Lepton flavour violation in minimal supersymmetric extensions to the Standard model

by
Terje R. Meisler

Dr. scient. thesis
Department of Physics
Faculty of Natural Sciences and Technology

NTNU 2003

ISBN 82-471-6247-4
ISBN 82-471-6246-6 (electronic)

URN:NBN:no-7281

Acknowledgements

The work presented in this thesis has been performed during the years 1995 - 2003 at the Norwegian University of Technology (NTNU), and Sør-Trøndelag University College (HiST). Mathematics and physics, and the use of these subjects to understand the Nature, has always fascinated me. I am therefore grateful to have been given the opportunity to study and do research in theoretical physics, the subject which connects physics and mathematics.

This thesis has been funded by NTNU, with prof. Kjell Mork as supervisor. Financial support has also been received from the Department of Physics, NTNU, and from Sør-Trøndelag University College (HiST).

I would like to thank my present employer, Sør-Trøndelag University College (HiST), who has supported me with software, several computers, and also have let me spend time to complete this work. I will also use this opportunity to thank all my fellow students from Lade (AVH), and to thank my family, my parents and siblings. But most of all a special thank you to Hanna and Jacob, and to Lise for listening to me when I eagerly have talked about supersymmetry and quantum fields.

Trondheim, December 2003

Terje R. Meisler

URN:NBN:no-7281

Contents

1 Introduction **1**

2 Lepton number violation in the Standard Model **5**
2.1 Experimental status of $l \to l'\gamma$ 6
2.2 Masses and gauge couplings 7
2.3 Massive neutrinos in the Standard Model 8
2.3.1 Dirac mass terms 9
2.3.2 Majorana mass terms 9
2.3.3 Dirac-Majorana mass terms 10
2.3.4 Neutrino masses, $l \to l'\gamma$ and the Standard Model 11

3 Supersymmetric models and massive neutrinos **13**
3.1 Extending MSSM 14
3.1.1 Dirac neutrinos - MSSM-D 14
3.1.2 Majorana neutrinos - MSSM-M 17
3.1.3 Dirac-Majorana neutrinos - MSSM-DM 19
3.2 Breaking of supersymmetry 21
3.2.1 Supergravity 22
3.2.2 Gauge mediated breaking of supersymmetry 23
3.2.3 Other scenarios 23

4 Dirac neutrinos and $l \to l'\gamma$ **25**
4.1 Reducing the parameter space of MSSM-D 26
4.2 The Higgs potential 27
4.2.1 The tadpole method 28
4.3 Mass matrices in MSSM-D 30
4.4 Running of parameters 32
4.4.1 Some results from MSSM 33
4.4.2 Qualitative analysis of the running 34
4.4.3 Numerical analysis of Y_ν, a_ν and M_n^2 38
4.5 Analysis of $\Gamma(l \to l'\gamma)$ in MSSM-D 39
4.5.1 Qualitative analysis of branching ratios 42
4.5.2 Numerical analysis of MSSM-D 43

5 Majorana neutrinos and $l \to l'\gamma$ **49**

5.1 The parameter space of MSSM-M . . . 49
5.2 Limits on R-parity violating couplings . . . 51
5.3 Mixing among down-type superfields . . . 51
5.3.1 Defining the $\hat{H}_d - L_i$-space . . . 51
5.3.2 Choice of basis . . . 54
5.4 Minimisation of tree-level scalar potential . . . 57
5.5 Mass matrices and mixing in MSSM-M . . . 59
5.5.1 Neutral fermions . . . 59
5.5.2 Charged fermions . . . 62
5.5.3 Charged scalar sector . . . 63
5.5.4 Neutral scalar sector . . . 64
5.6 Constraints from scalar masses . . . 66
5.7 Running of parameters in MSSM-M . . . 67
5.7.1 Analytic estimates . . . 67
5.7.2 Numerical analysis . . . 70
5.8 Qualitative analysis of $\Gamma(l \to l'\gamma)$ in MSSM-M . . . 76
5.9 Numerical analysis . . . 78
5.9.1 λ'_{ijk} vanishes . . . 78
5.9.2 λ_{ijk} vanishes . . . 82
5.9.3 Elements from both λ' and λ are non-vanishing . . . 83
5.9.4 Varying the MSSM parameters . . . 86
5.9.5 Beyond the supergravity scenario . . . 88

6 Dirac-Majorana neutrinos and $l \to l'\gamma$ 91
6.1 Lagrangian of MSSM-DM . . . 92
6.2 The tree-level scalar potential . . . 93
6.3 Mass matrices and mixing in MSSM-DM . . . 96
6.3.1 Neutral fermions . . . 96
6.3.2 Charged fermions . . . 98
6.3.3 Charged scalars . . . 99
6.3.4 Neutral scalars . . . 100
6.4 Constraints from mass matrices . . . 102
6.5 Running of parameters in MSSM-DM . . . 104
6.5.1 Qualitative analysis of renormalization group equations . . . 105
6.5.2 Numeric analysis of renormalization group equations . . . 108
6.6 Analysis of $\Gamma(l \to l'\gamma)$ in MSSM-DM . . . 116
6.6.1 Qualitative analysis of branching ratios . . . 116
6.6.2 Numerical analysis of branching ratios . . . 119

7 Summary and discussion 129

8 Conclusions 137

A Notation and supersymmetry 139
A.1 Notation . . . 139
A.2 A short introduction to supersymmetry . . . 142

A.2.1 Field content 146
A.3 R-parity 147

B Form factors and amplitudes **149**
B.1 Form factors and matrix elements 149
B.2 The decay rate 150
B.3 A toy model 151
B.4 Amplitudes in MSSM-DM 153
B.5 Amplitudes in MSSM-M 156
B.6 Amplitudes in MSSM-D 156

C Scalarpotentials **157**
C.1 Tree-level scalar potential 157
C.1.1 Neutral scalar potential 160
C.2 The tadpole method 161
C.2.1 The tree-level scalar potential 161
C.2.2 Tree-level tadpoles 162
C.2.3 The one-loop tadpoles 163

D Mass- and mixing-matrices **171**
D.1 Field content of MSSM-D 171
D.2 Mass matrices and mixing in MSSM-D 171
D.3 Field content of MSSM-DM 174
D.4 Mass-matrices in MSSM-DM 174
D.4.1 Neutral fermions in MSSM-DM 175
D.4.2 Charged Dirac fermions 175
D.4.3 Charged scalars 175
D.4.4 Neutral scalars 177
D.5 Mass-matrices in MSSM-M 180

E Feynman-rules **181**
E.1 Feynman-rules in MSSM-D 181
E.2 Feynman rules for MSSM-M and MSSM-DM 185
E.2.1 Weyl-spinors and mass-eigenstates 185
E.3 Feynman rules 190
E.4 Feynman rules for MSSM-M 193

F Renormalisation group equations **195**
F.1 MSSM-D 195
F.2 MSSM-DM 199
F.2.1 Quantum numbers and group properties 199
F.2.2 Gauge-couplings and gaugino-masses 200
F.2.3 Superpotential parameters 202
F.2.4 Soft-breaking terms 203

G Veltman-Passarino integrals **209**

G.1 Veltman-Passarino integrals 209
G.2 Solution by series expansion 213

H Numerical methods 219

Chapter 1

Introduction

In 1897 the era of particle physics started with J. J. Thompson's discovery of the electron [1]. Almost 50 years later, in 1945, C. F. Powell discovered a new electron-like particle in cosmic rays, which he named *muon*[1]. And in 1975 the third electron-like particle, the *tau* was discovered by M. L. Perl [3]. The existence of neutral fermions was first anticipated by Pauli with his famous "radioactive" letter in 1930 (see e.g., the virtual exhibition in Ref. [4]). It did however take more than 25 years until the first neutrino was discovered in 1956 by Cowan and Reines. In 1962 it was shown that at least two different kind of neutrinos must exist, one associated with the electron and one associated with the muon. These neutrinos was named electron-neutrinos and muon-neutrinos. Finally, in July 2000 Fermilab [5] could announce the first direct observation of the third neutrino, the tau-neutrino. These 3 charged and 3 neutral fermions make up the so-called *lepton-flavours*. An important observation made from detailed studies of Z-decay shows that nature only allows for these three lepton flavours [6]. That is, possible new leptons, beyond the existing ones, must be very heavy.

The mass and mean life-time (τ) for the charged leptons are established to a fairly good accuracy [6], i.e.,

$$m_e = 0.510998902 \pm 0.000000021\,\text{MeV}, \qquad \tau_e > 4.6 \cdot 10^{26}\,\text{yr}, \tag{1.1}$$

$$m_\mu = 105.658357 \pm 000005\,\text{MeV}, \qquad \tau_\mu = 2.19703 \pm 0.00004 \cdot 10^{-6}\,\text{s}, \tag{1.2}$$

$$m_\tau = 1776.99^{+0.29}_{-0.26}\,\text{MeV}, \qquad \tau_\tau = 290.6 \pm 1.1 \cdot 10^{-15}\text{s}. \tag{1.3}$$

However, the question whether the neutrinos are massless or not has for quite a long time been a puzzle. All accelerator experiments have been consistent with massless neutrinos. But the deficit of solar neutrinos have, since the 60's, indicated that the neutrinos are massive [7]. In 1998 the group working on the Super-Kamiokande experiment [8] confirmed the existence of neutrino oscillations for the first time. Later observations involving solar neutrinos (e.g., SNO [9, 10] and SAGE [11]), atmospheric neutrinos (e.g., MACRO [12] and Super-Kamiokande), accelerator neutrinos

[1]The name μ was chosen since π and μ was the only Greek letters on Powell's typewriter [2].

(e.g., K2K [13]) and reactor neutrinos (e.g., KAMLAND [14] and CHOOZ [15]) shows that neutrino oscillation is a real and physical effect. Moreover, these experiments shows that the neutrinos must be massive.

On the other hand, the Standard Model of particle physics is defined with massless neutrinos, i.e., the neutrinos are modelled by use of massless left-handed Weyl spinors. This leads to an accidental global symmetry [16] for the Lagrangian, with two important consequences: First, it leads to conservation of the number of leptons in all interactions. Second, it leads to conservation of the number of leptons from each lepton flavour. The quantum numbers describing these two symmetries are the lepton number and the three lepton flavour numbers, respectively. The conservation of these quantum numbers prohibits certain decay channels, such as $\tau^- \to \pi^-\pi^0$ and $\mu \to e\gamma$. Such decay channels have been studied extensively over the years, both theoretically and experimentally. And the constraints, especially for $\mu \to e\gamma$, do not leave much room for lepton flavour violation. Nevertheless, the existence of massive neutrinos may open such decay channels.

A very interesting possibility is that neutrinos can either be Dirac- or Majorana-fermions. One phenomenological difference between these two possibilities is that for a Dirac-fermion the lepton number is conserved, while the lepton flavour numbers may be broken. This is in analogy to the quark sector where baryon flavour is broken, and baryon number is conserved. On the other hand, a Majorana fermion breaks both lepton number and lepton flavour numbers. In more technical terms a Dirac fermion is defined by use of both left- and right-handed Weyl spinors. It therefore has four independent states with equal mass, i.e., particles with spin up (down), and anti-particles with spin up (down). On the other hand, a Majorana-fermion is its own anti-particle, with only two independent states. Also, both lepton number and lepton flavour numbers are broken for Majorana-fermions. These Majorana-fermions can be constructed either by use of only left-handed Weyl-spinors, or by a combination of left- and right-handed spinors. Majorana fermions constructed by both left- and right-handed Weyl-spinors, are often referred to as Dirac-Majorana fermions. Which of these three possibilities is the preferred one depends on the mass structure of the neutrinos.

The lack of a precise knowledge of the neutrino masses means that all three possibilities should be allowed in analysis of processes violating either lepton number or lepton flavour numbers. Such an analysis was made for three extensions of the Standard Model in Ref. [17]. It was found that the branching ratio for $\mu \to e\gamma$ was negligible for Dirac- and Majorana-neutrinos, but could be quite large for Dirac-Majorana neutrinos, almost in conflict with the upper limits. The reason for this large branching ratio for Dirac-Majorana neutrinos, is that light left-handed and heavy right-handed neutrino components will mix together. This mixing suppress cancellations among the different lepton flavours. Such cancellations are known as the GIM mechanism [18] in the quark sector, and as the MNS mechanism [19] in the lepton sector, in honour of Maki, Nakagawa and Sakata [19].

This thesis aims to continue the work made in Ref. [17] by analysing three minimal

supersymmetric extensions to the Standard Model, one including Dirac-neutrinos (MSSM-D), one including Majorana-neutrinos (MSSM-M), and one including Dirac-Majorana neutrinos (MSSM-DM). These three models are then analysed with special emphasis on lepton flavour violation. The three decay channels $\tau \to \mu\gamma$, $\tau \to e\gamma$ and $\mu \to e\gamma$ are analysed for all three models both by analytic and numeric methods.

The outline of this thesis is that Chapter 2 gives a brief review of the observations made for massive neutrinos, along with the description of neutrinos in the Standard Model and the extensions of it made in Ref. [17]. In Chapter 3 supersymmetry enters and the three models, MSSM-D, MSSM-M and MSSM-DM, are defined. Chapters 4 to 6 presents the analytic and numeric analysis of the phenomenology and the decay rates under study. In Chapter 7 the results will be summarised and discussed, and finally in Chapter 8 the conclusions are given. The notation used, and some detailed calculations are presented in the appendices.

URN:NBN:no-7281

Chapter 2

Lepton number violation in the Standard Model

The assumptions in the Standard Model, regarding massless neutrinos, lead to a global symmetry causing conservation of the lepton number, L, and of the three lepton flavour numbers, L_e, L_μ and L_τ.

Except for observations of neutrino oscillations there have been no other observations violating these quantum numbers[1]. An example of a process violating the lepton number is $\tau^- \to \pi^-\pi^0$. This process has not been observed, and has therefore an upper limit on its branching ratio [6] $Br(\tau^- \to \pi^-\pi^0) < 3.7 \times 10^{-4}$. Typical upper limits for branching ratios involving lepton number violating τ decays are $10^{-4}-10^{-6}$. An example of a lepton flavour violating decay channel is $\mu^- \to e^-e^+e^-$, with a branching ratio [6] $Br(\mu^- \to e^-e^+e^-) < 1.0 \times 10^{-12}$, which is a typical upper limit for branching ratios involving lepton flavour violating μ-decays. These example give the impression that both lepton number and the lepton flavour numbers are conserved quantum numbers, as prescribed by the Standard Model.

The confirmation of neutrino oscillations at Super-Kamiokande [8] in 1998 has changed this simple picture, since neutrino oscillations clearly break lepton flavour numbers, and also demands for massive neutrinos. Both phenomena not accounted for by the Standard Model. By introducing neutrino masses lepton flavour violating decay channels will now generally be a possibility. Thus a detailed understanding of these decay modes is important in order to understand the neutrinos, and to find a necessary extension of the Standard Model.

In this thesis the three lepton flavour number violating decay channels $\tau \to \mu\gamma$, $\tau \to e\gamma$ and $\mu \to e\gamma$, will be studied. For easy referencing these three modes are referred to by the generic term $l \to l'\gamma$.

[1] A group at the Heidelberg-Moscow double beta decay experiment claims to have observed neutrinoless double beta decays [20]. If confirmed this implies that both lepton number and lepton family numbers are violated, and also that the neutrinos are Majorana fermions.

This chapter will review the experimental status for the three relevant decay channels, and also present the possible neutrinos mass terms which may appear in a simple extension of the Standard Model. It must be stressed that the literature involving theory, phenomenology and experiments dealing with massive neutrinos is huge[2]. This chapter has therefore no intention of presenting a complete review, or even serve as a starting point to this most fascinating subject. Reference [21], and references therein, is a good starting point to the phenomenology of massive neutrinos. Also the web-page *The Neutrino Oscillation Industry* [22] presents updated information on this subject.

2.1 Experimental status of $l \to l'\gamma$

The masses and lifetimes for the charged leptons are all observed to great accuracy [23], see Eqs. (1.1) - (1.3). The upper limits for the various lepton flavour violating decay rates are also established to a fairly good accuracy. Especially the upper limit for $\mu \to e\gamma$ is impressive. The Particle Data Group [6] labels the three lepton flavour violating decay modes $\mu \to e\gamma$, $\tau \to e\gamma$ and $\tau \to \mu\gamma$ by the terms Γ_5, Γ_{128} and Γ_{129}, respectively. These are the names that will be used throughout this thesis for the experimentally measured upper limits. This to properly separate between the measured limits and the theoretically calculated values, which will appear in later chapters. The current upper limits for these decay modes are given as [6],

$$Br(\mu \to e\gamma) = \frac{\Gamma_5}{\Gamma(\mu \to \text{all})} < 1.2 \times 10^{-11}, \tag{2.1}$$

$$Br(\tau \to e\gamma) = \frac{\Gamma_{128}}{\Gamma(\tau \to \text{all})} < 2.7 \times 10^{-6}, \tag{2.2}$$

$$Br(\tau \to \mu\gamma) = \frac{\Gamma_{129}}{\Gamma(\tau \to \text{all})} < 1.1 \times 10^{-6}, \tag{2.3}$$

where $\Gamma(\mu \to \text{all})$ and $\Gamma(\tau \to \text{all})$ are the total μ- and τ-decay rates respectively. By combining Eqs. (2.1) - (2.3), and the lifetimes presented in Eqs. (1.2) and (1.3), the following upper limits for the three decay modes are obtained,

$$\Gamma_5 < 3.5951 \times 10^{-30}\,\text{GeV}, \tag{2.4}$$

$$\Gamma_{128} < 6.1282 \times 10^{-18}\,\text{GeV}, \tag{2.5}$$

$$\Gamma_{129} < 2.4967 \times 10^{-18}\,\text{GeV}. \tag{2.6}$$

Even though the limit for Γ_5 is impressive, a new experimental proposal has been approved by the Paul Scherrer Institute, Switzerland. This experiment [24] could push the limit for $Br(\mu \to c\gamma)$ down to 10^{-14}. Also for $Br(\tau \to \mu\gamma)$ a more

[2] A search at Slac-Spires with the keyword "neutrino" gave more than 17700 entries, and more than 520 entries only for 2002.

constraining upper limit of 10^{-9} may be reached in the near future [25]. Another possibility from these experiments is, of course, that a non-vanishing value is found for some or all of these decay channels.

2.2 Masses and gauge couplings

It is a well known fact that the masses and coupling constants in most quantum field theories run by energy scale[3]. That is, the values of these parameters depends on the energy scale in which they are measured. The details of this running is dictated by a set of differential equations, the renormalization group equations. The parameters of the Standard Model run by scale, and in order to solve the renormalization group equations some initial values of these parameters have to be known. In Ref. [26] the running of the fermion masses and the coupling constants of the Standard Model was studied, and the following values was obtained for the fermion masses at the M_Z-scale,

$$\begin{aligned} m_u &= 2.33^{+0.42}_{-0.45}\,\text{MeV}, & m_c &= 677^{+56}_{-61}\,\text{MeV}, & m_t &= (181 \pm 13)\,\text{GeV}, \\ m_d &= 4.69^{+0.60}_{-0.66}\,\text{MeV}, & m_s &= 93.4^{+11.8}_{-13.0}\,\text{MeV}, & m_b &= (3.00 \pm 0.11)\,\text{GeV}, \\ m_e &= (0.48684727 & m_\mu &= (102.75138 & m_\tau &= (1.74669 \\ &\quad \pm 0.00000014)\,\text{MeV}, & &\quad \pm 0.00033)\,\text{MeV}, & &\quad {}^{+0.00030}_{-0.00027})\,\text{GeV}. \end{aligned} \tag{2.7}$$

In the quark sector they also found the following quark mixing matrix, at the M_Z-scale,

$$V_{\text{CKM}} = \begin{pmatrix} 0.9754 & 0.2205 & 0.0030\,e^{-i\delta} \\ -0.2203 - 0.0001\,e^{i\delta} & 0.9747 & 0.0373 \\ 0.0082 - 0.0029\,e^{i\delta} & -0.0364 - 0.0007\,e^{i\delta} & 0.9993 \end{pmatrix}. \tag{2.8}$$

In this expression the standard parametrisation [6] of the CKM-matrix is used, and the phase δ lies in the range [6] $0 \leq \delta < 2\pi$.

The values for the three gauge couplings were also found, at the M_Z-scale, in this paper, i.e.,

$$\alpha_1(M_Z) = 0.016829 \pm 0.000017, \tag{2.9}$$
$$\alpha_2(M_Z) = 0.033493^{+0.000060}_{-0.000058}, \tag{2.10}$$
$$\alpha_3(M_Z) = 0.118 \pm 0.003. \tag{2.11}$$

These values are derived from

$$\alpha(M_Z) = (128.89 \pm 0.09)^{-1}, \tag{2.12}$$
$$\sin^2\theta_W = 0.23165 \pm 0.000024, \tag{2.13}$$

[3]The $N = 4$ supersymmetric Yang-Mills theory is an exception, in that the parameters do not run by scale.

and $\Lambda^5_{\overline{\rm MS}} = 209^{+39}_{33}$MeV. Here α is the fine structure constant determined from the quantum Hall effect, and $\sin\theta_W$ is the weak mixing angle. Finally, $\Lambda^5_{\overline{\rm MS}}$ parametrises the running of α_3. The index $\overline{\rm MS}$ means that modified minimal subtraction is used as the renormalization scheme, and the index 5 corresponds to the effective number of massless quarks. See Ref. [6] for further details on definitions and updated experimental limits for these parameters. The three gauge coupling constants are also defined to satisfy the relation,

$$\frac{1}{e^2} - \frac{5}{3}\frac{1}{g_1^2} + \frac{1}{g_2^2}, \tag{2.14}$$

and the $SU(5)$-GUT limit,

$$g_1 = g_2 = g_3. \tag{2.15}$$

The important point for the coming analysis is that Eqs. (2.7) - (2.11) provides us with the necessary boundary conditions at the M_Z scale. These boundary conditions also connects the Standard Model to the three supersymmetric models to be defined an analysed in later chapters.

2.3 Massive neutrinos in the Standard Model

The Standard Model is defined with massless neutrinos, but the neutrino oscillations shows that the neutrinos indeed are massive. These observations therefore imply that the Standard Model must be extended, or maybe even replaced by some other more general model. The simplest possible extension of the Standard Model is to add the necessary mass terms for the neutrinos by hand. Such an ad hoc method is not satisfactory since the neutrino masses are now treated different than the other fermions, i.e., the neutrino masses are not generated by the Higgs mechanism. Unfortunately, the use of the Standard Model Higgs mechanism, i.e., with one Higgs doublet, is not straight forward. The reason is that the neutrinos can be either Dirac- or Majorana-fermions. If the neutrinos are Dirac-fermions then a new Yukawa matrix, Y_ν, and the Standard Model Higgs mechanism will provide the necessary mass terms. But if the neutrinos are Majorana-fermions then the Standard Model Higgs mechanism is not sufficient to provide the necessary mass terms [21]. In this case an enlargement of the Higgs sector is required, that is, one must include additionally neutral scalars to the model.

The different options regarding the neutrino masses in the Standard Model will now be reviewed in greater detail. It will be shown that the fermionic nature of the neutrinos is determined by the mass terms. The neutrinos can therefore be Dirac, Majorana or Dirac-Majorana neutrinos. This section is based on the thorough review of neutrino oscillations presented in Ref. [21].

2.3.1 Dirac mass terms

A Dirac mass term is defined by the following Lagrangian,

$$\mathcal{L}_D = -\sum_{i,j} (\bar{\nu}_R)_i \; M^D_{ij} \; (\nu_L)_j + \text{h.c.}, \tag{2.16}$$

where M^D_{ij} is an arbitrary 3×3 complex mass matrix, and the lepton flavours are labelled by $i, j = e, \mu, \tau$. Also, $\nu_L\,(\nu_R)$ is a left- (right-) handed two-component Weyl spinor, and h.c. means Hermitian conjugation.

If $\mathcal{L}_D$ is the only mass term added to the Standard Model, one readily sees that the total Lagrangian still has a global symmetry involving leptons. That is, the lepton number (L) is still a conserved quantum number, but, depending on the details of M^D, the lepton flavour numbers may be broken. This is in close analogy with the baryon sector where the baryon number is conserved while the baryon flavour numbers are broken.

An important feature of Dirac neutrinos is that they acquire their masses by the very same Higgs mechanism as the charged fermions of the Standard Model. Thus, there is no need for any enlargement of the Higgs sector, only one new Yukawa matrix, Y_ν, must be included to parametrise these mass terms.

As for the quark sector of the Standard Model, a 3×3 mixing matrix determines the mixing between the three lepton flavours. In order to avoid confusion with the quark mixing matrix one often refers to this lepton mixing matrix as the MNS matrix. This to honour Maki, Nakagawa and Sakata [19] who first described mixing in the two flavour case, i.e., for ν_e and ν_μ. The general case was studied by Pontecorvo [27].

For Dirac neutrinos there is almost complete analogy to the quark sector. That is, there are 6 masses, 3 mixing angles and 1 complex phase associated with the lepton and quark flavours.

2.3.2 Majorana mass terms

A Majorana fermion is defined as its own anti-particle, thus neither lepton number nor lepton flavour numbers can be conserved. A Majorana mass term can now be defined in two ways. First, only left-handed Weyl spinors can be involved, and second both left- and right-handed spinors can be involved. Neutrino masses defined by the first option will be referred to as Majorana neutrinos, while neutrino masses defined by the last option are known as Dirac-Majorana neutrinos.

By allowing for left-handed Weyl spinors only, the following Majorana mass term is defined,

$$\mathcal{L}^L_M = -\frac{1}{2} \sum_{i,j} \left(\bar{\nu}^C_L\right)_i \; M^L_{ij} \; (\nu_L)_j + \text{h.c.}, \tag{2.17}$$

where M_{ij}^L is an arbitrary complex symmetric 3×3 matrix. The index C means charge conjugation, i.e.,

$$\nu_L^C = C\,\bar{\nu}_L^T, \tag{2.18}$$

where C is the unitary matrix of charge conjugation, see e.g., Refs. [28, 29] for further details and possible representations of this matrix.

A key observation, regarding $\mathcal{L}_M^L$, is that a Majorana mass term can not be accomplished by the Standard Model Higgs mechanism. That is, one needs to enlarge the neutral scalar sector of the Standard Model. This extension depends on how the neutrino masses are generated. If the Majorana mass terms are generated at tree-level a Higgs triplet is needed, in addition to the Standard Model Higgs doublet [21]. The neutrinos could also acquire a Majorana mass term at the one-loop level. However, this scenario also demands for an enlargement of the scalar sector. In this case one needs Higgs singlets and an additional Higgs doublet (1-loop), or a doubly charged Higgs singlet and an additional singly charged scalar (2-loop) [21].

2.3.3 Dirac-Majorana mass terms

The Dirac-Majorana mass term gives the most general mass term, in that both mass terms from Eqs. (2.16) and (2.17) are included. A Dirac-Majorana mass term adds the following piece to the Lagrangian,

$$\mathcal{L}_{DM} = \mathcal{L}_D + \mathcal{L}_M^L + \mathcal{L}_M^R, \tag{2.19}$$

where $\mathcal{L}_D$ and $\mathcal{L}_M^L$ are defined in Eqs. (2.16) and (2.17), respectively. The mass term $\mathcal{L}_M^R$ is defined as

$$\mathcal{L}_M^R = -\frac{1}{2}\sum_{i,j} (\nu_R)_i \; M_{ij}^R \; \left(\nu_R^C\right)_j + \text{h.c.}. \tag{2.20}$$

Here M^L and M^R are arbitrary complex symmetric 3×3 matrices, and M^D is a complex 3×3 matrix.

As for the Majorana neutrinos also the Dirac-Majorana mass term needs an enlargement of the scalar sector. In this case the Higgs sector must be extended with a Higgs triplet and a Higgs singlet [21].

Even if the Majorana and Dirac-Majorana mass terms need an enlargement of the Standard Model Higgs sector this scenario is quite popular in the literature. One reason is that the small neutrino masses can be understood by incorporating the see-saw mechanism, see Ref. [21].

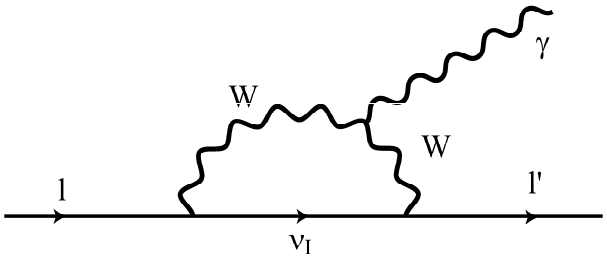

Figure 2.1: The figure shows the one-loop Feynman diagram, which contributes to the decay channels $l \to l'\gamma$ in the unitary gauge.

2.3.4 Neutrino masses, $l \to l'\gamma$ and the Standard Model

All mass terms, presented in Eqs. (2.16), (2.17) and (2.19) will, in general, lead to lepton flavour violation. Since the true fermionic nature of the neutrinos is not completely understood one should keep all possibilities open. That is, one should analyse lepton flavour violating decay rates by allowing for all three kinds of neutrino mass terms. Such an analysis has been made in Ref. [17], where the decay channel $\mu \to e\gamma$ was analysed for three extensions of the Standard Model.

In the unitary gauge the Standard Model contains only one Feynman diagram, at the one loop level, contributing to the lepton flavour violating decay channel $l \to l'\gamma$, see Fig. 2.1. In Ref. [30] the following branching ratio was obtained for Dirac or Majorana neutrinos,

$$\begin{aligned} Br\left(\mu \to e\gamma\right) &= \frac{\Gamma\left(\mu \to e\gamma\right)}{\Gamma\left(\mu \to e\nu_\mu \bar{\nu}_e\right)} \\ &= \frac{3\alpha}{32\pi}\left|U_{\mu i}U_{ei}\frac{m_i^2}{M_W^2}\right|^2, \end{aligned} \tag{2.21}$$

where U is the lepton mixing matrix, and m_i are the neutrino mass eigenstates, and M_W is the mass of the charged gauge boson W. If the neutrino-mass is assumed to be below 100 eV, this branching ratio was found to be extremely small, i.e., $Br\left(\mu \to e\gamma\right) \leq 10^{-40}$.

However, for a Dirac-Majorana neutrino the branching ratio was found to be as large as $Br\left(\mu \to e\gamma\right) \leq 10^{-13}$. The reason was found to be that the mass eigenstates are linear combinations of heavy right-handed and light left-handed components. This mixing of light and heavy components makes the neutrinos highly non-degenerate, and the MNS-mechanism is therefore suppressed.

Even if Eq. (2.21) is obtained for non-supersymmetric extensions of the Standard Model [17], this expression will be of great help in the forthcoming analysis to give a qualitative understanding of the decay rates. Roughly speaking, Eq. (2.21)

shows that $Br(\mu \to e\gamma)$ is determined by two competing phenomena. Assume for a moment that M_W and m_i are free, adjustable parameters of the model. Then $Br(\mu \to e\gamma)$ will decrease for increasing values of M_W. Also, this branching ratio will increase if m_i is scaled by a numeric factor. But more importantly, this branching ratio will increase if there is an increasing non-degeneracy among the neutrinos, see discussion in Appendix B.3. That is, this branching ratio may be small either if M_W^2 is large, or if the neutrinos are highly degenerate in mass. This dependency on the degeneracy among neutrinos, or on other particles, is referred to as the MNS mechanism, and is mathematically equivalent to the celebrated GIM mechanism [18] known from the quark sector.

Chapter 3

Supersymmetric models and massive neutrinos

If nature is supersymmetric at the electroweak scale, the three possible kinds of neutrino mass terms, have to enter the model as mass terms for the neutrino superfields. One can therefore construct three extensions of the Standard Model depending on the kind of neutrino masses one deals with. In the same manner one can also construct one minimal supersymmetric extension to each of these models. These three kinds of supersymmetric models will be constructed in this chapter, and their number of free parameters will be counted. This set of free parameters will be referred to as the parameter space for the model.

In order to separate properly among these three models the following terminology will be used. In this thesis the minimal supersymmetric extension of the Standard Model with massless neutrinos will be called MSSM. The minimal supersymmetric extension of the Standard Model including Dirac-neutrinos, Majorana neutrinos and Dirac-Majorana neutrinos will be called MSSM-D, MSSM-M and MSSM-DM, respectively.

An interesting consequence of these models is that they are all capable of giving masses, also to the Majorana neutrinos, by the Higgs-mechanism known from MSSM. That is, only the two Higgs doublets of MSSM are needed, for all kinds of neutrino masses.

Most often MSSM is divided into two broad categories, R-parity conserving and R-parity violating models. Each of these models may further be categorised in terms of different scenarios for the breaking of supersymmetry [31], e.g., gravity mediated supersymmetry breaking, gauge mediated supersymmetry breaking, or some other supersymmetry breaking mechanism. In this thesis a different, more natural, strategy for treating massive neutrinos will be used. These models will be constructed as minimal supersymmetric extensions to the Standard Model, by allowing all possible terms fulfilling the global symmetries implied by the various neutrino mass terms. That is, MSSM-D have both left- and right-handed neutrino

superfields, and conservation of the lepton number. The lepton flavour numbers may be broken in MSSM-D. In MSSM-M the neutrino mass terms are constructed by left-handed neutrino superfields only, and the lepton number is therefore broken. The neutrino mass terms in MSSM-DM are constructed of both left- and right-handed neutrino superfields, and the lepton number is therefore also broken. Note that if the lepton number is broken, than also the lepton flavour numbers are broken.

Additional global symmetries may also be enforced onto the Lagrangian. One such symmetry is a global baryon symmetry, which protects the proton against a too fast decay. In this thesis baryon symmetry will always be assumed, i.e., the Lagrangian is invariant under the action,

$$(Q, u, d, L, e, n, \hat{H}_u, \hat{H}_d) \to (-Q, -u, -d, L, e, n, \hat{H}_u, \hat{H}_d). \tag{3.1}$$

Here Q and L are doublets with superfields involving left-handed quarks and leptons, respectively, and u, d, e and n are the singlet superfields involving right-handed quarks and leptons. Finally, $\hat{H}_u$ and $\hat{H}_d$ are the left-handed doublets involving the two Higgs superfields of MSSM.

Also, a scenario for the breaking of supersymmetry must be chosen. This topic is discussed later in this chapter.

It should be stressed that other scenarios for supersymmetric extensions of the Standard Model could be used, e.g., one could extend the Standard Model Higgs sector with a Higgs triplet, in order to have massive Majorana neutrinos, and then one could make this model supersymmetric.

3.1 Extending MSSM

There exists lots of good introductions to supersymmetry, see e.g., Refs. [32, 29, 33], and also a lot of good reviews of MSSM, e.g., Refs. [28, 34]. However, to clarify the notation used and provide easy referencing, a short introduction to supersymmetry can be found in Appendix A.2.

3.1.1 Dirac neutrinos - MSSM-D

MSSM-D is defined as the minimal supersymmetric extension of the Standard Model, including right-handed neutrino superfields, n_i, and conservation of the lepton number. These demands defines the superpotential of MSSM-D, i.e.,

$$W_{\text{Dirac}} = Y_u Q \hat{H}_u u - Y_d Q \hat{H}_d d - Y_e L \hat{H}_d e + Y_\nu L \hat{H}_u n + \mu \hat{H}_u \hat{H}_d, \tag{3.2}$$

where the Yukawa matrices Y_u, Y_d, Y_e and Y_ν generally are arbitrary 3×3 complex matrices in flavour space. Here Q and L represent the chiral $SU(2)$ superfields of

the quark and lepton doublets, respectively. The chiral $SU(2)$ singlet superfields are denoted as, u, d, e and n, while $\hat{H}_u$ and $\hat{H}_d$ are the two Higgs doublets with hypercharge $Y = +1$ and $Y = -1$, respectively. The $SU(2)$ and $SU(3)$ indices have been suppressed. The sign convention in the superpotential follows the one from Ref. [35]. This convention has the advantage that the Yukawa couplings for the Standard Model fermions are positive.

Note that baryon symmetry, as defined by Eq. (3.1), do not allow for a term like $1/2\,\lambda''_{ijk} u_i\, d_j\, d_k$. Such a term will easily cause an unacceptable fast proton decay, see e.g., Ref. [35] and references therein.

The corresponding soft supersymmetry breaking terms becomes,

$$\begin{aligned} -\mathcal{L}_{\text{Dirac}} = {} & M_Q^2 \tilde{Q}^\dagger \tilde{Q} + M_L^2 \tilde{L}^\dagger \tilde{L} + M_{H_u}^2 H_u^\dagger H_u + M_{H_d}^2 H_d^\dagger H_d \\ & + M_u^2 \tilde{u}\tilde{u}^* + M_d^2 \tilde{d}\tilde{d}^* + M_e^2 \tilde{e}\tilde{e}^* + M_n^2 \tilde{n}\tilde{n}^* \\ & + \Big[a_u \tilde{Q} H_u \tilde{u} + a_d \tilde{Q} H_d \tilde{d} + a_e \tilde{L} H_d \tilde{e} + a_\nu \tilde{L} H_u \tilde{n} + b H_u H_d \\ & + \frac{1}{2} M_1 \tilde{B}^0 \tilde{B}^0 + \frac{1}{2} M_2 \tilde{W}^a \tilde{W}^a + \frac{1}{2} M_3 \tilde{G}^a \tilde{G}^a + \text{h.c.} \Big], \end{aligned} \tag{3.3}$$

where a_u, a_d, a_e and a_ν are arbitrary complex 3×3 matrices in flavour space, and $\tilde{Q}$, $\tilde{L}$, $\tilde{u}$, $\tilde{d}$, $\tilde{e}$, $\tilde{n}$, H_u and H_d are the scalar components of the corresponding supermultiplets. Also $M_{\tilde{Q}}^2$, $M_{\tilde{L}}^2$, $M_{\tilde{u}}^2$, $M_{\tilde{d}}^2$, $M_{\tilde{e}}^2$ and M_n^2 are 3×3 Hermitian matrices in flavour space, and M_3, M_2 and M_1 are the gaugino masses for the gauge-group $SU(3) \times SU(2) \times U(1)$. Note that the parameters which makes MSSM-D different from MSSM are Y_ν, a_ν and M_n^2. If these three matrices where to vanish then MSSM-D becomes equal to MSSM.

The parameter space for MSSM-D is defined as the set of all free parameters of MSSM-D. Thus a point in parameter space is a list of values for all free parameters of the model. Note that this parameter space also contains the parameter space of the Standard Model, especially the parameters of Eqs. 2.7 - 2.11 are included. The dimension of this parameter space is an important number to know. However, before this counting is performed it is instructive to count the parameter space of the Standard Model by the same counting procedure as will be used for MSSM-D. This counting procedure is as presented in Refs. [31, 36].

The Standard Model gauge sector consists of 3 real gauge couplings, g_1, g_2, g_3, and the QCD vacuum angle θ_{QCD}. The Higgs sector consists of the Higgs squared mass and one Higgs self coupling, i.e., the two real parameters m^2 and λ. The fermion sector consists of the three Yukawa-couplings, Y_u, Y_d and Y_e, which are arbitrary 3×3 complex matrices. A straight forward counting gives 60 free parameters to be determined. Fortunately, most of these degrees of freedom are unphysical, and can be removed from the Lagrangian. The gauge sector has a $U(3)^5$ flavour symmetry, corresponding to the three flavours of the five gauge multiplets: $(\nu_i, e_i^-)_L$, $(e_i^C)_L$, $(Q_i, u_i)_L$, $(u_i^C)_L$ and $(d_i^C)_L$. A $U(3)$ matrix can be parameterised by 3 real angles and 6 phases. Now, if all rotations of $U(3)^5$ flavour symmetry could be used 15

	Masses and couplings	Real parameters	Imaginary parameters
Gauge sector	$g_1,\ g_2,\ g_3,\ \theta_{\rm QCD}$	4	
	$M_1,\ M_2,\ M_3$	3	3
Higgs sector	$M_{H_u},\ M_{H_d}$	2	
	$b,\ \mu$	2	2
Flavour sector	$Y_u,\ Y_d,\ Y_e,\ Y_\nu,\ a_u,\ a_d,\ a_e,\ a_\nu$	72	72
	$M_Q^2,\ M_L^2,\ M_u^2,\ M_d^2,\ M_e^2,\ M_n^2$	36	18
Removable parameters	$U(3)^6 \times U_{\rm PQ}(1) \times U_{\rm R}(1)$	18	34
Degrees of freedom		102	34

Table 3.1: The table shows the degrees of freedom from the gauge-, Higgs-, and flavour-sector of MSSM-D. Some apparent degrees of freedom is removed by applying the flavour symmetries $U(3)^6 \times U_{\rm PQ}(1) \times U_{\rm R}(1)$, and taking conservation of baryon number and lepton number into account.

real parameters and 30 phases could be removed. However, the flavour sector of the Standard Model has four exact global $U(1)$ symmetries. These symmetries gives conservation of baryon number, B, and of lepton flavour numbers, L_e, L_μ and L_τ. Thus one can remove 15 real parameters and 26 phases. That is, the Standard Model consists of 18 real parameters, and 1 phase. Note that most of these parameters are associated with the Yukawa matrices, which determine the masses and mixing of the fermions.

The same counting procedure will now be used to count the degrees of freedom for MSSM-D. First, the gauge sector of MSSM-D consists of 4 real parameters, that is, g_1, g_2, g_3, and the QCD vacuum angle, $\theta_{\rm QCD}$. There are also 3 complex gaugino masses, M_1, M_2 and M_3. The Higgs sector contributes with two real Higgs masses, $M_{H_u}^2$ and $M_{H_d}^2$, and also two complex parameters, μ and b. The flavour sector brings in the largest amount of new parameters. In MSSM-D there are 8 arbitrary 3×3 complex matrices: Y_u, Y_d, Y_e, Y_ν, a_u, a_d, a_e and a_ν. And also 6 Hermitian 3×3 matrices, M_Q^2, M_L^2, $M_{\tilde{u}}^2$, $M_{\tilde{d}}^2$, $M_{\tilde{e}}^2$ and M_n^2. Note that a 3×3 Hermitian matrix can be parameterised with 6 real parameters and 3 phases.

The result of this counting procedure is shown in Table 3.1, and shows that MSSM-D may contribute with as much as 120 real and 95 imaginary parameters. However, as for the Standard Model many of these parameters are unphysical and can be removed from the Lagrangian. At this point it should be stressed that only the rotations on the superfields are made, since this preserves the form of the gaugino couplings [36]. The flavour symmetry of the gauge sector is $U(3)^6$, due to the 6 multiplets of the MSSM-D gauge group: $(\nu_i, e_i^-)_L$, $(e_i^C)_L$, $(\nu_i^C)_L$, $(Q_i, u_i)_L$, $(u_i^C)_L$ and $(d_i^C)_L$. In MSSM-D the baryon number, B and the lepton number, L, are conserved.

However, the lepton flavour numbers may still be broken. In addition there are two more flavour symmetries, $U_{\rm PQ}(1) \times U_R(1)$. This is a Peccei-Quinn symmetry, and a continuous R-symmetry [31]. Thus one may remove a total of 18 real parameters and 34 imaginary ones. Thus MSSM-D has a total of 163 free parameters, i.e., 102 real parameters and 61 phases, see Table 3.1. This to be compared with the 124 free parameters of MSSM [36]. Compared to the Standard Model MSSM-D has 144 new parameters, that is 84 new real parameters and 60 new phases. Each of these new parameters implies physics beyond the Standard Model.

The phenomenology of MSSM-D will be studied, both by analytic and numeric methods, in Chapter 4.

3.1.2 Majorana neutrinos - MSSM-M

MSSM-M is defined as the minimal supersymmetric extension of the Standard Model, including only left-handed neutrino superfields. The baryon number may or may not be broken, depending on the details of the model. Since all models in this thesis are assumed to be invariant under the action of Eq. (3.1) the baryon number is conserved, and the term $1/2\,\lambda''_{ijk} u_i d_j d_k$ is not allowed. The superpotential of MSSM-M becomes,

$$\begin{aligned} W_{\rm Majorana} &= Y_u Q \hat{H}_u u - Y_d Q \hat{H}_d d - Y_e L \hat{H}_d e + \mu \hat{H}_d \hat{H}_u \\ &\quad + \frac{1}{2}\lambda_{ijk} L_i L_j e_k + \lambda'_{ijk} L_i Q_j d_k + \mu_i L_i \hat{H}_u. \end{aligned} \tag{3.4}$$

Note that the R-parity violating terms appears as a consequence of the lepton number violation. By explicitly writing the $SU(2)$ indices it is straightforward to see that λ_{ijk} is antisymmetric in i and j.

The soft-breaking parameters of MSSM-M are given by,

$$\begin{aligned} -\mathcal{L}_{\rm Majorana} &= M_Q^2 \tilde{Q}^\dagger \tilde{Q} + M_L^2 \tilde{L}^\dagger \tilde{L} + M_{H_u}^2 H_u^\dagger H_u + M_{H_d}^2 H_d^\dagger H_d \\ &\quad + M_u^2 \tilde{u}\tilde{u}^* + M_d^2 \tilde{d}\tilde{d}^* + M_e^2 \tilde{e}\tilde{e}^* \\ &\quad + \Big[\varepsilon_i H_d^* \tilde{L}_i - b H_d H_u - b_i L_i H_u \\ &\quad + a_e H_d \tilde{L}\tilde{e} + a_d H_d \tilde{Q}\tilde{d} + a_u H_u \tilde{Q}\tilde{u} \\ &\quad + \frac{1}{2}\lambda^{\rm s}_{ijk} \tilde{L}_i \tilde{L}_j \tilde{e}_k + \lambda'^{\rm s}_{ijk} \tilde{L}_i \tilde{Q}_j \tilde{d}_k \\ &\quad + \frac{1}{2}\left(M_1 \tilde{B}\tilde{B} + M_2 \tilde{W}^a \tilde{W}^a + M_3 \tilde{g}\tilde{g} \right) + \text{h.c.} \Big]. \end{aligned} \tag{3.5}$$

The parameter space of MSSM-M is found by the same counting procedure as was used for MSSM-D. First, the gauge sector contribute with 4 real parameters: g_1, g_2, g_3 and the QCD vacuum angle $\theta_{\rm QCD}$. The gauge sector also consists of 3

	Masses and couplings	Real parameters	Imaginary parameters
Gauge sector	$g_1,\ g_2,\ g_3,\ \theta_{\rm QCD}$	4	
	$M_1,\ M_2,\ M_3$	3	3
Higgs sector	$M_{H_u},\ M_{H_d}$	2	
	$b,\ \mu$	2	2
Higgs-flavour sector	$\varepsilon_i,\ \mu_i,\ b_i$	9	9
Flavour sector	$Y_u,\ Y_d,\ Y_e,\ a_u,\ a_d,\ a_e,$	54	54
	$M_Q^2,\ M_L^2,\ M_u^2,\ M_d^2,\ M_e^2,$	30	15
	$\lambda_{ijk},\ \lambda^{\rm s}_{ijk},\ \lambda'_{ijk},\ \lambda'^{\rm s}_{ijk}$	72	72
Removable parameters	$U(3)^5 \times U(4) \times U_{\rm PQ}(1) \times U_{\rm R}(1)$	18	35
Degrees of freedom		158	120

Table 3.2: The table shows the degrees of freedom from the gauge-, Higgs-, Higgs-flavour-, and flavour-sector of MSSM-M. Some apparent degrees of freedom is removed by applying the flavour symmetries $U(3)^5 \times U(4) \times U_{\rm PQ}(1) \times U_{\rm R}(1)$, and taking conservation of baryon number into account.

complex gaugino masses M_1, M_2 and M_3. The Higgs sector contributes with 2 real masses $M^2_{H_u}$ and $M^2_{H_d}$, along with 2 complex parameters b and μ. A special characteristic of MSSM-M is that since there are no lepton number the superfields H_d and L_i have the same quantum numbers, and may therefore mix. Thus there exists a Higgs-flavour sector consisting of the 9 complex parameters μ_i, b_i and ε_i. The flavour sector contributes with 6 arbitrary complex 3×3 matrices: Y_u, Y_d, Y_e, a_u, a_d and a_e, and also of 5 Hermitian 3×3 matrices M_L^2, M_Q^2, M_u^2, M_d^2 and M_e^2. And finally there are 72 complex R-parity violating couplings: λ_{ijk}, λ^s_{ijk}, λ'_{ijk} and λ'^s_{ijk}.

That is, the model may have as much as 176 real and 155 imaginary parameters. The flavour symmetry for MSSM-M is $U(3)^4 \times U(1) \times U_{\rm PQ}(1) \times U_R(1)$. The $U(1)$ symmetry reflects the mixing among the $Y = -1$ doublets. A $U(4)$ matrix can be parameterised by 6 real and 10 imaginary parameters. Also note that only baryon number is conserved. Thus one finds that MSSM-M has 158 real parameters and 120 imaginary ones, a total of 278 free parameters, see Table 3.2.

Note that by including the trilinear coupling λ''_{ijk} and λ''^s_{ijk} another 18 complex parameters must be added to the model.

The phenomenology for Majorana neutrinos will be studied, both by analytic and numeric methods, in Chapter 5.

3.1.3 Dirac-Majorana neutrinos - MSSM-DM

MSSM-DM is defined as the minimal supersymmetric extension to the Standard Model, including left- and right-handed neutrino superfields, and violating the lepton number. The superpotential for MSSM-DM is defined as,

$$\begin{aligned} W_{\text{Dirac-Majorana}} &= Y_u Q\hat{H}_u u - Y_d Q\hat{H}_d d - Y_e L\hat{H}_d e + Y_\nu L\hat{H}_u n + Y_n \hat{H}_u\hat{H}_d n \\ &+ \mu\hat{H}_d\hat{H}_u + \mu_i L_i\hat{H}_u \\ &+ \frac{1}{2}\lambda_{ijk}L_iL_je_k + \lambda'_{ijk}L_iQ_jd_k \\ &+ \frac{1}{6}A_{ijk}n_in_jn_k + \frac{1}{2}B_{ij}\,n_in_j + C_in_i. \end{aligned} \tag{3.6}$$

Note the appearance of the self couplings, A_{ijk}, B_{ij} and C_i associated with the gauge singlet superfields n_i. These superfields, or the R-parity violating parameters, where not allowed in MSSM-D due to lepton number conservation.

The soft breaking terms are

$$\begin{aligned} -\mathcal{L}_{\text{Dirac-Majorana}} &= M_Q^2\tilde{Q}^\dagger\tilde{Q} + M_L^2\tilde{L}^\dagger\tilde{L} + M_{H_u}^2H_u^\dagger H_u + M_{H_d}^2H_d^\dagger H_d \\ &+ M_u^2\tilde{u}\tilde{u}^* + M_d^2\tilde{d}\tilde{d}^* + M_e^2\tilde{e}\tilde{e}^* + M_n^2\tilde{n}\tilde{n}^* + a_nH_uH_d\tilde{n} \\ &+ \Big[\varepsilon_iH_d^*\tilde{L}_i - bH_dH_u - b_iL_iH_u + a_nH_uH_d\tilde{n} \\ &+ a_eH_d\tilde{L}\tilde{e} + a_dH_d\tilde{Q}\tilde{d} + a_uH_u\tilde{Q}\tilde{u} + a_\nu H_u\tilde{L}\tilde{n} \\ &+ \frac{1}{2}\lambda^{\text{s}}_{ijk}\tilde{L}_i\tilde{L}_j\tilde{e}_k + \lambda'^{\text{s}}_{ijk}\tilde{L}_i\tilde{Q}_j\tilde{d}_k \\ &+ \frac{1}{2}\left(M_1\tilde{B}\tilde{B} + M_2\tilde{W}^a\tilde{W}^a + M_3\tilde{g}\tilde{g}\right) \\ &+ \frac{1}{6}A^{\text{s}}_{ijk}\tilde{n}_i\tilde{n}_j\tilde{n}_k + \frac{1}{2}B^{\text{s}}_{ij} + \text{h.c.}\Big]. \end{aligned} \tag{3.7}$$

Note that a linear term is not allowed as a soft-breaking term [37]. That is, a term like $C_i^{\text{s}}\,\tilde{n}_i$ does not appear in Eq. (3.7). Also note that Eqs. (3.6) and (3.7) includes MSSM, MSSM-D and MSSM-M.

The parameter space for MSSM-DM is found by the same counting procedure as for the previous models. First, the gauge sector contributes with 4 real parameters, g_1, g_2, g_3 and the QCD vacuum angle θ_{QCD}. The gauge sector also consists of the 3 complex gaugino masses M_1, M_2 and M_3. The Higgs sector contributes with 2 real masses $M_{H_u}^2$ and $M_{H_d}^2$, and 2 complex parameters μ and b. As for the Majorana neutrinos, there is mixing among the $Y = -1$ fields. Thus there is a Higgs-flavour sector, which contributes with 9 complex parameters, μ_i, b_i and ε_i.

	Masses and couplings	Real parameters	Imaginary parameters
Gauge sector	$g_1,\ g_2,\ g_3,\ \theta_{\rm QCD}$	4	
	$M_1,\ M_2,\ M_3$	3	3
Higgs sector	$M_{H_u},\ M_{H_d}$	2	
	$b,\ \mu$	2	2
Higgs-flavour sector	$b_i,\ \mu_i,\ \varepsilon_i$	9	9
Flavour sector	$Y_u,\ Y_d,\ Y_e,\ Y_\nu,\ Y_n,$		
	$a_u,\ a_d,\ a_e,\ a_\nu,\ a_n$	90	90
	$M_Q^2,\ M_L^2,\ M_u^2,\ M_d^2,\ M_e^2,\ M_\nu^2$	36	18
	$\lambda_{ijk},\ \lambda^{\rm s}_{ijk},\ \lambda'_{ijk},\ \lambda'^{\rm s}_{ijk}$	72	72
	$A_{ijk},\ A^{\rm s}_{ijk},\ B_{ij},\ B^{\rm s}_{ij},\ C_i$	33	33
Removable parameters	$U(3)^6 \times U(4) \times U_{\rm PQ}(1) \times U_{\rm R}(1)$	28	47
Degrees of freedom		223	180

Table 3.3: The table shows the degrees of freedom from the gauge-, Higgs-, Higgs-flavour-, and flavour-sector of MSSM-DM. Some apparent degrees of freedom is removed by applying the flavour symmetries $U(3)^6 \times U(4) \times U_{\rm PQ}(1) \times U_{\rm R}(1)$, and taking conservation of baryon number into account.

The flavour sector is quite large in MSSM-DM, and consists of 11 arbitrary complex 3×3 matrices, i.e., Y_u, Y_d, Y_e, Y_ν, Y_n, a_u, a_d, a_e, a_ν and a_n. Further, there are 6 Hermitian matrices, M_Q^2, M_L^2, M_u^2, M_d^2, M_e^2 and M_n^2. There are 4 R-parity violating complex trilinear couplings, i.e., λ_{ijk}, λ^s_{ijk}, λ'_{ijk} and λ'^s_{ijk}. And finally, there are 5 complex parameters associated with the gauge singlet sector, i.e., A_{ijk}, B_{ij}, C_i, A^s_{ijk} and B^s_{ij}.

That is, the model may have as much as 251 real and 227 imaginary parameters. However, the flavour symmetry, given by $U(3)^6 \times U(4) \times U_{\rm PQ}(1) \times U_R(1)$, will remove the unphysical parameters, see Table 3.3. This table shows that there are 223 real and 180 imaginary degrees of freedom in MSSM-DM, a total of 403 degrees of freedom. Most of these parameters implies physics beyond the Standard Model.

Note that by including the trilinear couplings λ''_{ijk} and λ''^s_{ijk} there will be 18 more complex degrees of freedom.

The phenomenology for Dirac-Majorana neutrinos in MSSM will be studied, both by analytic and numeric methods, in Chapter 6.

3.2 Breaking of supersymmetry

One of the historical motivations for introducing supersymmetry is that quadratic divergences are absent in models with exact supersymmetry [28]. This result is valid to all orders of perturbation theory, due to exact cancellations between graphs involving fermion and boson loops. On the other hand, no supersymmetric particle has been observed, and supersymmetry must therefore be broken, at best. In lack of any detailed understanding of the supersymmetric breaking mechanism one explicitly includes the soft-breaking terms [37] into the Lagrangian. These are the terms which breaks supersymmetry, but still keeps the model free from quadratic divergences.

As seen in Sec. 3.1, the parameter space associated with each model is huge. Tables 3.1 - 3.3 shows that most of the parameter spaces are associated with the soft-breaking terms. Thus, if these terms could be explained or calculated the number of unknown parameters would be reduced considerably.

A more disturbing problem with the models specified so far, is that, all kinds of phenomenological disasters can happen for most of the parameter space. That is, by choosing an arbitrary point in parameter space one can not ensure that even the electroweak symmetry breaking comes out properly. Further, such an arbitrary specification of the model would most probably lead to large flavour changing currents, leading to unacceptable fast proton decay. The electric dipole moments for the electron and neutrons are also most probably not acceptable [31]. One therefore finds that almost the complete parameter space is ruled out, and the phenomenologically acceptable points are rare.

In order to reduce the parameter space and to find a model, not in conflict with observations, further assumptions must be made. Most often one out of two approaches is used in order to explore the parameter space. The first approach makes use of the full parameter space at the electroweak scale, to search for the exclusive phenomenologically acceptable points. This is referred to as the low energy approach [31]. The second method, makes use of the dependency all parameters have on energy scale. This dependency is governed by the renormalization group equations, which connect the different energy scales together. Thus, by solving the renormalization group equations, the value for each parameter can be determined at an arbitrary scale, e.g., at the unification scale. This option will be explored in later chapters.

The renormalization group equations forms a coupled set of non-linear ordinary differential equations, and since the parameters of each model are specified either at the electroweak scale or at the unification scale, this is a boundary value problem.

By using the renormalization group equations supersymmetry breaking can occur at a much higher energy scale than the electroweak scale. In the literature there are roughly three different scenarios for the breaking of supersymmetry, see e.g., Ref. [31]. These are gravity mediated breaking (supergravity), gauge mediated su-

persymmetry breaking, and other possible scenarios. This last option may be a combination of the other two breaking mechanism, see Ref. [31] for further details and references regarding this last option.

Even though the supergravity breaking scenario is the one used throughout this thesis some of its alternatives will now be presented. This presentation does not intend to give a complete review of the possible options for supersymmetry breaking. But it aims to show that the popular supergravity breaking scenario is not the only possibility to gain some understanding of the parameter space.

3.2.1 Supergravity

In the supergravity breaking scenario it is assumed that supersymmetry is spontaneously broken in a hidden sector. There is also a visible sector consisting of the fields from e.g., MSSM-D. The breaking of supersymmetry in the hidden sector is transmitted to the visible sector by gravitational interactions. These interactions becomes important at the Planck scale where gravity can no longer be ignored. The interesting point, for this treatment of supersymmetry breaking, is that the resulting low energy effective theory includes all possible soft-breaking terms. Thus supergravity gives some rationale for these terms.

In the minimal supergravity breaking scenario the soft-breaking parameters take a special simple form at the unification scale, i.e.,

$$M_0: \quad \text{a common scalar mass,} \tag{3.8}$$

$$M_{1/2}: \quad \text{a common gaugino mass,} \tag{3.9}$$

$$A_0 Y_x: \quad \text{proportionality to the Yukawa couplings,} \tag{3.10}$$

where Y_x is shorthand for the Standard Model Yukawa matrices.

This makes it possible to define MSSM with only 5 free parameters, in addition to the ones given by the Standard Model, i.e., Eqs. (2.7) and (2.8). These parameters are

$$M_0,\ M_{1/2},\ \tan\beta = \frac{v_u}{v_d} \quad \text{and} \quad \text{sign}(\mu), \tag{3.11}$$

where v_u and v_d are the vacuum expectation values for the scalar fields H_u and H_d, respectively.

Following Ref. [31] this particular realisation of MSSM is referred to as MSSM-24. Here 19 parameters are identical to the ones from the Standard Model. MSSM-24 is the supersymmetric extension of the Standard Model which has been studied most thoroughly in the literature. This model conserves both lepton number and lepton flavour numbers, and the neutrinos are massless. Thus lepton flavour violating decay channels such as $l \to l'\gamma$ are forbidden in MSSM-24, as they are in the Standard Model. Since MSSM-24 can not explain lepton flavour changing processes, like neutrino oscillations, it must be extended with massive neutrinos.

This supersymmetric breaking scenario is the one which will be used throughout this thesis. Some deviations from minimal supergravity, defined by Eqs. (3.8) - (3.10) will also be studied.

3.2.2 Gauge mediated breaking of supersymmetry

Gauge mediated breaking of supersymmetry is an interesting alternative to supergravity breaking. Also in this scenario there exists a hidden sector where supersymmetry is spontaneously broken. The most important difference between this breaking scenario and supergravity breaking, is that the fields connecting the hidden and visible sector, i.e., the messenger sector, now have $SU(3) \times SU(2) \times U(1)$ gauge quantum numbers.

The two most important phenomenological differences, compared to supergravity breaking, is that the lightest neutralino is not the lightest supersymmetric particle. In this class of models the gravitino is the lightest supersymmetric particle. Thus the lightest neutralino is unstable and decays. Another interesting point is that the breaking scale does not have to be at, or even near, the Planck scale. It can be as low as 100 TeV [31].

This supersymmetry breaking scenario has a rich phenomenology, but it will not be explored further in this thesis. Further details and references regarding this scenario can be found in Ref. [31].

3.2.3 Other scenarios

A third option to break supersymmetry is to combine the two approaches described above. In this manner the scale at which the breaking occurs may vary from $10^2 - 10^{16}$ GeV. In these models the lightest supersymmetric particle can be either the gravitino or the neutralino.

Of course, one can also study other collections of points in the parameter space by methods not associated with any of these methods [31].

URN:NBN:no-7281

Chapter 4

Dirac neutrinos and $l \to l'\gamma$

In this chapter the phenomenology, relevant for the study of $l \to l'\gamma$ in MSSM-D, will be presented. As explained in last chapter, the parameter space of MSSM-D is very large, and some further assumptions must therefore be made in order to analyse this model properly. This chapter therefore starts with a presentation of the assumptions and simplifications which are to be used throughout this chapter. By using these assumptions the neutral scalar potential is minimised by use of the so-called tadpole method. This is the method which will be used in the numerical analysis of the neutral scalar potential. Further details regarding the tadpole method are presented in Appendix C.2. The only difference between MSSM-D and MSSM is the existence of the three gauge singlet superfields, n_i, in MSSM-D. Therefore, the mass matrices of MSSM-D are equal to the corresponding ones in MSSM, with the neutrino mass matrix and the squared sneutrino mass matrix as the only exceptions. For easy referencing, these mass matrices are presented in Sec. 4.3, and the other mass matrices are shown in Appendix D.2. An important feature with MSSM-D, and most quantum field theories, is that their parameters change by scale, e.g., the parameters are running. In Sec. 4.4 the running of the most important parameters of MSSM-D are analysed both by analytic and numeric methods. Finally, the numerical analysis of the decay channels $l \to l'\gamma$ is presented. The relevant Feynman rules and renormalization group equations are presented in Appendix E.1 and F.1, respectively.

4.1 Reducing the parameter space of MSSM-D

The Lagrangian for MSSM-D was defined in Eqs. (3.2) and (3.3), i.e.,

$$W_{\text{MSSM-D}} = Y_u Q \hat{H}_u u - Y_d Q \hat{H}_d d - Y_e L \hat{H}_d e + Y_\nu L \hat{H}_u n + \mu \hat{H}_u \hat{H}_d,$$

$$\begin{aligned} -\mathcal{L}_{\text{MSSM-D}} = {} & M_Q^2 \tilde{Q}^\dagger \tilde{Q} + M_L^2 \tilde{L}^\dagger \tilde{L} + M_{H_u}^2 H_u^\dagger H_u + M_{H_d}^2 H_d^\dagger H_d \\ & + M_u^2 \tilde{u}\tilde{u}^* + M_d^2 \tilde{d}\tilde{d}^* + M_e^2 \tilde{e}\tilde{e}^* + M_n^2 \tilde{n}\tilde{n}^* \\ & + \Big[a_u \tilde{Q} H_u \tilde{u} + a_d \tilde{Q} H_d \tilde{d} + a_e \tilde{L} H_d \tilde{e} + a_\nu \tilde{L} H_u \tilde{n} + b H_u H_d \\ & + \frac{1}{2} M_1 \tilde{B}^0 \tilde{B}^0 + \frac{1}{2} M_2 \tilde{W}^a \tilde{W}^a + \frac{1}{2} M_3 \tilde{G}^a \tilde{G}^a + \text{h.c.} \Big]. \end{aligned}$$

Note that both $SU(2)$ and $SU(3)$ indices are suppressed in these expressions.

The analysis of Sec. 3.1.1 showed that, in general, 163 parameters must be defined in order to completely specify MSSM-D. This is too much in order to give a phenomenological analysis of the model. Also, as explained in Sec. 3.1.1, most of the parameter space leads to realisations of MSSM-D in conflict with the phenomenological constraints. Therefore, several simplifications will be made. The first of these simplifications is to assume that all parameters are real, and also to neglect the QCD vacuum angle, θ_{QCD}. Next, the supergravity inspired boundary conditions, presented in Eqs. (3.8) - (3.10), will be used. This defines the soft-breaking terms at the unification scale (GUT scale). Table 3.1 shows that by neglecting the imaginary parameters the parameter space is now reduced to 100 parameters, with 17 parameters determined from the Standard Model[1]. All of the remaining 83 parameters still left in the model represent physics beyond the Standard Model.

By assuming minimal supergravity breaking the number of free parameters are reduced considerably, and one only needs the 5 parameters from MSSM-24 to determine all soft-breaking couplings and masses, i.e.,

$$M_Q^2 = M_L^2 = M_u^2 = M_d^2 = M_e^2 = M_n^2 = M_0^2\, 1_{3\times 3}, \tag{4.1}$$

$$M_{H_u}^2 = M_{H_d}^2 = M_0^2, \tag{4.2}$$

$$a_u = A_0 Y_u,\ a_d = A_0 Y_d,\ a_e = A_0 Y_e,\ a_\nu = A_0 Y_\nu \tag{4.3}$$

$$M_1 = M_2 = M_3 = M_{1/2}, \tag{4.4}$$

These boundary conditions will be the starting point for the analysis of MSSM-D. However, also some smaller violations of Eqs. (4.1) and (4.3) will be studied in Sec. 4.5.2.

By using the renormalization group equations, and the minimisation conditions, the low energy values of all parameters can be obtained. As explained in Sec. 2.7, the

[1] There are 12 parameters determining the masses and mixing angles for the quarks and charged leptons. There are also 3 gauge couplings, and two parameters representing the Higgs sector.

gauge couplings and the masses of gauge bosons and masses of the Standard Model fermions are all determined at the M_Z-scale by Eqs. (2.7) - (2.11). The 3 neutrino masses and the 3 mixing angles associated with the lepton sector will be considered as free parameters, only constrained by observational limits.

This discussion shows that a minimal version of MSSM-D can be defined in terms of 11 free parameters, 5 of these parameters are identical to the ones in MSSM-24, and 6 parameters are associated with the neutrino Yukawa matrix, Y_ν. In this analysis of MSSM-D, the most interesting parameters are the ones making MSSM-D an extension of MSSM. Thus, most attention will be paid in the analysis of Y_ν, a_ν and M_n^2.

4.2 The Higgs potential

In order to achieve a correct electroweak symmetry breaking, and to find the mass matrices of MSSM-D, the scalar potential has to be analysed and the neutral scalar potential must be minimised. In this chapter the minimum of the one-loop neutral scalar potential is found by use of the tadpole method [38].

The scalar potential of MSSM-D consists of three terms, i.e.,

$$V_{\text{scalar}} = V_F + V_D + V_{\text{soft}}. \tag{4.5}$$

Here V_F denotes the F-terms obtained from the superpotential by

$$V_F = \sum_\phi \left| \frac{dW}{d\phi} \right|^2 , \tag{4.6}$$

and ϕ is shorthand for all scalar fields of MSSM-D. The D-terms, V_D, are found as,

$$V_D = \frac{1}{2} \left[D^a D^a + (D')^2 \right] , \tag{4.7}$$

where D^a and D' are the auxiliary fields associated with the scalar potential of $SU(2)$ and $U(1)$. The soft-breaking terms, V_{soft}, were presented in Eq. (3.3).

Putting these terms together one finds the following tree-level neutral scalar potential,

$$\begin{aligned} V_0 = & \left(m_{H_u}^2 + \mu^2 \right) |H_u|^2 + \left(m_{H_d}^2 + \mu^2 \right) |H_d|^2 + b \left(H_u H_d + \text{h.c.} \right) \\ & + \frac{1}{8} \left(g^2 + g'^2 \right) \left[|H_u|^2 - |H_d|^2 \right]^2 + \frac{1}{2} g^2 |H_u H_d|^2 \\ & + M_{\tilde{n}}^2 \tilde{n} \tilde{n}^* + \left[(Y_\nu + a_\nu) \tilde{L} \, H_u \, \tilde{n} + \text{h.c.} \right] . \end{aligned} \tag{4.8}$$

The only difference between MSSM and MSSM-D is the existence of the three right-handed neutrino gauge singlets, n_i, in MSSM-D. These neutral scalar fields leads to

the contribution shown in the last line of Eq. (4.8). However, due to conservation of the lepton number none of these three scalar fields develops any vacuum expectation value. And the tree-level minimisation conditions are equal in MSSM-D and MSSM. In later chapters it will be shown that vacuum expectation values associated with $\tilde{n}_i$ becomes important MSSM-DM.

4.2.1 The tadpole method

The minimum of the one-loop neutral scalar potential is found by use of the so-called tadpole method [38]. Further details regarding this method are presented in Ref. [38] and also in Appendix C.2. It is, however, instructive to use this method to minimise the tree-level scalar potential of Eq. (4.8).

The two Higgs doublets H_u and H_d are the only scalar fields which contributes to the neutral scalar potential of MSSM-D. These two doublets takes the explicit form,

$$H_u = \begin{pmatrix} H_u^+ \\ H_u^0 \end{pmatrix} \equiv \begin{pmatrix} H_u^+ \\ \frac{1}{\sqrt{2}}\left(v_u + \psi_u + i\phi_u\right) \end{pmatrix}, \tag{4.9}$$

$$H_d = \begin{pmatrix} H_d^0 \\ H_d^- \end{pmatrix} \equiv \begin{pmatrix} \frac{1}{\sqrt{2}}\left(v_d + \psi_d + i\phi_d\right) \\ H_d^- \end{pmatrix}. \tag{4.10}$$

By combining these expressions for H_u and H_d with the scalar potential of Eq. (4.8), and putting all other fields to zero, the following term is identified,

$$V_0 = V_{\text{tadpole}} + \cdots = t_u\psi_u + t_d\psi_d + \cdots . \tag{4.11}$$

Here t_u and t_d are the tree-level tadpoles, i.e.,

$$t_u = \left(m_{H_u}^2 + \mu^2\right) v_u + bv_u - \frac{1}{8}\left(g^2 + g'^2\right) v_u \left(v_d^2 - v_u^2\right), \tag{4.12}$$

$$t_d = \left(m_{H_d}^2 + \mu^2\right) v_d + bv_d + \frac{1}{8}\left(g^2 + g'^2\right) v_d \left(v_d^2 - v_u^2\right). \tag{4.13}$$

The minimum of the Higgs potential is now found as the critical points of V_{tadpole}, i.e.,

$$\frac{\partial V_0}{\partial \psi_i} = \frac{\partial V_{\text{tadpole}}}{\partial \psi_i} = 0. \tag{4.14}$$

This shows that both tadpoles have to vanish at the minimum, i.e., $t_u = t_d = 0$ at the minimum.

It is not a necessity, but in order to simplify the minimisation conditions the following rotation is performed,

$$\begin{pmatrix} T_u \\ T_d \end{pmatrix} = \begin{pmatrix} \cos\beta & -\sin\beta \\ \sin\beta & \cos\beta \end{pmatrix} \begin{pmatrix} t_u \\ t_d \end{pmatrix}, \tag{4.15}$$

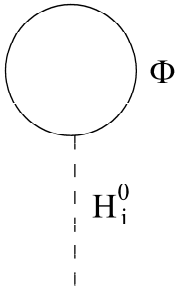

Figure 4.1: This figure shows the one-loop tadpole. Here $H_i^0, i = 1, 2$ are the two CP-even neutral Higgs-fields and Φ is shorthand for all fields of MSSM-D.

where, as usual, $\tan\beta = v_u/v_d$. This rotation gives,

$$T_u = v\left[\frac{1}{2}\left(m_{H_u}^2 + m_{H_d}^2 + 2\mu^2\right)\sin 2\beta + b\right], \tag{4.16}$$

$$T_d = v\left[\left(m_{H_d}^2 + \mu^2\right)\cos^2\beta - \left(m_{H_u}^2 + \mu^2\right)\sin^2\beta + \frac{1}{2}M_Z^2\cos 2\beta\right], \tag{4.17}$$

and $v = \sqrt{v_u^2 + v_d^2}$.

From these expressions one can now obtain the well known tree-level minimisation conditions from MSSM. First, by setting $T_u = 0$ and dividing by v the following minimisation condition is found,

$$-b = \frac{1}{2}\left(m_{H_u}^2 + m_{H_d}^2 + 2\mu^2\right)\sin 2\beta. \tag{4.18}$$

Next, by setting $T_d = 0$ and dividing by $v\cos 2\beta$ the other minimisation condition is found,

$$\mu^2 = \frac{m_{H_d}^2 - m_{H_u}^2\tan^2\beta}{\tan^2\beta - 1} - \frac{1}{2}M_Z^2. \tag{4.19}$$

These are the two minimisation conditions known from MSSM. One-loop corrections to these minimisation conditions can now be obtained by including the one-loop tadpoles, as shown in Fig. 4.1. The contributions from these tadpoles are calculated and added to the tree-level contributions, i.e., added to Eqs. (4.16) and (4.17). From these expressions the one-loop corrected values for the parameters b and $|\mu|^2$ are found by solving two coupled linear equations, analogous to Eqs. (4.16) and (4.17). Appendix C.2 shows the general expressions for the one-loop contributions to T_u and T_d. These expressions are more general than those presented in Ref. [38] since non-diagonal squared mass matrices are taken into account. Also some minor errors of Ref. [38] have been corrected.

The rationale for the tadpole method is the observation that the nth-derivative of the scalar potential is related to the tadpole diagrams with n external lines [38]. Thus, by generalising the tadpole method the solutions of

$$\frac{d^n V_0}{d\phi^n} = 0, \tag{4.20}$$

can be found.

It should be stressed that the tadpole method only finds the solutions to Eq. (4.14). It does not address questions regarding the stability of these solutions, or even if the solutions found defines a global minimum for V_0. A deeper insight into the scalar potential should be gained by using other, perhaps numerical, methods.

4.3 Mass matrices in MSSM-D

The only difference between MSSM and MSSM-D is the existence of the 3×3 matrices Y_ν, a_ν and M_n^2 in MSSM-D. These matrices enters the Lagrangian due to the existence of the three gauge singlet superfields n_i. Since MSSM-D conserves the lepton number the neutral fields, n_i, only affect the neutrino and sneutrino masses. Thus, apart from these two mass matrices all of the other mass matrices are equal to the corresponding ones known from MSSM. For completeness and easy reference all mass matrices of MSSM-D are presented in Appendix D.2. Only the neutrino mass matrix and the squared sneutrino mass matrix will be discussed in this section.

One of the nice features of Dirac neutrinos is that they acquire mass by the same mechanism as the other fermions of the Standard Model. That is, the charged and neutral lepton mass matrices are defined in terms of the two Yukawa matrices Y_e and Y_ν, respectively, i.e.,

$$M_e = \frac{v \cos\beta}{\sqrt{2}} Y_e, \tag{4.21}$$

$$M_\nu = \frac{v \sin\beta}{\sqrt{2}} Y_\nu. \tag{4.22}$$

These 3×3 mass matrices are generally not symmetric, and two unitary matrices are therefore needed in order to diagonalise each of them, i.e.,

$$U_L^e \, M_e \, U_R^{e\dagger} = D_e, \tag{4.23}$$

$$U_L^\nu \, M_\nu \, U_R^{\nu\dagger} = D_\nu. \tag{4.24}$$

This also defines the two diagonal matrices $D_e = \mathrm{diag}(m_e, m_\mu, m_\tau)$ and $D_\nu = \mathrm{diag}(m_{\nu_1}, m_{\nu_2}, m_{\nu_3})$, where m_e, m_μ and m_τ are the observed masses for the three charged leptons, as shown in Eqs. (1.1) - (1.3). And, m_{ν_1}, m_{ν_2} and m_{ν_3} are the three

neutrino mass eigenstates. In analogy with the quark sector [26], the lepton flavour mixing matrix is defined by

$$V_{\rm MNS} = U_L^e\, U_L^{\nu\dagger}. \tag{4.25}$$

The standard parametrisation, advocated for the quark mixing matrix [6], will also be used to represent $V_{\rm MNS}$, i.e.,

$$V_{\rm MNS} = \begin{pmatrix} c_{12}c_{13} & s_{12}c_{13} & s_{13}\, e^{-i\delta_{13}} \\ -s_{12}c_{23} - c_{12}s_{23}s_{13}\, e^{i\delta_{13}} & c_{12}c_{23} - s_{12}s_{23}s_{13}\, e^{i\delta_{13}} & s_{23}c_{13} \\ s_{12}s_{23} - c_{12}c_{23}s_{13}\, e^{i\delta_{13}} & -c_{12}s_{23} - s_{12}c_{23}s_{13}\, e^{i\delta_{13}} & c_{23}c_{13} \end{pmatrix}, \tag{4.26}$$

where $c_{ij} = \cos\theta_{ij}$ and $s_{ij} = \sin\theta_{ij}$, and δ_{13} is a CP-violating phase, and $i, j = e, \mu\tau$.

The analogy with the quark sector is followed in that it is possible to chose a flavour basis where one of the matrices M_e or M_ν is diagonal. In this thesis a basis is chosen such that the charged lepton mass matrix, i.e., M_e, is diagonal. Thus, in general, there are 7 new parameters associated with the lepton sector, that is, 3 neutrino masses, and 3 mixing angles and 1 CP-violating phase. The CP-violation phase, δ_{13}, will be neglected in the forthcoming analysis, in accordance with the assumption of using only real parameters.

As seen from Eq. (4.22), the elements of Y_ν are determined from the neutrino masses and mixing angles. These parameters are not known, since observations of neutrino oscillations only reveal information on the squared mass differences, i.e., $\Delta m_{ij}^2 = m_i^2 - m_j^2$. On the other hand, these observations shows that the mass eigenstates are almost degenerate, with Δm^2 ranging from 10^{-3} to 10^{-5} [6]. Also, maximal mixing seems to be preferred [39]. The bounds from direct observations of the neutrino masses are less stringent, and the current limits [6] are $m_{\nu_e} < 3\,\text{eV}$, $m_{\nu_\mu} < 0.19\,\text{MeV}$ and $m_{\nu_\tau} < 18.2\,\text{MeV}$. As an example, assume that the mixing angles are neglected and that the neutrinos are degenerate in mass, i.e., $m_{\nu_1} = m_{\nu_2} = m_{\nu_3} = m_\nu = 1$ eV, then one finds the following upper bounds on Y_ν, i.e.,

$$(Y_\nu)_{ii} = \frac{\sqrt{2}}{v \sin\beta}\, m_\nu < 10^{-11}, \qquad i = 1, 2, 3. \tag{4.27}$$

This indicates that the neutrino masses does not give any important contribution to the decay rates under study. However, due to the boundary condition of Eq. (4.3), the values for the trilinear soft-breaking couplings a_ν are determined at the GUT scale by Y_ν. Thus, even if the eigenvalues of Y_ν are small, the large mixing angles indicated for Y_ν may be of importance.

The most important feature with the non-vanishing neutrino masses in MSSM-D is not the masses themselves, but the fact that these mass terms demands for an extension of the squared sneutrino mass matrix. The sneutrinos are neutral, but complex scalars, and the gauge basis to be used is,

$$\Phi_{\tilde\nu}^T = (\tilde\nu_L^e, \tilde\nu_L^\mu, \tilde\nu_L^\tau, \tilde\nu_R^{e*}, \tilde\nu_R^{\mu*}, \tilde\nu_R^{\tau*}), \tag{4.28}$$

where * means complex conjugation. In this basis the squared sneutrino mass matrix takes the form,

$$M^2_{\tilde{\nu}} = \begin{pmatrix} M_L^2 + M_\nu^2 + \frac{1}{2}M_Z^2 \cos 2\beta & v\,(a_\nu \sin\beta - \mu Y_\nu \cos\beta) \\ v\left(a_\nu^\dagger \sin\beta - \mu^* Y_\nu^\dagger \cos\beta\right) & M_n^2 + M_\nu^2 \end{pmatrix}. \tag{4.29}$$

This is a 6×6 symmetric matrix, and is therefore diagonalised by one unitary matrix, i.e.,

$$Z_{\tilde{\nu}}^\dagger\, M^2_{\tilde{\nu}}\, Z_{\tilde{\nu}} = \mathrm{diag}(m^2_{\tilde{\nu}_i}), \quad i = 1, 2, \ldots, 6. \tag{4.30}$$

The mass eigenstates, $\tilde{\nu}_i$ and gauge eigenstates are related as follows,

$$\nu_L^I = Z_{\tilde{\nu}}^{Ii*}\, \tilde{\nu}_i^*, \quad \text{and} \quad \nu_R^I = Z_{\tilde{\nu}}^{(I+3)i}\, \tilde{\nu}_i, \tag{4.31}$$

where $I = e, \mu, \tau$, and $i = 1, 2, 3$.

Note that due to the supergravity boundary conditions both a_ν and Y_ν have off-diagonal elements at the electroweak scale. Thus there will always be lepton flavour mixing associated with the sneutrinos.

4.4 Running of parameters

As in most quantum field theories, all couplings and masses of MSSM-D depends upon which energy scale the experiments takes place. That is, the numerical value for these parameters changes if the energy scale is changed. One says that these parameters run by scale, or simply that they are running. The details of this running is governed by a system of ordinary differential equations, the renormalization group equations. The two-loop renormalization group equations for a general minimal supersymmetric model were presented in Ref. [34]. And since MSSM-D belongs to this class of supersymmetric models, the general results of [34] are therefore used extensively. In the analysis of MSSM-D two-loop renormalization group equations are used for the gauge couplings and the gaugino masses, while one-loop renormalization group equations are used for all other parameters. The complete set of renormalization group equations are presented in Appendix F.2.

The renormalization group equations for the parameters of MSSM have been studied by many authors[2], therefore only a few of the more important results will be reviewed in this section. The running of the parameters Y_ν, a_ν and M_n^2 are the most interesting ones, since these are the parameters associated with the three gauge singlet superfields n_i. In this section the renormalization group equations for these parameters are analysed qualitatively and by numerical methods.

[2] A search, in March 2003, at the SLAC-Spires database [40] on the topics supersymmetry and renormalization group ended in more than 1700 entries.

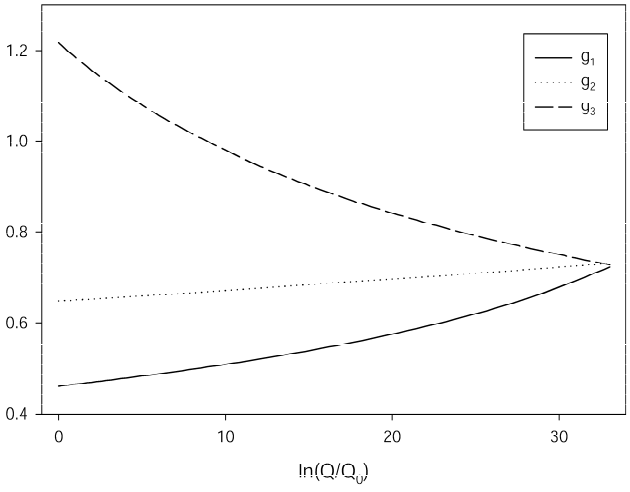

Figure 4.2: The figure shows the running of the gauge couplings in MSSM-D. Note that the three gauge couplings does not completely unify at high energies.

4.4.1 Some results from MSSM

The most celebrated result, from studies of the renormalization group equations of MSSM, is that the three gauge couplings, g_i, associated with the gauge group $SU(3) \times SU(2) \times U(1)$, seems to unify at high energies. The energy scale where this unification (almost) takes place is referred to as the unification scale, or simply as the GUT-scale. The two-loop renormalization group equations for the three gauge couplings are shown in Eq. (F.1). An example of the running of the gauge couplings is shown in Fig. 4.2. This figure shows that the three gauge couplings does not unify completely. This is the case both for the Standard Model and for MSSM. On the other hand, a very interesting result, regarding this unification, was presented in Ref. [41], where it was shown that by introducing R-parity violating couplings, the unification was improved. These R-parity violating couplings are absent in MSSM-D, but becomes important in MSSM-M and MSSM-DM.

The top-quark Yukawa coupling, y_t, has also been studied extensively in the literature. One of the most interesting results from these analysis, is that y_t has a quasi-fix point at low energies [42, 43]. That is, its value at the electroweak scale is only affected to a small part on its value at the unification scale. This is exemplified in Fig. 4.3, which shows the running of y_t for some choices of $\tan\beta$.

The value for y_t is determined from the top-quark mass by the relation,

$$Y_u = \frac{\sqrt{2}}{v \sin\beta} M_u, \tag{4.32}$$

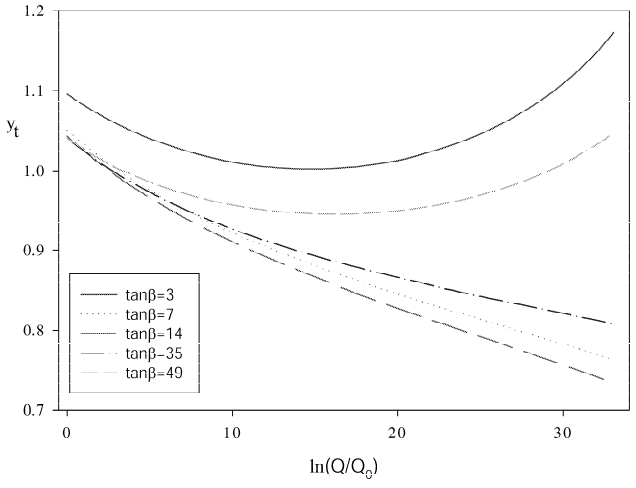

Figure 4.3: The figure shows the running of the top quark Yukawa coupling, y_t, for some choices of $\tan\beta$.

where M_u is a 3×3 matrix with the top-quark mass m_{top} as the element $(M_u)_{3,3}$ and y_t as the element $(Y_u)_{3,3}$. Due to the large top-quark mass y_t also takes large values, especially for small values of $\tan\beta$. These large values are problematic for two reasons. First, the running of y_l may hit a Landau pole before it reaches the GUT-scale. Second, y_t may grow out of the perturbative regime, which makes it impossible to use perturbation theory. To prevent these scenarios y_t will be assumed to be in the perturbative regime. This leads to the following rough estimates [35] for $\tan\beta$,

$$1.2 < \tan\beta < 65. \tag{4.33}$$

Another interesting result obtained from analysis of the renormalization group equations, is the possibility for a unification between the bottom-quark and tau Yukawa couplings, i.e., the possibility for y_b and y_τ to be equal at the GUT-scale, see e.g., Ref. [44, 45]. This possibility will not be pursued any further in this work.

4.4.2 Qualitative analysis of the running

The complete set of renormalization group equations, as presented in Appendix F.2, must be solved by numerical methods. But a qualitative analysis can be obtained.

The neutrino Yukawa matrix Y_ν have small off-diagonal elements at the electroweak scale, and also at the GUT scale. Due to the boundary condition

$$a_\nu = A_0\, Y_\nu, \tag{4.34}$$

also the matrix a_ν have off-diagonal elements at the GUT-scale, and also at the electroweak scale.

The renormalization group equation for the charged lepton Yukawa couplings Y_e, is shown in Eq. (F.9). This equation shows that Y_e will develop off-diagonal elements due to the term

$$Y_e Y_\nu^\dagger Y_\nu, \tag{4.35}$$

in its renormalization group equation. These elements are, however, very small due to the smallness of the elements of Y_ν.

The renormalization group equations for the soft-breaking bilinear couplings M_L^2, M_e^2 and M_n^2, i.e., Eqs. (F.22), (F.25) and (F.26), shows that all of these matrices have, small, but non-vanishing off-diagonal elements at the electroweak scales. Thus the lepton flavour numbers are broken at the electroweak scale by all particles that have mass matrices depending upon Y_ν, a_ν, M_L^2, M_e^2 and M_n^2. These are the neutrinos, the sneutrinos and charged sleptons.

By making some additional assumptions analytic solutions of the renormalization group equations can be obtained for Y_ν, a_ν and M_n^2.

The renormalization group equations for Y_ν, a_ν and M_n^2 are presented in Eqs. (F.10), (F.17) and (F.26). These equations shows that the running of Y_ν only depends on gauge couplings and on other Yukawa couplings. The running of the soft-breaking trilinear coupling a_ν depends upon gauge couplings, Yukawa couplings and other soft-breaking trilinear couplings. And the running of M_n^2 depends upon all parameters, that is, gauge couplings, Yukawa couplings, soft-breaking trilinear and bilinear couplings. Due to this increase in complexity the running of Y_ν will be studied first, then the running of a_ν and M_n^2 will be analysed.

The estimate of the elements of Y_ν, which was presented in Eq. (4.27), shows that all of these elements are very small at the electroweak scale. It is therefore reasonable to assume that the running of gauge couplings, and of all other Yukawa couplings, do not depend on Y_ν. To further simplify the equations, one may assume that all elements of Y_u and Y_ν vanishes, except for $(Y_u)_{33} = y_t$ and $(Y_\nu)_{33} = \nu_\tau$. This is a very good approximation for Y_u, and is often used in the literature, e.g., Ref. [35]. But since observations shows that the neutrino masses are almost degenerate in mass, the approximation made for Y_ν is more dubious. Nevertheless, these assumptions will be used in order to make an analytic analyse of the renormalization group equations for the elements of Y_ν.

The assumptions made above simplifies the renormalization group equations for Y_ν considerably. And Eq. (F.10) takes the simple form,

$$\frac{d}{dt}\nu_\tau = \frac{1}{16\pi^2}\,\nu_\tau f_1(t), \tag{4.36}$$

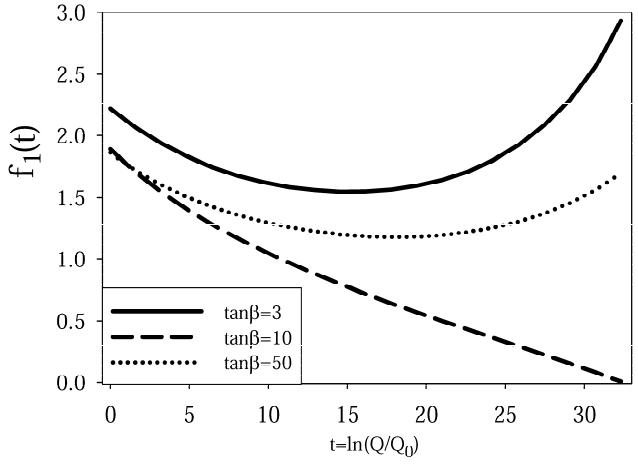

Figure 4.4: The figure shows the running of $f_1(t) = 3y_t^2 - \frac{3}{5}g_1^2 - 3g_2^2$ for three choices of $\tan\beta$.

where

$$f_1(t) = 3y_t^2 - \frac{3}{5}g_1^2 - 3g_2^2. \tag{4.37}$$

The energy scale, Q, is parametrised by

$$t = \ln\frac{Q}{M_Z}, \tag{4.38}$$

Equation (4.36) shows that for $f_1(t) > 0$ the neutrino Yukawa coupling, ν_τ, increases, as the energy increases. In Fig. 4.4 some examples of the running of $f_1(t)$ are shown. This figure shows that $f_1(t)$ is positive for most choices of $\tan\beta$, and the elements of Y_ν will therefore take larger values at the GUT-scale than they do at the electroweak scale.

A solution to Eq. (4.36) is found by straight forward integration, i.e.,

$$\nu_\tau(t) = \nu_\tau^0 \exp\left\{\frac{1}{16\pi^2}\int_0^t f_1(u)\,du\right\}, \tag{4.39}$$

where ν_τ^0 is the initial value for ν_τ, e.g., its value at the electroweak scale.

A rough estimate of ν_τ at the GUT-scale, i.e., of $\nu_\tau^{\rm GUT}$, can now be obtained by making the approximations

$$y_t \approx 1, \quad g_1 \approx g_2 \approx 0.6, \tag{4.40}$$

$$f_1(t) \approx 1.7. \tag{4.41}$$

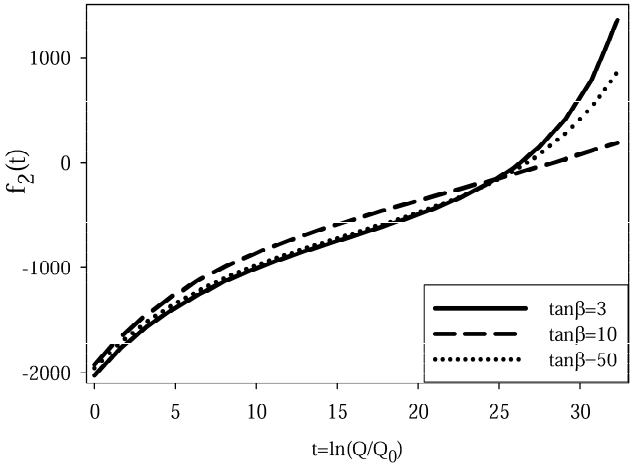

Figure 4.5: The figure shows the running of $f_2(t) = 6a_\ell y_\ell - \frac{6}{5}g_1^2 M_1 - 6g_2^2 M_2$ for three choices of $\tan\beta$.

Which gives the following estimate,

$$\frac{\nu_\tau^{\rm GUT}}{\nu_\tau^0} \approx \exp\left\{\frac{t_{\rm GUT}}{16\pi^2}\cdot 1.7\right\} \approx 1.4, \tag{4.42}$$

which are motivated from the results presented in Figs. 4.2 and 4.3.

That is, even if some rough assumptions have been made, this example shows that the neutrino Yukawa couplings will increase for increasing energies, but their values are still very small for all energies.

Next, the running of the trilinear soft-breaking couplings defined by matrix a_ν will be analysed. In addition to the assumptions leading to Eq. (4.36), some additional assumptions must be made. First, it is assumed that the running of all other soft-breaking trilinear couplings do not depend upon a_ν. It is also assumed that all elements of a_u and a_ν vanishes, except for $(a_u)_{33} = a_t$ and $(a_\nu)_{33} = \tilde{\nu}_\tau$. As for Y_u and Y_ν, this is a reasonable assumption also for a_u, but a more dubious one for a_ν. These assumptions simplify the renormalization group equation for a_ν, i.e., Eq. (F.17), considerably,

$$\frac{d}{dt}\tilde{\nu}_\tau = \frac{1}{16\pi^2}\left(\tilde{\nu}_\tau f_1(t) + \nu_\tau f_2(t)\right), \tag{4.43}$$

$$f_2(t) = 6a_t y_t - \frac{6}{5}g_1^2 M_1 - 6g_2^2 M_2, \tag{4.44}$$

and $f_1(t)$ is defined in Eq. (4.37). The assumptions made above mean that $f_2(t)$ does not depend upon $\tilde{\nu}_\tau$. Some examples of the running of $f_2(t)$ are shown in Fig. 4.5,

for three values of $\tan\beta$. This figure shows that $f_2(t)$ is negative for most of the integration region, and $\tilde{\nu}_\tau$ will decrease for increasing values of t.

An analytic solution to Eq. (4.43) can also be obtained, i.e.,

$$\begin{aligned}\tilde{\nu}_\tau(l) &= \frac{1}{F_1(t)}\left(\tilde{\nu}_\tau^{\mathrm{GUT}} - \frac{1}{16\pi^2}\int_t^{t_{\mathrm{GUT}}} \nu_\tau(u) f_2(u) F_1(u) du\right) \\ &= \frac{1}{F_1(t)}\nu_\tau^{\mathrm{GUT}}\,(A_0 - F_2(l))\,, \end{aligned} \tag{4.45}$$

where

$$F_1(t) = \exp\left\{\frac{1}{16\pi^2}\int_t^{t_{\mathrm{GUT}}} f_1(u)du\right\}, \tag{4.46}$$

$$F_2(t) = \frac{1}{16\pi^2}\int_t^{t_{\mathrm{GUT}}} f_2(u)du. \tag{4.47}$$

The solution for $\tilde{\nu}_\tau$ and the boundary value

$$\tilde{\nu}_\tau^{\mathrm{GUT}} = A_0\,\nu_\tau^{\mathrm{GUT}}, \tag{4.48}$$

have been used to obtain the final form of Eq. (4.45).

The renormalization group equations for M_n^2, i.e., Eq. (F.26), show that the running of M_n^2 depends on the square of Y_ν and a_ν. And since both ν_τ and $\tilde{\nu}_\tau$ are small the values for each element of M_n^2 do not change much as the energy scale is changed from the electroweak scale to the GUT-scale. Only if the supergravity inspired boundary conditions are violated, and a_ν is allowed to take arbitrary large values, M_n^2 will change its value.

A summary of this discussion is therefore that the elements of Y_ν increase, and the elements of a_ν decrease for increasing values of t. While the elements of M_n^2 are nearly constant.

4.4.3 Numerical analysis of Y_ν, a_ν and M_n^2

By using the method outlined in Appendix H one can obtain numerical stable solutions for the complete set of renormalization group equations for MSSM-D. It should be stressed again that no threshold effects have been taken into account, neither at the electroweak nor at the unification scale. See e.g., Ref. [46] for further comments and analysis of threshold effects.

Some examples of the running of $(Y_\nu)_{3,3}$ and $(a_\nu)_{3,3}$ are shown in Figs. 4.6 and 4.7. These solutions confirm the analytic solutions of Eqs. (4.39) and (4.45), in that $(Y_\nu)_{3,3}$ increases and $(a_\nu)_{3,3}$ decreases for increasing energies. These two figures also show that the running of $(Y_\nu)_{3,3}$ and $(a_\nu)_{3,3}$ are well behaved, and their values are

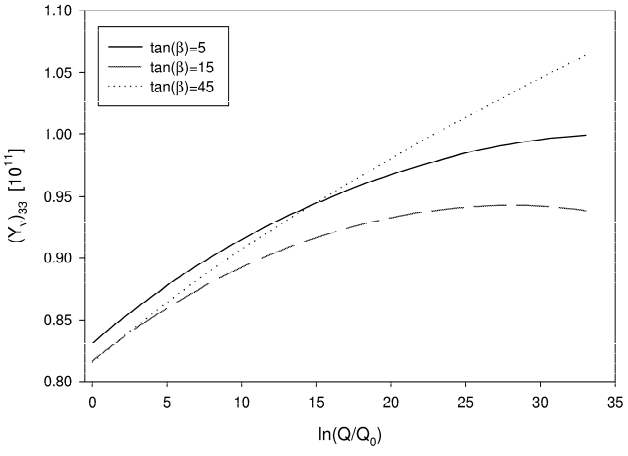

Figure 4.6: The figure shows the running of the Yukawa coupling $(Y_\nu)_{3,3}$ for three choices of $\tan\beta$.

small throughout the complete integration region. This smallness of Y_ν, and the supergravity boundary conditions of Eqs. (4.1) - (4.4), means that a_e, a_ν, M_L^2, M_e^2 and M_n^2 all have off diagonal elements at the electroweak scale. These elements are, however, very small. As an example, assume that the following boundary conditions are used at the electroweak and GUT-scale,

$$\begin{aligned} M_0 &= 200\,\text{GeV}, & A_0 &= 250\,\text{GeV}, \quad M_{1/2} = 300\,\text{GeV}, \\ \tan\beta &= 5, & \text{sign}(\mu) &= +1, \\ m_{\nu_1} &= 1.0\,\text{eV}, & m_{\nu_2} &= 2.0\,\text{eV}, \qquad m_{\nu_3} = 1.0\,\text{eV}, \\ \theta_{12} &= \theta_{13} = \theta_{23} = 45^o. \end{aligned} \tag{4.49}$$

The largest off-diagonal elements appear for a_ν, where they are of the order 10^{-11}, and the diagonal elements are of the order 10^{-9}. For the other matrices, i.e., M_L^2, M_e^2 and M_n^2, the off-diagonal elements are even smaller.

4.5 Analysis of $\Gamma(l \to l'\gamma)$ in MSSM-D

In this section the three decay rates $\mu \to e\gamma$, $\tau \to e\gamma$ and $tau \to \mu\gamma$ will be analysed qualitatively and by numerical methods.

The Feynman rules, necessary for this analysis, are presented in Appendix E. These Feynman rules lead to 8 possible kinds of Feynman diagrams for $l \to l'\gamma$ at the one-loop level, see Fig. 4.8. However, not all of them contribute to the lepton

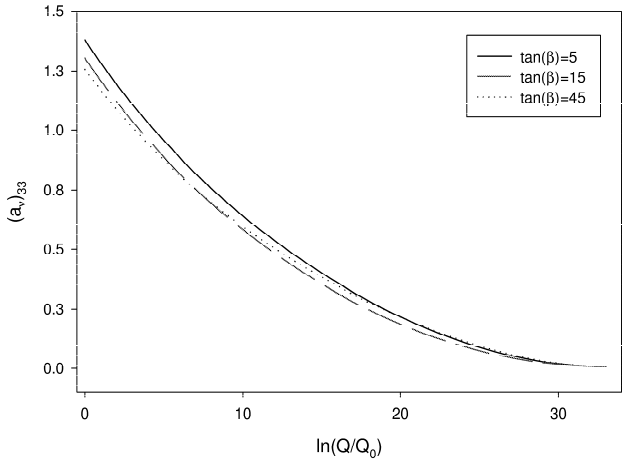

Figure 4.7: The figure shows the running of the coupling $(a_\nu)_{3,3}$ for three choices of $\tan\beta$. The supergravity boundary condition of Eq. (4.3) have been used and $A_0 = 120$.

flavour violating decay rates under study. This is most easily seen by grouping the 8 diagrams into three subgroups. The first subgroup consists of the diagrams in Fig. 4.8 a) and b). These two kinds of diagrams involves supersymmetric particles and will give the largest contribution to the decay rates. The second subgroup consists of the diagrams shown in c) and d). These diagrams have neutral gauge bosons and a neutral Goldstone boson in the loop. None of these diagrams gives lepton flavour violation, and therefore do not contribute to the decay rates under study. Finally, the last group consisting of diagrams e), f), g) and h), have charged gauge boson and charged Goldstone boson together with the three massive neutrinos as intermediate particles. Since the neutrinos break lepton flavour numbers the amplitudes from this group of diagrams will contribute to the decay rates under study.

In the Standard Model, and by using the unitary gauge, the diagram shown in Fig. 2.1 is the only one that contributes. This diagram is identical to the one in Fig. 4.8 e). In Ref. [17] it was shown that this diagram does lead to lepton flavour violation, but its contribution is very small, i.e., $Br\,(\mu \to e\gamma) \leq 10^{-40}$. Observations of neutrino oscillations show that the neutrino masses must be highly degenerate [6]. From the discussion in Sec. 2.3.4 and the toy model analysed in Appendix B.3, one sees that none of the diagrams in e) - h) can give any interesting contribution. These diagrams are therefore neglected in the forthcoming analysis.

This shows that the only interesting contribution comes from the amplitudes of Fig. 4.8 a) and b), that is, the only diagrams where sparticles are involved.

Before these diagrams are analysed one should comment on the gauge used for the

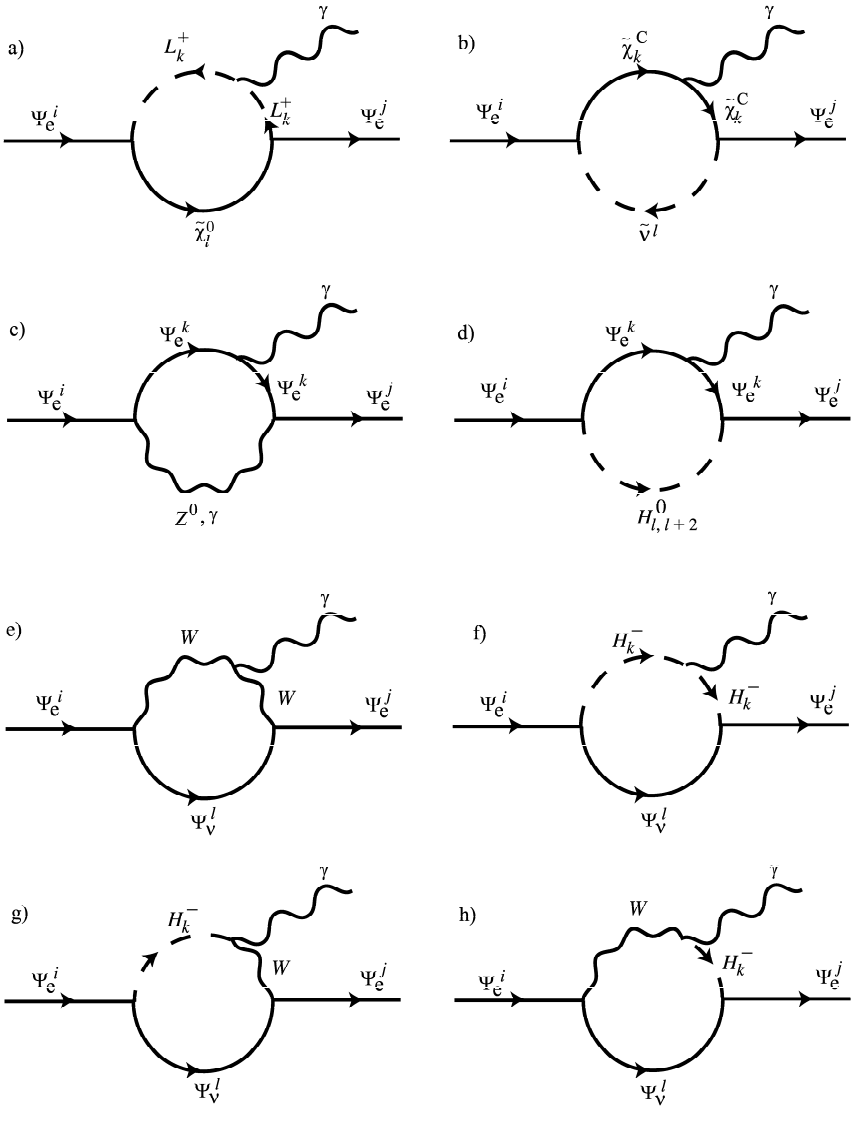

Figure 4.8: The figure shows the eight kinds of Feynman-diagrams which may contribute to the decay channels $l \to l'\gamma$ in MSSM-D. The diagrams d), f), g) and h) does not appear in the unitary gauge.

quantisation of MSSM-D. The Feynman rules, presented in Appendix E, extend the Feynman rules of MSSM. In Ref. [47] the complete set of Feynman rules for MSSM was obtained in the Feynman gauge. Therefore the Feynman gauge is used throughout this analysis too. On the other hand, if the unitary gauge is used there will be fewer diagrams, since the effects from diagrams d), f), g) and h) now are included in the propagators of the massive gauge bosons. The physical results, such as branching ratios, are of course independent on the gauge which is used.

4.5.1 Qualitative analysis of branching ratios

The amplitudes shown in Figs. 4.8 a) and b) are calculated by combining the general expressions from Appendix B with the Feynman rules of Appendix E. These amplitudes will be analysed by numerical methods, but some qualitative understanding is useful too. First, one should remember that the lepton number is conserved in MSSM-D, while the lepton flavour numbers are broken. In Fig. 4.8 a) the lepton number is transmitted through the loop by the 6 selectrons, and in b) the 6 sneutrinos transmits these flavour numbers.

As explained in Sec. 2.3.4, decoupling and mass degeneracy are the two mechanisms which determines the decay rates. Decoupling means that the contribution from one diagram will decrease if the masses in the loop are increasing. The mass degeneracy is important since a larger degeneracy among particles, with equal quantum numbers, will decrease the contribution from the specific diagram.

By using this knowledge one can give a qualitative analysis of the contribution each of diagrams of Fig. 4.8 a) and b) will give. In diagram a) the selectron masses are important. The squared mass matrix for these scalars is equal in MSSM and MSSM-D. It is shown in Eq. (D.5). However, due to the non-vanishing neutrino mixing angles it has been explained that M_L^2 and M_e^2 will have off-diagonal elements at the electroweak scale. These off-diagonal elements leads to flavour mixing and a larger non-degeneracy among the selectron masses. Thus, the selectrons break the lepton flavour numbers, and the amplitudes of Fig. 4.8 a) contributes to the decay rates under study.

The amplitudes represented by Fig. 4.8 b) involves the sneutrinos. Equation (4.29) shows the squared mass matrix for these neutral scalars. This matrix shows that the sneutrino masses depends upon Y_ν, M_L^2 and M_n^2, which all have off-diagonal elements at the electroweak scale. Therefore, also these diagrams gives a non-vanishing contribution to the decay rates under study. From MSSM-24 it is well known that the sneutrinos are highly degenerate in mass [35]. And the analysis of Sec. 4.4 shows that all elements of Y_ν and a_ν are very small. Since the mixing between the left- and right-handed components of the squared sneutrino mass matrix is determined from these couplings, one would only expect a small mixing between these components. The sneutrinos are therefore expected to be highly degenerate also in MSSM-D.

To conclude this qualitative analysis, we see that the only interesting contributions

comes from the amplitudes of Figs. 4.8 a) and b). By using the supergravity inspired scenario, i.e., Eqs. (4.1) - (4.4), the mass degeneracy for both selectrons and sneutrinos depends strongly upon the neutrino mixing angles. Since the elements of Y_ν are small it is expected that the decay rates are small also in this model. Finally, the decay rates will not be sensitive on M_n^2. That is, the boundary condition

$$M_n^2 = M_0^2 \, 1_{3\times 3}, \tag{4.50}$$

may be severely broken at the GUT-scale without leading to any violations of the upper limits for the decay rates.

The actual size of the contributions and a detailed analysis of these amplitudes must be made by numerical methods. This is the topic of the next section.

4.5.2 Numerical analysis of MSSM-D

In this section the numerical analysis of the three decay rates $\Gamma(l \to l'\gamma)$ will be presented. In order to have a well defined model all free parameters of MSSM-D must be specified. This will be referred to as a realisation of MSSM-D, or as a particular scenario for MSSM-D. The supergravity inspired boundary conditions of Eqs. (3.8) - (3.11), defines MSSM-D in terms of the 5 parameters from MSSM-24, i.e., M_0, A_0, $M_{1/2}$, $\tan\beta$ and $\mathrm{sign}(\mu)$, and 6 new parameters, which defines the neutrino Yukawa matrix, Y_ν. One possible choice for the 5 MSSM-24 parameters is the following set of parameters,

$$\begin{aligned} M_0 = 111\,\mathrm{GeV}, \qquad & A_0 = 278\,\mathrm{GeV}, \quad M_{1/2} = 247\,\mathrm{GeV}, \\ \tan\beta = 5, \qquad & \mathrm{sign}(\mu) = +1. \end{aligned} \tag{4.51}$$

This particular choice of parameters was analysed in Ref. [46], and leads to a phenomenologically acceptable solution for MSSM-24. Some of the parameters, and the associated masses are shown in Table 4.1. This table shows the tree-level mass for the lightest Higgs boson, and also an improvement [48] of this mass. The tree level result is used in the numerical calculations, i.e., in the one-loop calculations of the minimisation conditions for the neutral scalar potential.

In Ref. [46] the GUT-scale is defined as the scale where the two gauge couplings g_1 and g_2 unifies. The strong coupling, g_3, is defined by the unification conditions, $g_1 = g_2 = g_3$, at this particular scale. Next, the renormalization group equations are solved, and the values for the three gauge coupling constants, at the electroweak scale, are found. The value obtained for g_3 can now be compared with its measured value. In this thesis a slightly different approach is used, in that the values for g_1, g_2 and g_3 are defined at the M_Z-scale by Eqs. (2.9) - (2.11). The unification scale is now defined as the scale $M_{\mathrm{GUT}} = 2.04 \cdot 10^{16}\,\mathrm{GeV}$, and the renormalization group equations are run up to this scale, where the boundary conditions of Eqs. (4.1) -

Parameters	Masses and couplings
M_0, A_0, $M_{1/2}$	111, 278, 247
$\tan\beta$, $\mathrm{sign}(\mu)$	5, +1
$\tilde{e}_1$, $\tilde{e}_2$, $\tilde{e}_3$,	148, 152, 152,
$\tilde{e}_4$, $\tilde{e}_5$, $\tilde{e}_6$	219, 219, 221
$\tilde{\nu}_i, \quad i = 1, 2, \ldots, 6$	216, 216, 215, 111, 111, 111
$\tilde{\chi}_1^0$, $\tilde{\chi}_2^0$, $\tilde{\chi}_3^0$, $\tilde{\chi}_4^0$	93, 171, 431, 447
$\tilde{\chi}_1$, $\tilde{\chi}_2$	183, 442
$\tilde{u}_1$, $\tilde{u}_2$, $\tilde{u}_3$,	421, 622, 622,
$\tilde{u}_4$, $\tilde{u}_5$, $\tilde{u}_6$	638, 638, 680
$\tilde{d}_1$, $\tilde{d}_2$, $\tilde{d}_3$,	580, 620, 620
$\tilde{d}_4$, $\tilde{d}_5$, $\tilde{d}_6$	622, 644, 644
M_h, M_H, M_{A^0}, $M_{H^\pm}$	84, 479, 477, 483
Improved M_h, M_H	103, 511
$\mu(M_Z)$	427
M_1, M_2, M_3	97, 184, 671
g_1, g_2, $g_3\,(M_{\mathrm{GUT}})$	0.722, 0.730, 0.727

Table 4.1: The table shows the parameters which have been used in the numerical calculations in this chapter. An improvement [48] of the lightest neutral Higgs mass is also shown. All masses are given in GeV.

(4.4) are used. Thus, complete unification of the three gauge coupling constants is not imposed on the model, but may come out as a consequence of this approach. On the other hand, the correct values for the gauge couplings will be used in the forthcoming calculations.

In addition to the values of Eq. (4.51), the 3 neutrino masses and 3 mixing angles must also be specified. However, numerical calculations shows that for neutrino masses of the order 1 eV, and for all mixing angles, the decay rate $\mu \to e\gamma$ is of the order 10^{-40}, or smaller. The other two decay rates are even further away from breaking any phenomenological limits.

The parameter choices in Eq. (4.51) were rather arbitrarily, but numerical calculations with other choices for these parameters do not lead to violations of the upper limits for any of the decay rates under study. Thus MSSM-D, with the supergravity inspired scenario easily fulfils the phenomenologically constraints, i.e., Eqs. (2.4) - (2.6). These calculations are in accordance with the qualitative analysis made in Sec. 4.5.1.

A'_0	$\tau \to \mu\gamma$	$\tau \to e\gamma$	$\mu \to e\gamma$
10^8	10^{-39}	10^{-40}	10^{-47}
10^{10}	10^{-31}	10^{-32}	10^{-39}
10^{12}	10^{-23}	10^{-24}	10^{-31}

Table 4.2: The table shows the decay rate for the three decay rates under study, for three values of A'_0.

Beyond the supergravity boundary conditions

The supergravity inspired boundary conditions of Eqs. (4.1) - (4.4), are imposed by hand. It is therefore interesting to analyse MSSM-D also for small violations of these boundary conditions. Four scenarios, each violating some of these boundary conditions will now be analysed.

These cases are defined as violations of the following boundary conditions,

$$a_\nu = A_0\, Y_\nu, \tag{4.52}$$

$$M_n^2 = M_0^2\, 1_{3\times 3}, \tag{4.53}$$

$$M_e^2 = M_0^2\, 1_{3\times 3}, \tag{4.54}$$

$$M_L^2 = M_0^2\, 1_{3\times 3}. \tag{4.55}$$

In all of these scenarios the numerical values for the 5 MSSM parameters, which was presented in Eq. (4.51), are used. And the neutrino Yukawa matrix is determined by the following parameters,

$$m_{\nu_1} = 1\,\text{eV}, \quad m_{\nu_2} = 2\,\text{eV}, \quad m_{\nu_3} = 3\,\text{eV}, \tag{4.56}$$

$$\theta_{12} = \theta_{13} = \theta_{23} = 45^\circ. \tag{4.57}$$

The first of these examples is defined as a violation of Eq. (4.52). A new parameter A'_0 is introduced to the model, and the boundary condition of Eq. (4.52) is replaced by,

$$a_\nu = A'_0\, Y_\nu. \tag{4.58}$$

Numerical calculations show that this new parameter must be very large in order to make any influence on the decay rates, see Table 4.2. For such large values of A'_0, the elements of a_ν are of the same order of magnitude or larger than the diagonal elements of a_e. For the remaining analysis of MSSM-D, it will be assumed that all elements of a_ν are small, i.e., of the order 10^{-9} or smaller.

In the next case the boundary condition for M_n^2 is extended. A new parameter, M'_0, is introduced such that Eq. (4.53) is replaced by,

$$M_n^2 = M_0'^2\, 1_{3\times 3}. \tag{4.59}$$

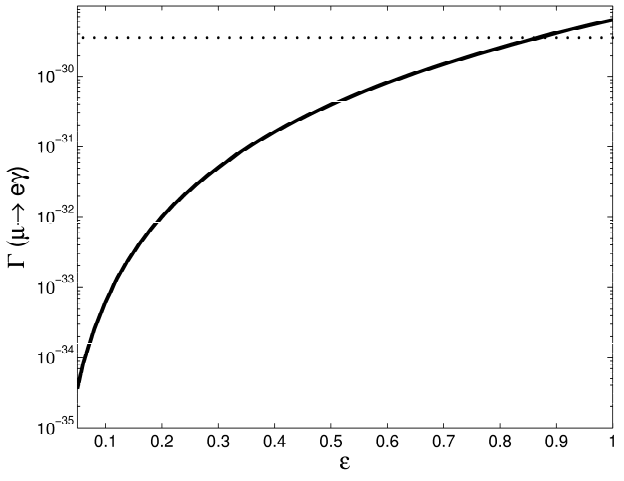

Figure 4.9: The figure shows the decay rate as a function of the off-diagonal elements of M_e^2, i.e., ε^2. The horizontal line shows the present upper limit for $\mu \to e\gamma$.

Numerical calculations show that M_0' must be very large, of the order 10^{10}, or larger, in order to give any interesting contribution to the decay rates. Such a large value for M_0' make the right-handed sneutrinos very heavy, i.e., $\tilde{\nu_R} \sim M_0' \sim 10^{10}\,\mathrm{GeV}$ compared to the light left-handed sneutrinos. Through the remaining analysis of MSSM-D it will be assumed that the masses for left- and right-handed sneutrinos are of the same order of magnitude.

Both of the matrices a_ν and M_n^2 appear only in the squared sneutrino mass matrix. Thus, apart from small renormalization group effects, this means that the analysis so far has only involved the Feynman diagrams represented by Fig. 4.8 b). On the other hand, matrix M_e^2 appears only in the squared mass matrix for the selectrons, and therefore only affects the Feynman diagram in Fig. 4.8 a). If M_e is diagonal at the GUT scale, the off-diagonal elements at the electroweak scale are non-vanishing, but still very small. This is reflected in the numerical calculations, which show no violations of the upper limits for any of the decay rates in this case. It is therefore more interesting to assume that M_e^2 do have small off-diagonal elements at the GUT-scale. As an example, the boundary condition of Eq. (4.54) will be replaced with,

$$M_e^2 = \begin{cases} M_0^2 & \text{for } i = j, \\ \varepsilon^2 & \text{for } i \neq j. \end{cases} \tag{4.60}$$

The result of the numerical calculations is shown in Fig. 4.9. This figure shows that the off-diagonal elements of M_e^2, i.e., ε^2 must be small in order to not conflict with the upper limit for $\mu \to e\gamma$. This figure also shows that the off-diagonal elements must decrease if the upper limit for $\mu \to e\gamma$ is improved.

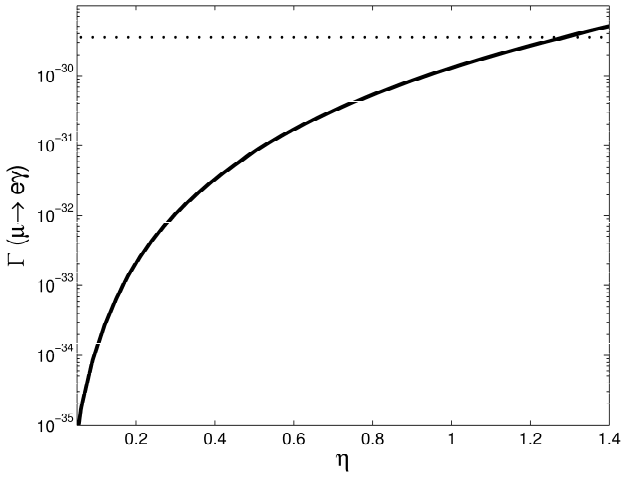

Figure 4.10: The figure shows the decay rate as a function of the off-diagonal elements of M_L^2, i.e., η^2. The horizontal line shows the present upper limit for $\mu \to e\gamma$.

In the final scenario it is assumed that M_L^2 have off-diagonal elements at the GUT-scale, and the boundary condition of Eq. (4.55) is replaced with,

$$M_L^2 = \begin{cases} M_0^2 & \text{for } i = j, \\ \eta^2 & \text{for } i \neq j. \end{cases} \tag{4.61}$$

Figure 4.10 shows the decay rate $\mu \to e\gamma$ as a function of the off-diagonal elements of M_L^2, i.e., η^2.

These two figures show that the constraints for ε and η are of roughly equal size. These constraints, for the off-diagonal elements, are weakened if the slepton and sneutrino masses are increased. Such an increase will occur if M_0 is larger.

The important finding from this analysis is that even small deviations from the supergravity inspired breaking scenario will lead to phenomenologically unacceptable values for the decay rates. Especially the off-diagonal elements of M_L^2 and M_e^2 must be small, of the order 10^{-4} times the diagonal elements.

In this analysis these off-diagonal elements were put into the model by hand, but it will be shown in the next chapters that such off-diagonal elements become a natural consequence of adding R-parity violating terms. These terms are important ingredients of both MSSM-M and MSSM-DM.

URN:NBN:no-7281

Chapter 5

Majorana neutrinos and $l \to l'\gamma$

5.1 The parameter space of MSSM-M

In this chapter MSSM-M will be studied with respect to the three lepton flavour violating decay channels $\tau \to \mu\gamma$, $\tau \to e\gamma$ and $\mu \to e\gamma$. As explained in Sec. 3.1.2 the three neutrinos of MSSM-M are of the Majorana type, that is, they are their own anti-particles. Consequently, neither the lepton number nor the lepton family numbers are conserved in MSSM-M. This violation of lepton number mens that there are no quantum numbers which can distinguish between the superfields $\hat{H}_d$ and L_i, $i = 1, 2, 3$. Thus these 4 superfields may mix together, giving rise to a new global $U(4)$ symmetry between $\hat{H}_d$ and L_i. In Sec. 5.3 this new $U(4)$-symmetry will be explored, and a convenient notation based on it will be presented. Another important feature of MSSM-M is that the neutrinos are constructed from left-handed fields only. Thus the right-handed gauge singlets, n_i, which appeared in MSSM-D are absent in MSSM-M.

The breaking of the lepton number also makes it possible to introduce R-parity violating couplings. These couplings leads to a new and rich phenomenology, but also to a lot of new free parameters of the model.

As shown in Sec. 3.1.2 the superpotential for MSSM-M is given by,

$$W = W_{\text{MSSM}} + W_{\not R}, \tag{5.1}$$

where

$$W_{\text{MSSM}} = Y_u Q \hat{H}_u u - Y_d Q \hat{H}_d d - Y_e L \hat{H}_d e + \mu \hat{H}_d \hat{H}_u, \tag{5.2}$$

and

$$W_{\not R} = \frac{1}{2}\lambda_{ijk} L_i L_j e_k + \lambda'_{ijk} L_i Q_j d_k + \frac{1}{2}\lambda''_{ijk} u_i d_j d_k + \mu_i L_i \hat{H}_u. \tag{5.3}$$

Here i, j and k label the three families of the Standard Model, and the $SU(2) \times SU(3)$-indices have been suppressed. By explicitly taking the $SU(2)$ indices into

account one finds that λ_{ijk} is antisymmetric in i and j, while λ''_{ijk} is symmetric in j and k.

The proton lifetime is very sensitive to the coupling λ''_{ijk}. As an example, assume that all elements of both λ'_{ijk} and λ''_{ijk} are non-vanishing and of order unity. In this case the proton lifetime would be hours or minutes [35]. To prevent such a disaster, the coupling λ''_{ijk} will be assumed to vanish. This is achieved by imposing a global symmetry on the Lagrangian, which action is given by,

$$(Q, u, d, L, e, n, \hat{H}_u, \hat{H}_d) \to (-Q, -u, -d, L, e, n, \hat{H}_u, \hat{H}_d). \tag{5.4}$$

This symmetry is referred to as a *baryon symmetry*. The relevant renormalization group equation, i.e., Eq. (F.56), shows that the β-function for λ''_{ijk} is proportional to λ''_{ijk}, a consequence of the non-renormalization theorem [34]. Thus once the couplings λ''_{ijk} vanish at an arbitrary scale they vanish at all scales. That is, this particular choice for λ''_{ijk} is renormalization group invariant, i.e., a fixed point for Eq. (F.56). Equation (F.65) shows that if both λ''_{ijk} and $\lambda''^{\rm s}_{ijk}$ vanish at an arbitrary scale, then $\lambda''^{\rm s}_{ijk}$ vanishes at all scales. Thus by choosing vanishing values for λ''_{ijk} and $\lambda''^{\rm s}_{ijk}$ these parameters will not appear on any scales in the model. These parameters will therefore not appear in the model to be analysed.

Including the baryon symmetry the most general soft-breaking terms for MSSM-M becomes,

$$\begin{aligned}
-\mathcal{L}_{\rm soft} =& M_Q^2 \tilde{Q}^\dagger \tilde{Q} + \left(M_{\tilde{L}}^2\right) \tilde{L}^\dagger \tilde{L} + M_{H_u}^2 H_u^\dagger H_u + M_{H_d}^2 H_d^\dagger H_d \\
&+ M_{\tilde{u}} \tilde{u} \tilde{u}^* + M_{\tilde{d}}^2 \tilde{d} \tilde{d}^* + M_{\tilde{e}}^2 \tilde{e} \tilde{e}^* + \Big[\varepsilon_i H_d^\dagger \tilde{L}_i - b H_d H_u - b_i L_i H_u \\
&+ a_e \tilde{L} H_d \tilde{e}_K + a_d \tilde{Q} H_d \tilde{d}_K + a_u \tilde{Q} H_u \tilde{u} \\
&+ \lambda^{\rm s}_{ijk} \tilde{L}_i \tilde{L}_j \tilde{e}_k + \lambda'^{\rm s}_{ijk} \tilde{L}_i \tilde{Q}_j \tilde{d}_k \\
&+ \frac{1}{2} \left(M_1 \tilde{B} \tilde{B} + M_2 \tilde{W}^a \tilde{W}^a + M_3 \tilde{g} \tilde{g} \right) + \text{h.c.} \Big] .
\end{aligned} \tag{5.5}$$

The superpotential and soft-breaking terms, from Eqs. (5.1) - (5.3) and (5.5), show that the difference between MSSM-M and MSSM-D is that MSSM-M allows for R-parity violation, but not for right-handed neutrino singlets. That is, the following R-parity violating couplings exist in MSSM-M: μ_i, λ_{ijk}, λ'_{ijk}, b_i, $\lambda^{\rm s}_{ijk}$, $\lambda'^{\rm s}_{ijk}$ and ε_i. On the other hand, the field content of MSSM-M is identical to the one for MSSM.

As explained in Sec. 3.1.2 MSSM-M will generally consist of 278 free parameters. To obtain a phenomenological interesting model some simplifications have to be made. First, all parameters are assumed to be real, and $\theta_{\rm QCD}$ is neglected.

This leaves 157 real parameters. Most of these parameters are associated with the soft-breaking terms, as shown in Table 3.2, page 18. However, if also the supergravity boundary conditions of Eqs. (3.8) - (3.10) are imposed the number of free parameters

will be considerably reduced. As will be explained in Sec. 5.9 MSSM-M, constrained by the supergravity boundary conditions, consists of 41 free parameters. These are the 5 parameters known from MSSM-24, i.e., $\tan\beta$, sign(μ), M_0, $M_{1/2}$ and A_0, in addition to the 36 parameters defining the R-parity violating couplings λ_{ijk} and λ'_{ijk}.

5.2 Limits on R-parity violating couplings

In Ref. [41] limits was obtained for the trilinear couplings, λ_{ijk} and λ'_{ijk}. These limits are shown in Table 5.1. For details regarding the methods to extract these data, see Ref. [41], and references therein.

The most important finding from this table is that most bounds depend upon on a particular scalar mass. That is, the bounds get weaker the more massive the sparticle spectrum is. But for scalar masses of the order 10^2 GeV all limits are of the order 10^{-3}. Table 5.1 also shows that the bounds for the various elements of λ_{ijk} and λ'_{ijk} are roughly of the same order of magnitude.

In this thesis upper limits for the couplings λ_{ijk} and λ'_{ijk} will be obtained by numerical studies of the decay rates $l \to l'\gamma$. In Ref. [41] no upper limits was obtained for the soft-breaking trilinear couplings $\lambda^{\rm s}_{ijk}$ and $\lambda'^{\rm s}_{ijk}$. In this chapter upper limits will be found for these couplings, and also upper limits for the soft-breaking bilinear couplings b_i and ε_i.

5.3 Mixing among down-type superfields

Due to the existence of R-parity violating couplings, the lepton number is violated. Since the lepton number is the only quantum number to distinguish the supermultiplets $\hat{H}_d$ and L_i, these doublets may therefore mix together in MSSM-M. In this section the $\hat{H}_d$-L_i-space will be presented, together with two convenient bases, which are frequently used in the literature. In Sec. 5.5 it will be shown that, in one of these bases, the mass matrices take an almost identical form in MSSM-M as they do in MSSM. This bases will therefore be the preferred one for the analysis of MSSM-M.

5.3.1 Defining the $\hat{H}_d - L_i$-space

The mixing among superfields $\hat{H}_d$ and L_i makes it useful to define a vector space spanned by $\hat{H}$ and L_i. This space will be referred to as the $\hat{H}_d$-L_i-space. The superfields $\hat{H}_d$ and L_i can now be assembled into a $U(4)$-vector, the vector L_α, defined by,

$$L_\alpha = \left(\hat{H}_d, L_i\right), \ \alpha = 0,1,2,3, \quad i = 1,2,3. \tag{5.6}$$

Coupling	Bound	Coupling	Bound
λ_{121}	$0.049 \cdot m_{\tilde{c}_R}/100\,\mathrm{GeV}$	λ_{231}	$0.070 \cdot m_{\tilde{c}_R}/100\,\mathrm{GeV}$
λ_{122}	$0.049 \cdot m_{\tilde{\mu}_R}/100\,\mathrm{GeV}$	λ_{232}	$0.070 \cdot m_{\tilde{\mu}_R}/100\,\mathrm{GeV}$
λ_{123}	$0.049 \cdot m_{\tilde{\tau}_R}/100\,\mathrm{GeV}$	λ_{233}	$0.070 \cdot m_{\tilde{\tau}_R}/100\,\mathrm{GeV}$
λ_{131}	$0.062 \cdot m_{\tilde{e}_R}/100\,\mathrm{GeV}$		
λ_{132}	$0.062 \cdot m_{\tilde{\mu}_R}/100\,\mathrm{GeV}$		
λ_{133}	$0.0060 \cdot \sqrt{m_{\tilde{\tau}}/100\,\mathrm{GeV}}$		
λ'_{111}	$5.2 \cdot 10^{-4}\, f(\tilde{m})$	λ'_{231}	$0.18 \cdot m_{\tilde{b}_L}/100\,\mathrm{GeV}$ (1.12)
λ'_{112}	$0.021 \cdot m_{\tilde{s}_R}/100\,\mathrm{GeV}$	λ'_{232}	0.56 (1.04)
λ'_{113}	$0.021 \cdot m_{\tilde{b}_R}/100\,\mathrm{GeV}$	λ'_{233}	$0.15\sqrt{m_{\tilde{b}_R}/100\,\mathrm{GeV}}$
λ'_{121}	$0.043 \cdot m_{\tilde{d}_R}/100\,\mathrm{GeV}$	λ'_{311}	$0.11 \cdot m_{\tilde{d}_R}/100\,\mathrm{GeV}$ (1.12)
λ'_{122}	$0.043 \cdot m_{\tilde{s}_R}/100\,\mathrm{GeV}$	λ'_{312}	$0.11 \cdot m_{\tilde{s}_R}/100\,\mathrm{GeV}$ (1.12)
λ'_{123}	$0.043 \cdot m_{\tilde{b}_R}/100\,\mathrm{GeV}$	λ'_{313}	$0.11 \cdot m_{\tilde{b}_R}/100\,\mathrm{GeV}$ (1.12)
λ'_{131}	$0.019 \cdot m_{\tilde{t}_L}/100\,\mathrm{GeV}$	λ'_{321}	$0.52 \cdot m_{\tilde{d}_R}/100\,\mathrm{GeV}$ (1.12)
λ'_{132}	$0.28 \cdot m_{\tilde{t}_L}/100\,\mathrm{GeV}$ (1.04)	λ'_{322}	$0.52 \cdot m_{\tilde{s}_R}/100\,\mathrm{GeV}$ (1.12)
λ'_{133}	$1.4 \cdot 10^{-3}\sqrt{m_{\tilde{b}}/100\,\mathrm{GeV}}$	λ'_{323}	$0.52 \cdot m_{\tilde{b}_R}/100\,\mathrm{GeV}$ (1.12)
λ'_{211}	$0.059 \cdot m_{\tilde{d}_R}/100\,\mathrm{GeV}$	λ'_{331}	0.45 (1.04)
λ'_{212}	$0.059 \cdot m_{\tilde{s}_R}/100\,\mathrm{GeV}$	λ'_{332}	0.45 (1.04)
λ'_{213}	$0.059 \cdot m_{\tilde{b}_R}/100\,\mathrm{GeV}$	λ'_{333}	0.45 (1.04)
λ'_{221}	$0.18 \cdot m_{\tilde{s}_R}/100\,\mathrm{GeV}$ (1.12)		
λ'_{222}	$0.21 \cdot m_{\tilde{s}_R}/100\,\mathrm{GeV}$ (1.12)		
λ'_{223}	$0.21 \cdot m_{\tilde{b}_R}/100\,\mathrm{GeV}$ (1.12)		

Table 5.1: The table shows the limits, at the 2σ-level, for λ_{ijk} and λ'_{ijk} at the electroweak scale, obtained from Ref. [41]. The following definition is used $f(\tilde{m}) = (m_{\tilde{e}}/100\ \mathrm{GeV})^2 \cdot (m_{\tilde{\chi}^0}/100\ \mathrm{GeV}^2)^{1/2}$. When the perturbative bounds are more stringent than the empirical bounds these bounds are shown in parenthesis.

This vector can be rotated in $U(4)$-space by applying a unitary 4×4 mixing matrix, X, i.e.,

$$L^a_\alpha = X_{\alpha\beta} L_\beta, \tag{5.7}$$

where L^a_α is the rotated $U(4)$ vector.

It is also useful to define the following 7 new $U(4)$-vectors and -tensors:

$$\lambda_{\alpha\beta k} = \begin{pmatrix} 0 & -(Y_e^*)_{jk} \\ (Y_e)_{jk} & \lambda_{ijk} \end{pmatrix}, \tag{5.8}$$

$$\lambda'_{\alpha jk} = \left(-(Y_d)_{jk}, \lambda'_{ijk}\right), \tag{5.9}$$

$$\mu_\alpha = (\mu, \mu_i), \tag{5.10}$$

$$\left(M_L^2\right)_{\alpha\beta} = \begin{pmatrix} M_{H_d}^2 & \epsilon_i \\ \epsilon_i & \left(M_{\tilde{L}}^2\right)_{ij} \end{pmatrix}, \tag{5.11}$$

$$\lambda^{\rm s}_{\alpha\beta k} = \begin{pmatrix} 0 & (a_e)_{jk} \\ -(a_c)_{jk} & \lambda^{\rm s}_{ijk} \end{pmatrix}, \tag{5.12}$$

$$\lambda'^{\rm s}_{\alpha jk} = ((a_b)_{jk}, \lambda'^{\rm s}_{ijk}), \tag{5.13}$$

$$b_\alpha = (b_0, b_i). \tag{5.14}$$

In these definitions, and for the remaining analysis, small Greek letters label the $U(4)$ space, and small Latin indices label the three lepton families of the Standard Model, i.e., $\alpha,\ \beta = 0,1,2,3$ and $i,j,k = 1,2,3$. The definition of Eq. (5.8) shows that $\lambda_{\alpha\beta k}$ is antisymmetric in its two first indices, α and β, just like λ_{ijk} was antisymmetric in i and j.

In terms of these $U(4)$ invariant parameters, the superpotential and soft-breaking terms, i.e., Eqs. (5.1) and (5.5), can be expressed in a $U(4)$-manifest notation, i.e.,

$$W = Y_u Q \hat{H}_u u + \frac{1}{2}\lambda_{\alpha\beta k} L_\alpha L_\beta e_k + \lambda'_{\alpha jk} L_\alpha Q_j d_k + \mu_\alpha L_\alpha \hat{H}_u, \tag{5.15}$$

$$\begin{aligned} -\mathcal{L}_{\rm soft} &= M_{\tilde{Q}}^2 \tilde{Q}^\dagger \tilde{Q} + \left(M_{\tilde{L}}^2\right)_{\alpha\beta} \tilde{L}^\dagger_\alpha \tilde{L}_\beta + M_{H_u}^2 H_u^\dagger H_u \\ &\quad + M_{\tilde{u}}^2 \tilde{u}\tilde{u}^* + M_{\tilde{d}}^2 \tilde{d}\tilde{d}^* + M_{\tilde{e}}^2 \tilde{e}\tilde{e}^* - (b_\alpha \tilde{L}_\alpha H_u + \text{h.c.}) \\ &\quad + \Big[a_u H_u \tilde{Q}\tilde{u} + \frac{1}{2}\lambda^{\rm s}_{\alpha\beta k} \tilde{L}_\alpha \tilde{L}_\beta \tilde{e}_k + \lambda'^{\rm s}_{\alpha jk} \tilde{L}_\alpha \tilde{Q}_j \tilde{d}_k \\ &\quad + \frac{1}{2}\left(M_1 \tilde{B}\tilde{B} + M_2 \tilde{W}^a \tilde{W}^a + M_3 \tilde{g}\tilde{g}\right) + \text{h.c.} \Big]. \end{aligned} \tag{5.16}$$

This explicitly shows the covariance of the Lagrangian under rotations in $\hat{H}$-L_i-space, and is the form for the Lagrangian that will be used throughout this thesis.

Only when necessary, e.g., for comparisons with the literature will the non-covariant form of Eqs. (5.1) and (5.5) be used.

5.3.2 Choice of basis

Generally, the $U(4)$-vectors and -tensors of Eqs. (5.6) and (5.8) - (5.14) will change under a $U(4)$ rotation. The transformation rules are easily found by rotating the superfield L_α, and demanding a covariant Lagrangian, i.e.,

$$W \to W^a = Y_u Q \hat{H}_d u + \frac{1}{2}\lambda^a_{\alpha\beta k} L^a_\alpha L^a_\beta e_k + \lambda'^a_{\alpha j k} L^a_\alpha Q_j d_k + \mu^a_\alpha L^a_\alpha \hat{H}_u, \qquad (5.17)$$

and for the soft breaking terms

$$\begin{aligned} -\mathcal{L}_{\text{soft}} \to -\mathcal{L}^a_{\text{soft}} = {} & M^2_{\tilde{Q}} \tilde{Q}^\dagger \tilde{Q} + \left(M^2_{\tilde{L}}\right)^a \tilde{L}^{a\dagger}_\alpha \tilde{L}^a_\beta + M^2_{H_u} H^\dagger_u H_u \\ & + M^2_{\tilde{u}} \tilde{u}\tilde{u}^* + M^2_{\tilde{d}} \tilde{d}\tilde{d}^* + M^2_{\tilde{e}} \tilde{e}\tilde{e}^* - (b^a_\alpha \tilde{L}^a_\alpha H_u + \text{h.c.}) \\ & + \Bigg[\frac{1}{2}\lambda^{s\,a}_{\alpha\beta k} \tilde{L}^a_\alpha \tilde{L}^a_\beta \tilde{e}_k + \lambda'^{s\,a}_{\alpha j k} \tilde{L}^a_\alpha \tilde{Q}_j \tilde{d}_k + a_u H_u \tilde{Q}\tilde{u} \\ & + \frac{1}{2}\left(M_1 \tilde{B}\tilde{B} + M_2 \tilde{W}^a \tilde{W}^a + M_3 \tilde{g}\tilde{g}\right) + \text{h.c.}\Bigg], \end{aligned} \qquad (5.18)$$

where the index a labels the rotated fields and transformed parameters. The transformation rule for L_α under the action of the unitary matrix X can be found by solving Eq. (5.7) in terms of L_α. That is,

$$L_\alpha = X^\dagger_{\alpha\beta} L^a_\alpha. \qquad (5.19)$$

By substituting this expression into Eqs. (5.15) and (5.16) the following transformation rules are obtained,

$$\mu^a_\alpha = X^\dagger_{\alpha\rho}\, \mu_\rho, \qquad (5.20)$$

$$\lambda'^a_{\alpha j k} = X^\dagger_{\alpha\rho}\, \lambda'_{\rho j k}, \qquad (5.21)$$

$$\lambda^a_{\alpha\beta k} = X^\dagger_{\alpha\rho} X^\dagger_{\beta\sigma}\, \lambda_{\rho\sigma k}, \qquad (5.22)$$

$$b^a_\alpha = X^\dagger_{\alpha\rho}\, b_\rho, \qquad (5.23)$$

$$\lambda'^{s\,a}_{\alpha j k} = X^\dagger_{\alpha\rho}\, \lambda'^s_{\rho j k}, \qquad (5.24)$$

$$\left(M^2_{\tilde{L}}\right)^a_{\alpha\beta} = X^\dagger_{\alpha\rho} X^\dagger_{\beta\sigma} \left(M^2_{\tilde{L}}\right)_{\rho\sigma}, \qquad (5.25)$$

$$\lambda^{s\,a}_{\alpha\beta k} = X^\dagger_{\alpha\rho} X^\dagger_{\beta\sigma}\, \lambda^s_{\rho\sigma k}. \qquad (5.26)$$

Rotate away the bilinear term

The $U(4)$ symmetry described above can now be used to simplify the Lagrangian. One application is to rotate away the bilinear superpotential term μ_i. This is achieved by using the $U(4)$ symmetry to define the following rotated superfields,

$$\hat{H}_d^a = \frac{\mu \hat{H}_d + \mu_i L_i}{\sqrt{\mu^2 + \mu_i^2}} \quad \text{and} \quad L_i^a = \frac{\mu_i \hat{H}_d - \mu L_i}{\sqrt{\mu^2 + \mu_i^2}}. \tag{5.27}$$

Using these definitions the bilinear terms of Eqs. (5.2) and (5.3) become,

$$\begin{aligned} \mu \hat{H}_u \hat{H}_d + \mu_i L_i \hat{H}_u \to \mu \hat{H}_d^a \hat{H}_u + \mu_i L_i^a \hat{H}_u \\ = \sqrt{\mu^2 + \mu_i^2}\, \hat{H}_d \hat{H}_u = \mu^a \hat{H}_d \hat{H}_u, \end{aligned} \tag{5.28}$$

where $\mu^a = \sqrt{\mu^2 + \mu_i^2}$. Thus the parameter μ_i does not appear anymore in the Lagrangian. In this case, the X-matrix is defined such that,

$$\mu_\alpha^a = X_{\alpha\beta}\, \mu_\beta = (\mu^a, 0, 0, 0). \tag{5.29}$$

Of course, also the other elements of $U(4)$ space will be altered by this rotation, according to Eqs. (5.21) - (5.26). Unfortunately, the rotation of Eq. (5.27) is not preserved under the action of the renormalization group equations, that is, even if the parameter μ_i vanish at a particular scale it will reappear at an arbitrary scale, see discussion in Sec. 5.7. The mass matrices are also rather complicated in this basis.

Rotate away the sneutrino vacuum expectation values

An important observation is that due to the mixing between the superfields $\hat{H}_d$ and L_i, also the sneutrino fields acquires vacuum expectation values. The scalar fields $\tilde{L}_\alpha$ takes the form,

$$\tilde{L}_\alpha = \begin{pmatrix} \frac{1}{\sqrt{2}} (v_\alpha + \psi_\alpha + i\phi_\alpha) \\ \tilde{L}_\alpha^- \end{pmatrix}. \tag{5.30}$$

This shows that also v_α is a $U(4)$ vector. It is therefore possible to choose a particular rotation matrix X, in $U(4)$-space such that

$$v_\alpha^a = X_{\alpha\beta}\, v_\beta = (v_d, 0, 0, 0). \tag{5.31}$$

Since X is unitary, the length of v_α must be preserved under the action of X. That is,

$$v_d^2 = \sum_{\alpha=0}^{3} v_\alpha^2. \tag{5.32}$$

This basis, where v_i vanishes, will be referred to as the v_i-basis, and is the preferred basis for the rest of this thesis. The definition of v_d also makes it possible to define

$$\tan\beta = \frac{v_u}{v_d}, \tag{5.33}$$

in analogy to MSSM and MSSM-D.

By following Ref. [49] the correct X-matrix fulfilling Eq. (5.31) is found in terms of the three mixing angles θ, ϕ and η, i.e.,

$$\sin\theta = \frac{v_1}{\sqrt{v_0^2 + v_1^2}}, \tag{5.34}$$

$$\sin\phi = \frac{v_2}{\sqrt{v_0^2 + v_1^2 + v_2^2}}, \tag{5.35}$$

$$\sin\eta = \frac{v_3}{\sqrt{v_0^2 + v_1^2 + v_2^2 + v_3^2}}. \tag{5.36}$$

The mixing matrix X is now defined [49] as

$$X = R_1 \cdot R_2 \cdot R_3, \tag{5.37}$$

where

$$R_1 = \begin{pmatrix} \cos\eta & 0 & 0 & \sin\eta \\ 0 & 1 & 0 & 0 \\ 0 & 0 & 1 & 0 \\ -\sin\eta & 0 & 0 & \cos\eta \end{pmatrix}, \tag{5.38}$$

$$R_2 = \begin{pmatrix} \cos\phi & 0 & \sin\phi & 0 \\ 0 & 1 & 0 & 0 \\ -\sin\phi & 0 & \cos\phi & 0 \\ 0 & 0 & 0 & 1 \end{pmatrix}, \tag{5.39}$$

$$R_3 = \begin{pmatrix} \cos\theta & \sin\theta & 0 & 0 \\ -\sin\theta & \cos\theta & 0 & 0 \\ 0 & 0 & 1 & 0 \\ 0 & 0 & 0 & 1 \end{pmatrix}. \tag{5.40}$$

Multiplying these matrices together one finds the explicit expression for X, i.e.,

$$X = \begin{pmatrix} \cos\eta\cos\phi\cos\theta & \cos\eta\cos\phi\sin\theta & \cos\eta\sin\phi & \sin\eta \\ -\sin\theta & \cos\theta & 0 & 0 \\ -\sin\phi\cos\theta & -\sin\phi\sin\theta & \cos\phi & 0 \\ -\sin\eta\cos\phi\cos\theta & -\sin\eta\cos\phi\sin\theta & -\sin\eta\sin\phi & \cos\eta \end{pmatrix}. \tag{5.41}$$

It should be remarked that neither this basis is conserved under the action of the renormalization group equations. However, by using some additionally assumptions the mass matrices of MSSM-M take particularly simple forms in this basis. This is the rationale for using the v_i-basis in this thesis.

5.4 Minimisation of tree-level scalar potential

Due to the R-parity violating couplings and the associated $U(4)$ invariance, MSSM-M contains five doublets contributing to the neutral part of the tree-level scalar potential, i.e.,

$$H_u = \begin{pmatrix} H_u^+ \\ \frac{1}{\sqrt{2}}(v_u + \psi_u + i\phi_u) \end{pmatrix}, \tag{5.42}$$

$$\tilde{L}_\alpha = \begin{pmatrix} \frac{1}{\sqrt{2}}(v_\alpha + \psi_\alpha + i\phi_\alpha) \\ \tilde{L}_\alpha^- \end{pmatrix}. \tag{5.43}$$

In Appendix C.1 the neutral part of the tree-level scalar Higgs potential for MSSM-M is found as

$$\begin{aligned} V = &\left(M_{H_u}^2 + |\mu_\alpha|^2\right)|H_u|^2 + \left((M_L)_{\alpha\beta} + \mu_\alpha\mu_\beta^*\right)\tilde{L}_\alpha^i\tilde{L}_\beta^{i*} \\ &- \left(\varepsilon_{ij}b_\alpha\tilde{L}_\alpha^i H_u^j + \text{h.c.}\right) + \frac{1}{8}\left(g^2+g'^2\right)\left(|H_u|^2 - \left|\tilde{L}_\alpha\right|^2\right)^2, \end{aligned} \tag{5.44}$$

where small Latin indices denote $SU(2)$ indices. The minimum is found as a critical point of V, i.e., the following relations must be fulfilled at the minimisation scale,

$$\frac{\partial V}{\partial H_u^0} = 0, \tag{5.45}$$

$$\frac{\partial V}{\partial \tilde{L}_\alpha^0} = 0. \tag{5.46}$$

Straightforward differentiation gives the following tree-level minimisation conditions,

$$\left(M_{H_u}^2 + |\mu_\alpha|^2\right)v_u = b_\alpha v_\alpha - \frac{1}{8}\left(g^2+g'^2\right)\left(v_u^2 - v_d^2\right)v_u, \tag{5.47}$$

$$\left((M_L)_{\alpha\beta} + \mu_\alpha\mu_\beta^*\right)v_\beta = b_\alpha v_u + \frac{1}{8}\left(g^2+g'^2\right)\left(v_u^2 - v_d^2\right)v_\alpha. \tag{5.48}$$

Here v_d is defined by Eq. (5.32).

By rotating away the sneutrino vacuum expectation values, the minimisation conditions, Eqs. (5.47) and (5.48), take the following simplified forms,

$$M_{H_u}^2 + |\mu|^2 = b_0 \cot\beta + \frac{M_Z^2}{2}\cos 2\beta, \tag{5.49}$$

$$M_{H_d}^2 + |\mu|^2 = b_0 \tan\beta - \frac{M_Z^2}{2}\cos 2\beta, \tag{5.50}$$

$$\varepsilon_i + \mu_i \mu_0^* = b_i \tan\beta. \tag{5.51}$$

In the next section it will be argued that the coupling μ_i must be almost vanishing in order to keep the neutrino masses light enough. One can therefore assume that μ_i can be completely rotated away along with v_i, a choice which will be referred to as *complete alignment*. Complete alignment gives the following minimisation conditions,

$$M_{H_u}^2 + |\mu|^2 = b\cot\beta + \frac{M_Z^2}{2}\cos(2\beta), \tag{5.52}$$

$$M_{H_d}^2 + |\mu|^2 = b\tan\beta - \frac{M_Z^2}{2}\cos(2\beta), \tag{5.53}$$

$$\varepsilon_i = b_i \tan\beta. \tag{5.54}$$

Here $|\mu|^2$ is defined by

$$|\mu|^2 = \sum_{\alpha=0}^{3} |\mu_\alpha|^2. \tag{5.55}$$

Note that if also the couplings μ_i and b_i where to vanish, then the tree-level minimisation conditions of MSSM-M are equal to the ones from MSSM-D (and MSSM, see e.g., Ref. [35]). The assumptions leading to this equality between MSSM-M and MSSM can be summarised as follows,

$$v_\alpha^a = (v_d, 0, 0, 0), \tag{5.56}$$

$$\mu_\alpha^a = (\mu, 0, 0, 0), \tag{5.57}$$

$$b_\alpha^a = (b_0, 0, 0, 0). \tag{5.58}$$

Also the definition from Eq. (5.32) is used.

Note that under the assumptions of Eqs. (5.56) - (5.58) the minimisation conditions lead to a vanishing ε_i, at the minimisation scale.

It is important to realize that these parameters run differently under the action of the renormalization group equations. That is, alignment made at the electroweak scale will not be maintained at other scales. This fact will be further explored in Sec. 5.7.

5.5 Mass matrices and mixing in MSSM-M

Due to the baryon symmetry of Eq. (3.1), the quark (and gluino) mass-matrices are equal to the corresponding ones in MSSM. However, the mixing of $\hat{H}_d$ and L_i affects all other mass matrices of MSSM-M. Especially, there will be mixing among MSSM leptons and charginos, which leads to 5 charged Dirac fermions. The neutrinos and neutralinos of MSSM will also mix together, leading to 7 neutral Majorana fermions. Also the sparticles will mix due to the $U(4)$-symmetry, and there are 8 charged and 10 neutral scalars.

Despite this mixing it will be shown that under complete alignment, and by using the v_i-basis, the mass matrices of MSSM-M take almost identical forms as they do in MSSM. Thus also the Feynman rules of MSSM [47] only need minor changes in order to be adopted to MSSM-M.

5.5.1 Neutral fermions

As explained above, there are 7 neutral Majorana fermions in MSSM-M. These will be referred to as *neutral fermions*, and the terms neutralinos will be reserved to the neutral Majorana fermions of MSSM and MSSM-D.

In the basis $\Phi_N^T = \left\{\lambda_B, \lambda_A^3, \psi_{H_u^0}, \psi_{L_\alpha^0}\right\}$ the 7×7 mass matrix for the neutral fermions becomes,

$$M_N = \begin{pmatrix} M_1 & 0 & M_Z s_w s_\beta & -M_Z s_W v_\beta/v \\ 0 & M_2 & -M_Z c_W s_\beta & M_Z c_W v_\beta/v \\ M_Z s_W s_\beta & -M_Z c_W s_\beta & 0 & \mu_\beta \\ -M_Z s_W v_\alpha/v & M_Z c_W v_\alpha/v & \mu_\alpha & 0_{\alpha\beta} \end{pmatrix}, \tag{5.59}$$

where $s_W = \sin\theta_W$, $c_W = \cos\theta_W$, $s_\beta = \sin\beta$ and $c_\beta = \cos\beta$.

Since this mass matrix is symmetric it can be diagonalised by use of one unitary matrix, i.e.,

$$Z_N^T M_N Z_N = \mathrm{diag}\left(m_{\tilde{\chi}_i^0}, m_{\nu_j}\right),\ i = 1,2,3,4,\ \text{and}\ j = 1,2,3, \tag{5.60}$$

where m_{ν_j} is identified with the observed neutrino masses. Using the mixing matrix, Z_N, the mass eigenstates are related to Φ_N as follows,

$$\lambda_B = iZ_N^{1i}\,\tilde{\chi}_i^0, \tag{5.61}$$
$$\lambda_A^3 = iZ_N^{2i}\,\tilde{\chi}_i^0, \tag{5.62}$$
$$\psi_{H_u^0} = Z_N^{3i}\,\tilde{\chi}_i^0, \tag{5.63}$$
$$\psi_{L_\alpha^0} = Z_N^{(\alpha+4)i}\,\tilde{\chi}_i^0. \tag{5.64}$$

Neutrino masses and alignment

The mass matrix of Eq. (5.59) shows that there may be mixing among the gauge eigenstates ν_α and the other neutral gauge eigenstates, i.e., the neutral gauge fermions and neutral higgsinos. In the v_i-basis the only parameter associated with this mixing is the bilinear term μ_α. If this parameter also vanishes in the v_i-basis, then there are no mixing among the neutrinos and neutralinos of MSSM. This choice means that v_α and μ_α are aligned in the $U(4)$-space. It turns out that this alignment is crucial in order to obtain phenomenologically acceptable neutrino masses in MSSM-M.

To study this alignment in greater detail it is useful to introduce the following definition,

$$\cos\xi \equiv \frac{\sum_\alpha v_\alpha \mu_\alpha}{v_d \mu}, \tag{5.65}$$

where Eqs. (5.56) and (5.57) have been used.

Generally, 2 of the 7 eigenvalues of the mass matrix, Eq. (5.59), always vanish. These two eigenvalues are to be identified with two of the three observed neutrinos. Unfortunately, the third would-be-neutrino acquire a large mass due to mixing among neutral gauginos and higgsinos. Its mass is of the order of the mass for the neutralinos of MSSM, i.e., of the order 100 GeV. To see this the following estimate for the alignment can be made.

First, the largest neutrino mass from Eq. (5.59) is found to be of order [50],

$$m_\nu \sim M_Z \cos^2\beta \sin^2\xi, \tag{5.66}$$

assuming all relevant masses are at the electroweak scale. A rough estimate for the alignment is then obtained by using the following conservative estimate for the neutrino masses, $m_{\nu_3} < 18.2$ MeV. This estimate obtained from direct search [51], gives the following limit for the amount of alignment,

$$\sin^2\xi < \frac{18.2\,\text{MeV}}{M_Z}\left(1+\tan^2\beta\right) \simeq 10^{-3}, \quad \text{for} \quad \tan\beta = 2. \tag{5.67}$$

One should, however, note that recent observations favour a degenerate set of neutrino masses (see e.g., Ref. [52]), that is, all neutrino masses could be of the order 1 eV. Such a small neutrino mass will lead to a much more stringent bound for the alignment, i.e,

$$\sin^2\xi \sim 10^{-11}. \tag{5.68}$$

The exact values for the neutrino masses are not of crucial importance for this thesis. The important observation is that in order to achieve the small neutrino masses indicated by neutrino oscillation observations, there must be almost complete alignment. Thus a reasonable assumption is simply to assume that one indeed has complete alignment, that is, $\mu_i = 0$ in the v_i-basis.

At this point one should note that these considerations regarding the neutrino masses are only valid at the tree-level. At the one-loop level the neutrinos acquires small

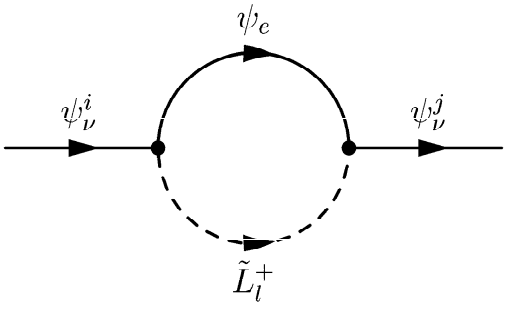

Figure 5.1: The figure shows an example of the kind of diagrams which will contribute to the neutrino mass matrix at the one-loop level. In MSSM-M also quark-squark pairs will contribute to the one-loop neutral fermion mass matrix.

masses from loop-diagrams like the one shown in Fig. 5.1, see e.g, Ref. [50]. It is an interesting observation that this one-loop contribution to the neutral fermion mass matrix has to be finite. In fact, a counter-term in the $\overline{\text{DR}}$-scheme is actually forbidden by hypercharge conservation, see also discussion in sec. 2.1.

Rotate away the sneutrino vacuum expectation values
By rotating away the sneutrino vacuum expectation values and assuming complete alignment, the mass matrix M_N, takes the simpler form,

$$M_N^a = \begin{pmatrix} M_1 & 0 & M_Z s_W s_\beta & -M_Z s_W c_\beta & 0_{1\times 3} \\ 0 & M_2 & -M_Z c_W s_\beta & M_Z c_W c_\beta & 0_{1\times 3} \\ M_Z s_W s_\beta & -M_Z c_W s_\beta & 0 & \mu^a & 0_{1\times 3} \\ -M_Z s_W c_\beta & M_Z c_W c_\beta & \mu^a & 0 & 0_{1\times 3} \\ 0_{3\times 1} & 0_{3\times 1} & 0_{3\times 1} & 0_{3\times 1} & 0_{3\times 3} \end{pmatrix}, \tag{5.69}$$

where $s_W = \sin\theta_W$, $c_W = \cos\theta_W$, $s_\beta = \sin\beta$ and $c_\beta = \cos\beta$.

This mass matrix has a 4×4 submatrix identical to the neutralino mass matrix in MSSM. It is also clear from Eq. (5.69) that there are three vanishing eigenvalues, i.e., the three neutrino masses vanishes.

5.5.2 Charged fermions

Also the charged Higgsinos, the charged gauginos and the charged leptons may mix due to the $U(4)$-symmetry. These mixed states will be referred to as *charged fermions*. In the basis

$$\Psi^{-T} = \left(\lambda_A^-, \psi_{L_\alpha^-}\right) \quad \text{and} \quad \Psi^{+T} = \left(\lambda_A^+, \psi_{H_u^+}, \psi_{e_i^+}\right), \tag{5.70}$$

where

$$\lambda_A^\pm = \frac{1}{\sqrt{2}}\left(\lambda_A^1 \mp i\lambda_A^2\right), \tag{5.71}$$

the 5×5 charged fermion mass matrix take the form,

$$M_C = \begin{pmatrix} M_2 & \sqrt{2}M_W \sin\beta & 0_{1\times 3} \\ \sqrt{2}M_W v_\alpha / v & -\mu_\alpha & -\frac{1}{\sqrt{2}}\lambda_{\alpha\beta k} v_\beta \end{pmatrix}. \tag{5.72}$$

Generally, two unitary matrices are needed to diagonalise this mass matrix, i.e.,

$$(Z_-)^\dagger M_C Z_+ = \mathrm{diag}\left(m_{\tilde{\kappa}_1^-}, m_{\tilde{\kappa}_2^-}, m_i\right). \tag{5.73}$$

This is in analogy to the chargino mass matrix of MSSM. Here the mass-eigenstates $m_{\tilde{\chi}_i}$ is to be identified with the charginos of MSSM, and the eigenstates m_i with the positively charged leptons of the Standard Model.

The mass eigenstates $\tilde{\kappa}_i$ are defined as,

$$\tilde{\kappa}_i = \begin{pmatrix} \tilde{\kappa}_i^+ \\ \bar{\tilde{\kappa}}_i^- \end{pmatrix}, \qquad i = 1, 2, \ldots, 5. \tag{5.74}$$

In terms of these mass-eigenstates the basis-elements of $\Psi^\pm$ can be expressed as,

$$\lambda_A^\pm = iZ_\pm^{1i}\tilde{\kappa}_i^\pm, \qquad \psi_{H_u^+} = Z_+^{2i}\tilde{\kappa}_i^+, \tag{5.75}$$

$$\psi_{H_d^-} = Z_-^{2i}\tilde{\kappa}_i^-, \qquad \psi_{e_i^+} = Z_+^{2+i,j}\tilde{\kappa}_j^+, \tag{5.76}$$

$$\psi_{L_i^-} = Z_-^{2+i,j}\tilde{\kappa}_j^-. \tag{5.77}$$

Rotate away the sneutrino vacuum expectation values
Under complete alignment in the v_i-basis the chargino mass matrix takes the simpler form,

$$M_C^a = \begin{pmatrix} X_{2\times 2} & 0_{2\times 3} \\ 0_{3\times 2} & \frac{1}{\sqrt{2}} v_d \left(Y_e^a\right)_{3\times 3} \end{pmatrix}, \tag{5.78}$$

where

$$X = \begin{pmatrix} M_2 & \sqrt{2}M_W \sin\beta \\ \sqrt{2}M_W \cos\beta & -\mu \end{pmatrix}. \tag{5.79}$$

Thus, in the v_i-basis the charged fermion mass matrix, M_C^a, is reduced into two block-matrices of dimension 2×2 and 3×3. The 2×2 matrix, X, is identical to the mass matrix for the charged scalar Higgs bosons of MSSM. And the 3×3 matrix, Y_e^a, is equal to the Yukawa matrix for the charged leptons of the Standard Model.

At this stage the Yukawa-matrix, Y_e^a, does not have to be diagonal. However, after making the rotation to the v_i-basis a new rotation among the superfields L_i^a can be made. Thus one can always define a basis for L_i where this Yukawa-matrix is diagonal. These diagonal elements are then related to the Standard Model charged leptons in the usual way, i.e.,

$$(Y_e)_{ii} = \frac{\sqrt{2}m_e^i}{v\cos\beta}, \qquad i = 1,2,3. \tag{5.80}$$

Due to this simple form for the mass matrix, explicit expressions can be obtained for the mixing matrix and eigenvalues. Following Ref. [28] the mixing matrices takes the following form,

$$Z^- = \begin{pmatrix} U_{2\times 2} & 0_{2\times 3} \\ 0_{3\times 2} & \mathbf{1}_{3\times 3} \end{pmatrix}, \qquad Z^+ = \begin{pmatrix} V_{2\times 2} & 0_{2\times 3} \\ 0_{3\times 2} & \mathbf{1}_{3\times 3} \end{pmatrix}, \tag{5.81}$$

where

$$U = O_-, \quad V = \begin{cases} O_+, & \det X \geq 0, \\ \sigma^3 O_+, & \det X < 0, \end{cases} \quad O_\pm = \begin{pmatrix} \cos\phi_\pm & \sin\phi_\pm \\ \sin\phi_+ & \cos\phi_+ \end{pmatrix}. \tag{5.82}$$

The mixing angles are given by

$$\tan 2\phi_+ = \frac{2\sqrt{2}M_W\mu\cos\theta_W + M_2\sin\theta_W}{M_2^2 - \mu^2 \mp 2M_W^2\cos 2\theta_W}, \tag{5.83}$$

$$\tan 2\phi_- = \frac{2\sqrt{2}M_W\mu\sin\theta_W + M_2\cos\theta_W}{M_2^2 - \mu^2 + 2M_W^2\cos 2\theta_W}. \tag{5.84}$$

Explicit expressions for the masses can be obtained, see Eq. (D.13).

5.5.3 Charged scalar sector

The 8×8 squared mass matrix for the charged scalars in the gauge-basis $\Phi_{\rm CS}^T = \left(H_u^+, \tilde{L}_\alpha^{2*}, \tilde{e}_i\right)$ is shown in Eq. (D.30). By rotating to the v_i-basis, and assuming

complete alignment, this matrix simplifies considerably, i.e.,

$$M^2_{\rm cs} = \begin{pmatrix} M_W^2 \cos^2\beta + b_0 \cot\beta & M_W^2 \sin\beta\cos\beta + b_0 & b_j & 0_j \\ M_W^2 \sin\beta\cos\beta + b_0 & M_W^2 \sin^2\beta + b_0 \tan\beta & b_j \tan\beta & 0_j \\ b_i & b_i \tan\beta & \left(M^2_{\tilde{L}}\right)_{ij} & \left(M^2_{\tilde{L}}\right)_{i,3+j} \\ 0 & 0 & \left(M^2_{\tilde{L}}\right)_{3+i,j} & \left(M^2_{\tilde{L}}\right)_{3+i,3+j} \end{pmatrix}, \tag{5.85}$$

where $M^2_{\tilde{L}}$ is the 6×6 squared mass matrix for the sleptons in MSSM, see Eq. (D.5), i.e.,

$$M^2_L = \begin{pmatrix} M_L^2 + M_l^2 + \Delta_L & v\left(a_e \cos\beta + \mu Y_e \sin\beta\right) \\ v\left(a_e^\dagger \cos\beta + \mu^* Y_e^\dagger \sin\beta\right) & M_e^2 + M_l^2 + \Delta_e \end{pmatrix}, \tag{5.86}$$

where

$$\Delta_L = M_Z^2 \left(\frac{1}{2} + \sin^2\theta_W\right)\cos(2\beta), \tag{5.87}$$

$$\Delta_e = M_Z^2 \sin^2\theta_W \cos(2\beta). \tag{5.88}$$

The squared mass matrix for the charged scalars is symmetric and is therefore diagonalised by only one matrix, i.e.,

$$Z_L^\dagger\, M^2_{\tilde{L}}\, Z_L = \mathrm{diag}(m^2_{L_i}), \qquad i = 1, 2, \ldots, 8. \tag{5.89}$$

By using this mixing matrix the gauge eigenstates and mass eigenstates are related as follows,

$$H_u^- = Z_L^{1i}\, \tilde{L}_i, \tag{5.90}$$

$$\tilde{L}^{2*}_\alpha = Z_L^{(2+\alpha)i*}\, \tilde{L}_i, \tag{5.91}$$

$$\tilde{e}_j = Z_L^{(5+j)i}\, \tilde{L}_i. \tag{5.92}$$

Note that if b_i vanishes there will be no mixing among the MSSM charged Higgs scalars and sleptons.

Finally, we note that the squared mass matrix, Eq. (5.85), always has one vanishing eigenvalue. This is the Goldstone boson, which appears explicitly in the Feynman gauge used in this thesis, see e.g., Ref. [47]. In the physical (unitary) gauge this degree of freedom is absorbed by the W bosons.

5.5.4 Neutral scalar sector

The squared mass matrix for the CP-even neutral scalars is shown in Eq. (D.39) for the gauge basis $\Phi_0^T = (\psi_u, \psi_\alpha)$. By assuming complete alignment in the v_i-basis the

squared mass matrix for the CP-even neutral scalars takes the simpler form,

$$M^2_{\text{even}} = \begin{pmatrix} M_Z^2 \sin^2\beta + b_0 \cot\beta & -M_Z^2 \cos\beta \sin\beta - b_0 & b_j \\ -M_Z^2 \cos\beta \sin\beta - b_0 & M_Z^2 \cos^2\beta + b_0 \tan\beta & b_j \tan\beta \\ b_i & b_i \tan\beta & (M^2_{\text{even}})_{2+i,2+j} \end{pmatrix}, \quad (5.93)$$

where

$$\left(M^2_{\text{even}}\right)_{i,j} = \left(M_L^2\right)_{ij} + \frac{M_Z^2}{2} \cos 2\beta\, \delta_{ij}. \quad (5.94)$$

The squared mass matrix for these CP-even neutral scalars is symmetric and is therefore diagonalised by only one matrix, i.e.,

$$Z_R^\dagger\, M^2_{\text{even}}\, Z_R = \text{diag}(m^2_{\text{e}_i}), \qquad i = 1, 2, \ldots, 5. \quad (5.95)$$

By using this mixing matrix the gauge eigenstates and mass eigenstates are relate as follows,

$$\psi_u = Z_R^{1i}\, \Phi_{\text{e}\,i}, \quad (5.96)$$

$$\psi_\alpha = Z_R^{(2+\alpha)i}\, \Phi_{\text{e}\,i}. \quad (5.97)$$

The squared mass matrix for the CP-odd neutral scalars is shown in Eq. (D.47) for the gauge basis $\Phi^T_{\text{even}} = (\phi_u, \phi_\alpha)$. Under complete alignment in the v_i-basis also this matrix simplifies considerably, i.e.,

$$M^2_{\text{odd}} - \begin{pmatrix} b_0 \cot\beta & b_0 & b_j \\ b_0 & b_0 \tan\beta & b_j \tan\beta \\ b_i & b_i \tan\beta & (M^2_{\text{odd}})_{2+i,2+j} \end{pmatrix}, \quad (5.98)$$

where

$$\left(M^2_{\text{odd}}\right)_{i,j} = \left(M_L^2\right)_{ij} + \frac{M_Z^2}{2} \cos 2\beta\, \delta_{ij}. \quad (5.99)$$

Also this squared mass matrix is symmetric and is therefore diagonalised by only one matrix, i.e.,

$$Z_H^\dagger\, M^2_{\text{even}}\, Z_H = \text{diag}(m^2_{\text{o}_i}), \qquad i = 1, 2, \ldots, 5. \quad (5.100)$$

By using this mixing matrix the gauge eigenstates and mass eigenstates are related as follows,

$$\phi_u = Z_H^{1i}\, \Phi_{\text{o},i}, \quad (5.101)$$

$$\phi_\alpha = Z_R^{(2+\alpha)i}\, \Phi_{\text{o},i}. \quad (5.102)$$

As for the squared mass matrix for the charged scalars, the squared mass matrix for the CP-odd neutral scalars, i.e., Eq. (5.98), has one vanishing eigenvalue. This is the Goldstone boson, which appears explicitly in the Feynman-gauge. In the physical (unitary) gauge this degree of freedom is absorbed by the Z-boson.

To conclude this section, it is found that under complete alignment in the v_i-basis all mass matrices in MSSM-M takes rather simple forms. If also b_i were to vanish then there are no mixing among the (s)particles known from MSSM. On the other hand, if b_i turns out to be too large the squared charged and neutral mass matrices, i.e., Eqs. (5.85), (5.93) and (5.98), will lead to unacceptable light scalar masses. This soft-breaking bilinear parameter is therefore one of the most important parameters of MSSM-M. The mixing matrices, defined in this section, are also of crucial importance to obtain the proper Feynman rules for MSSM-M. All Feynman rules relevant for the calculations in this thesis are shown in Appendix E.4.

5.6 Constraints from scalar masses

The squared mass matrices presented in last section clearly show the importance of the three bilinear couplings b_i. These couplings cause mixing among the scalars of H_d and $\tilde{L}_i$. In Sec. 5.9 stringent upper limits will be obtained for these three bilinear couplings. It is, however, useful also to analyse whether the scalar masses put any limits on these parameters.

By using the supergravity scenario, defined by Eqs. (3.8) - (3.10), the parameters b_i are determined at the electroweak scale by use of the minimisation conditions,

$$b_i = \varepsilon_i \cot\beta. \tag{5.103}$$

One would expect that both ε_i and b_i takes small non-vanishing values at the electroweak scale, since $\varepsilon_i = (M_L^2)_{0i} = 0$ at the GUT-scale. Therefore, any non-vanishing values at the electroweak scale must be caused by renormalization group effects, and consequently small.

In this section the squared mass matrices for charged and neutral scalars will be analysed by a different method. It is assumed that the bilinear couplings b_i are three free parameters of the model, and that ε_i is determined from the minimisation condition of Eq. (5.103). The other relevant parameters are chosen by hand as follows,

$$\tan\beta = 10, \qquad \mu = 400, \qquad b_0 = 25000\,\mathrm{GeV}^2, \tag{5.104}$$

$$M_L^2 = 70000 \cdot 1_{4\times4}\,\mathrm{GeV}^2, \quad M_e^2 = 45000 \cdot 1_{3\times3}\,\mathrm{GeV}^2, \quad a_e = 200 \cdot Y_e. \tag{5.105}$$

Even though these values are chosen rather arbitrarily they are typical representations for the values obtained by using the boundary conditions of Eqs. (3.8) - (3.10), and the renormalization group equations.

The present observational limit [23] on the charged scalars of MSSM is $m_{\tilde{\tau}} > 80$ GeV. This limit will also be used in MSSM-M. By assuming that the three bilinear couplings are equal, i.e., $b_1 = b_2 = b_3 = b$, one finds that the lightest charged scalar violates the phenomenological limit for $b \gtrsim 7000\,\mathrm{GeV}^2$. This is a large value, much larger than the ones obtained by use of the supergravity inspired boundary conditions and the renormalization group equations. It will be shown that the decay rates under study put much stronger limits on these bilinear couplings.

Finally, two observations regarding the sign of b_i should be mentioned. First, b_i can take negative values even if b_0 can always be chosen to be positive [35]. An example of its values is shown in Table 5.2. Second, the scalar masses will depend upon the sign of b_i, but only as long as all elements of λ_{ijk} or λ'_{ijk} do not vanish.

5.7 Running of parameters in MSSM-M

As for most other quantum field theories, the parameters of MSSM-M runs with energy scale. This running is determined by the renormalization group equations shown in Appendix F.2. In this section the running of some of the most important parameters of MSSM-M will be studied by analytic and numeric methods.

5.7.1 Analytic estimates

The full set of renormalization group equations must be solved by numerical methods. However, some insight into the general behaviour of the running of these parameters can be obtained by analytic methods. In order to obtain analytic approximate solutions some simplifications must be made. First, the following assumptions are made,

$$(Y_u)_{33} = y_t \neq 0, \quad \text{else} \quad Y_u = 0, \tag{5.106}$$

$$\lambda'_{033} = y_b \neq 0 \quad \text{and} \quad \lambda'_{333} \neq 0, \quad \text{else} \quad \lambda'_{\alpha ij} = 0, \tag{5.107}$$

$$\lambda_{033} = y_\tau \neq 0 \quad \text{and} \quad \lambda_{233} = -\lambda_{323} \neq 0, \quad \text{else} \quad \lambda_{\alpha\beta k} = 0. \tag{5.108}$$

Secondly, also the following hierarchy is assumed among the Yukawa couplings at the electroweak scale,

$$y_t > y_b \gtrsim y_\tau \gtrsim \lambda'_{333} \sim \lambda_{233}. \tag{5.109}$$

Running of gauge coupling constants

The running of the gauge coupling constants do not depend on the Yukawa couplings at the one-loop level. First at the two-loop level the Yukawa couplings will make their influence, see Eqs. (F.38) - (F.40). These two-loop renormalization group

equations can be written in the more compact form,

$$\frac{dg_i}{dt} = \beta_{g_i}^{\rm MSSM} + \Delta\beta_{g_i},\ i = 1,2,3 \qquad \text{where} \tag{5.110}$$

$$\Delta\beta_{g_i} = -\frac{g_i^4}{(16\pi^2)^2} B_i\, \lambda'^2_{333}, \quad \text{and} \quad B_i = \left(\frac{14}{5}, 6, -4\right). \tag{5.111}$$

Here $\beta_{g_i}^{\rm MSSM}$ is the two-loop β-function obtained in MSSM, and $\Delta\beta_{g_i}$ is the contribution from the trilinear couplings.

This shows that the effect of the R-parity violating couplings will lower the values for g_1 and g_2, and raise the value for g_3 at the GUT-scale. By comparing with the running of the gauge couplings obtained in Sec. 4.4, see Fig. 4.2, one observes that the inclusion of the R-parity violating couplings makes the gauge couplings unify better. Such an analysis has been made in Ref. [53] and confirms these qualitative statements.

Running of Yukawa couplings

The renormalization group equation of Eq. (F.53) shows that the running of the top-quark Yukawa coupling, y_t, depends on λ'_{ijk} but not on $\lambda_{\alpha jk}$. However, due to the hierarchy assumed in Eq. (5.109) the running of y_t is almost unaffected by the existence of these small R-parity violating couplings. That is, to a good approximation y_t will run in MSSM-M as it does in MSSM, or MSSM-D. By the same reasoning this conclusion is also valid for the two Yukawa couplings y_b and y_τ. That is, to a first approximation these parameters run in MSSM-M as they do in MSSM.

Moreover, since the couplings λ_{233} and y_τ are elements of the same $U(4)$-tensor one would expect these parameters to change by almost the same amount. Such a behaviour is also expected for the parameters of $\lambda'_{\alpha jk}$, that is, y_b and λ'_{333}.

It is important to realize that these R-parity violating couplings will lead to off-diagonal elements for the Yukawa matrix Y_e at the GUT-scale. Due to the existence of off-diagonal elements in the neutrino Yukawa matrix Y_ν, the Yukawa matrix Y_e also developed small off-diagonal elements in MSSM-D. In MSSM-M this neutrino Yukawa matrix is absent, and the off-diagonal elements of Y_e are associated with existence of the R-parity violating couplings, or equivalently associated with the existence of the $U(4)$-symmetry.

By using the supergravity boundary values of Eq. (3.10), i.e.,

$$\lambda^{\rm s}_{\alpha jk} = A_0\, \lambda_{\alpha jk}, \tag{5.112}$$

$$\lambda'^{\rm s}_{\alpha jk} = A_0\, \lambda'_{\alpha jk}, \tag{5.113}$$

one sees that also the soft-breaking trilinear couplings have off-diagonal elements at the GUT-scale, and also at the electroweak scale.

Running of bilinear term, μ_α

Since the bilinear term μ_α is a superpotential term, the non-renormalization the-

orem [54] applies and makes its renormalization group equation rather simple, see Eq. (F.59).

The assumptions of Eqs. (5.106) and (5.107) leads to the following renormalization group equations for μ_0 and μ_3,

$$16\pi^2 \frac{d}{dt}\mu_0 = \mu_0 \left(3y_t^2 - \frac{3}{5}g_1^2 - 3g_2^2 \right) + 3\mu_3 y_b \lambda'_{333}, \tag{5.114}$$

$$16\pi^2 \frac{d}{dt}\mu_3 = \mu_3 \left(3y_t^2 - \frac{3}{5}g_1^2 - 3g_2^2 \right) + 3\mu_0 \lambda'^2_{333}. \tag{5.115}$$

The renormalization groups for μ_1 and μ_2 does not depend upon λ'_{333}, and these parameters therefore vanish at all scales if take vanishing values at the electroweak scale.

Equations (5.114) and (5.115) shows that the running of the parameters μ_0 and μ_3 are coupled to each other only through the R-parity violating coupling λ'_{333}. Also due to the hierarchy shown in Eq. (5.109) the running of μ_3 is less dependent on the running of μ_0 than the running of μ_0 depends on μ_3. Also note that if the R-parity violating coupling λ'_{333} vanishes the renormalization group equation for μ_0 becomes equal to the corresponding one from MSSM, see e.g., Ref. [35]. Equation (5.115) also shows that even if μ_3 vanishes at the M_Z-scale, it will take small non-vanishing values at an arbitrary scale. That is, complete alignment is only fulfilled at the M_Z-scale.

The renormalization group equations for the Yukawa couplings, Eqs. (F.53) - (F.55), show that their running do not depend on μ_α. Thus the general solutions of Eqs. (5.114) and (5.115) can be found by straight forward methods, i.e.,

$$\mu_0(t) = \frac{1}{16\pi^2} E_1(t) \left(16\pi^2 \mu_0^0 + 3\mu_3 \int_0^t \frac{y_b \lambda'_{333}}{E_1(t')} dt' \right), \tag{5.116}$$

$$\mu_3(t) = \frac{1}{16\pi^2} E_1(t) \left(16\pi^2 \mu_3^0 + 3\mu_0 \int_0^t \frac{\lambda'^2_{333}}{E_1(t')} dt' \right), \tag{5.117}$$

where μ_0^0 and μ_3^0 are the initial values for μ_0 and μ_3. The following definition has also been used,

$$E_1(t) = \exp\left\{ \frac{1}{16\pi^2} \int_0^t \left(3y_t^2 - \frac{3}{5}g_1^2 - 3g_2^2 \right) dt' \right\}. \tag{5.118}$$

As explained in Sec. 4.4 the combination $3y_t^2 - \frac{3}{5}g_1^2 - 3g_2^2 > 0$ for most of the parameter space. Thus we expect both μ_0 and μ_3 to be increasing functions with increasing values for t. This is confirmed by a full numerical solution of the renormalization group equations.

This ends the qualitative analysis of the running of the superpotential parameters.

Particles	Masses (in GeV)
Charged fermions	$4.87 \cdot 10^{-4}$, 0.102, 1.75, 175, 459
Neutral fermions	0, 0, 0, 94.6, 181.1, 448.4, 452.1
Charged scalars	80.41, 198.1, 210.9, 211.0, 258.6, 258.6, 266.4, 512.8
Neutral scalars, CP-even	89.3, 261.9, 262.2, 262.2, 506.8
CP-odd	91.2, 261.9, 262.2, 262.2, 506.5
Squarks, up-type	448.9, 658.5, 658.5, 676.9, 676.9, 698.6
down-type	599.4, 656.8, 656.8, 664.4, 682.6, 682.6
b_i	(25400, -0.56, -0.56, -0.54)

Table 5.2: The table shows the masses and parameters which are obtained by using the supergravity input parameters $\tan\beta = 10$, $\mathrm{sign}(\mu) = +1$, $M_0 = 200\,\mathrm{GeV}$, $M_{1/2} = 250\,\mathrm{GeV}$ and $A_0 = 200\,\mathrm{GeV}$. All masses are in GeV.

5.7.2 Numerical analysis

The full set of renormalization group equations is quite complicated in MSSM-M and has to be solved by numeric methods. In this thesis the 2-loop renormalization group equations for the gauge-coupling constants and gaugino masses, and the 1-loop renormalization group equations for the Yukawa couplings and soft-breaking parameters are used. This set of differential equations has been solved by Fortran-routines provided by the Numerical Algorithm Group [55].

At the electroweak scale the Yukawa matrix Y_e is related to the known charged lepton masses, see Eq. (5.80). After specifying the boundary values for the gauge- and Yukawa couplings at the electroweak scale, the renormalization group equations are run up to the GUT-scale where the supergravity inspired boundary values of Eqs. (3.8) - (3.10) are used. Finally, all renormalization group equations are run down to the electroweak scale, where the scalar potential is minimised. This process is iterated until a stable solution, satisfying all boundary values and the minimisation conditions, is found. In the literature this method is referred to as the shooting method [56], or the ambidextrous approach [38].

The following numerical values will be used in order to discuss the running of the most important parameters of MSSM-M,

$$\tan\beta = 10, 30, 50, \quad \mathrm{sign}(\mu) = +1, \tag{5.119}$$

$$M_0 = 200\,\mathrm{GeV}, \quad A_0 = 200\,\mathrm{GeV}, \quad M_{1/2} = 250\,\mathrm{GeV}, \tag{5.120}$$

$$\lambda_{ijk} = -\lambda_{jik} = 0.05, \tag{5.121}$$

$$\lambda'_{ijk} = 0.05, \quad \text{for all } i, j, k = 1, 2, 3. \tag{5.122}$$

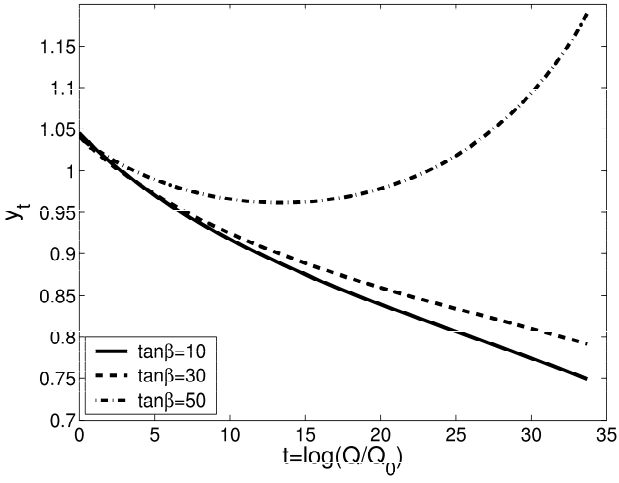

Figure 5.2: The figure shows the running of the top-quark Yukawa coupling y_t, for three values of $\tan\beta$.

By solving the renormalization group equations and the minimisation conditions a consistent set of parameters are found. These parameters determine all masses and couplings of one particular realisation of MSSM-M. Table 5.2 shows the particle masses obtained by the boundary conditions.

Due to its size the top-quark Yukawa coupling is the most important Yukawa coupling, determining the running for the other parameters. Its running is shown in Fig. 5.2. Even if the R-parity violating coupling λ'_{ijk} contributes to its running, the running of Y_u is almost identical to the one obtained in MSSM-D, see Fig. 4.3.

Complete alignment, as defined in Sec. 5.5, means that the three superpotential couplings μ_i vanishes at the minimisation scale. However, as explained in last section, these couplings takes non-vanishing values at all other scales, due to renormalization group effects. Examples of the running of μ_0 and μ_3 are shown in Fig. 5.3, for $\tan\beta = 10$, 30 and 50. These figures shows that μ_3 does not vary much, however, the largest variation comes for large values of $\tan\beta$. This is due to the dependency of the top-quark Yukawa coupling. This also confirms the qualitative discussion in the last section.

The three soft-breaking bilinear couplings ε_i are defined by $\varepsilon_i = (M_L^2)_{0i} = (M_L^2)_{i0}$, and vanishes at the GUT-scale due to the supergravity inspired boundary condition $(M_L^2)_{\alpha\beta} = M_0^2\, 1_{\alpha\beta}$. At the electroweak scale these parameters and the minimisation conditions determine b_i. Figure 5.4 shows some examples of the running of these parameters for three values of $\tan\beta$. These figures show that neither of the parameters b_1 and ε_1 suffers from large changes. The largest contribution come from large values of $\tan\beta$, due to the dependency of the large top-quark Yukawa coupling. This

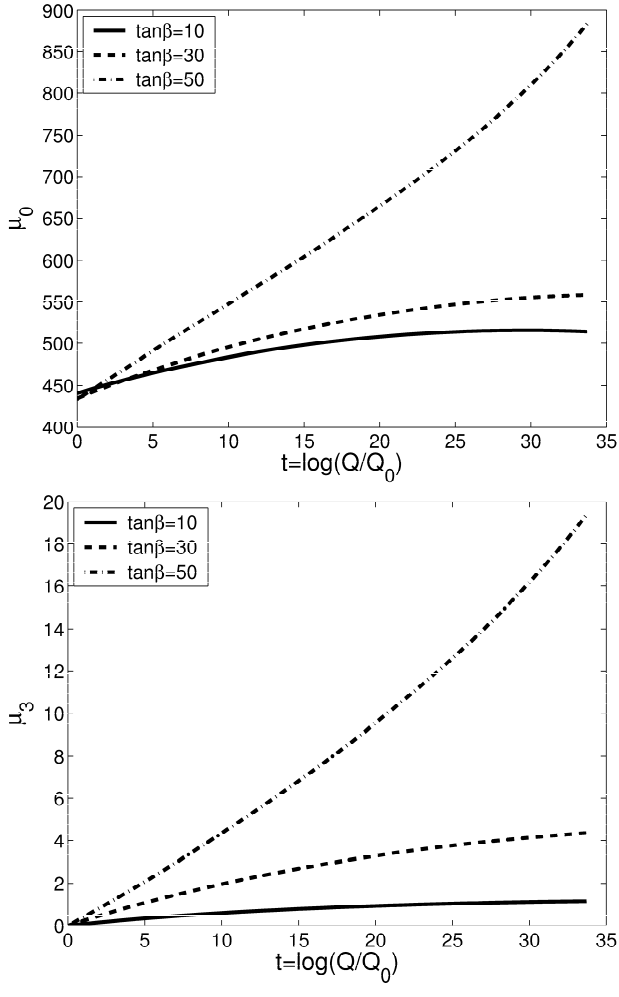

Figure 5.3: The figure shows the running of the bilinear superpotential parameters μ_0 and μ_3, for three values of $\tan\beta$.

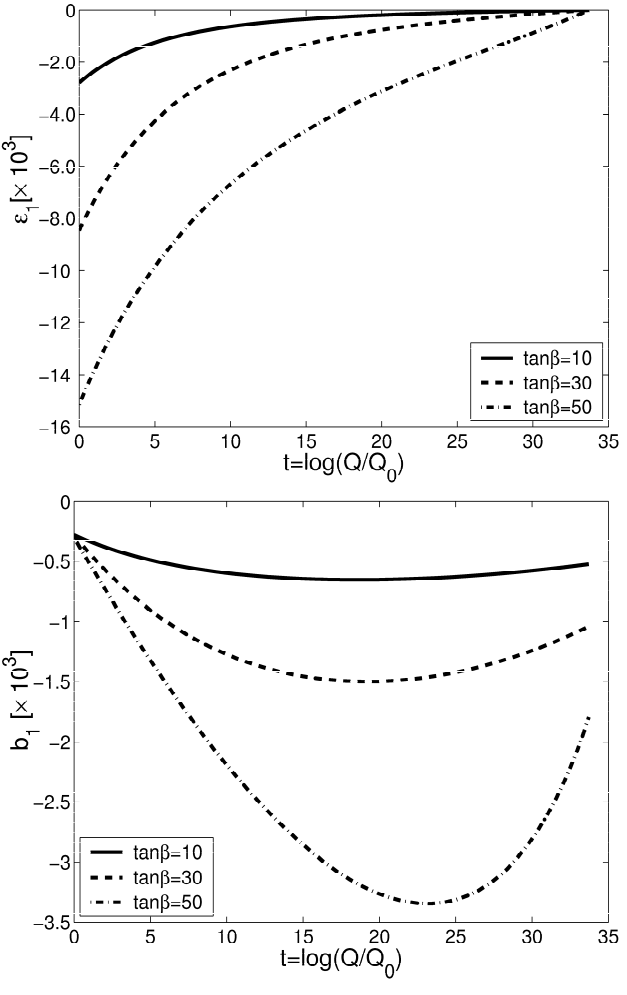

Figure 5.4: The figure shows the running of the bilinear soft-breaking parameters ε_1 and b_1, for three values of $\tan\beta$.

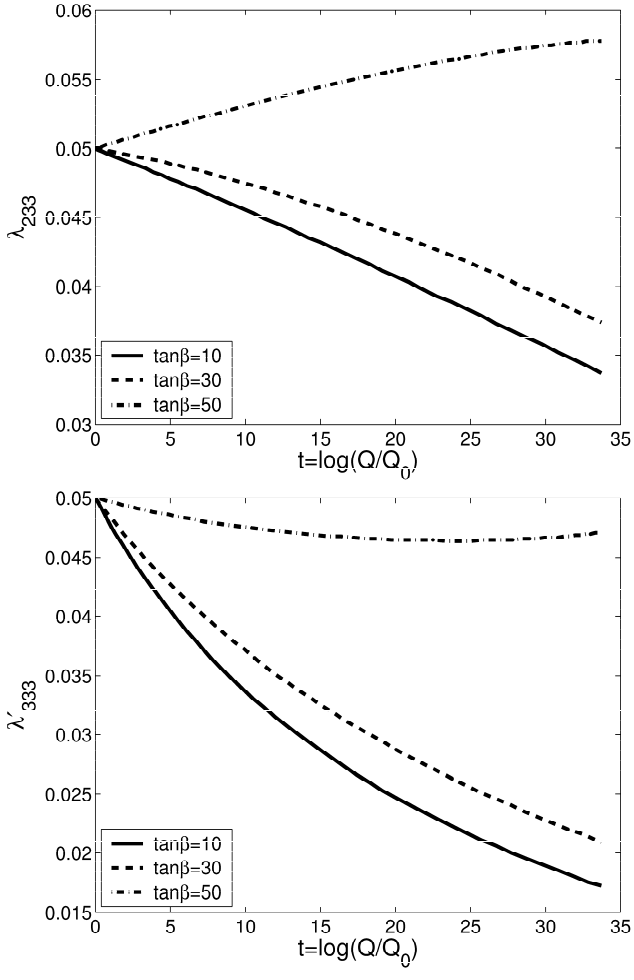

Figure 5.5: The figure shows the running of the trilinear R-parity violating superpotential parameters λ_{233} and λ'_{333}, for three values of $\tan\beta$.

confirms the analytic solutions obtained in Eq. (5.117).

It is also of importance to know the running of the trilinear couplings λ_{ijk}, λ'_{ijk}, λ^{s}_{ijk} and λ''^{s}_{ijk}. Examples of the running of λ_{ijk} and λ'_{ijk} for the values $\tan\beta = 10$, 30 and 50, are shown in Fig. 5.5. And the running of the soft-breaking parameters λ^{s}_{233} and λ'^{s}_{333} are shown in Fig. 5.6 for three values of $\tan\beta$.

The running of the gauge couplings are of special interest. In Ref. [53] it was shown that the R-parity breaking parameters will alter the running of the gauge couplings at the two-loop level. This is clearly seen from the renormalization group equations

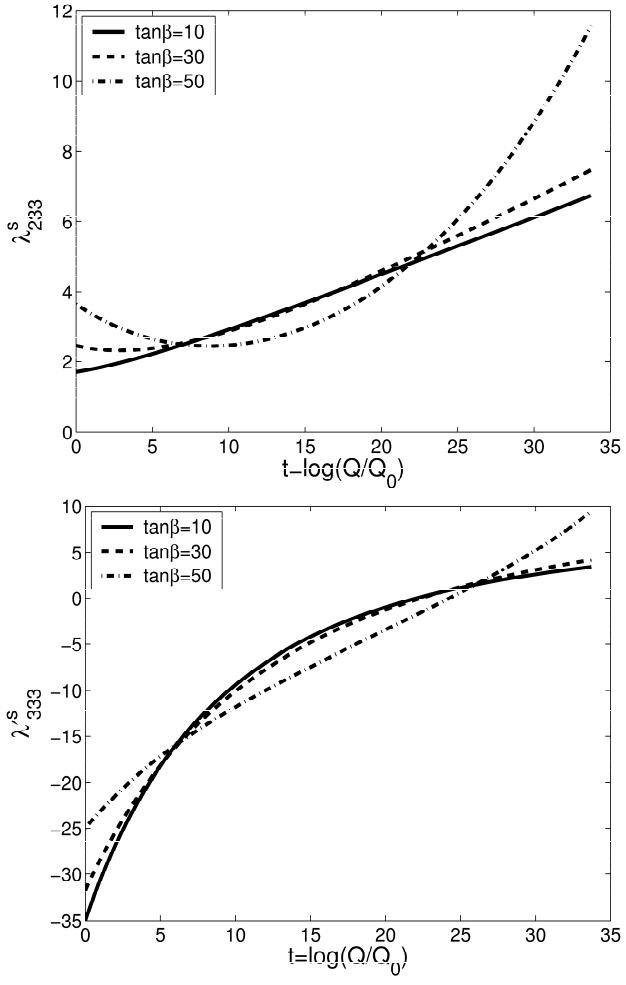

Figure 5.6: The figure shows the running of the soft-breaking trilinear parameters λ^s_{233} and λ^s_{333}, for three values of $\tan\beta$.

in Eq. (F.38) - (F.40). The running of the gauge coupling constant is almost identical to the one found in MSSM-D, see Fig. 4.2. For a thorough analysis of the influence the R-parity violating couplings will have on the running of the gauge coupling constants, please refer to Ref. [53].

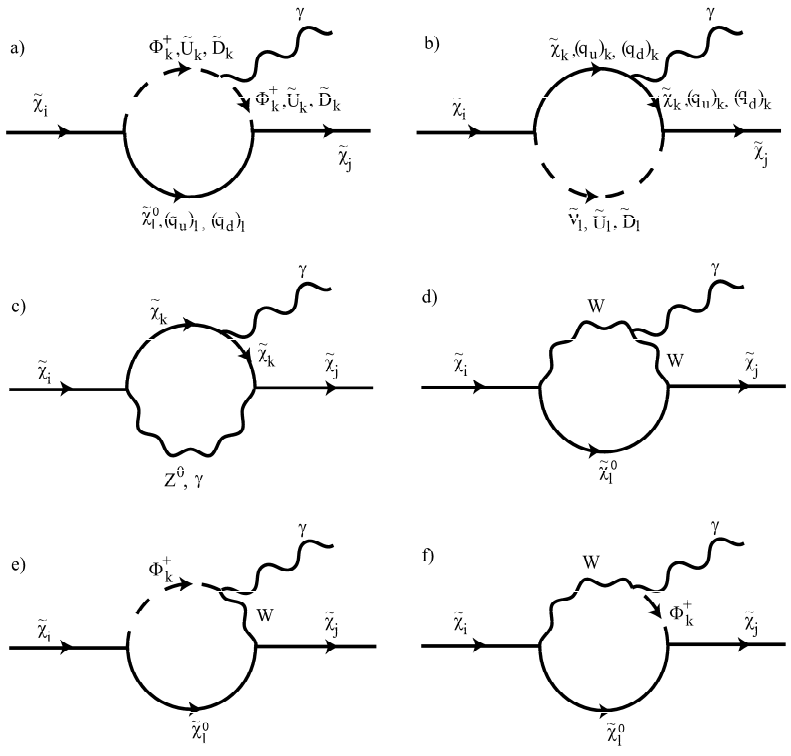

Figure 5.7: The figure shows all Feynman diagrams, at the one-loop level, which may contribute to the decay channels $l \to l'\gamma$ in MSSM-M. Note that (s)quarks will also contribute.

5.8 Qualitative analysis of $\Gamma(l \to l'\gamma)$ in MSSM-M

In next section the numerical analysis of the decay rates $\Gamma(l \to l'\gamma)$ will be presented. It is, however, necessary to make some qualitative discussion of the importance of the different R-parity violating parameters.

All amplitudes, which may contribute to the decay channels $l \to l'\gamma$ in MSSM-M, are shown in Fig. 5.7. Note that due to the existence of the trilinear R-parity violating couplings λ'_{ijk}, also quarks and squarks will contribute to these decay rates.

The Feynman rules, relevant for these decay rates, are presented in Appendix E.2, and general expressions for the amplitudes are presented in Appendix B.5. As in the sections above, the assumption of complete alignment in the v_i-basis will be used throughout this analysis, that is, $v_i = \mu_i = 0$, at the electroweak scale.

The diagrams represented by Fig. 5.7 a) and b) are the important ones. These dia-

grams involve sparticles and charged and neutral leptons from the Standard Model, and also the (s)quark contribution.

The other diagrams, i.e., the diagrams of Fig. 5.7 c) - f), do not contribute under the assumption of complete alignment in the v_i-basis. This is most easily seen from the charged and neutral fermion mass matrices, i.e., Eqs. (5.78) and (5.69). Both of these mass matrices have a diagonal lower 3×3 sub-matrix, associated with the Standard Model charged and neutral leptons, respectively. This means that neither charged nor neutral fermions mix with each other, or with any of the Higgs superfields $\hat{H}_u$ or $\hat{H}_d$. Thus, there are no lepton family violations associated with either charged nor neutral leptons of the Standard Model. It should be stressed that this conclusion is valid only at the one-loop level, and at a particular energy scale. Taking higher loop corrections into account, the neutrinos will be massive and mix together.

The mass matrices presented in Sec. 5.5 shows that, under complete alignment, the neutral and charged fermion mass matrices have no explicit dependency on the R-parity violating parameters λ_{ijk} or λ'_{ijk}, or on any of the soft breaking parameters λ^{s}_{ijk}, λ'^{s}_{ijk}, b_i or ε_i. On the other hand, the three soft breaking bilinear parameters b_i appears explicitly in the squared mass matrices for the charged and neutral scalars, i.e., in Eqs. (5.85), (5.93) and (5.98). A first rough upper limit for b_i was obtained in Sec. 5.6 by imposing lower limits for the charged scalar masses.

The Feynman rules presented in Appendix E.3 shows that the decay rates do not have any explicit dependency on the soft breaking trilinear couplings, λ^{s}_{ijk} and λ'^{s}_{ijk}. These trilinear soft breaking couplings therefore only make their appearance through renormalization group effects. Upper limits on the soft-breaking trilinear couplings may therefore be difficult to obtain from the decay rates under study.

It is important to note that if all elements of λ'_{ijk} and λ_{ijk} vanishes, except for two elements of λ_{ijk}, e.g., $\lambda_{123} = -\lambda_{213} \neq 0$, then there can be no interesting contribution from the amplitudes of Fig. 5.7 a) and b). This is also the case if all elements of λ_{iik} and λ'_{ijk} vanish except for one element of λ'_{ijk}, e.g., $\lambda'_{123} \neq 0$.

Since b_i is a vital parameter in the squared scalar mass matrices, the numerical calculations will also analyse the decay rates by assuming that b_i are free parameters at the electroweak scale. In such a scenario, it is important to have at least two non-vanishing components of b_i, in order to ensure a non-vanishing contribution to the decay rates.

This discussion thus shows that one needs at least one of the following scenarios to be fulfilled in order to observe lepton flavour violations in the decay rates $l \to l'\gamma$,

1. At least four non-vanishing elements of λ_{ijk}.
2. At least two non-vanishing elements of λ'_{ijk}. These elements must affect the leptons, that is, the index i must take at least two different values.
3. At least two non-vanishing elements of λ_{ijk} and one non-vanishing element of λ'_{ijk}.

4. At least two non-vanishing elements of b_i.

5. At least two non-vanishing elements of λ_{ijk} or one non-vanishing element from λ'_{ijk}, and one non-vanishing element of b_i. More than one lepton flavours must be involved.

5.9 Numerical analysis

In this section the numerical analysis of the three lepton flavour violating decay channels $l \to l'\gamma$, calculated in MSSM-M, will be presented. This model is much more complicated than both MSSM and MSSM-D, since there are many new free parameters. The field content is, however, identical to MSSM. That is, there are no right-handed gauge singlet superfields in either MSSM or MSSM-M.

By using the supergravity inspired boundary conditions, there are 41 free parameters of MSSM-M. These are the 5 MSSM parameters, i.e., $\tan\beta$, sign(μ), M_0, A_0 and $M_{1/2}$, together with the 9 and 27 free parameters of λ_{ijk} and λ'_{ijk}, respectively.

The main purpose of this part of the analysis is to obtain constraints for λ_{ijk} and λ'_{ijk}, from the decay channels $l \to l'\gamma$. In order to have a well defined realisation of MSSM-M all 41 free parameters must be specified. Our strategy is to first choose a set of values for the 5 MSSM parameters. Then a texture for λ_{ijk} and λ'_{ijk} is chosen, thus reducing the number of free parameters considerably. Our primary choice for the MSSM parameters are the values shown in Eqs. (5.104) and (5.105). The masses, and some important parameters, associated with this choice, are shown in Table 5.2.

The analysis will follow the list presented in last section.

5.9.1 λ'_{ijk} vanishes

By assuming that all components of λ'_{ijk} vanishes, there will be no (s)quark contributions to the decay channels. To fully specify the model a texture for λ_{ijk} must be assumed. At this point one should remember that λ_{ijk} is anti-symmetric in its two first indices, i.e., $\lambda_{ijk} = -\lambda_{jik}$ for $i \neq j$. This antisymmetric property must, of course, always be taken into account in any texture of λ_{ijk}.

As explained in Sec. 5.8, these decay rates vanish if all elements λ_{ijk} vanish. They also vanish if only two elements of λ_{ijk} are non-vanishing, e.g., $\lambda_{123} = -\lambda_{213} \neq 0$. These two special cases are confirmed by numerical calculations, thus serving as two simple consistency checks on the numerical routines.

The first non-trivial texture to be explored, is defined by assuming that all elements of λ_{ijk} are as equal as possible, i.e.,

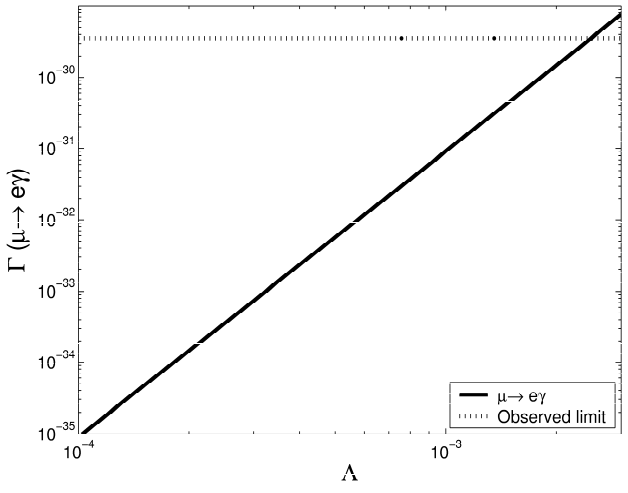

Figure 5.8: The figure shows the decay rate $\mu \to e\gamma$ calculated for varying values of Λ. Λ is defined by Eq. (5.123). The dotted horizontal line denotes the present observational limit.

$$\lambda_{ijk} = \begin{cases} \lambda_{ijk} = -\lambda_{jik} = \Lambda, & \text{for } i \neq j, \\ 0, & \text{else.} \end{cases} \tag{5.123}$$

This texture will be referred to as a uniform texture for λ_{ijk}.

The results from the numerical calculations, using this texture, are summarised in Fig. 5.8. These calculations put an upper limit of $\Lambda \leq 2.5 \cdot 10^{-3}$, for the decay rate $\mu \to e\gamma$. The other two decay rates lead to weaker bounds for Λ, i.e., $\Lambda \leq 5.9 \cdot 10^{-2}$ and $\Lambda \leq 7.4 \cdot 10^{-2}$ for $\tau \to \mu\gamma$ and $\tau \to e\gamma$, respectively. Figure 5.8 also shows that if the upper limit on $\mu \to e\gamma$ where to be improved by a factor 10000, the upper limit on Λ would roughly be lowered by a factor 10. Figure 5.8 also shows that this decay rate may be approximated by

$$\Gamma(\mu \to e\gamma) \sim \Lambda^4, \tag{5.124}$$

in its dependency on Λ, also see discussion in Appendix B.3.

The decay rates have also been calculated by assuming the following three textures,

$$\lambda_{231} = \lambda_{232} \neq 0. \tag{5.125}$$
$$\lambda_{231} = \lambda_{233} \neq 0, \tag{5.126}$$
$$\lambda_{232} = \lambda_{233} \neq 0, \tag{5.127}$$

and all other elements vanishing for each of the three textures. The antisymmetric property of λ_{ijk} must of course be implemented into each texture, i.e., $\lambda_{ijk} = -\lambda_{jik}$, for $i \neq j$.

The upper limits obtained from these three textures are shown in Table 5.3. In this table $\lambda_{2,3,2}$ and $\lambda_{2,3,3}$ are abbreviated to $\lambda_{23\binom{2}{3}}$, with equal notation for the other two columns. These calculations have also been performed for the six analogous textures

$$\lambda_{12\binom{1}{2}} \neq 0, \quad \lambda_{12\binom{1}{3}} \neq 0, \quad \lambda_{12\binom{2}{3}} \neq 0, \tag{5.128}$$

$$\lambda_{13\binom{1}{2}} \neq 0, \quad \lambda_{13\binom{1}{3}} \neq 0, \quad \lambda_{13\binom{2}{3}} \neq 0, \tag{5.129}$$

and all other elements of λ_{ijk} vanishing for each texture. The upper limits obtained for the textures shown in Eq. (5.128) are presented in Table 5.4. The textures represented by Eq. (5.129) have also been used. But the limits are only slightly weaker than the ones shown in Table 5.4. Table 5.3 and 5.4 shows the important observation that the decay rates $\tau \to \mu\gamma$ and $\tau \to e\gamma$ put the strongest constraints on some textures.

The textures of Eqs. (5.125) - (5.129) show that the strongest constraint on λ_{ijk} does not always come from $\mu \to e\gamma$. For some textures the other two decay rates will be the most constraining ones.

The following two textures have also been used,

$$\lambda_{231} = \lambda_{232} = \lambda_{233} \equiv \lambda_{23k} \neq 0, \quad k = 1, 2, 3. \tag{5.130}$$

$$\lambda_{121} = \lambda_{131} = \lambda_{231} \neq 0. \tag{5.131}$$

The results of using these textures are shown in Table 5.5. The textures defined by λ_{12k} or λ_{13k} have also been used, but the results are comparable with the ones above made from the texture presented in Eq. (5.130). As seen from the superpotential of Eq. (5.3) the last parameter of λ_{ijk} determines the contribution from the right-handed component.

The results of using the texture from Eq. (5.131) are shown in the third column of Table 5.5.

The textures of Eqs. (5.130) and (5.131) again show that $\mu \to e\gamma$ puts the strongest limits on λ_{ijk}.

To summarise this part of the analysis. The three decay rates have been calculated under the assumption that all elements of λ'_{ijk} vanish, and for several textures of λ_{ijk}. It has been shown that $\mu \to e\gamma$ puts the strongest constraint on λ'_{ijk}. But there are also textures in which the other two decay rates are the most constraining ones.

Decay channel	$\lambda_{23\binom{1}{2}} = 4.2 \cdot 10^{-3}$	$\lambda_{23\binom{1}{3}} = 1.30 \cdot 10^{-1}$	$\lambda_{23\binom{2}{3}} = 1.04 \cdot 10^{-1}$
$\tau \to \mu\gamma$	0	0	$2.5 \cdot 10^{-18}$
$\tau \to e\gamma$	0	$6.3 \cdot 10^{-18}$	0
$\mu \to e\gamma$	$3.6 \cdot 10^{-30}$	0	0

Table 5.3: This table shows the upper limits for the three decay rates. It is assumed that all elements of λ'_{ijk} vanish, and the textures presented Eqs. (5.125) - (5.127) are used. The MSSM parameters are defined in Eqs. (5.104) - (5.105).

Decay channel	$\lambda_{12\binom{1}{2}} = 4.1 \cdot 10^{-3}$	$\lambda_{12\binom{1}{3}} = 1.30 \cdot 10^{-1}$	$\lambda_{12\binom{2}{3}} = 1.04 \cdot 10^{-1}$
$\tau \to \mu\gamma$	0	0	$2.5 \cdot 10^{-18}$
$\tau \to e\gamma$	0	$6.1 \cdot 10^{-18}$	0
$\mu \to e\gamma$	$3.6 \cdot 10^{-30}$	0	0

Table 5.4: This table shows the upper limits for the three decay rates. It is assumed that all elements of λ'_{ijk} vanish, and the texture presented in Eq. (5.128) is used. The MSSM parameters are defined in Eqs. (5.104) - (5.105).

Decay channel	$\lambda_{23k} = 4.1 \cdot 10^{-3}$	$\lambda_{ij1} = 1.2 \cdot 10^{-2}$
$\tau \to \mu\gamma$	$5.1 \cdot 10^{-24}$	$3.8 \cdot 10^{-24}$
$\tau \to e\gamma$	$5.0 \cdot 10^{-24}$	$3.9 \cdot 10^{-24}$
$\mu \to e\gamma$	$3.6 \cdot 10^{-30}$	$3.6 \cdot 10^{-30}$

Table 5.5: This table shows the upper limits for the three decay rates under study. All elements of λ'_{ijk} are assumed to vanish. The textures presented in Eqs. (5.130) - (5.131) are used. The MSSM parameters are defined in Eqs. (5.104) - (5.105).

5.9.2 λ_{ijk} vanishes

If λ'_{ijk} has non-vanishing elements (s)quarks may also contribute to the decay rates under study, and it is therefore of interest to study possible limits on these trilinear couplings. It is now assumed that all elements of λ_{ijk} vanish, and several textures for λ'_{ijk} will be explored by numerical methods, and upper limits for λ'_{ijk} will be established.

One should recall that the first index of λ'_{ijk}, i.e., index i, label the lepton fields, while the next two indices, i.e., j and k, labels the (s)quarks. As explained in Sec. 5.8 the index i must take at least two different values in order to give a non-vanishing contribution to the decay-rates. This is confirmed by numerical calculations, and serves as a simple consistency check on the numerical routines.

As for the analysis above, the first nontrivial texture is to assume that all elements of λ'_{ijk} are equal, i.e.,

$$\lambda'_{ijk} = \Lambda', \quad \text{for all } i, j \text{ and } k. \tag{5.132}$$

The second column of Table 5.6 shows the upper limit obtained from this texture. This texture puts the most stringent upper limits on λ'_{ijk}. In Fig. 5.9 the decay rate $\mu \to e\gamma$ has been calculated by varying Λ'. This figure shows that the decay rates follow a power law in close analogy to Eq. (5.124), i.e.,

$$\Gamma(\mu \to e\gamma) \sim \Lambda'^4, \tag{5.133}$$

see discussion in Appendix B.3. Figure 5.9 shows that if the upper bounds on $\mu \to e\gamma$ is lowered by a factor 10000, then the upper limit on Λ' will be lowered roughly by a factor 10.

The following three textures have also been used,

$$\lambda'_{133} = \lambda'_{233} = \lambda'_{333} \neq 0, \tag{5.134}$$
$$\lambda'_{111} = \lambda'_{211} = \lambda'_{311} \neq 0, \tag{5.135}$$
$$\lambda'_{122} = \lambda'_{222} = \lambda'_{322} \neq 0, \tag{5.136}$$

and all other elements are vanishing.

The results obtained by using the texture of Eq. (5.134) is shown in the third column of Table 5.6. The decay rates have also been calculated by using the textures of Eqs. (5.135) and (5.136). These textures, however, only gives slighter weaker bounds on the trilinear couplings than the texture of Eq. (5.134).

It is also possible to choose a texture of λ'_{ijk} in such a manner that either $\tau \to \mu\gamma$ or $\tau \to e\gamma$ puts the most stringent constraints on λ'_{ijk}. Some examples are shown in Table 5.7.

These calculations shows that the lepton flavour violating decay rates also put upper

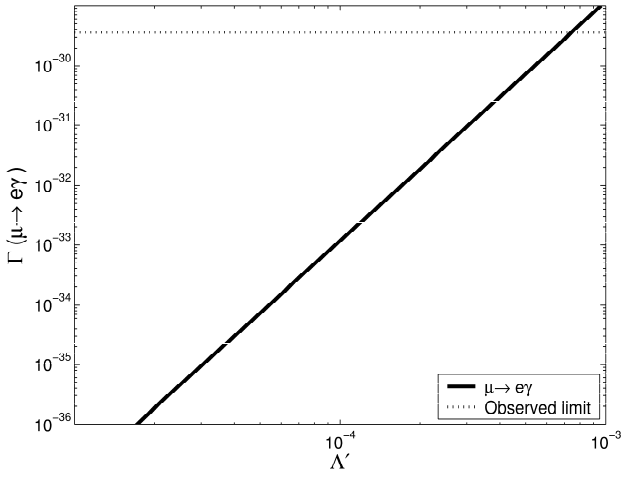

Figure 5.9: The figure shows the decay rate $\mu \to e\gamma$ calculated for varying values of Λ'. Λ' is defined by Eq. (5.132). The dotted horizontal line denotes the present observational limit.

Decay channel	$\Lambda' = 7.5 \cdot 10^{-4}$	$\lambda'_{i33} = 2.4 \cdot 10^{-3}$
$\tau \to \mu\gamma$	$6.0 \cdot 10^{-24}$	$6.0 \cdot 10^{-24}$
$\tau \to e\gamma$	$5.8 \cdot 10^{-24}$	$5.8 \cdot 10^{-24}$
$\mu \to e\gamma$	$3.6 \cdot 10^{-30}$	$3.6 \cdot 10^{-30}$

Table 5.6: The table shows the numeric results for the upper limits of the decay rates under study, obtained by assuming all elements of λ_{ijk} are vanishing. The texture of Eq. (5.132) are used. The MSSM parameters are shown in Eqs. (5.104) - (5.105).

limits on the R-parity violating couplings λ_{ijk}. The limits are also found to be an order of magnitude stronger than the limits for λ_{ijk}.

5.9.3 Elements from both λ' and λ are non-vanishing

It is, of course, also possible that both λ and λ' have non-vanishing elements. As the analysis from the two preceding subsections shows, the most constraining textures are the uniform ones. By using the uniform textures, i.e.,

$$\lambda_{ijk} = -\lambda_{jik} = \Lambda, \quad \text{for} \quad i \neq j, \tag{5.137}$$
$$\lambda'_{ijk} = \Lambda', \tag{5.138}$$

Decay channel	$\lambda'_{\binom{1}{2}33} = 2.4 \cdot 10^{-3}$	$\lambda'_{\binom{1}{3}33} = 7.6 \cdot 10^{-2}$	$\lambda'_{\binom{2}{3}33} = 6.1 \cdot 10^{-2}$
$\tau \to \mu\gamma$	0	0	$2.5 \cdot 10^{-18}$
$\tau \to e\gamma$	0	$6.1 \cdot 10^{-18}$	0
$\mu \to e\gamma$	$3.6 \cdot 10^{-30}$	0	0

Table 5.7: The Table shows the numeric results obtained by putting $\lambda_{ijk} = 0$. Only components of λ'_{ijk} may be non-vanishing. The model is specified by Eqs. (5.104) - (5.105).

the upper limit is found as $\Lambda = \Lambda' = 7.8 \cdot 10^{-4}$, for $\mu \to e\gamma$. This limiting value gives $7.5 \cdot 10^{-24}$ and $6.7 \cdot 10^{-24}$ for the decay rates $\tau \to \mu\gamma$ and $\tau \to e\gamma$, respectively.

In Fig. 5.10 the decay rate $\Gamma(\mu \to e\gamma)$ is calculated by first fixing a value for Λ' and then varying Λ.

In the last two subsections it has been shown that neither of the decay rates will give any non-vanishing contribution if there are only two non-vanishing elements of λ_{ijk}, i.e., $\lambda_{ijk} = \lambda_{jik} \neq 0$, for $i \neq j$. It has also been shown that at least two elements of λ'_{ijk} must be non-vanishing in order to give a non-vanishing contribution for the decay rates. But if there are some non-vanishing elements of both λ_{ijk} and λ'_{ijk} there will be contributions.

The following 6 textures have therefore been calculated,

$$\lambda'_{333} = \lambda_{121} = -\lambda_{211}, \quad \lambda'_{333} = \lambda_{233} = -\lambda_{323}, \tag{5.139}$$
$$\lambda'_{333} = \lambda_{122} = -\lambda_{212}, \quad \lambda'_{333} = \lambda_{133} = -\lambda_{313}, \tag{5.140}$$
$$\lambda'_{333} = \lambda_{132} = -\lambda_{312}, \quad \lambda'_{333} = \lambda_{231} = -\lambda_{321}. \tag{5.141}$$

Each of these textures gives a non-vanishing value for only one of the decay rates under study. These are the only textures for λ_{ijk}, combined with λ_{333}, which give any non-vanishing contribution to the decay rates. The limits obtained from the last texture of Eqs. (5.139) - (5.141) are shown in Table 5.8. In this table the upper limits shown in columns 2 and 3 are obtained from lower limits[1] for the charged scalar masses. That is, for larger values than the one shown in these two columns the lightest charged scalar is lighter than 81GeV.

The first textures of Eqs. (5.139) and (5.140) give much weaker bounds than the ones shown in Table 5.8. The first texture of Eq. (5.141) gives the same bound as the one shown in column two of Table 5.8.

[1]The lower limit[6] for the $\tilde{\tau}$ (stau) is used also in MSSM-M, i.e., $m_{\tilde{\tau}} > 81\,\mathrm{GeV}$.

Decay channel	$\lambda_{231} = -\lambda_{321} = \lambda'_{333} = 5.9 \cdot 10^{-3}$	$\lambda_{133} = -\lambda_{311} = \lambda'_{333} = 0.387$	$\lambda_{233} = -\lambda_{322} = \lambda'_{333} = 0.387$
$\tau \to \mu\gamma$	0	0	$3.3 \cdot 10^{-20}$
$\tau \to e\gamma$	0	$2.4 \cdot 10^{-20}$	0
$\mu \to e\gamma$	$3.6 \cdot 10^{-30}$	0	0

Table 5.8: The table shows the results obtained by using the textures shown in Eqs.. (5.139) - (5.141). The model is specified by Eqs. (5.104) - (5.105).

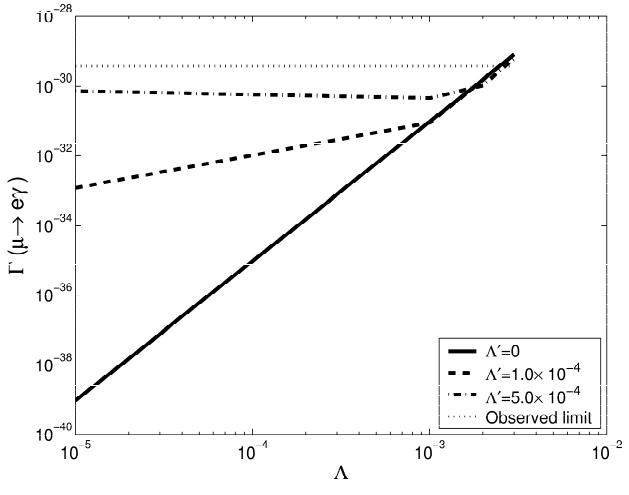

Figure 5.10: The figure shows the decay rates for $\mu \to e\gamma$ calculated by varying Λ and Λ'. The model is specified by Eqs. (5.104) - (5.105).

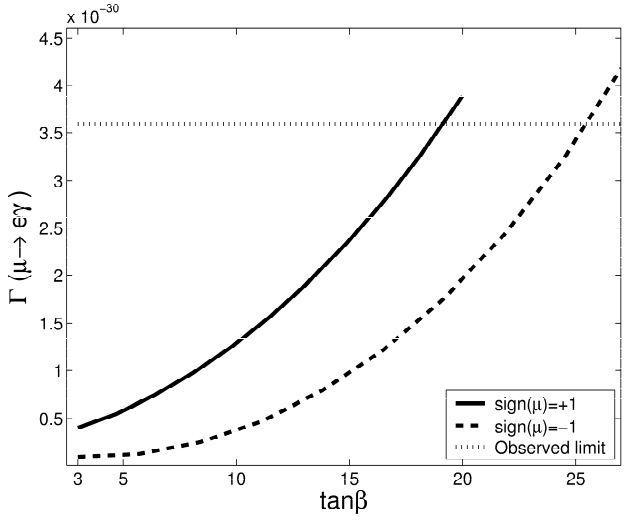

Figure 5.11: The figure shows the decay rate for $\mu \to e\gamma$, obtained by varying $\tan\beta$, and for positive and negative values of signμ.

5.9.4 Varying the MSSM parameters

In the numerical calculations made above the 5 MSSM parameters were kept constant throughout the calculations, i.e., they where defined by Eqs. (5.104) - (5.105). It is, of course, also possible that these parameters take other values, and it is therefore necessary to study the decay rates by varying these MSSM parameters too. Since the uniform textures, i.e., Eqs. (5.123) and (5.132), give the most stringent upper bounds on the decay rates, these textures are used in this part of the analysis. It is further assumed that $\Lambda = \Lambda' = 7.0 \cdot 10^{-4}$ throughout the analysis, unless otherwise stated.

The starting point is to use the 5 MSSM parameters from Eqs. (5.104) - (5.105), and then vary one parameter at time.

The results of this procedure are shown in Figs. 5.11 - 5.14. In all of these figures the decay rate $\mu \to e\gamma$ is found to give the strongest constraint on the parameters. Figure 5.11 shows the dependency this decay rate have on $\tan\beta$ and also on the sign of μ. Figures 5.12 and 5.14 shows the dependency this decay rate has on $M_{1/2}$ and M_0, respectively. They also shows the dependency on $\tan\beta$. These figures shows that small values of M_0 and $M_{1/2}$ and a large value of $\tan\beta$ together with a negative sign for μ leads to the strongest limits for the decay rates. This confirms the analytic analysis of Sec. 5.6.

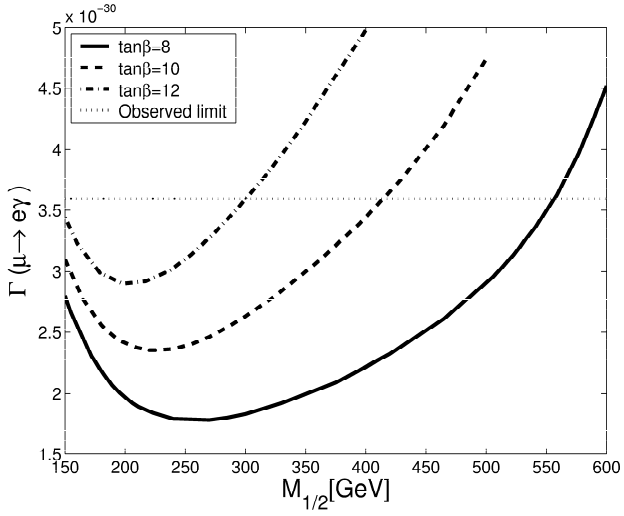

Figure 5.12: The figure shows the decay rate for $\mu \to e\gamma$, obtained by varying $M_{1/2}$, and for three values of $\tan\beta$.

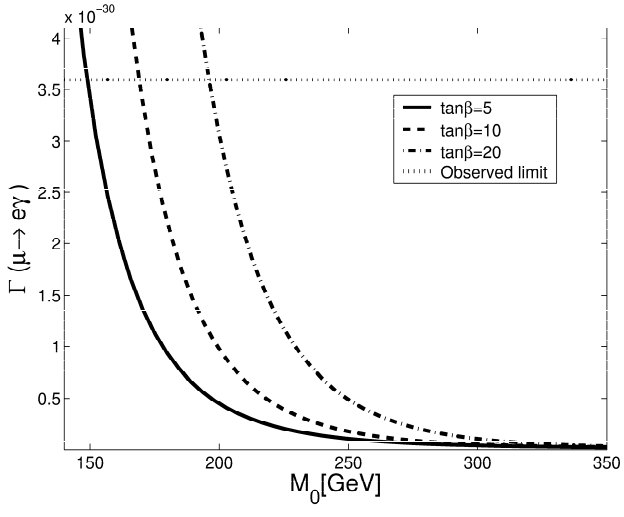

Figure 5.13: The figure shows the decay rate for $\mu \to e\gamma$, obtained by varying M_0, and for three values of $\tan\beta$.

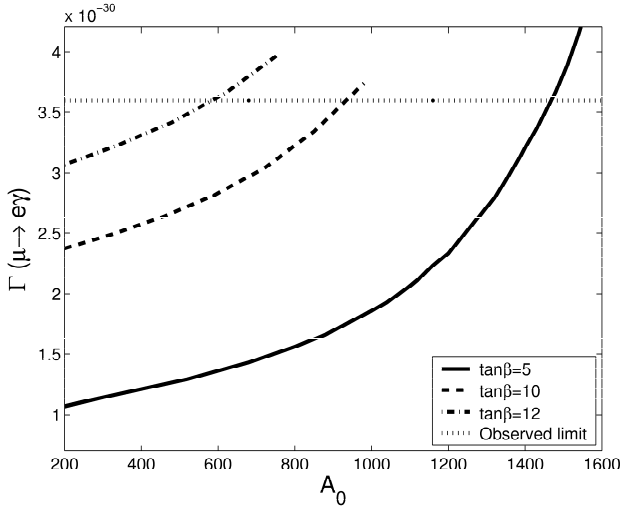

Figure 5.14: The figure shows the decay rate for $\mu \to e\gamma$, obtained by varying A_0, and for three values of $\tan\beta$.

5.9.5 Beyond the supergravity scenario

Up until now, the supergravity inspired breaking scenario of Eqs. (3.8) - (3.10) have been used. In this scenario the three soft-breaking bilinear couplings b_i are determined by the minimisation conditions at the electroweak scale. Table 5.2 show that these couplings are small. The squared mass matrices of the scalars, presented in Sec. 5.5 shows that these couplings are important since they lead to greater non-degeneracy among the scalars. It is therefore interesting to make some smaller deviation from the supergravity breaking scenario, and to study the couplings b_i as free parameters. The minimisation conditions must, of course, still be fulfilled, and they are used to determine ε_i in terms of b_i, i.e.,

$$\varepsilon_i = b_i \cot\beta. \tag{5.142}$$

Since $\varepsilon = (M_L^2)_{01} = (M_L^2)_{10}$ the running of M_L^2 will be influenced by the specific choice made for b_i. And since the running of all soft-breaking bilinear couplings depends upon M_L^2, all of these parameters will, in general, be affected by the choice made for b_i at the electroweak scale. However, if all elements of λ_{ijk} and λ'_{ijk} vanish ε_i does not couple to any of the other components of any couplings. Thus, in this case the supergravity inspired breaking conditions of Eqs. (3.8) - (3.10) are still fulfilled. On the other hand for small non-vanishing values for the elements of λ_{ijk} and λ'_{ijk} the supergravity conditions will be violated.

The 5 MSSM parameters from Eqs. (5.104) - (5.105), will be used together with the uniform textures of Eqs. (5.123) and (5.132), i.e., $\Lambda = \Lambda'$.

Decay channel	$b_{\binom{1}{2}} = 37.2\,\mathrm{GeV}^2$	$b_{\binom{1}{3}} = 2.62 \times 10^3\,\mathrm{GeV}^2$	$b_{\binom{2}{3}} = 2.11 \times 10^3\,\mathrm{GeV}^2$
$\tau \to \mu\gamma$	0	0	$2.5 \cdot 10^{-18}$
$\tau \to e\gamma$	0	$6.1 \cdot 10^{-18}$	0
$\mu \to e\gamma$	$3.6 \cdot 10^{-30}$	0	0

Table 5.9: The table shows the three decay rates calculated by varying b_i. The uniform textures are used for λ_{ijk} and λ'_{ijk}, i.e., $\Lambda = \Lambda' = 0$. The model is specified by Eqs. (5.104) - (5.105).

If only one of the components of b_i is non-vanishing, say b_1 and $\Lambda = 0$ there can be no contribution to the decay rates. But if two of the components are non-vanishing there will be some contributions, see Table 5.9.

Another rather simple scenario is to assume all three couplings are equal, i.e., $b_1 = b_2 = b_3 = b$. By specifying some values for Λ and varying b the plots shown in Fig. 5.15 was obtained. This figure shows that the parameter b must take rather large values, compared to the values for b_i presented in Table 5.2, in order to break the phenomenological limit for $\mu \to e\gamma$. Nevertheless, all of these scenarios put much stronger limits on b_i than was made in Sec. 5.6.

It is also of interest to find possible limits on the soft-breaking parameters $\lambda^{\mathrm{s}}_{ijk}$ and $\lambda'^{\mathrm{s}}_{ijk}$. The renormalization group equations for M^2_L and M^2_e shows that the running of these parameters depends upon these trilinear soft-breaking parameters. One therefore expects that these parameters leads to lepton flavour violation through renormalization group effects.

Assume that all elements of λ_{ijk} and λ'_{ijk} vanishes, and further that $\lambda^{\mathrm{s}}_{ijk}$ and $\lambda'^{\mathrm{s}}_{ijk}$ are defined in terms of uniform textures at the GUT-scale, i.e.,

$$\lambda^{\mathrm{s}}_{ijk} = \begin{cases} \lambda^{\mathrm{s}}_{ijk} = -\lambda^{\mathrm{s}}_{jik} = \Lambda^{\mathrm{s}}, & \text{for } i \neq j, \\ 0, & \text{else.} \end{cases}, \tag{5.143}$$

$$\lambda'^{\mathrm{s}}_{ijk} - \Lambda'^{\mathrm{s}}, \text{ for all } i, j, k = 1, 2, 3. \tag{5.144}$$

In Fig. 5.16 it is assumed that $\Lambda'^{\mathrm{s}} = \Lambda^{\mathrm{s}}$. The straight line shows that even if all elements of λ_{ijk} and λ'_{ijk} vanishes, the decay channel $\mu \to e\gamma$ put limits on the soft-breaking trilinear couplings. In this case the upper limit $\Lambda^{\mathrm{s}} < 0.24$ is obtained. Slightly weaker limits are found for the other two decay rates. This figure also shows the decay rate $\mu \to e\gamma$ by using uniform textures for λ_{ijk} and λ'_{ijk}, i.e., $\Lambda = \Lambda' = 7.0 \times 10^{-4}$. In this case an upper limit $\Lambda = 0.26$ is found.

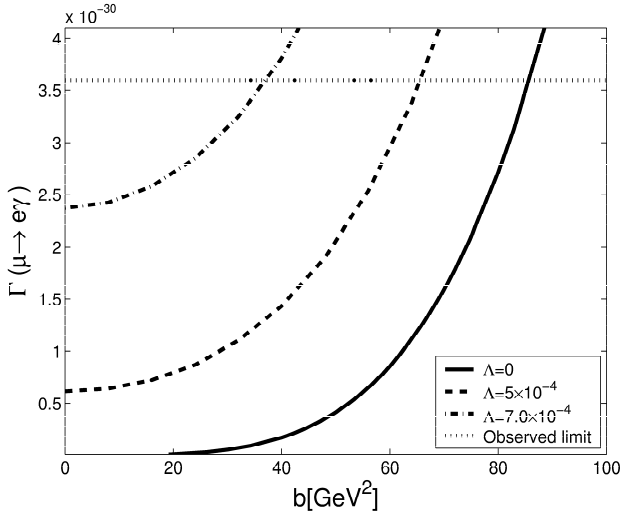

Figure 5.15: The figure shows the decay rate for $\mu \to e\gamma$, obtained by varying b_i, and for three values of Λ.

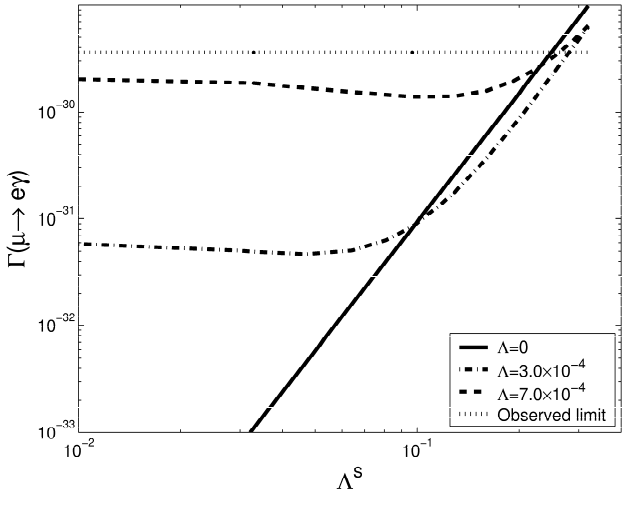

Figure 5.16: The figure shows the decay rate for $\mu \to e\gamma$, obtained by varying Λ^s.

Chapter 6

Dirac-Majorana neutrinos and $l \to l'\gamma$

The most complicated of the three models to be studied in this thesis is MSSM-DM. In Sec. 3.1.3 it was shown that this model, in general, has 387 free parameters, with only 19 of these parameters known from the Standard Model[1] It was also shown that this parameter space also includes the parameter spaces of MSSM, MSSM-D and MSSM-M.

This chapter starts with a presentation of the MSSM-DM Lagrangian, written in terms of the $U(4)$-manifest notation from Chapter 5. In Sec. 6.2 the tree-level scalar potential of MSSM-DM is defined, and the minimisation conditions are presented. In Sec. 6.3 all mass matrices, relevant for our analysis, are presented. The existence of the three right-handed superfields n_i, and the violation of the lepton number, allows for self-couplings between these superfields. These couplings will lead to major modifications of the neutral fermion and the neutral scalar masses. The mass matrices for the charged fermions and charged scalars are, only with minor exceptions, identical to the corresponding ones from MSSM-M. Next, in Sec. 6.4 the squared mass matrices for the neutral scalars are analysed, and some constraints are obtained on the gauge singlet parameters. As for most quantum field theories, the parameters of MSSM-DM will run by scale, and in Sec. 6.5 the running of some of the most important parameters is analysed, both qualitatively and by numerical methods. Finally, in Sec. 6.6.2 the qualitatively and numerical analysis of the lepton flavour violating decay rates, $l \to l'\gamma$, will be presented.

[1]The 3 neutrino masses and 3 mixing angles and possible complex phase are considered as known parameters in this count.

6.1 Lagrangian of MSSM-DM

In Sec. 3.1.3 the model MSSM-DM was defined in terms of its superpotential and soft-breaking terms, i.e., by Eqs. (3.6) and (3.7). It was shown that due to the R-parity violating couplings the lepton quantum number is not conserved. As for MSSM-M, this causes the superfields $\hat{H}_d$ and L_i to have identical quantum numbers, and these fields can therefore mix together. This mixing introduces a global $U(4)$ symmetry on the Lagrangian, and it can be rewritten in terms of the $U(4)$-vectors and -tensors defined in Sec. 5.3, and the two $U(4)$-tensors to be defined in Eqs. (6.3) and (6.4). In terms of these $U(4)$-vectors and -tensors the superpotential and soft-breaking terms take the more compact form,

$$\begin{aligned} W = {} & Y_u Q \hat{H}_u u + \frac{1}{2}\lambda_{\alpha\beta k} L_\alpha L_\beta e_k + \lambda'_{\alpha jk} L_\alpha Q_j d_k \\ & + \lambda'''_{\alpha i} L_\alpha \hat{H}_u n_i + \mu_\alpha L_\alpha \hat{H}_u \\ & + \frac{1}{6} A_{ijk} n_i n_j n_k + \frac{1}{2} B_{ij}\, n_i n_j + C_i n_i, \end{aligned} \tag{6.1}$$

$$\begin{aligned} -\mathcal{L}_{\text{soft}} = {} & M^2_{\tilde{Q}} \tilde{Q}^\dagger \tilde{Q} + \left(M^2_{\tilde{L}}\right)_{\alpha\beta} \tilde{L}^\dagger_\alpha \tilde{L}_\beta + M^2_{H_u} H^\dagger_u H_u \\ & + M^2_{\tilde{u}} \tilde{u}\tilde{u}^* + M^2_{\tilde{d}} \tilde{d}\tilde{d}^* + M^2_{\tilde{e}} \tilde{e}\tilde{e}^* + M^2_{\tilde{n}} \tilde{n}\tilde{n}^* \\ & + \Big[-b_\alpha \tilde{L}_\alpha H_u + a_u H_u \tilde{Q} \tilde{u} \\ & + \frac{1}{2}\lambda^{\text{s}}_{\alpha\beta k} \tilde{L}_\alpha \tilde{L}_\beta \tilde{c}_k + \lambda'^{\text{s}}_{\alpha jk} \tilde{L}_\alpha \tilde{Q}_j \tilde{d}_k + \lambda'''^{\text{s}}_{\alpha i} \tilde{L}_\alpha H_u \tilde{n}_i \\ & + \frac{1}{2}\left(M_1 \tilde{B}\tilde{B} + M_2 \tilde{W}^a \tilde{W}^a + M_3 \tilde{g}\tilde{g} \right) \\ & + \frac{1}{6} A^{\text{s}}_{ijk} \tilde{n}_i \tilde{n}_j \tilde{n}_k + \frac{1}{2} B^{\text{s}}_{ij} \tilde{n}_i \tilde{n}_j + \text{h.c.} \Big]. \end{aligned} \tag{6.2}$$

In this chapter the following definitions for indices will be used, small Latin indices counts the flavours known from the Standard Model, e.g., $i, j, k = 1, 2, 3$, and small Greek indices labels the $U(4)$-vectors and tensors, e.g., $\alpha = 0, 1, 2, 3$.

Note that a linear term, such as $C^{\text{s}}_i \tilde{n}_i$, is not a soft-breaking term [37].

This form for the superpotential and soft-breaking terms will be used throughout this thesis. Only when necessary, e.g., for comparison with the literature, will the non $U(4)$-manifest notation of Eqs. (3.6) and (3.7) be used. In Appendices C.1, D.4, E.2 and F.2 the scalar potential, the mass matrices, the Feynman rules and the renormalization group equations are presented by use of this manifest $U(4)$-notation.

As for MSSM-M baryon symmetry will be imposed by hand to ensure proton stability, see discussion in Sec. 5.1. That is, it is always assumed that all elements of both λ''_{ijk} and $\lambda''^{\text{s}}_{ijk}$ vanishes.

In addition to the $U(4)$-vectors and -tensors defined in Eqs. (5.8) - (5.14), two new $U(4)$-vectors are also needed in MSSM-DM,

$$\lambda'''_{\alpha j} = ((Y_n)_j, (Y_\nu)_{ij}) \,, \tag{6.3}$$

$$\lambda'''^{\rm s}_{\alpha j} = ((a_n)_j, (a_\nu)_{ij}) \,. \tag{6.4}$$

Note that λ'''_{ij} and $\lambda'''^{\rm s}_{ij}$ are the neutrino Yukawa matrix and its associated soft-breaking trilinear couplings. Both of these matrices appeared in MSSM-D.

These two matrices are the only couplings in MSSM-DM that connect the right-handed gauge singlets to the other fields of MSSM-DM. Thus, if all elements of both $\lambda'''_{\alpha j}$ and $\lambda'''^{\rm s}_{\alpha j}$ where to vanish then the gauge singlet superfields fields, n_i, can not interact with any of the other fields. Such a scenario will be referred to as having an *invisible gauge singlet sector*. In the literature these right-handed neutrinos are often referred to as sterile neutrinos, see e.g., Ref. [21]. If an invisible gauge sector exist then the visible sector, that is, the collection of all other fields, is identical to the field content of MSSM-M. Thus to have an interesting model, phenomenologically different from MSSM-M, at least one of the elements of $\lambda'''_{\alpha i}$ or $\lambda'''^{\rm s}_{\alpha i}$ must be non-vanishing.

As for MSSM-D and MSSM-M some simplifications have to be made in order to make a sensible analysis of this model. The assumptions, which will be used, are analogous to the ones already seen in preceding chapters. That is, all parameters are assumed to be real, and the supergravity inspired boundary conditions of Eqs. (3.8) - (3.11) are used, i.e.,

$$M^2_{H_u} = M^2_0, \quad M^2_{\tilde{X}} = M^2_0 \, \mathbf{1}, \tag{6.5}$$

$$M_1 = M_2 = M_3 = M_{1/2}, \tag{6.6}$$

$$\lambda^{\rm s}_{\alpha\beta k} = A_0 \, \lambda_{\alpha\beta k}, \tag{6.7}$$

$$\lambda'^{\rm s}_{\alpha jk} = A_0 \, \lambda'_{\alpha\beta k}, \tag{6.8}$$

$$\lambda'''^{\rm s}_{\alpha j} = A_0 \, \lambda'''_{\alpha j}, \tag{6.9}$$

$$A^{\rm s}_{ijk} = A_0 \, A_{ijk}, \tag{6.10}$$

$$B^{\rm s}_{ij} = B_0 \, B_{ij}, \tag{6.11}$$

at the GUT-scale. Here $\tilde{X}$ is shorthand for $M^2_{\tilde{Q}}$, $M^2_{\tilde{L}}$, $M^2_{\tilde{u}}$, $M^2_{\tilde{d}}$, $M^2_{\tilde{e}}$ and $M^2_{\tilde{n}}$. Note that B_0 is a new parameter associated with the gauge singlet sector of MSSM-DM, and should not be confused with the parameter B_0 appearing in some treatments of MSSM, e.g., in Ref. [35]. In next section it will be shown that the three superpotential parameters C_i are determined by minimising the neutral scalar potential.

6.2 The tree-level scalar potential

The complete tree-level scalar potential of MSSM-DM is presented in Appendix C.1. Due to the existence of both right-handed gauge singlets and R-parity violating cou-

plings, this scalar potential is quite complicated. This complication is a consequence of the gauge singlet scalar fields which also contribute to the neutral scalar potential. Thus, in MSSM-DM there are 8 scalar fields contributing to the neutral scalar potential, i.e.,

$$H_u = \begin{pmatrix} H_u^+ \\ H_u^0 \end{pmatrix} = \begin{pmatrix} H_u^+ \\ \frac{1}{\sqrt{2}}(v_u + \psi_u + i\phi_u) \end{pmatrix}, \tag{6.12}$$

$$\tilde{L}_\alpha = \begin{pmatrix} \tilde{L}_\alpha^0 \\ \tilde{L}_\alpha^- \end{pmatrix} = \begin{pmatrix} \frac{1}{\sqrt{2}}(v_\alpha + \psi_\alpha + i\phi_\alpha) \\ \tilde{L}_\alpha^- \end{pmatrix}, \tag{6.13}$$

$$\tilde{n}_i = \frac{1}{\sqrt{2}}\left(w_i + \rho_i + i\eta_i\right). \tag{6.14}$$

Since the gauge singlets do not contribute to the electroweak symmetry breaking, their vacuum expectation values do not have to be acquired at the electroweak scale. Thus, in addition to the electroweak scale, there may exist another breaking scale, what will be referred to as the n-scale. This breaking scale will be assumed to exist somewhere well above the electroweak scale and below the GUT-scale, i.e.,

$$M_Z \ll M_{n\text{-scale}} \leqslant M_{\text{GUT}}. \tag{6.15}$$

It is further assumed that all gauge singlet scalar fields, $\tilde{n}_i$, acquire a vacuum expectation value, ω_i, at the same scale. Finally, these vacuum expectation values are assumed to be of the same order of magnitude as the breaking scale itself, that is, $\omega_i \sim M_{n\text{-scale}}$.

The minimum of the neutral scalar potential is found as a solution of the following 8 minimisation conditions,

$$\frac{\partial V}{\partial H_u^0} = 0, \quad \frac{\partial V}{\partial \tilde{L}_\alpha^0} = 0, \tag{6.16}$$

$$\frac{\partial V}{\partial \tilde{n}_i} = 0. \tag{6.17}$$

Since the n-scale is assumed to exist at a much larger energy scale than the electroweak scale, only the gauge singlets will acquire vacuum expectation values at this scale. This somewhat simplifies the minimisation conditions at the n-scale, and they take the following form,

$$\begin{aligned} 0 = {} & \frac{1}{2\sqrt{2}} A_{ijl} A_{pql}\, \omega_j \omega_p \omega_q \\ & + \frac{1}{4}\omega_j \omega_k \left(\Lambda_{ijk}^s + 2\sqrt{2}\Lambda_{ijl} B_{kl} + \Lambda_{jkl} B_{il}\right) \\ & + \frac{1}{\sqrt{2}}\omega_j \left(A_{ijl} C_l + \left(M_n^2\right)_{ij} + B_{ij}^s + 2B_{il}B_{jl}\right) + B_{il}C_l. \end{aligned} \tag{6.18}$$

This is a linear set of 3 equations in terms of C_i, and the minimisation conditions at the n-scale will therefore be solved with respect to C_i. Of course, these minimisation conditions could be used to solve for three other parameters, e.g., the diagonal elements of B_{ij} or in terms of ω_i.

Also, some further assumptions will be made for A_{ijk} and B_{ij}. Both of these parameters will be defined at the electroweak scale by use of the least amount of free parameters. This demand is accomplished by assuming that both A_{ijk} and B_{ij} are diagonal at the electroweak scale. That is, the following textures for A_{ijk} and B_{ij} will be used,

$$A_{ijk} = P\,\delta_{ij}\delta_{jk}, \tag{6.19}$$

$$B_{ij} = Q\,\delta_{ij}, \qquad i,j,k = 1,2,3. \tag{6.20}$$

The actual size of these parameters will be discussed in later sections, but as a general rule it will be shown that P is small and Q is large.

Note that if both A_{ijk} and A^{s}_{ijk} vanish, then the minimisation conditions of Eq. (6.18) take the simpler form

$$B_{ij}C_j + \frac{1}{\sqrt{2}}\omega_j\left(\left(M_n^2\right)_{ij} + B^{\mathrm{s}}_{ij} + 2B_{il}B_{lj}\right) = 0. \tag{6.21}$$

To further streamline the notation the following definitions will be used,

$$\hat{\mu}_\alpha = \mu_\alpha + \frac{1}{\sqrt{2}}\lambda'''_{\alpha j}w_j, \tag{6.22}$$

$$\hat{b}_\alpha = b_\alpha + \frac{1}{\sqrt{2}}\lambda'''^{\mathrm{s}}_{\alpha j}w_j + \lambda'''_{\alpha l}\left(\frac{1}{4}w_iw_jA_{ijl} + \frac{1}{\sqrt{2}}w_iB_{il} + C_l\right). \tag{6.23}$$

By using these parameters the minimisation conditions, from Eq. (6.16), take almost identical forms as the minimisation conditions of MSSM-M, i.e.,

$$\left(M^2_{H_u} + |\hat{\mu}_\alpha|^2\right)v_u = \hat{b}_\alpha v_\alpha + \frac{M_Z^2}{2}\cos(2\beta)v_u, \tag{6.24}$$

$$\left(\left(M_L^2\right)_{\alpha\beta} + \hat{\mu}_\alpha\hat{\mu}^*_\beta\right)v_\beta = \hat{b}_\alpha v_u - \frac{M_Z^2}{2}\cos(2\beta)v_\alpha. \tag{6.25}$$

The only difference between these minimisation conditions, and the ones found for MSSM-M, is the use of the hatted parameters defined in Eqs. (6.22) and (6.23).

It is also useful to introduce the term complete alignment in MSSM-DM. However, when dealing with MSSM-DM the phrase *complete alignment* will mean that $\hat{\mu}_i$ and v_i are completely aligned, that is, $\hat{\mu}_i = 0$ in the v_i-basis. Note that complete alignment does not imply that $\hat{b}_i$ has to vanish. A more thorough analysis of complete alignment is made in the next section when discussing the mass matrix for the neutral fermions.

By assuming complete alignment the minimisation conditions of Eqs. (6.24) and (6.25) now take the form,

$$M_{H_u}^2 + |\hat{\mu}_0|^2 = \hat{b}_0 \cot\beta + \frac{M_Z^2}{2}\cos 2\beta, \tag{6.26}$$

$$M_{H_d}^2 + |\hat{\mu}_0|^2 = \hat{b}_0 \tan\beta - \frac{M_Z^2}{2}\cos 2\beta, \tag{6.27}$$

$$\varepsilon_i = \hat{b}_i \tan\beta. \tag{6.28}$$

Here $\tan\beta$ was defined in Eq. (5.33), and the definition of Eq. (5.11) has been used, i.e., $(M_L^2)_{00} = M_{H_d}^2$ and $(M_L^2)_{0i} = (M_L^2)_{i0} = \varepsilon_i$.

As for MSSM-M these minimisation conditions do not determine either μ_α nor b_α. Instead, they determine the hatted parameters $|\hat{\mu}_0|$ and $\hat{b}_\alpha$. It is therefore interesting to note that the mass matrices, to be presented in the next section, only depend upon these hatted parameters.

6.3 Mass matrices and mixing in MSSM-DM

The mass matrix for the charged fermions, and the squared mass matrices for the charged scalars (including squarks), are almost identical to the corresponding mass matrices found for MSSM-M. The only difference is the use of $\hat{\mu}_\alpha$ and $\hat{b}_\alpha$. On the other hand, the mass matrix for the neutral fermions and the squared mass matrices for the neutral scalars are modified due to the presence of the right-handed gauge singlets and the violation of the lepton number. In this section the relevant mass matrices of MSSM-DM will be presented, always under the assumption of complete alignment in the v_i-basis. The general expressions for these mass matrices are shown in Appendix D.4.

6.3.1 Neutral fermions

In the gauge-basis $\Phi_N^T = \left(\lambda_B, \lambda_A^3, \psi_{H_u^0}, \psi_{L_\alpha^0}, \psi_{n_i}\right)$, the masses for the 10 neutral fermions are determined by the following 10×10 symmetric mass matrix,

$$M_N = \begin{pmatrix} M_1 & 0 & M_Z s_\theta s_\beta & -M_Z s_\theta v_\alpha/v & 0 \\ 0 & M_2 & -M_Z c_\theta s_\beta & M_Z c_\theta v_\beta/v & 0 \\ M_Z s_\theta s_\beta & -M_Z c_\theta s_\beta & 0 & \hat{\mu}_\alpha & \frac{1}{\sqrt{2}}\lambda'''_{\alpha j} v_\alpha \\ -M_Z s_\theta v_\alpha/v & M_Z c_\theta v_\beta/v & \hat{\mu}_\alpha & 0 & \frac{1}{\sqrt{2}}\lambda'''_{\alpha j} v_u \\ 0 & 0 & \frac{1}{\sqrt{2}}\lambda'''_{\alpha i} v_\alpha & \frac{1}{\sqrt{2}}\lambda'''_{\alpha i} v_u & \frac{1}{2}\hat{B}_{ij} \end{pmatrix}. \tag{6.29}$$

Here $s_\theta = \sin\theta_W$, $c_\theta = \cos\theta_W$, $s_\beta = \sin\beta$, $c_\beta = \cos\beta$ and $\hat{\mu}_\alpha$ is defined by Eq. (6.22).

Also $\hat{B}_{ij}$ is defined by,

$$\hat{B}_{ij} = B_{ij} + \frac{1}{\sqrt{2}} w_p A_{ijp}. \tag{6.30}$$

This symmetric matrix is diagonalised by the unitary matrix, Z_N, i.e.,

$$Z_N^\dagger M_N Z_N = \mathrm{diag}\left(m_{\tilde{\chi}_i}\right), \quad i = 1, \ldots, 10. \tag{6.31}$$

By using Z_N the gauge eigenstates can be expressed in terms of the mass eigenstates, ψ_i^0, i.e.,

$$\lambda_B = i Z_N^{1i}\, \psi_i^0, \qquad \lambda_A^3 = i Z_N^{2i}\, \psi_i^0, \tag{6.32}$$

$$\psi_{H_u^0} = Z_N^{3i}\, \psi_i^0, \qquad \psi_{L_\alpha^0} = Z_N^{4+\alpha,i}\, \psi_i^0, \tag{6.33}$$

$$\psi_{n_j} = Z_N^{7+j,i}\, \psi_i^0. \tag{6.34}$$

These 2-component spinors can be combined into five 4-component Majorana spinors, i.e.,

$$\tilde{\chi}_i^0 = \begin{pmatrix} \tilde{\psi}_i^0 \\ \bar{\tilde{\psi}}_i^0 \end{pmatrix}, \quad i = 1, 2, \ldots, 5. \tag{6.35}$$

The mass matrix M_N suffers from the same kind of problem that hampered the neutral fermion mass matrix of MSSM-M, that is, one of the neutrino masses will generally be too heavy. In Sec. 5.5 this problem was overcome by assuming complete alignment between v_α and μ_α. However, due to the explicit appearance of $\lambda'''_{\alpha i}$ in the definition of $\hat{\mu}_\alpha$, the phrase complete alignment must be slightly modified in MSSM-DM. The obvious generalisation is to define complete alignment to mean that $\hat{\mu}_\alpha$ is completely aligned to v_α. As in MSSM-M this ensures that there are three small eigenvalues of M_N to be associated with the Standard Model neutrino masses.

Note that even if $\hat{\mu}_i$ vanishes in the v_i-basis this does not mean that λ'''_{ij} has to vanish. A cancellation between μ_i and $\frac{1}{\sqrt{2}} w_j \lambda_{ij}$ will suffice to align $\hat{\mu}_\alpha$ to v_α. However, if λ'''_{ij} takes the same size as found in Chapter 4, i.e., of the order 10^{-11}, these values can safely be neglected in the forthcoming analysis. On the other hand, λ'''_{0i} may generally take non-vanishing values. These parameters are now the only parameters in M_N which connect the gauge singlet fields to the other fields of MSSM-DM.

If $\lambda'''_{\alpha i}$ vanishes completely there are 3 vanishing eigenvalues, and 3 large eigenvalues determined from $\hat{B}_{ij}$, and 4 eigenvalues determined from a 4×4 matrix almost identical to the neutralino mass matrix of MSSM. In such a case there are no mixing between the gauge singlets and the other fields in this case.

As for MSSM-M, radiative corrections will lead to small non-vanishing masses for the neutrinos. These radiative corrections are, however, not taken into account in this thesis.

The assumptions discussed so far lead to the following simplified neutral fermion mass matrix, i.e.,

$$M_N = \begin{pmatrix} (M_N)_{4\times4} & 0_{4\times3} & C_{4\times3} \\ 0_{3\times4} & 0_{3\times3} & 0_{3\times3} \\ C^T_{3\times4} & 0_{3\times3} & \frac{1}{2}\hat{B}_{3\times3} \end{pmatrix}. \tag{6.36}$$

Here $(M_N)_{4\times4}$ is identical to the neutralino mass matrix of MSSM, that is, identical to Eq. (D.20). The matrix $\hat{B}_{ij}$ was defined in Eq. (6.30) and C_{ij} is defined as,

$$C_{ij} = \frac{v_d}{\sqrt{2}} \begin{pmatrix} 0 & 0 & 0 \\ 0 & 0 & 0 \\ \lambda'''_{01} & \lambda'''_{02} & \lambda'''_{03} \\ \lambda'''_{01}\tan\beta & \lambda'''_{02}\tan\beta & \lambda'''_{03}\tan\beta \end{pmatrix}. \tag{6.37}$$

This means that the matrix C is the part of M_N connecting the left- and right-handed components together.

6.3.2 Charged fermions

The charged fermion mass matrix is almost identical to the corresponding mass matrix from MSSM-M. The only difference, is the appearance of $\hat{\mu}_0$. In the gauge bases $\Psi^{-T} = \left(\tilde{W}^-, \psi_{L^-_\alpha}\right)$ and $\Psi^{+T} = \left(\tilde{W}^+, \psi_{H^+_u}, \psi_{e^+_i}\right)$ the 5×5 charged fermion mass matrix takes the following form [49] in the v_i-basis,

$$M_C = \begin{pmatrix} M_2 & \sqrt{2}M_Z\sin\beta & 0_{1\times3} \\ \sqrt{2}M_Z\cos\beta & -\hat{\mu}_0 & 0_{1\times3} \\ 0_{3\times1} & 0_{3\times1} & \frac{1}{\sqrt{2}}v_d\,(Y_e)_{ij} \end{pmatrix}. \tag{6.38}$$

This mass matrix must be diagonalised by use of two unitary matrices, i.e.,

$$Z_-^T M_C Z_+ = \mathrm{diag}\left(m_{\chi^-_1}, m_{\chi^-_2}, m_i\right). \tag{6.39}$$

By using Z_+ and Z_- the gauge eigenstates can be written in terms of the mass eigenstates, i.e.,

$$\lambda^\pm_A = iZ^\pm_{1i}\tilde{\chi}^\pm_i, \qquad \psi_{H^+_u} = Z^+_{2i}\tilde{\chi}^+_i, \tag{6.40}$$

$$\psi_{L^-_\alpha} = Z^-_{2+\alpha,i}\tilde{\chi}^-_i, \quad \psi_{e^+_j} = Z^+_{2+j,i}\tilde{\chi}^+_i, \quad i = 1,2,\ldots,5, \tag{6.41}$$

where

$$\lambda^\pm_A = \frac{\lambda^1_A \mp i\lambda^2_A}{\sqrt{2}}. \tag{6.42}$$

The two 4-component Dirac spinors are now defined by,

$$\chi_i = \begin{pmatrix} \tilde{\chi}_i^+ \\ \bar{\tilde{\chi}}_i^- \end{pmatrix}, \quad i = 1, 2. \tag{6.43}$$

As for MSSM-M complete alignment in the v_i-basis ensures that there are no mixing between the MSSM-like charginos and MSSM-like charged leptons. As noted in Sec. 5.5 one can make another rotation among the superfields L_i such that the Yukawa-matrix Y_e is diagonal in the v_i basis. Its diagonal elements are associated with the three charged lepton masses known from the Standard Model, see Eq. (5.80). Note that this mass matrix describes the positive charged leptons known from the Standard Model.

By following Ref. [28], it is now straight forward to obtain analytic expressions for the mixing matrices Z^+ and Z^-. These expressions are identical to the corresponding ones obtained for MSSM-M, see Eqs. (5.81) - (5.84).

6.3.3 Charged scalars

The squared mass matrix for the charged scalars is almost identical to the corresponding matrix found in MSSM-M. The only difference is the appearance of the hatted parameters $\hat{\mu}_0$ and $\hat{b}_\alpha$ in MSSM-DM. Working in the gauge-basis $\Phi_{\rm CS}^T = \left(H_u^+, \tilde{L}_\beta^{2*}, \tilde{e}_j\right)$, and assuming complete alignment in the v_i-basis, the squared mass matrix for the charged scalars takes the form,

$$M_{\rm cs}^2 = \begin{pmatrix} M_W^2 \cos^2\beta + \hat{b}_0 \cot\beta & M_W^2 \sin\beta\cos\beta + \hat{b}_0 & \hat{b}_j & 0_j \\ M_W^2 \sin\beta\cos\beta + \hat{b}_0 & M_W^2 \sin^2\beta + \hat{b}_0 \tan\beta & \hat{b}_j \tan\beta & 0_j \\ \hat{b}_i & \hat{b}_i \tan\beta & \left(M_{\tilde{L}}^2\right)_{ij} & \left(M_{\tilde{L}}^2\right)_{i,3+j} \\ 0_i & 0_i & \left(M_{\tilde{L}}^2\right)_{3+i,j} & \left(M_{\tilde{L}}^2\right)_{3+i,3+j} \end{pmatrix}, \tag{6.44}$$

where $i, j = 1, 2, 3$, and $M_{\tilde{L}}^2$ is analogous to the squared mass matrix for the selectrons of MSSM, that is, it is analogous to Eq. (D.5). The only modification from MSSM-M is a change from μ to $\hat{\mu}_0$. Also, the upper left 2×2 submatrix is analogous to the squared mass matrix for the charged Higgs scalars of MSSM. As for the charged scalar squared mass matrix of MSSM-M, are the bilinear couplings represented by $\hat{b}_\alpha$ important parameters, which connect the MSSM-like charged Higgs scalars to the selectrons.

This matrix is symmetric and is therefore diagonalised by using only one unitary matrix, i.e.,

$$Z_{\rm cs}^\dagger M_{\rm cs}^2 Z_{\rm cs} = \text{diag}\left(m_1^2, m_2^2, \ldots, m_8^2\right).$$

By using this unitary matrix the mass eigenstates become

$$H_u^1 = Z_L^{1i}\,\tilde{L}_i^+, \qquad \tilde{L}_\alpha^2 = Z_L^{2+\alpha,i*}\,\tilde{L}_i^+, \tag{6.45}$$

$$\tilde{c}_{R,j} = Z_L^{5+j,i}\,\tilde{L}_i^+, \qquad i = 1,2,\ldots,8. \tag{6.46}$$

Due to the existence of $\lambda'''_{\alpha i}$ the squared mass matrices for the up- and down-type squarks will also be modified. However, this modification only involves a change from μ to $\hat{\mu}_0$.

Finally, we note that the squared mass matrix, Eq. (6.44), always has one vanishing eigenvalue. This is the Goldstone boson which appears explicitly in the Feynman gauge used in this thesis, see e.g., Ref. [47]. In the physical (unitary) gauge this degree of freedom is absorbed by the W bosons.

6.3.4 Neutral scalars

As for MSSM one can reduce the neutral scalars into two classes, according to their CP eigenvalues, see e.g., Ref. [47].

The general form for the squared mass matrix for the CP-even neutral scalars obtained in the gauge basis $\Phi_0^T = (\psi_u, \psi_\alpha, \rho_i)$ is shown in Appendix D.4. This matrix simplifies considerably under complete alignment, i.e.,

$$M^2_{\text{even}} = \begin{pmatrix} M_Z^2 \sin^2\beta + \hat{b}_0 \cot\beta & -M_Z^2 \cos\beta\sin\beta - \hat{b}_0 & \hat{b}_i & (M^2_{\text{even}})_{1,5+j} \\ -M_Z^2 \cos\beta\sin\beta - \hat{b}_0 & M_Z^2 \cos^2\beta + \hat{b}_0 \tan\beta & \hat{b}_i \tan\beta & (M^2_{\text{even}})_{2,5+j} \\ \hat{b}_i & \hat{b}_i \tan\beta & (M^2_{\text{even}})_{2+i,2+j} & 0 \\ (M^2_{\text{even}})_{5+j,1} & (M^2_{\text{even}})_{5+j,2} & 0 & (M^2_{\text{even}})_{5+i,5+j} \end{pmatrix}, \tag{6.47}$$

where

$$\begin{aligned}
\left(M^2_{\text{even}}\right)_{1,5+i} &= \left(M^2_{\text{even}}\right)_{5+i,1} \\
&= \frac{1}{\sqrt{2}} v\cos\beta\left(\lambda'''^{\text{s}}_{0i} + \lambda'''_{0l}\hat{B}_{il}\right) + \sqrt{2} v \sin\beta\,\hat{\mu}_0\lambda'''_{0i}, && (6.48)\\
\left(M^2_{\text{even}}\right)_{2,5+i} &= \left(M^2_{\text{even}}\right)_{5+i,2} \\
&= \frac{1}{\sqrt{2}} v\sin\beta\left(\lambda'''^{\text{s}}_{0i} + \lambda'''_{0l}\hat{B}_{il}\right) + \sqrt{2} v \cos\beta\,\hat{\mu}_0\lambda'''_{0i}, && (6.49)\\
\left(M^2_{\text{even}}\right)_{2+i,2+j} &= \left(M_L^2\right)_{ij} + \frac{M_Z^2}{2}\cos 2\beta\,\delta_{ij}, && (6.50)\\
\left(M^2_{\text{even}}\right)_{5+i,5+j} &= \frac{1}{2}v^2\lambda'''_{0i}\lambda'''_{0j} + \left(M_n^2\right)_{ij} + \hat{B}^{\text{s}}_{ij} + \hat{B}_{ik}\hat{B}_{jk} \\
&\quad + A_{ijk}\left(\frac{1}{4}v^2\sin(2\beta)\lambda'''_{0k} + C_k + \frac{1}{\sqrt{2}}w_p B_{pk} + \frac{1}{4}w_p w_q A_{pqk}\right). && (6.51)
\end{aligned}$$

Here the definition of $\hat{B}_{ij}$ made in Eq. (6.30) is used along with

$$\hat{B}^{s}_{ij} = B^{s}_{ij} + \frac{1}{\sqrt{2}} w_k A^{s}_{ijk}. \tag{6.52}$$

The squared mass-matrix for the CP-odd neutral scalars was also obtained in Appendix D.4 in the gauge basis $\Phi^T_{\text{even}} = (\phi_u, \phi_\alpha, \eta_i)$. Under complete alignment in the v_i-basis this matrix also simplifies considerably, i.e.,

$$M^2_{\text{odd}} = \begin{pmatrix} \hat{b}_0 \cot\beta & \hat{b}_0 & \hat{b}_i & (M^2_{\text{odd}})_{1,5+j} \\ \hat{b}_0 & \hat{b}_0 \tan\beta & \hat{b}_i \tan\beta & (M^2_{\text{odd}})_{2,5+j} \\ \hat{b}_i & \hat{b}_i \tan\beta & (M^2_{\text{odd}})_{2+i,2+j} & 0 \\ (M^2_{\text{odd}})_{5+i,1} & (M^2_{\text{odd}})_{5+i,2} & 0 & (M^2_{\text{odd}})_{5+i,5+j} \end{pmatrix}, \tag{6.53}$$

where

$$\left(M^2_{\text{odd}}\right)_{1,5+i} = \left(M^2_{\text{odd}}\right)_{5+i,1} = \frac{1}{\sqrt{2}} v \cos\beta \left(-\lambda'''^{s}_{0i} + \lambda'''_{0l} \hat{B}_{il}\right), \tag{6.54}$$

$$\left(M^2_{\text{odd}}\right)_{2,5+i} = \left(M^2_{\text{odd}}\right)_{5+i,2} = \frac{1}{\sqrt{2}} v \sin\beta \left(-\lambda'''^{s}_{0i} + \lambda'''_{0l} \hat{B}_{il}\right), \tag{6.55}$$

$$\left(M^2_{\text{odd}}\right)_{2+i,2+j} = \left(M^2_L\right)_{ij} + \frac{M^2_Z}{2} \cos 2\beta\, \delta_{ij}, \tag{6.56}$$

$$\begin{aligned} \left(M^2_{\text{odd}}\right)_{5+i,5+j} &= v_u^2 \lambda'''_{0i} \lambda'''_{0j} + 2 \left(M^2_n\right)_{ij} - \hat{B}^{s}_{ij} + \hat{B}_{ik} \hat{B}_{jk} \\ &\quad - A_{ijk} \left(v_u v_d \lambda'''_{0k} + C_k + \frac{1}{\sqrt{2}} w_p B_{pk} + \frac{1}{4} w_p w_q A_{pqk}\right). \end{aligned} \tag{6.57}$$

The definitions made in Eqs. (6.30) and (6.52) have also been used for this matrix.

As for the squared mass matrix for the neutral CP-odd Higgs scalars of MSSM, the matrix of Eq. (6.53) has one vanishing eigenvalue. This is the Goldstone boson which appears explicitly in the Feynman-gauge. In the physical gauge this degree of freedom is absorbed by the Z-boson.

The lightest neutral CP-even scalar is associated with the Higgs boson from the Standard Model. This mass, and its sensitivity on the other parameters is further analysed in the next section.

Each of the squared mass matrices, Eqs. (6.47) and (6.53), are diagonalised by use of only one unitary matrix. However, as explained in Appendix E.2.1, the 16 eigenstates for the neutral scalars will be assembled into one complex neutral eigenvector, Φ^i_{NS}. By using this eigenvector the mass eigenstates are obtained as

$$H^2_u = \frac{1}{\sqrt{2}} \left(Z^{1i}_{NS} + i Z^{9i}_{NS}\right) \Phi^i_{NS}, \tag{6.58}$$

$$\tilde{L}^{1}_{\alpha} = \frac{1}{\sqrt{2}} \left(Z^{2+\alpha,i}_{NS} + i Z^{10+\alpha,i}_{NS}\right) \Phi^i_{NS}, \tag{6.59}$$

$$\tilde{n}_j = \frac{1}{\sqrt{2}} \left(Z^{5+j,i}_{NS} + i Z^{13+j,i}_{NS}\right) \Phi^i_{NS}, \quad i = 1, 2, \ldots, 16. \tag{6.60}$$

In this section the mass matrices have been presented in the v_i basis. It has been shown that all mass matrices of MSSM are modified to some degree. However, by assuming complete alignment it is found that these modifications are small. That is, one still finds the mass matrices of MSSM, but now as sub-matrices in the mass matrices of MSSM-DM. The mixing between MSSM-like particles is made possible by the couplings λ'''_{0i}, $\lambda'''^{s}_{\alpha j}$ and $\hat{b}_\alpha$.

6.4 Constraints from mass matrices

As shown in the last section, the parameters λ'''_{0i} and $\lambda'''^{s}_{\alpha i}$ cause the heavy modes, associated with the right-handed singlets, to mix with the lighter modes of MSSM-DM. It is therefore of interest to find out whether the observed mass bounds reported by Ref. [23] will put any constraints on these two parameters.

The mass matrices presented in the last section show that neither the mass matrix for the charged fermions, nor the squared mass matrix for the charged scalars, will put any limits on the elements of λ'''_{0i} or $\lambda'''^{s}_{\alpha i}$. In addition, if one assumes that $\bar{M}_Z \ll \hat{B}_{ij} \leqslant \bar{M}_{\rm GUT}$ then neither the neutral fermion mass matrix constrains λ'''_{0i}. In fact, the larger the parameter $\hat{B}$ is, the larger λ'''_{0i} can be without breaking the phenomenological constraints of Ref. [23]. As an example, assume that $\hat{B}_{ij} = 10^8\,\delta_{ij}$ and $\lambda'''_{0i} = k$, $i = 1, 2, 3$. Then k has to be larger than 1000 for the lightest neutralino mass to break the lower limit on 32.5 GeV. This is clearly an unacceptable value for perturbative calculations, and for the forthcoming analysis it will always be assumed that $|\lambda'''_{0i}| < 1$ for each $i = 1, 2, 3$

The observed limits on possible neutral scalar masses reported by Ref. [23], i.e., $m_{\tilde{\chi}^0_1} > 23\,\text{GeV}$, may put some constraint on $\lambda'''_{\alpha j}$. One should, however, remember that neutral scalar masses are subject to large radiative corrections, see e.g., Ref. [57]. Thus one should not take any limits found from tree-level calculations too literally. Aside from this cautionary remark, it is interesting to see what kind of restrictions the tree-level squared mass matrices do put on the neutral scalar masses. In the forthcoming numerical analysis these tree-level mass matrices will be used.

In the full numerical analysis, to be presented in Sec. 6.6, the elements of all mass matrices are determined by solving the renormalization group equations and by minimising the tree-level neutral scalar potential. For now, only some rough assumptions will be made for the relevant parameters.

The most interesting neutral scalar mass is the lightest one. To study this mass the following three assumptions are made. First, it is assumed that $(M^2_{\rm even})_{5+i,5+j}$ is diagonal, i.e.,

$$\left(M^2_{\rm even}\right)_{5+i,5+j} = M^2_R\,\delta_{ij}, \qquad i, j = 1, 2, 3. \tag{6.61}$$

Then it is assumed that $\hat{b}_0$ is large, but still fulfilling the relation $\hat{b}_0 \ll M^2_{\rm R}$, and also that $\hat{b}_i$ can be neglected. Also, assume that the matrix elements $(M^2_{\rm even})_{1,5+i}$ and

$(M^2_{\rm even})_{2,5+i}$ are related as follows,

$$\left(M^2_{\rm even}\right)_{1,5+i} = M_T^2, \tag{6.62}$$

$$\left(M^2_{\rm even}\right)_{2,5+i} = M_T^2 \, \tan\beta. \tag{6.63}$$

By using these assumptions the squared mass matrix of Eq. (6.47) takes the following simplified form,

$$M^2_{\rm even} = \begin{pmatrix} M_Z^2 \sin^2\beta + \hat{b}_0 \cot\beta & -M_Z^2 \cos\beta \sin\beta - \hat{b}_0 & 0_j & M_T^2 \, \hat{e}_j \\ -M_Z^2 \cos\beta \sin\beta - \hat{b}_0 & M_Z^2 \cos^2\beta + \hat{b}_0 \tan\beta & 0_j & M_T^2 \, \tan\beta \, \hat{e}_j \\ 0_i & 0_i & (M^2_{\rm even})_{2+i,2+j} & 0 \\ M_T^2 \, \hat{e}_i & M_T^2 \, \tan\beta \, \hat{e}_i & 0 & M_R^2 \, \delta_{i,j} \end{pmatrix}, \tag{6.64}$$

where the unit vectors $\hat{e}_i$ are defined by

$$\hat{e}_1 = (1,0,0), \quad \hat{e}_2 = (0,1,0), \quad \hat{e}_3 = (0,0,1). \tag{6.65}$$

Note that these assumptions means that M_T^2 is now the only parameter causing the light and heavy elements of $M^2_{\rm even}$ to mix together.

This simplified mass matrix shows that 3 of its eigenvalues are obtained from $(M^2_{\rm even})_{2+i,2+j}$. Two more eigenvalues will be equal to M_R, as can be shown from the characteristic polynomial. Thus, only the last 3 eigenvalues may possible depend on M_T^2.

To proceed the following numerical values will be used,

$$\tan\beta = 10, \tag{6.66}$$

$$M_R^2 = 10^{20}\,\mathrm{GeV}^2, \tag{6.67}$$

$$b_0 = 30000\,\mathrm{GeV}^2. \tag{6.68}$$

In Figure 6.1 the lightest neutral scalar mass is shown as a function of M_T^2. It clearly shows that M_T^2 must be very large, of the order 10^{11}, in order to give some interesting contribution to the lightest neutral scalar mass.

One may also use this upper bound for M_T^2 to find a rough upper limit for λ'''_{0i}. From Eq. (6.48) one can make the following approximation,

$$\left(M^2_{\rm even}\right)_{1,5+i} = M_T^2 \approx \frac{1}{\sqrt{2}} \, v \cos\beta \, \lambda'''_{0l} \, \hat{B}_{il}. \tag{6.69}$$

By assuming $\hat{B}_{ij} = Q \, \delta_{ij}$, where $Q \sim M_R^2 \sim 10^{20}\,\mathrm{GeV}^2$, one finds the following upper bounds from Eq. (6.69) and Fig. 6.1,

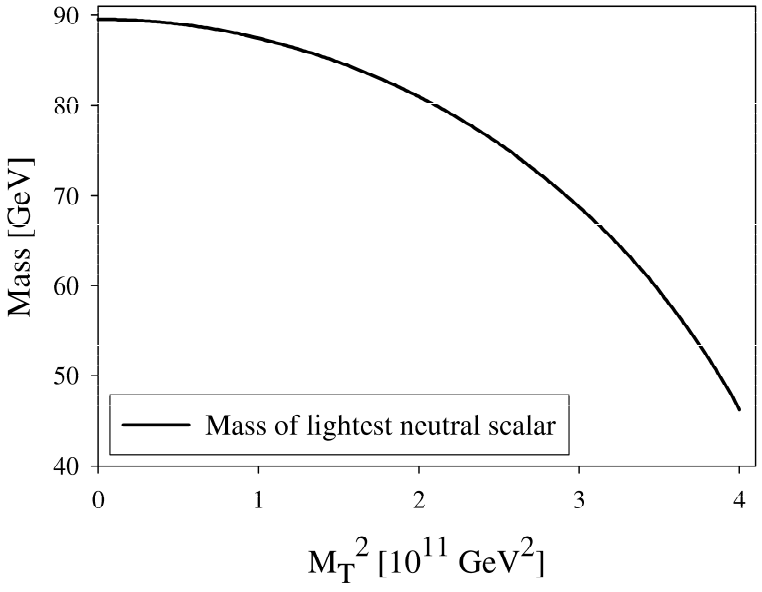

Figure 6.1: The figure shows the mass of the lightest neutral scalar as a function of M_T^2, see Eq. (6.62).

$$\lambda'''_{01} \lesssim \frac{10^{11}}{M_R}\frac{\sqrt{2}}{3}\frac{\sqrt{1+\tan^2\beta}}{v} \sim 10^{-1}. \tag{6.70}$$

This limit is rather arbitrary for two reasons. First, only approximate methods have been used, and secondly, it is well known that the neutral scalar masses are sensitive to radiative corrections. Thus to give a more thorough analysis of the neutral scalar masses one should include these loop effects. These corrections have not been analysed or included in this thesis.

Also, no limits were obtained for $\lambda'''^{s}_{\alpha j}$, although one would expect these elements to be of the order 10, based on experience on the relation between the superpotential and soft-breaking trilinear couplings. In later sections the decay rates $\Gamma(l \to l'\gamma)$ will be explored, qualitatively and numerically, in order to improve these rough estimates for both λ'''_{0i} and $\lambda'''^{s}_{\alpha i}$.

6.5 Running of parameters in MSSM-DM

In this section the running of some of the most important parameters of MSSM-DM will be analysed both by analytic and numeric methods. The constrained supergravity inspired boundary conditions will be used, i.e., Eqs. (6.5) - (6.11). Also, the

boundary conditions from Eqs. (6.19) and (6.20) are used to determine A_{ijk} and B_{ij} at the electroweak scale, i.e.,

$$\begin{aligned} A_{ijk} &= P\,\delta_{ij}\delta_{jk}, \\ B_{ij} &= Q\,\delta_{ij}, \qquad i,j,k = 1,2,3, \end{aligned}$$

Finally, one parameter, ω, is needed at the n-scale, i.e.,

$$\omega_i = \omega\,\hat{e}_i, \qquad i = 1,2,3, \tag{6.71}$$

and the unit vectors $\hat{e}_i$ are defined in Eq. (6.65).

This means that in addition to the Standard Model couplings, masses and mixing angles, MSSM-DM now has 48 free parameters. The superpotential parameters λ_{ijk}, λ'_{ijk}, λ'''_{0i}, P and Q, contribute with 41 parameters at the electroweak scale[2]. Five of the remaining parameters are known from MSSM, i.e., $\tan\beta$, M_0, $M_{1/2}$, A_0 and $\mathrm{sign}(\hat{\mu}_0)$. And the last two parameters are B_0 and ω.

6.5.1 Qualitative analysis of renormalization group equations

Even if the full set of renormalization group equations must be solved by numerical methods, it is important to gain some qualitative understanding of the running of the most important parameters of MSSM-DM. In this part of the analysis the running of $\lambda'''_{\alpha i}$, $\lambda'''^{\mathrm{s}}_{\alpha i}$, A_{ijk}, A^{s}_{ijk}, B_{ij}, B^{s}_{ij} and C_i will be studied. It will be shown that all elements of C_i are huge, while the elements of both A_{ijk} and A^{s}_{ijk} are very small. In fact, these trilinear couplings will be assumed to vanish.

As stated several times in this chapter, the most important parameters of MSSM-DM are the elements of $\lambda'''_{\alpha i}$. This is for two reasons. First, it causes the gauge singlets to mix with the other fields. Secondly, due to the boundary condition, Eq. (6.9), it also determines $\lambda'''^{\mathrm{s}}_{\alpha i}$ at the GUT-scale.

The running of $\lambda'''_{\alpha j}$ is determined by Eq. (F.57). This equation shows that even if λ'''_{ij} vanishes at the electroweak scale, non-vanishing values will reappear at higher scales. This renormalization group effect is due to the R-parity violating couplings λ_{ijk} and λ'_{ijk}. The renormalization group equation of Eq. (F.57) also shows that the running of $\lambda'''_{\alpha j}$ is quite sensitive to the top-quark Yukawa coupling. Since the top-quark Yukawa coupling was found to depend strongly on $\tan\beta$, also $\lambda'''_{\alpha i}$ will show the same dependency. Note that $\lambda'''_{ij} = (Y_\nu)_{ij}$, therefore much of the analysis made for Y_ν in Sec. 4.4 still applies for $\lambda'''_{\alpha i}$.

[2]The parameters λ_{ijk}, λ'_{ijk}, λ'''_{0i}, P and Q contribute with 9, 27, 3, 1 and 1 parameters, respectively.

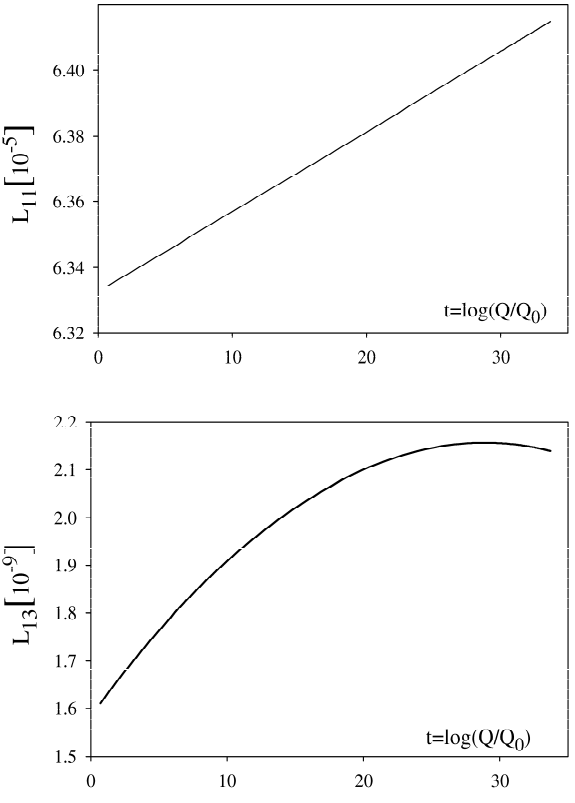

Figure 6.2: The figure shows the running of L_{11} and L_{13}. The values to be specified in Sec. 6.5.2 and $\tan\beta = 10$ are used.

The boundary condition, Eq. (6.9), shows that, generally, also $\lambda'''^{s}_{\alpha j}$ takes non-vanishing values at the GUT scale, and also at the electroweak scale. These non-vanishing values cause mixing between left- and right-handed neutral scalars.

The renormalization group equations for the gauge singlet self couplings, A_{ijk}, B_{ij} and C_i, are presented in Eqs. (F.58), (F.60) and (F.61), respectively. The running of all of these parameters depends upon the term

$$L_{ij} = \frac{1}{16\pi^2}\left(\lambda'''_{\alpha i}\lambda'''_{\alpha j} + A_{ikl}A_{jkl}\right) \lesssim 10^{-5}. \tag{6.72}$$

The upper limit was obtained by assuming $\lambda_{0i} < 0.1\,\hat{e}_i$, which was the limit established in Sec. 6.4. It has also been assumed that each component of A_{ijk} has the same upper limit, i.e., $A_{ijk} < 0.1$ for each i, j and k. Figure 6.2 shows the running of L_{11} and L_{13}. This figure shows that L_{11} does not change much, and may

be treated as a constant throughout the integration region. One also sees that L_{13} is very small. The results for the other diagonal and off-diagonal elements of L_{ij} are equal to L_{11} and L_{13}, respectively. Figure 6.2 means that neither of the gauge singlet self couplings, i.e., A_{ijk}, B_{ij} and C_i, suffers from any large relative changes throughout the integration region, and they may therefore be treated as constants.

In Sec. 6.3 it was shown that B_{ij} will be assumed diagonal at the electroweak scale, i.e.,

$$B_{ij} = Q\,\delta_{ij}, \tag{6.73}$$

and that Q is large, i.e.,

$$Q \sim \omega \sim 10^{10}\,\mathrm{GeV}. \tag{6.74}$$

It will now be shown that this causes the elements C_i to take very large values, e.g., of the order $10^{20}\,\mathrm{GeV}^2$, and that the elements of A_{ijk} must be small, that is

$$A_{ijk} < 1, \text{ for each } i,\ j \text{ and } k. \tag{6.75}$$

The elements of B^{s}_{ij} are fixed at the GUT-scale by the boundary condition shown in Eq. (6.11). This means that its elements are of roughly the same order of magnitude as the elements of B_{ij}. If one neglects the trilinear couplings A_{ijk} and A^{s}_{ijk}, then the minimisation condition of Eq. (6.18) takes the simpler approximate form,

$$C_1 = C_2 = C_3 = R \approx 3\sqrt{2}\,Q\,\omega \sim 10^{20}\mathrm{GeV}^2. \tag{6.76}$$

Such large values may have large impact on other parameters due to renormalization group effects. This is clearly seen in the running of B^{s}_{ij}. Its renormalization group equation, i.e., Eq. (F.70), shows that the running of B^{s}_{ij} depends on b_α. But the minimisation conditions do not determine b_α, they determine the hatted parameter $\hat{b}_\alpha$. Thus b_α must be determined at the electroweak scale by Eq. (6.23). Due to the large values for ω, P, Q and R it is found that b_0 may be approximated by,

$$b_0 \approx -\lambda'''_{0l}\left(\frac{3}{4}\,\omega^2\,P + \frac{3}{\sqrt{2}}\,\omega\,Q + R\right) \sim -10^{20}\,\mathrm{GeV}^2, \tag{6.77}$$

at the electroweak scale.

The important fact is not the values for b_0, but that the running of B^{s}_{ij} depends upon b_0. An approximate solution of the renormalization group equation for B^{s}_{ij} can easily be found, i.e.,

$$B^{s}_{ij} = \left(B_0\,Q - \frac{3}{8\pi^2}\,b_0\,P\,\lambda'''_{01}\,t_{GUT}\right)\delta_{ij}. \tag{6.78}$$

Note that the last term is the dominating one due to the large size of b_0. In the preceding analysis it has been assumed that B^{s}_{ij} and B_{ij} are of roughly the same

magnitude. Solution (6.78) shows that this can be achieved if P is small, or if it vanishes completely. Alternatively, one can assume that λ'''_{01} is small, of the order 10^{-7}. But this means that there are hardly any coupling between the visible and invisible sector, and MSSM-DM will be phenomenologically equal to MSSM-M. One can also obtain small values for B^{s}_{ij} at the electroweak scale if there are some cancellations among the terms in Eq. (6.78).

This motivates the assumption that all elements of A_{ijk} vanishes. Note that due to the boundary conditions at the GUT scale, i.e., Eq. (6.10), also all elements of A^{s}_{ijk} vanishes.

The vanishing of A_{ijk} has several advantages. First, the squared mass matrices for the neutral scalars, Eq. (6.47) and (6.53), are simplified. Next, the minimisation conditions at the n-scale, i.e., Eq. (6.18), are also simplified. Finally, the vanishing of A_{ijk} prevents B^{s}_{ij} to take large values. This also makes the numerical routines more stable.

In the next section the running of A_{ijk} and A^{s}_{ijk} are, however, presented in order to confirm the qualitative analysis made in this section.

6.5.2 Numeric analysis of renormalization group equations

The full set of renormalization group equations, as presented in Appendix F.2, has to be solved by numerical methods. In MSSM-DM this is a large set of coupled differential equations, which in general takes more than 30.000 lines of Fortran code only to define.

The numerical method, presented in Sec. H, only needs some small modifications to give a proper treatment of the n-scale. This modified procedure starts by solving the renormalization group equations, but neglecting the n-scale, and the large parameters B^{s}_{ij}, b_α and C_i. After a solution is obtained, these parameters, and the n-scale, are included. The value for the soft breaking parameter B^{s}_{ij} is fixed at the GUT scale by the boundary condition Eq. (6.11). Next, the equations are run down to the n-scale, and a value for C_i is found. From the qualitative analysis it is known that that this value can be treated as a constant throughout the integration region. Finally, a value for b_α is obtained at the electroweak scale. The renormalization group equations are now iterated between the electroweak scale, the n-scale and the GUT scale until a stable solution is obtained. As explained in the analytic analysis, most of these parameters will not suffer from any large renormalization group effects, and a stable solution is obtained from only a few iterations. Note that the running of B^{s}_{ij}, b_α and C_i does not affect the running of any of the other parameters.

The following set of MSSM parameters will be used throughout this section,

$$\tan\beta \in \{10, 30, 50\}, \tag{6.79}$$
$$\text{sign}(\mu) = +1, \tag{6.80}$$
$$M_0 = 200\,\text{GeV}, \tag{6.81}$$
$$M_{1/2} = 250\,\text{GeV}, \tag{6.82}$$
$$A_0 = 200\,\text{GeV}. \tag{6.83}$$

The following texture has been used,

$$\lambda'''_{\alpha i} = \begin{cases} \Lambda''' & \text{for } \alpha = 0 \text{ and } i = 1,2,3, \\ 0 & \text{else.} \end{cases} \tag{6.84}$$

This particular texture will be referred to as a uniform texture for λ'''. The uniform textures, defined by Eqs. (5.123) and (5.132), are also used with the following choices,

$$\Lambda = \Lambda' = \Lambda''' = 5.0 \cdot 10^{-4}. \tag{6.85}$$

These choices are motivated from the analysis made in Chapter 5, where the uniform texture did put the strongest limits on the R-parity violating parameters.

By using these values the running of λ'''_{03} and λ'''_{33} has been calculated for three values of $\tan\beta$. The results are shown in Fig. 6.3. These two figures show that even if λ'''_{03} and λ'''_{33} may have a large relative change throughout the integration region, the values are still very small. These figures also shows that only for large values of $\tan\beta$ will there be a large relative change in the value for $\lambda'''_{\alpha j}$. As explained in the analytic analysis of $\lambda'''_{\alpha i}$, this dependency on $\tan\beta$ is a consequence of the dependency the renormalization group equation for $\lambda'''_{\alpha i}$ has on the large top-quark Yukawa coupling, y_t. See Fig. 5.2 for examples on the running of y_t.

The running of λ'''_{33} shows that even if this parameter starts off being zero, non-vanishing values have reappeared at the GUT-scale. As explained in the analytic analysis this is a consequence of the non-vanishing R-parity violating couplings. Even though the values for $\lambda'''_{\alpha i}$ are small, they are important for fixing the values of $\lambda'''^{s}_{\alpha i}$ at the GUT scale.

Figure 6.4 shows some examples of the running of λ'''^{s}_{03} and λ'''^{s}_{33}, also for the three choices of $\tan\beta$. These figures show that λ'''^{s}_{03} and λ'''^{s}_{33} take small, but non-vanishing values at the electroweak scale. As for the running of $\lambda'''_{\alpha i}$, the running for the soft-breaking trilinear coupling, $\lambda'''^{s}_{\alpha i}$, will depend on the top-quark trilinear couplings y_t and a_t. Thus, also for $\lambda'''^{s}_{\alpha i}$ the greatest relative change will come from large values of $\tan\beta$.

The running of the gauge singlet parameters is found by specifying values for P, Q,

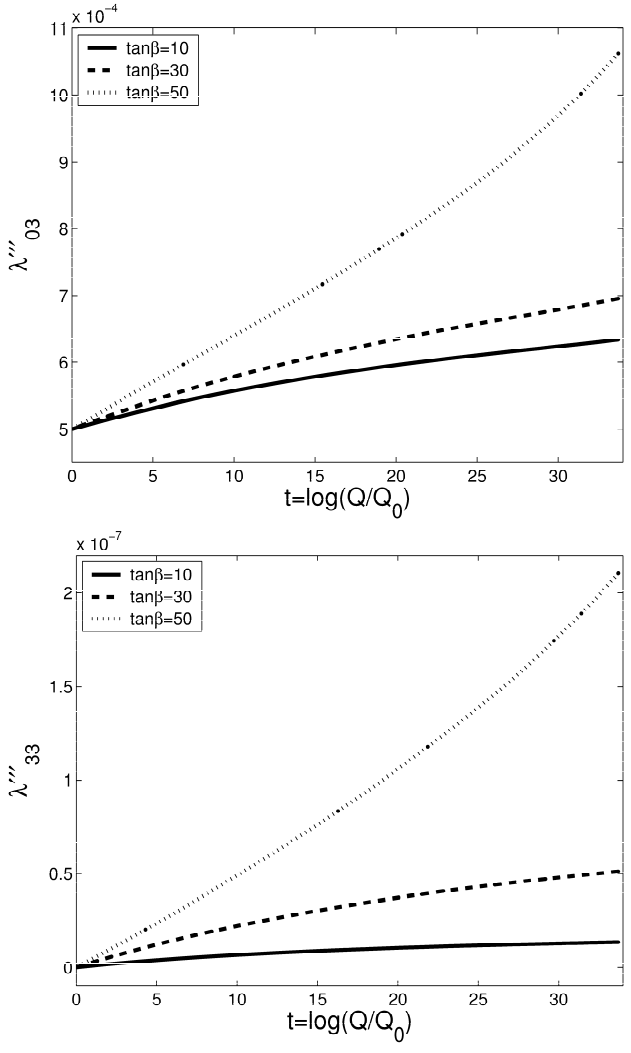

Figure 6.3: The figure shows the running of λ'''_{03} and λ'''_{33} for some choices for $\tan\beta$.

B_0 and ω, see Eqs. (6.19), (6.20) and (6.71). Some, rather arbitrary, values are,

$$P = 10^{-1}, \tag{6.86}$$
$$Q = 10^{10}\,\text{GeV}, \tag{6.87}$$
$$B_0 = 1, \tag{6.88}$$
$$\omega = 10^{11}\,\text{GeV}. \tag{6.89}$$

By using these values it is found that none of the diagonal elements of A suffer from

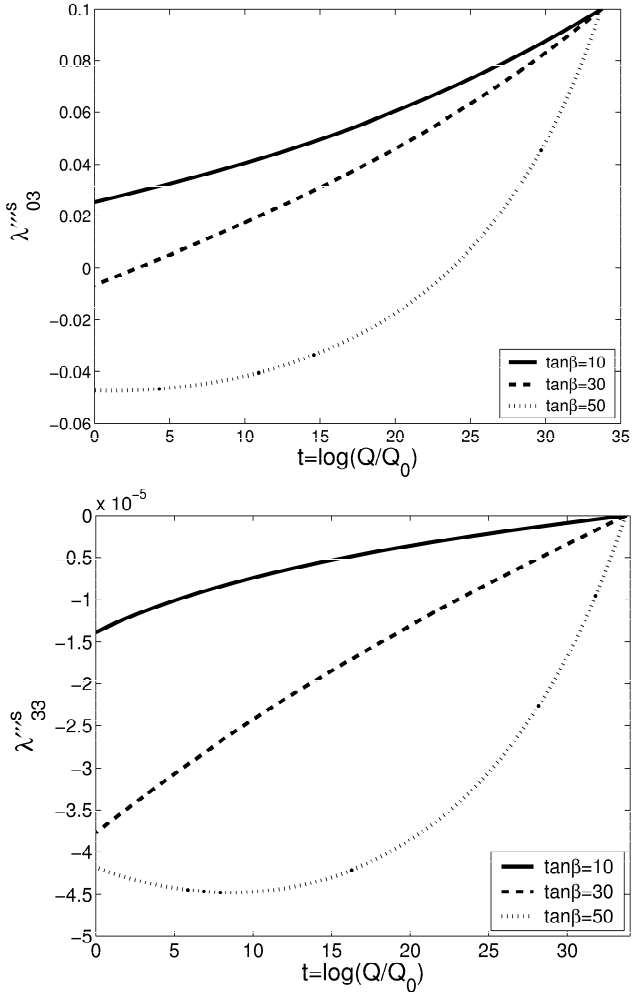

Figure 6.4: The figure shows the running of the soft breaking trilinear couplings λ'''^{s}_{03} and λ'''^{s}_{33}.

any large relative change, even for large values of $\tan\beta$. The off-diagonal elements of A_{ijk} take non-vanishing values at the GUT scale, depending on $\tan\beta$ and on the R-parity violating couplings. Examples of the running of A_{113} are shown in Fig. 6.5.

The value for the trilinear soft breaking coupling, A^{s}_{ijk}, is totally fixed by A_0 and the value of A_{ijk} at the GUT-scale. It is found that the diagonal elements of A^{s} do not suffer from any large relative changes. Though these changes are larger than the ones for A_{ijk}. Figure 6.5 shows the running of the element A^{s}_{113} for three values of $\tan\beta$.

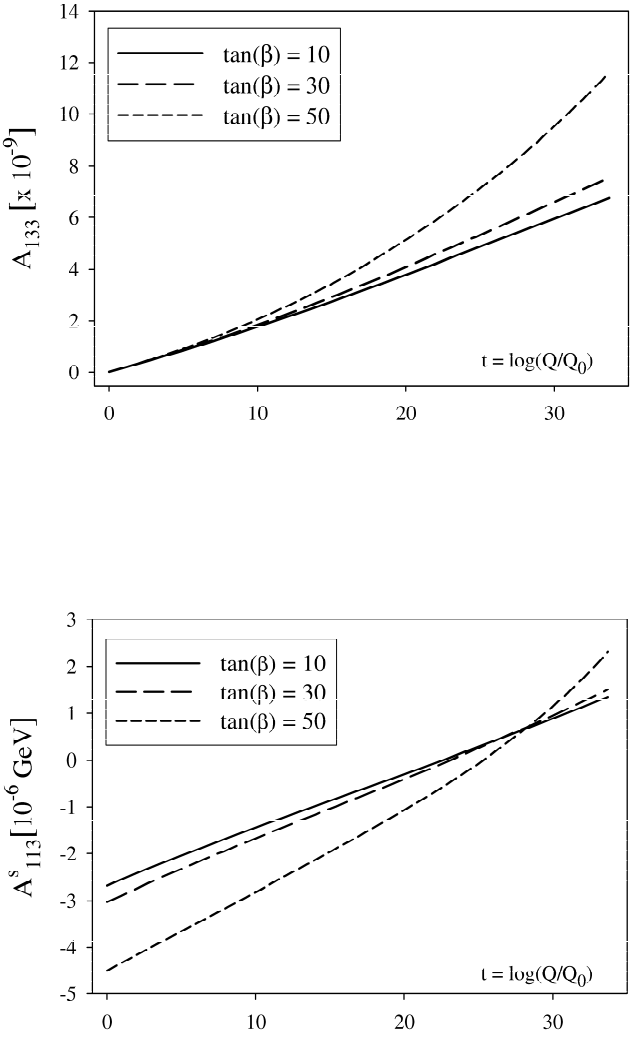

Figure 6.5: The figure shows the running of the parameters A_{113} and A^s_{113} for three values of $\tan\beta$.

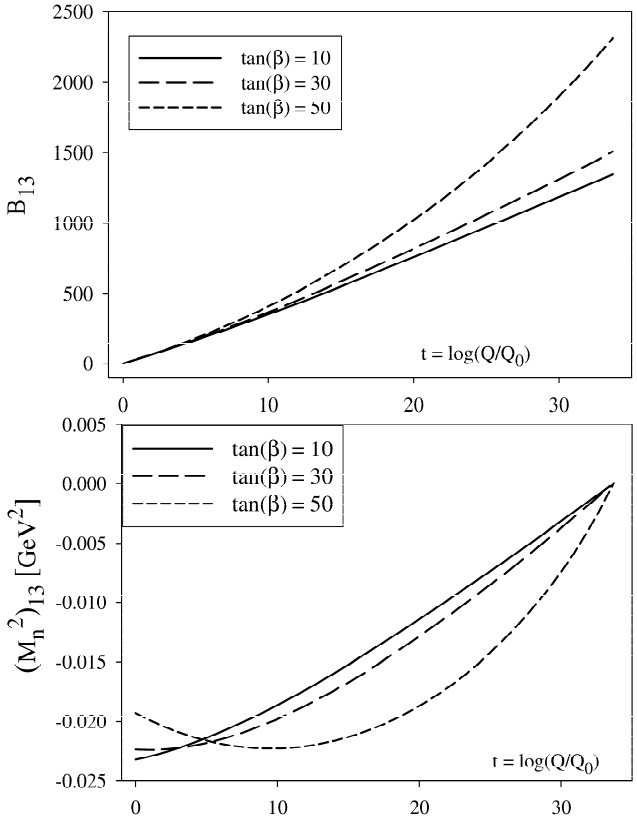

Figure 6.6: The figure shows the running of the parameters B_{13} and $(M_n)_{13}$.

Also, the running of the diagonal elements of B_{ij} is found to have a small relative change. However, also in this case the off-diagonal elements will take non-vanishing values at scales above the electroweak scale. Examples on the running of B_{13} are shown in Fig. 6.6.

A qualitative analysis of the running of $B^{\rm s}_{ij}$ was presented in Sec. 6.5.1. In this analysis it was shown that $B^{\rm s}_{ij}$ had an indirect dependency on C_i via the parameter b_α. Some examples of the running of $B^{\rm s}_{ij}$ are shown in Fig. 6.7. This figure shows that even though the elements of $B^{\rm s}_{ij}$ change over the integration region, they are still very large.

The soft-breaking parameter $M^2_{\tilde{n}}$ appears explicitly in the renormalization group equations for $M^2_{H_u}$ and $(M^2_L)_{\alpha\beta}$, but always in combination with the small parameters $\lambda'''_{\alpha j}$. It is found that the diagonal elements do not change much over the integration interval. These elements are also more or less unaffected by the different values for $\tan\beta$. An example of the running of $(M^2_{\tilde{n}})_{13}$ is shown in Fig. 6.6.

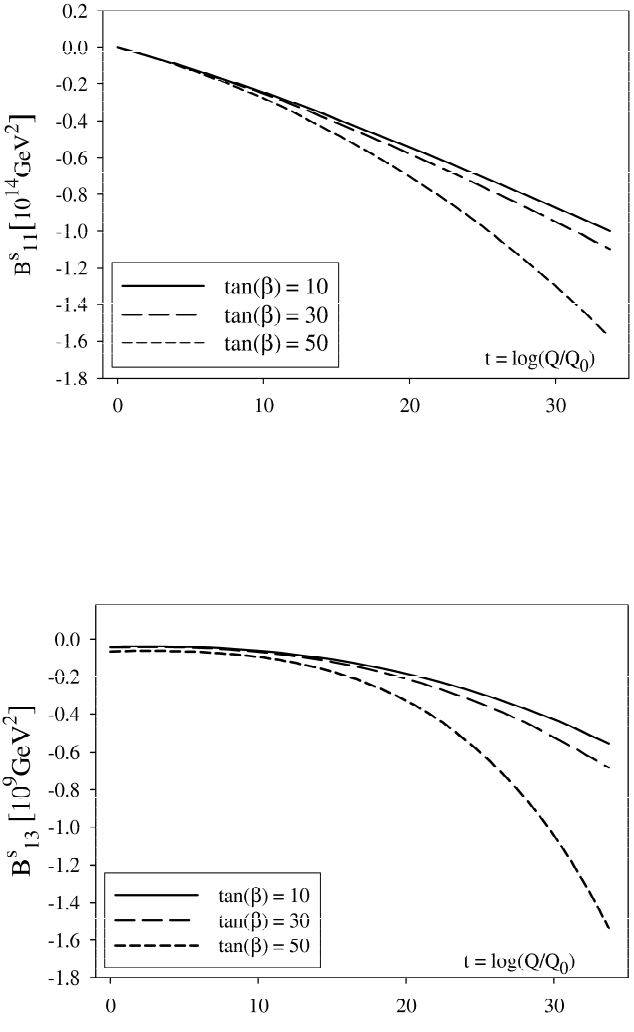

Figure 6.7: The figure shows the running of the parameters B^s_{11} and B^s_{13}.

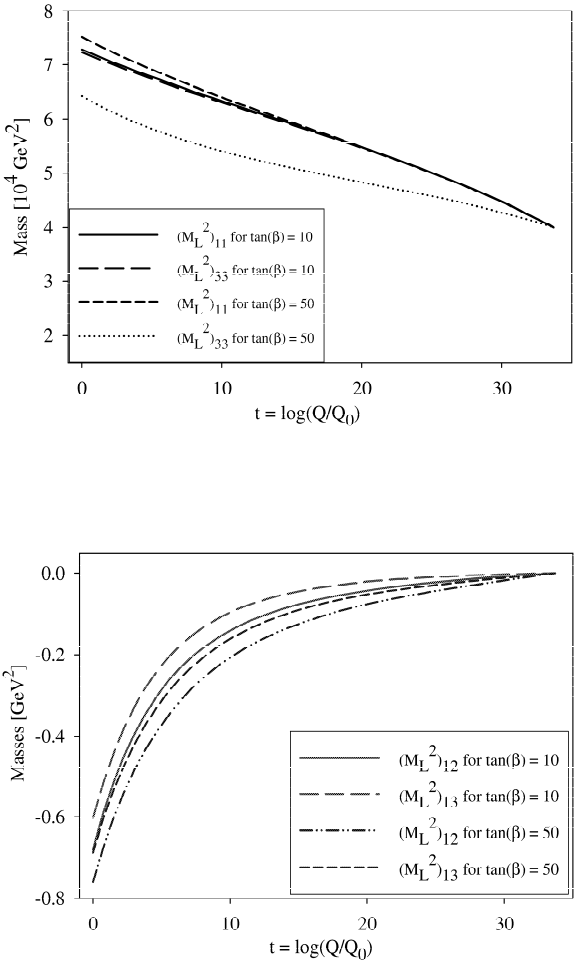

Figure 6.8: The figure shows examples of the running of the diagonal elements and off-diagonal elements of M_L^2, for two values of $\tan\beta$.

As seen from the analysis of MSSM-D and MSSM-M, the off-diagonal elements of M_L^2 are of crucial importance to the decay rates under study. The reason is, of course, that this matrix appears in the squared mass matrices for all scalars. The running of both the diagonal and the off-diagonal elements are shown in Fig. 6.8. This figure shows that the off-diagonal elements are small. Their size also depends on $\tan\beta$.

To summarise the analysis of this section. The renormalization group equations have been analysed, both by qualitatively and by numerical methods. Special attention has been paid to analyse the parameters which involve the right-handed gauge singlets. It has been argued that there is a hierarchy among the right-handed gauge singlet self-couplings, i.e.,

$$A_{ijk} \ll B_{pq} \ll C_l. \tag{6.90}$$

And that the trilinear couplings A_{ijk} and $A^{\rm s}_{ijk}$ may be assumed to vanish. The remaining self-couplings, i.e., B_{ij}, $B^{\rm s}_{ij}$ and C_i may all be approximated as constants throughout the integration region. They all take large values.

6.6 Analysis of $\Gamma(l \to l'\gamma)$ in MSSM-DM

In Ref. [17] it was found that the upper limits for $Br(l \to l'\gamma)$ could easily be violated if the Standard Model was extended with three Dirac-Majorana neutrinos. This violation is caused by mixing among the light left-handed components and the heavy right-handed components, of the neutrino mass matrix. In this section a similar analysis of the decay rates $\mu \to e\gamma$ will be analysed by use of MSSM-DM.

Except for an enlargement of the neutral sector the Feynman amplitudes, which contributes to the decay rates, are equal to the ones from MSSM-M. These Feynman diagrams were all presented in Chapter 5, Fig. 5.7.

The analysis of the preceding sections clearly demonstrates that the most important parameters of MSSM-DM are $\lambda'''_{\alpha i}$ and $\lambda'''^{\rm s}_{\alpha i}$, that is the parameters which connects the gauge singlet fields to the other fields. Thus, if these parameters vanish at the electroweak scale, the gauge singlet sector becomes invisible. In this case the visible sector is equal to MSSM-M, and the analysis of Chapter 5 applies. It is therefore always assumed, throughout this analysis, that at least one of the elements $\lambda'''_{\alpha i}$ or $\lambda'''^{\rm s}_{\alpha i}$ are non-vanishing in the ν_i-basis.

6.6.1 Qualitative analysis of branching ratios

The amplitudes and Feynman rules presented in Appendices B.4 and E.3, show that the diagrams from Fig. 5.7 c), d), e) and f) do not lead to lepton flavour violation. This was also the case in MSSM-M, see discussion in Sec. 5.8. Thus only the diagrams of Fig. 5.7 a) and b) may possible cause any lepton flavour violation.

As seen in MSSM-M, the existence of the R-parity violating coupling λ'_{ijk} will cause quarks and squarks to contribute to these lepton flavour violating decay rates.

In order to analyse the lepton flavour violating decay rates properly, it is useful to discuss the possible flavour violating sources which will contribute to the amplitudes in Fig. 5.7 a) and b). The first of these sources is the direct appearance of R-parity violating couplings in the Feynman rules, see Appendix E.3. And the second source is lepton flavour mixing caused by off-diagonal elements in the mass matrices. In this analysis it will be shown that the off-diagonal elements of the squared scalar mass matrices are the most important sources to lepton flavour violation. The flavour mixing shows up in the vertex factors through the various mixing matrices. Finally, the renormalization group equations may cause the soft-breaking parameters to break lepton flavour at the electroweak scale. The renormalization group equations were studied both by analytic and numeric methods in Sec. 6.5. The most important result from this analysis is that non-vanishing values for λ_{ijk} and λ'_{ijk} lead to off-diagonal elements for the soft-breaking parameters at the electroweak scale. This will also give off-diagonal elements in the mass matrices, and the lepton flavour violation appears from the mixing matrices.

We will now discuss the importance of each of these three sources, with respect to the decay rates under study.

The Feynman rules presented in Eqs. (E.65) - (E.72) show that none of the soft breaking parameters appear directly in the amplitudes. Moreover, since λ_{0ij} is assumed to be diagonal at the electroweak scale, the mixing matrices Z^+ and Z^- will take particular simple forms, see Eq. (5.81). By using these expressions one finds that none of the vertex factors have any direct dependency on λ''_{0i}. That is, the vertex factors only have a direct dependency on λ_{ijk} and λ'_{ijk}.

The mass matrices of MSSM-DM were presented in Sec. 6.3, and a first analysis was made in Sec. 6.4. This analysis shows that neither neutral nor charged fermion mass matrices will give any interesting constraints on the parameters of MSSM-DM. The charged fermion mass matrix, Eq. (6.38), shows that there can be no lepton flavour violation associated with the charged fermions.

The neutral fermion mass matrix has been studied rather thoroughly in Sec. 6.3.1. In this analysis it was shown that in order to obtain phenomenologically acceptable neutrino masses almost complete alignment had to be assumed. Under complete alignment the neutral fermion mass matrix will have three vanishing eigenvalues, which are associated with the masses for the Standard Model neutrinos. This means that the left-handed neutrino components do not mix with any of the other neutral fermions, and any possible lepton flavour violation, caused by the neutral fermion mass matrix, must be caused by mixing between the heavy right-handed gauge singlets and the lighter MSSM-like neutralinos.

If either of the parameters λ^s_{0ij}, $(M^2_L)_{ij}$ or $(M^2_e)_{ij}$ have off-diagonal elements, then the charged scalars will also be a source to lepton flavour mixing. Flavour mixing also takes place for non-vanishing values of $\hat{b}_i$. In Sec. 6.5 it was found that all of

these matrices have small off-diagonal elements at the electroweak scale, if either of the R-parity violating parameters, λ_{ijk} or λ'_{ijk} are non-vanishing.

A special case

The comments made above can now be used to analyse the amplitudes of Fig. 5.7 for the special case that all R-parity violating couplings vanish except λ'''_{0i}. Under these assumptions it will be shown that the lepton flavour number is broken, but there is no contribution to the decay rates under study.

The vanishing of the neutrino masses means that a part of the neutral fermion mixing matrix is diagonal, i.e.,

$$Z_N^{4+i,4+j} = \delta_{ij}, \quad i,j = 1,2,3. \tag{6.91}$$

Next the mixing matrices for the neutral scalars will be discussed. The analysis of the renormalization group equations shows that if the superpotential parameters λ_{ijk}, λ'_{ijk} and λ'''_{ij} all vanish at the electroweak scale, these parameters vanish at all scales. Due to the supergravity inspired boundary conditions this implies that also λ^{s}_{ijk}, λ'^{s}_{ijk} and λ'''^{s}_{ij} vanish at all scales. Further, one finds that M_L^2 and M_c^2 are diagonal at all scales. The vanishing of $(M_L^2)_{0i} = \varepsilon_i$ and the minimisation condition of Eq. (6.23) means that also $\hat{b}_i$ vanishes at the electroweak scale. In fact, this parameter vanishes at all scales. On the other hand, the matrices $\bar{M}_n^2$ and $\bar{B}_n^s$ do have off-diagonal elements as a consequence of the couplings λ'''_{0i}.

By inspecting the squared neutral scalar mass matrices, i.e., Eqs. (6.47) and (6.53), one finds that also parts of the corresponding mixing matrices are diagonal, i.e.,

$$Z_{NS}^{3+i,3+j} = Z_{NS}^{11+i,11+j} = \delta_{ij}, \quad i,j = 1,2,3. \tag{6.92}$$

By combining these mixing matrices with the Feynman rules of Appendix E.3 one finds that there is no contribution to the decay rates under study.

This result can also be understood from the Lagrangian, i.e., Eq. (6.1) and (6.2). In this case the vanishing of λ_{ijk}, λ^{s}_{ijk}, λ'_{ijk}, λ'^{s}_{ijk} and λ'''_{ij} gives rise to a global symmetry involving the superfields L_i. This global symmetry protects the different components of L_i from mixing together or mixing with any other superfield. Thus any violation of the lepton flavour numbers is associated only with the right-handed gauge singlet fields. Since the amplitudes of Fig. 5.7 involves a chirality flip, the left-handed charged fermions are always involved. This means that the global symmetry among L_i acts as the lepton flavour numbers, and ensures that the decay rates vanish for this special case.

This result is also confirmed by numerical calculations. As a final comment, regarding this example, it should be noted that parts of the numerical calculations had to be made to great accuracy. In fact, the Veltman-Passarino integrals was calculated to 60 decimals accuracy by use of the series expansion described in Appendix G.1.

This analysis again shows the importance of λ_{ijk} and λ'_{ijk}. As for the other models studied in this work, small deviations from the most constraining scenario will be made. This is the subject for the numerical analysis of next section.

6.6.2 Numerical analysis of branching ratios

In order to proceed the analysis of MSSM-DM, the following numerical values for the 5 MSSM parameters will be used,

$$\tan\beta = 10, \tag{6.93}$$
$$\text{sign}(\hat{\mu}_0) = +1, \tag{6.94}$$
$$M_0 = 200\,\text{GeV}, \tag{6.95}$$
$$M_{1/2} = 250\,\text{GeV}, \tag{6.96}$$
$$A_0 = 200\,\text{GeV}. \tag{6.97}$$

Also the following values define the gauge singlet sector,

$$\omega = 10^{11}\text{GeV}, \tag{6.98}$$
$$B_0 = 1\,\text{GeV}, \tag{6.99}$$
$$P = 0, \tag{6.100}$$
$$Q = 10^{10}\,\text{GeV}. \tag{6.101}$$

The uniform textures will also be used for the R-parity violating parameters λ_{ijk} and λ'_{ijk}, i.e., Eqs. (5.123) and (5.132). It is also assumed that

$$\Lambda' = \Lambda. \tag{6.102}$$

Constraints for these parameters were obtained in Chapter 5. However, since the most important parameters of MSSM-DM are the ones connecting the gauge singlet fields to the other fields, the detailed structure of λ_{ijk} and λ'_{ijk} is not of any crucial importance for this analysis.

The texture presented in Eq. (6.84) will be used for $\lambda'''_{\alpha i}$. Finally, all soft breaking parameters are determined at the GUT-scale by the supergravity inspired boundary conditions of Eqs. (3.8) - (3.11). By combining these assumptions one finds that the only free parameters left are Λ''' and Λ. Thus, each of the decay rates are therefore now a function of these two parameters only.

The decay rates have been calculated for several choices of these two parameters. These calculations confirm the analytical analysis made in Sec. 6.6.1. That is, the decay rates are found to vanish if Λ vanishes, independent of the values of Λ'''. Albeit not a very interesting result, this serves as an important check of the computer code.

In order to obtain non-vanishing values for the decay rates non-vanishing values are assumed for Λ. Figure 6.9 shows the results of the numerical calculations of

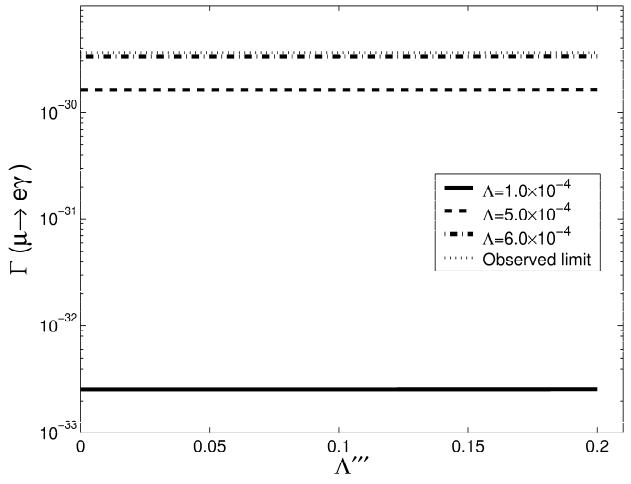

Figure 6.9: The figure shows $\Gamma(\mu \to e\gamma)$, as a function of Λ''', calculated for three values of Λ. Λ logarithmic scale has been used for the decay rate.

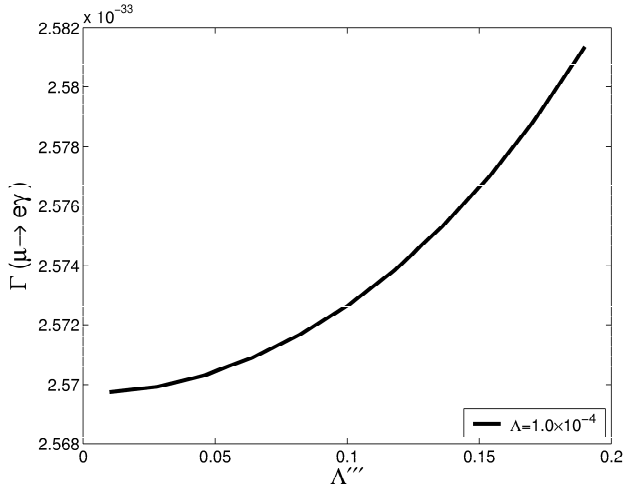

Figure 6.10: The figure shows the decay rate $\Gamma(\mu \to e\gamma)$ as a function of Λ''', for $\Lambda''' = 1.0 \times 10^{-4}$.

$\Gamma(\mu \to e\gamma)/\Gamma_5$, obtained for three different values of Λ, and by varying Λ'''. In this figure Γ_5 means the upper limit [6] for $\mu \to e\gamma$, see Eq. (2.4). Figure 6.9 clearly shows that this particular decay rate do not put any further constraints on $\lambda'''_{\alpha i}$, beyond the ones already obtained from the analysis of the mass matrices. The figure also shows that this decay rate is quite sensitive to Λ. Analogous results were also obtained for the other two decay rates under study. Though the limits was found to be even less constraining than the ones shown in Fig. 6.9. This sensitivity on λ_{ijk} and λ'_{ijk} have been analysed in chapter 5, and will not be pursued any further in this chapter.

Figure 6.9 may give the impression that the decay rates are completely independent of Λ'''. This is, however, not the case. A closer inspection of these figures shows that the decay rates indeed have some weak dependency on Λ''', see Fig. 6.10. This figure shows $\Gamma(\mu \to e\gamma)$ calculated as a function of Λ''' for the choice $\Lambda = 1.0 \times 10^{-4}$. It shows that the decay rate $\mu \to e\gamma$ indeed depends on Λ''', and that this decay rate increases with increasing values for Λ'''. This is as expected from the qualitative analysis, since increasing values for Λ''' will lead to an increasing mixing between the light and heavy modes of the neutral scalars. That is, increasing values for Λ''' lead to a greater non-degeneracy among the neutral scalars, and an enhancement of the decay rates.

These calculations show that the most constraining scenario, in which the boundary values for the soft-breaking terms are chosen in accordance to Eqs. (3.8) - (3.11), have no dependency on $\lambda'''_{\alpha i}$. On the other hand, the decay rates show a strong dependency on the R-parity violating parameters λ_{ijk} and λ'_{ijk}. As shown in chapter 5, this was also the case for MSSM-M.

Thus, it has been shown that the mass matrices put the strongest constraints on the parameter $\lambda'''_{\alpha i}$. The decay rates $\Gamma(l \to l'\gamma)$ do not show any phenomenologically interesting sensitivity on $\lambda'''_{\alpha i}$.

The masses of all particles in MSSM-DM are presented in Table 6.1 for two scenarios of Λ and Λ'''. In the first scenario $\Lambda = 10^{-3}$ and $\Lambda''' = 0$, while in the other scenario $\Lambda = 10^{-3}$ and $\Lambda''' = 0.3$. As the table shows all masses are almost identical for both scenarios. The masses for a third scenario, i.e., $\Lambda = 10^{-4}$ and $\Lambda''' = 0$, where identical to the second column of this table. Note that in order to find possible contributions to the decay rates under study also the mixing matrices have to be taken properly into account.

Beyond the supergravity boundary conditions

It is also interesting to analyse the decay rates if some of the assumptions made above are violated. As stated several times, the most interesting parameters to analyse in MSSM-DM are the ones which make MSSM-DM different from MSSM-M, that is, $\lambda_{\alpha i}$ and $\lambda'''_{\alpha i}$s. In this part of the numerical analysis three scenarios, all violating all or parts of the constraints dictated by the supergravity inspired boundary conditions will be analysed. In the first scenario $\hat{b}_i$ is assumed to be a free parameter at the

Particles	$\Lambda = 10^{-3}$ and $\Lambda''' = 0$	$\Lambda = 10^{-3}$ and $\Lambda''' = 0.3$
$\tilde{\chi}_i^0$	0, 0, 0, 92.7, 174.9, 446.0, 457.8 5.0×10^9, 5.0×10^9, 5.0×10^9	0,0,0 92.7, 175.8, 460,1, 471.3, 5.0×10^9, 5.0×10^9, 5.0×10^9
$\tilde{\chi}_j$	4.87×10^{-4}, 0.103, 1.75, 180.2, 460.7	4.87×10^{-4}, 0.103, 1.75, 181.0, 474.2
$\Phi_{\mathrm{cs},k}$	80.41, 208.0, 219.7, 219.7, 270.1, 270.1, 276.5, 512.7	80.41, 210.2, 223.1, 223.2 268.8, 268.8, 276.3, 516.6
Φ_l^0	89.3, 261.2, 262.2, 262.2, 506.7 80.41, 261.2, 262.2, 262.2, 512.7 10^{10}, 10^{10}, 10^{10}, 10^{10}, 10^{10}, 10^{10}	87.3, 259.8, 260.8, 260.8, 503.0 80.41, 259.8, 260.8, 260.8, 508.7 10^{10}, 10^{10}, 10^{10}, 10^{10}, 10^{10}, 10^{10}
$\tilde{U}_{\tilde{p}}$ and $\tilde{D}_{\tilde{p}}$	450.0, 659.7, 659.7, 678.1, 678.1, 700.0 600.5, 658.0, 658.0, 665.6, 683.7, 683.8	445.1, 660.5, 660.5, 677.8, 677.8, 699.3 598.3, 658.6, 658.7, 666.3, 683.4, 683.5
$\hat{b}_q$	-6,-6,-5	-6,-6,-5

Table 6.1: The table shows the masses of MSSM-DM, obtained by using the parameters specified by Eqs. (6.93) - (6.84). All masses are in GeV. The particles are labelled according to: $i = 1, 2, \ldots, 10$, $j = 1, 2, \ldots, 5$, $k = 1, 2, \ldots, 8$, $l = 1, 2, \ldots, 16$, $p = 1, 2, \ldots, 6$ and $q = 1, 2, 3$.

electroweak scale. And in the second and third scenario the boundary conditions

$$\lambda'''^{s}_{\alpha i} = A_0 \lambda'''_{\alpha i}, \tag{6.103}$$

and

$$M_n^2 = M_0^2 \, 1_{3\times 3}, \tag{6.104}$$

are violated at the GUT scale.

Varying $\hat{b}_i$

In this scenario $\hat{b}_i$ is assumed to be a free parameter at the electroweak scale. Thus, the model now has five free parameters, i.e., Λ, Λ''' and $\hat{b}_i$, $i = 1, 2, 3$. However, to simplify, the following choice for Λ and Λ''' is used, i.e.,

$$\Lambda = \Lambda''' = 5.0 \times 10^{-4}. \tag{6.105}$$

Also, the following simplifying assumption is used for $\hat{b}_i$,

$$\hat{b}_i = B', \quad \text{for } i = 1, 2, 3, \tag{6.106}$$

i.e., all elements of $\hat{b}_i$ are equal. Using these assumptions, i.e., Eqs. (6.105) and (6.106), there is now only one free parameter left in MSSM-DM, i.e., B'.

This scenario is interesting since $\hat{b}_i$ determines the mixing between left-handed components and Higgs scalars in the squared mass matrices for charged and neutral scalars.

Of course, all minimisation conditions must be fulfilled. Thus, in this scenario the minimisation condition of Eq. (6.23) determines $\varepsilon_i = (M_L^2)_{0i}$, in terms of $\hat{b}_i$ at the electroweak scale. The numerical procedure used in this scenario is to first obtain a stable solution for the renormalization group equations, as for the preceding numerical analysis. Next, a value for $\hat{b}_i$ is chosen and a value for ε_i is calculated from Eq. (6.23). It is not an important issue to find the corresponding values for the soft-breaking parameters at the GUT-scale. But one readily sees that this procedure will give off-diagonal elements to M_L at the electroweak scale. Due to the renormalization group equations this means that most soft-breaking parameters also acquire off-diagonal elements at the GUT-scale. Two examples are,

$$M_L^2 = \begin{pmatrix} 40001 & 4094 & 4093 & 4082 \\ 4094 & 40000 & 0.5 & 0.2 \\ 4093 & 0.5 & 40000 & 0.4 \\ 4082 & 0.2 & 0.4 & 40001 \end{pmatrix}, \tag{6.107}$$

and

$$M_e^2 = \begin{pmatrix} 40000 & 0 & 0.5 \\ 0 & 40000 & 0.5 \\ 0.5 & 0.5 & 40001 \end{pmatrix}. \tag{6.108}$$

Both of the matrices M_L^2 and M_e^2 break the supergravity inspired boundary condition of Eq. (3.8), i.e.,

$$M_L^2 = \bar{M}_0^2\, 1_{\alpha\times\beta}, \quad \text{and} \quad M_e^2 = \bar{M}_0^2\, 1_{3\times 3}. \tag{6.109}$$

Equation (6.108) shows that the violation of this boundary condition is quite weak. The reason for this weak violation is that the running of M_e^2 has a dependency on M_L^2 proportional to Λ^2. The same conclusion is also valid for the other soft-breaking bilinear parameters, that is, the running of these parameters depends upon M_L^2, but only proportional to the small parameters Λ^2 or Λ''^2. Finally, one should also note that the boundary conditions for the soft-breaking trilinear couplings are still fulfilled, since the running of these parameters do not depend upon $\bar{M}_L^2$.

Figure 6.11 shows the results of the numerical calculations obtained by varying B'. This figure shows that the decay rates are independent on the sign of $\hat{b}_i$. This is in accordance with the general analysis of Sec. 6.6.1, and also in accordance with the analysis of MSSM-M, made in chapter 5. Figure 6.11 also shows that $|B'|$ should be less than $173\,\mathrm{GeV}^2$, for this scenario. This is a much larger value than the one found from the most constraining scenario, see Table. 6.1.

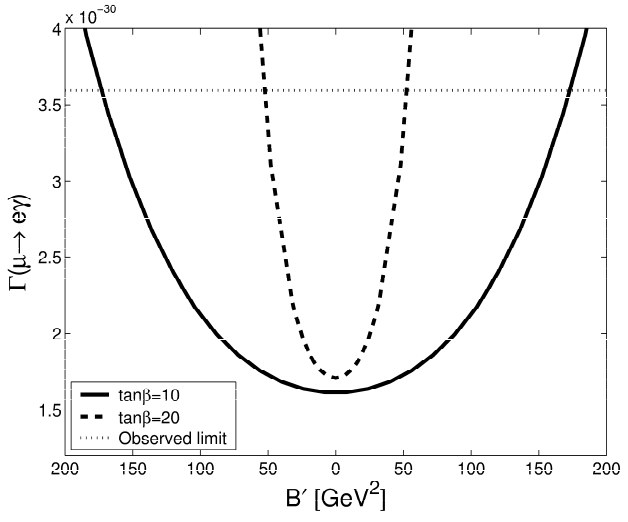

Figure 6.11: The figure shows $\Gamma(\mu \to e\gamma)$, obtained by varying B' for two values of $\tan\beta$.

Varying $\lambda'''^{s}_{\alpha i}$

A violation of the boundary condition

$$\lambda'''^{s}_{\alpha i} = A_0 \lambda'''_{\alpha i}, \tag{6.110}$$

at the GUT-scale, will alter the squared mass matrices for charged and neutral scalars. This may give an enhancement of the decay rates under study. However, $\lambda'''^{s}_{\alpha i}$ can not grow too large since this will lead to phenomenologically unacceptable light scalar masses. Another important observation is that the running of all soft-breaking parameters depends upon $\lambda'''^{s}_{\alpha i}$. Thus a violation of Eq. (6.110) will affect the values for all soft-breaking parameters at the electroweak scale. Some examples are shown in Table 6.2.

In the preceding analysis it has been shown that the uniform texture always gives the most constraining scenario for the parameters. Thus, the following texture is used,

$$\lambda'''^{s}_{\alpha i} = \Lambda'''^{s}, \quad \text{for all } \alpha = 0, 1, 2, 3 \text{ and } i = 1, 2, 3. \tag{6.111}$$

This will be referred to as a uniform texture for λ'''^{s}. The results of the numerical calculations are shown in Fig. 6.12. In this figure $\Lambda = \Lambda''' = 0, 1.0 \times 10^{-4}$ and 4.0×10^{-4}. The decay rate $\mu \to e\gamma$ is independent of the sign of Λ'''^{s}. This figure gives an upper limit $|\Lambda'''^{s}| < 5.5$ for $\Lambda = \Lambda''' = 0$ and 1.0×10^{-4}, and the upper limit $|\Lambda'''^{s}| < 3.6$ for $\Lambda = \Lambda''' = 4.0 \times 10^{-4}$. The other two decay rates under study have also been calculated, but the constraints obtained from these decay rates are less stringent than the ones from Fig. 6.12.

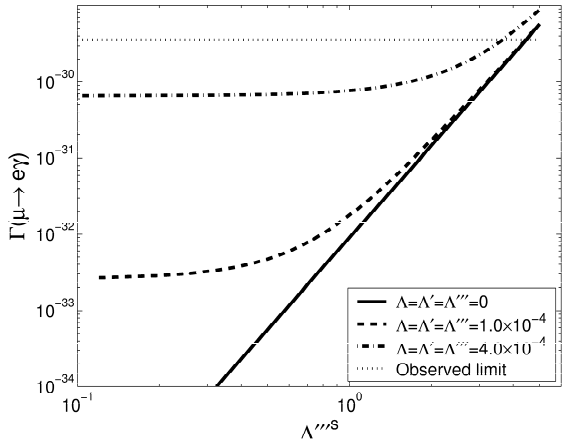

Figure 6.12: The figure shows $\Gamma(\mu \to e\gamma)$, obtained by varying Λ'''^{s} for three values of Λ, Λ' and Λ'''.

Figure 6.12 also shows another interesting characteristic of this scenario. That is, non-vanishing values are obtained for the decay rates even if Λ and Λ''' vanishes. This is in opposition to the general conclusion, found in Sec. 6.6.1 and in the numerical analysis above, where it has been shown that the decay rates vanish if Λ vanishes. The reason for the non-vanishing decay rates in the scenario defined by Eq. (6.111) is that all soft-breaking parameters have acquired off-diagonal elements at the electroweak scale, see Table 6.2.

The following textures have also been employed,

$$\Lambda' = \Lambda = 0 \quad \text{and} \quad \Lambda''' = 4.0 \times 10^{-4}, \tag{6.112}$$

$$\lambda'''^{s}_{0i} = A_0 \lambda'''_{0i} \quad \text{and} \quad \lambda'''^{s}_{ij} = \Lambda'''^{s}, \quad \text{for each } i,j = 1,2,3. \tag{6.113}$$

The upper limit $|\Lambda'''^{s}| < 4.4$ is obtained in this case.

Varying M_n^2

Since M_n^2 only appears in the squared mass matrices for the neutral scalars, a violation of the boundary condition

$$M_n^2 - M_0^2\, 1_{3\times3}, \tag{6.114}$$

at the GUT-scale, will alter these scalar masses. Further, due to renormalization group effects the values for M_L^2 and M_e^2 may also depend upon M_n^2. Thus the lepton numbers may be broken at the electroweak scale also by the charged scalars. However, this dependence is quite small, since the running of M_L^2 and M_e^2 have a dependency upon M_n^2 proportional to λ'''. In order to ensure that this coupling between M_n^2 and M_L^2 exists the uniform texture for λ, i.e., Eq. (5.123) will be used.

	$\Lambda'''^{s} = 0$	$\Lambda'''^{s} = 7$
$\lambda'''^{s}_{\alpha i}$	0	5.2 (all elements equal)
M_L^2	$\begin{pmatrix} 63926 & 0 & 0 & 0 \\ 0 & 72809 & 0 & 0 \\ 0 & 0 & 72807 & 0 \\ 0 & 0 & 0 & 72306 \end{pmatrix}$	$\begin{pmatrix} 63878 & -50 & -50 & -51 \\ -50 & 72760 & -51 & -51 \\ -50 & -51 & 72758 & -51 \\ -51 & -51 & -51 & 72258 \end{pmatrix}$
M_n^2	$200^2\,\delta_{ij}$	$\begin{pmatrix} 39932 & -68 & -68 \\ -68 & 39932 & -68 \\ -68 & -68 & 39932 \end{pmatrix}$

Table 6.2: The table shows the values for some the parameters at the electroweak scale. The choice $\Lambda = \Lambda''' = 0$ is used.

The uniform texture of Eq. (5.138) will also be assumed for λ', and it will be assumed that

$$\Lambda = \Lambda' = 6.2 \times 10^{-4}, \tag{6.115}$$

in this part of the analyses. Due to the supergravity boundary conditions these assumptions also determines λ^s and λ'^s.

The uniform texture of Eq. (6.84) is also used with the choice

$$\Lambda''' = 0.1. \tag{6.116}$$

This choice, together with the supergravity boundary conditions, also define the soft-breaking trilinear couplings $\lambda'''^{s}_{\alpha i}$.

The decay rate $\mu \to e\gamma$ has now been calculated for various values of Λ''' by varying M_0'. Some of the results are presented in Fig. 6.13. This figure also shows the same decay rate by assuming the uniform texture Eq. (6.111) with

$$\Lambda'''^{s} = 1.0. \tag{6.117}$$

In this section the three decay rates $\tau \to \mu\gamma$, $\tau \to e\gamma$ and $\mu \to e\gamma$ have been analysed both by qualitative and numerical methods. It was not possible to find any limits on $\lambda'''_{\alpha i}$, beyond those already obtained in previous sections, from these decay rates. Some examples, where the supergravity breaking scenario is violated, have also been explored. It has been shown that these scenarios easily come in conflict with the upper bounds for the decay rates under study. Limits on the soft-breaking parameters $\lambda'''^{s}_{\alpha i}$ have been obtained.

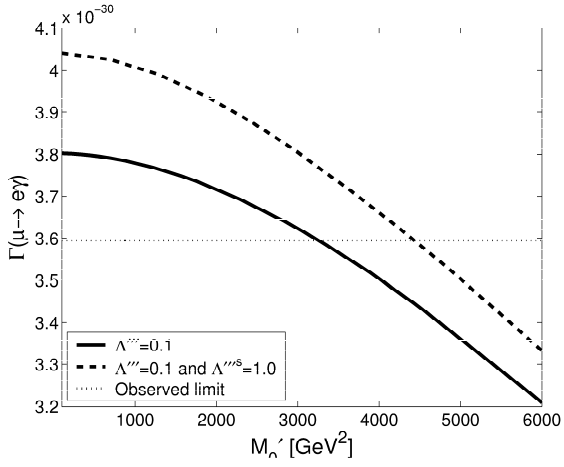

Figure 6.13: The figure shows $\Gamma(\mu \to e\gamma)$ as a function of M_0'.

URN:NBN:no-7281

Chapter 7

Summary and discussion

The starting point for this thesis is the confirmation of non-vanishing neutrino masses [8] - the very first direct evidence for physics beyond the Standard Model. These neutrino masses raise several interesting questions, both to the experimentalist and to the theoretical physicist. An experimentalist would like to measure parameters like masses, mixing angles and decay rates, all challenging tasks due to the elusive nature of the neutrinos. These measurements are important in order to gain a proper understanding of the neutrino masses, and also in order to distinguish between various extensions of the Standard Model. However, as a theoretical physicist, one of the most intriguing challenges, regarding the neutrino masses, is to understand the mechanism which causes them. In the Standard Model all charged fermions acquire their mass from the electroweak symmetry breaking and the Yukawa couplings. However, this approach does not necessarily apply to the generation of neutrino masses, since the neutrinos may be either Dirac or Majorana fermions.

If the neutrinos where Dirac fermions, their masses may indeed be generated by the same mechanism as the charged fermion masses, that is, by the electroweak symmetry breaking and one Yukawa matrix, Y_ν. Such an approach extends the Standard Model with at least 7 new parameters, that is, 3 neutrino masses and 3 mixing angles and 1 CP-violating phase, see discussion in Sec. 3.1.1. Unfortunately, this model does not give any explanation for the smallness of the neutrino masses, nor does it explain the lepton mixing angles, or give any fundamental knowledge of the fermions. The most important phenomenological signature of Dirac neutrinos is that lepton number is a conserved quantum number, while the three lepton flavour numbers are broken. Thus lepton number violating processes, like double β-decay, are not allowed, while lepton flavour violating processes, like $\mu \to e\gamma$, are allowed. As explained in Sec. 3.1.1, depending on the details of Y_ν, there may exist a CP-violating phase in the lepton sector. This makes the lepton sector analogous to the quark sector, i.e., baryon and lepton numbers are conserved, while the baryon and lepton flavour numbers are broken.

On the other hand, the neutrinos may exist as Majorana fermions, that is, they are their own anti-particles. In this case neither lepton nor lepton flavour numbers are conserved, i.e., double β-decay and $\mu \to e\gamma$ are both allowed. Due to the Majorana property there can be no CP-violating phase associated with the lepton sector, see Sec. 3.1.3. Even more important the Standard Model Higgs mechanism can not give masses to these Majorana fermions. As explained in Sec. 2.3, one must enlarge the neutral scalar sector with singlets, more doublets or even triplets [21].

At the moment, the fermionic nature of the neutrinos is not completely understood. Recent results from the HEIDELBERG-MOSCOW experiment at Gran-Sasso (Italy) claims that double β-decay is already observed [20]. If confirmed, this proves that the neutrinos are Majorana fermions. However, it is too early to draw any definite conclusion from this experiment, and one should still allow for both Dirac and Majorana neutrinos in any phenomenological analysis.

In this thesis three minimal supersymmetric extensions of the Standard Model have been defined and analysed, both by analytical and numerical methods. These three models are all motivated, and defined, by exploring the global symmetries allowed by the neutrino mass terms [21], i.e., Dirac mass terms, Majorana mass terms and Dirac-Majorana mass terms. The three minimal supersymmetric models are labelled in accordance with these mass terms as MSSM-D, MSSM-M and MSSM-DM, respectively.

Each of these models is an extension of MSSM, only constrained by the global symmetries dictated by the neutrino mass terms and proton stability. The parameter spaces have been defined as the collection of all free parameters of the model, and the degrees of freedom is the number of free parameters of each model. This number of free parameters have been found for each model, and the result is presented in Tables 3.1 - 3.3.

The R-parity violating couplings, which appears in MSSM-M and MSSM-DM, allows the superfields $\hat{H}_d$ and L_i to mix together, thus causing a new global $U(4)$-symmetry on the Lagrangian. By exploring this symmetry the Lagrangian for MSSM-M and MSSM-DM can be formulated in a $U(4)$ manifest manner, i.e., in terms of $U(4)$ -vectors and -tensors. These vectors and tensors are defined in Eqs. (5.8) - (5.14) and Eqs. (6.3) and (6.4). The tree-level scalar potential, the tree-level minimisation conditions, the mass matrices, the Feynman rules and the renormalization group equations for MSSM-M and MSSM-DM have all been written by use of this notation. These expressions have also been obtained for MSSM-D by use of the more traditional notation known from MSSM. The results are presented in Appendices C - F. A more detailed summary and discussion, of each of these subjects, will now be presented.

Parameter spaces

As shown in Tables 3.1 - 3.3 the parameter spaces are huge for all three models. Thus, in order to perform any phenomenological analyses, further constraints and assumptions have to be imposed on each model. In this work, the two most im-

portant assumptions are that all parameters are real, and that the soft breaking parameters are fixed at the GUT-scale. The first assumption seems reasonable since the decay rates does not have any dependence on any complex phase. The second assumption, referred to as the supergravity inspired scenario is less well motivated. It is, however, quite popular in the literature, and hints for models even beyond the supersymmetric models, e.g., supergravity or string theory. In the supergravity inspired scenario the low energy values for the soft-breaking parameters are found by solving the renormalization group equations and the minimisation conditions.

Scalar potential and minimisation conditions
The tree-level neutral scalar potential for MSSM-DM is presented in Appendix C.1. This scalar potential is an extension of the scalar potentials for MSSM-D and MSSM-M, and the tree-level minimisation conditions for each model are therefore obtained from this potential. By using the manifest $U(4)$ notation it is shown that all three models have almost identical minimisation conditions at the electroweak scale. MSSM-DM also have three minimisation conditions at a much higher scale, the so-called n-scale.

For MSSM-D the one loop minimisation conditions have been obtained by the so-called tadpole method [38]. Some small errors in the expressions from Ref. [38] have been corrected, and the one-loop corrections to the minimisation conditions have been calculated. The result obtained by including these one-loop corrections are small, and for MSSM-M and MSSM-DM only the tree level neutral scalar potential have been used. For a future work the one-loop neutral scalar potential should be included and thoroughly studied for all models.

Mass matrices
The mass matrices for charged and neutral fermions, and the squared mass matrices for the charged and neutral scalars have been found for each of the models MSSM-D, MSSM-M and MSSM-DM. It has been shown that all of these matrices extends the mass matrices known from MSSM.

The charged fermion mass matrices of MSSM-D are equal to the ones from MSSM. But in MSSM-M and MSSM-DM the charginos and charged leptons mix due to the violation of the lepton number. These mixed states are referred to as the charged fermions of MSSM-M and MSSM-DM. It has been shown that it is still possible to define the Standard Model leptons in this model.

The neutral fermions of MSSM-D consists of the left-handed neutrinos and the neutralinos. The neutrino masses are non-vanishing due to a neutrino Yukawa matrix, Y_ν. Due to the violation of the lepton number, the neutrinos and neutralinos will mix together in MSSM-M and MSSM-DM. These mixed states are referred to as neutral fermions. There are 5 neutral fermions in MSSM-M, and as much as 8 in MSSM-DM. The smallness of the neutrino masses puts stringent limits on the parameters of MSSM-M and MSSM-DM. To simplify the calculations it has been assumed that the neutrino masses vanishes at tree level in MSSM-M and MSSM-DM. In a future work the loop-corrections should be implemented.

The squared mass matrices for the charged and neutral scalars are all found from the scalar potential, presented in Appendix C. And the squared mass matrices are shown in Appendix D.

In MSSM-D the squared mass matrices for the charged scalars are identical to the corresponding ones from MSSM. But in MSSM-M and MSSM-DM the charged Higgs scalars and sleptons mix, also due to the violation of the lepton number. There are therefore 8 charged scalars in both of these models.

The neutral scalars of MSSM-DM are extended with the right-handed singlets, and the sneutrino mass matrix of MSSM-D is therefore a 6×6 matrix. Due to the violation of lepton number in MSSM-M and MSSM-DM the neutral Higgs scalars and sneutrinos will mix together. There are as much as 10 and 16 neutral scalars in MSSM-M and MSSM-DM, respectively.

The scalar masses have been analysed in MSSM-M and MSSM-DM in order to find any constraints on the parameter spaces. The most important finding from this analysis is the demand for alignment between v_i and μ_i, from the neutral fermion mass matrices of MSSM-M and MSSM-DM. Only for MSSM-DM does the squared neutral scalar mass matrices put any interesting constraint on the parameter space.

In this analysis only the tree-level matrices have been used. For most particles this is a good approximation. But for the neutral scalars it is known that there are large one loop-contributions, see e.g., Ref. [58]. Loop corrections should be included in a future analysis of these models.

Renormalization group equations

General expressions for the 2-loop renormalization group equations of any $N = 1$ supersymmetric extension to the Standard Model already exist in the literature [34]. However, the renormalization group equations for MSSM-D, MSSM-M and MSSM-DM had all to be found from these general expressions. These renormalization group equations are presented in Appendix F. Two-loop renormalization group equations have been used for the gauge and gaugino couplings, and one-loop renormalization group equations for all other parameters. No decoupling is assumed in the analysis of these renormalization group equations.

The renormalization group equations have been analysed, for each model, both qualitatively and by numerical methods. It has been of special interest to analyse the dependency the running of the parameters have on each other. In this thesis, the only model with non-vanishing tree-level neutrino masses is MSSM-D. Therefore, the running of the Yukawa-couplings, from the neutrino Yukawa matrix Y_ν, have been studied thoroughly in Sec. 4.4. Approximate analytic solutions to the neutrino Yukawa couplings have been obtained, in Sec. 4.4. These analytic solutions clearly shows the dependency the elements of Y_ν have on the top-quark Yukawa coupling, Y_t. It is well known (see e.g., Ref. [38]) that the top-quark Yukawa-coupling has a (quasi-) fixed point solution at low energies. And it would be interesting if such a fixed point solution also could be found for the elements of Y_ν, giving some rationale for the smallness of the neutrino masses. Such a fix point solution was, however,

not found in MSSM-D.

The renormalization group equations for MSSM-M and MSSM-DM have also been analysed qualitatively and by numerical methods. It is known [53] that the R-parity violating couplings are important for the running of the gauge coupling constants. In this thesis, the dependence the Yukawa couplings have on the R-parity violating parameters have been studied. To accomplish such an analysis it has been of invaluable importance to formulate the renormalization group equations in terms of the manifest $U(4)$ notation, see Appendix F. This formulation clearly shows the dependence between R-parity violating couplings and the Yukawa couplings. In fact, the $U(4)$ symmetry makes it impossible to distinguish between R-parity violating parameters and Yukawa couplings.

A general result of this analysis is that even if the off-diagonal elements of Y_e vanish at the electroweak scale, they reappear at higher scales due to their coupling to the R-parity violating couplings. Since the supergravity inspired scenario relates the soft breaking trilinear couplings to the Yukawa matrices at the GUT scale, i.e.,

$$a_x = A_0 Y_x, \tag{7.1}$$

these soft breaking parameters also have off-diagonal elements at the GUT scale. By solving the renormalization group equations one finds that the trilinear soft breaking parameters have off-diagonal elements at the electroweak scale. Thus the existence of R-parity violating couplings, and the supergravity inspired scenario, leads to lepton flavour violations both in the fermionic and in the scalar sector.

The numerical analysis, for the full set of renormalization group equations, in MSSM-D, MSSM-M and MSSM-DM are presented in Secs. 4.4, 5.7 and 6.5, respectively.

Lepton flavour violating decay channels

In this thesis the three lepton flavour violating decay channels $\tau \to \mu\gamma$, $\tau \to e\gamma$ and $\mu \to e\gamma$, have been analysed in three minimal supersymmetric extensions of the Standard Model, i.e., MSSM-D, MSSM-M and MSSM-DM. These three decay rates are referred to as $l \to l'\gamma$. The general conclusion from this analysis is that none of the models can be completely ruled out from this analysis only. However, the three lepton flavour violating decay channels do put important constraints on each of the parameter spaces.

It should come as no surprise that the model with the largest parameter space, MSSM-DM, is quite difficult to analyse. This difficulty is due to the existence of both gauge singlet superfields and R-parity violating couplings. However, the Lagrangian of MSSM-DM, i.e., Eqs. (6.1) and (6.2), shows that if the parameters $\lambda'''_{\alpha i}$ and $\lambda'''^{\mathrm{s}}_{\alpha i}$ vanishes, then the three right-handed gauge singlet fields, n_i, will not interact with any of the other fields. In this case MSSM-DM is indistinguishable from MSSM-M, at least with respect to the decay rates under study. The analysis of Chapter 5 therefore covers this situation too, and the analysis of MSSM-DM has therefore been focused on possible constraints for $\lambda'''_{\alpha i}$ and $\lambda'''^{\mathrm{s}}_{\alpha i}$.

The analysis of Chapter 6 shows that in order to obtain phenomenologically acceptable neutrino masses $\lambda'''_{\alpha i}$ must be severely constrained. It has also been shown that no further limits are obtained on these parameters from analysis of the other mass matrices or from analysis of the decay rates.

Thus, the phenomenologically most interesting models are MSSM-D and MSSM-M. The main difference between these two models is that the lepton number is conserved in MSSM-D, and violated in MSSM-M. This violation of lepton number manifest itself in the existence of R-parity violating couplings in MSSM-D.

The main conclusion from the analysis of MSSM-D, presented in Sec. 4.5.2, is that this model easily fulfils the constraints dictated by the three lepton flavour violating decay rates. The reason is that due to the almost vanishing neutrino masses, all elements of Y_ν have to be very small. Thus even for maximal mixing the necessary lepton flavour violation will be too small to conflict with the upper limits [23] for $l \to l'\gamma$. On the other hand, the limits on the decay rates could easily be violated if one leaves the simple scheme of supergravity inspired boundary conditions. This is also known from MSSM.

The existence of R-parity violating couplings in MSSM-M leads to a rich and interesting phenomenology. The analysis of MSSM-M, as presented in Chapter 5, has as its main conclusion that the decay channels $l \to l'\gamma$ do indeed constrain the R-parity violating couplings. However, due to the dependence these parameters have on each other, is it difficult to give simple expressions for these constraints.

Deviations from the constrained supergravity scenario
For all models it has been shown that even small deviations from the most constrained scenario lead to considerable effects for the decay rates under study. It has been especially interesting to see that all three decay rates are important in determining limits for the parameter space. Even though the decay channel $\mu \to e\gamma$ is the one with strongest upper limit, the two τ-decays are also important. As has been shown for all models it is possible to choose the parameters in such a manner that the limits for $\mu \to e\gamma$ is fulfilled, while one or both of the limits for the τ-decays are violated.

Numerical analysis
For each of the three models a computer program has been written in Fortran. Each of these computer programs takes a set of parameters as input and gives the decay rates as output. In order to obtain a stable and accurate code numerical routines from the Numerical Algorithm Group (NAG) [55] have been used where possible. From the start the libraries FF and Looptools [72] was used to solve the Veltman-Passarino integrals. Especially the numerical calculations involving MSSM-DM showed large numerical fluctuations when these libraries was used. Therefore, the series expansions, presented in Appendix G.1, have been used in the final versions of each program. The Fortran library FM [59, 60] has also been used to calculate the Veltman-Passarino integrals with multiple precision, i.e., by using 100 digits.

Also the renormalization group equations possessed computational challenges. This

is mostly due to the huge number of coupled differential equations, which had to be solved. To be able to both proof-read and tailor the numerical code to the relevant model the following procedure has been used. First, the renormalization group equations where written in Maple [61]. Then they where translated into Fortran code by use of Maple's Fortran generator. The largest set of differential equations, generated by this procedure, extended over 30.000 lines of Fortran code. Such a large set of differential equations was necessary to properly analyse the running of parameters in MSSM-DM. Several numerical methods, all provided by the Numerical Algorithm Group [55], have been used to check for speed, accuracy and stability in the solution of the renormalization group equations. However, in the end a Runge-Kutta method was enough to meet all demands for speed, accuracy and stability. The reason that such a huge set of coupled non-linear differential equations solves so easily, is that the renormalization group equations are obtained from a perturbative method. Thus, these equations make up a set of ordinary polynomial differential equations, i.e., the dependent variables are only polynomial.

URN:NBN:no-7281

Chapter 8

Conclusions

In this thesis three minimal supersymmetric extensions to the Standard Model have been defined and analysed. These models have been defined in terms of the possible global symmetries, which are allowed by the Dirac-, Majorana- and Dirac-Majorana mass terms. The models are therefore labelled in accordance with these mass terms as MSSM-D, MSSM-M and MSSM-DM, respectively. For each model the accompanying parameter spaces, neutral scalar potentials, minimisation conditions, mass matrices, Feynman rules and renormalization group equations have been found and analysed. These models have been used to analyse the three lepton flavour violating decay rates $\tau \to \mu\gamma$, $\tau \to e\gamma$ and $\mu \to e\gamma$.

In order to accomplish such an analysis several assumptions have been made for each model. The most important ones are the assumption of using only real parameters, and that the soft breaking terms are defined by the supergravity inspired boundary condition at the unification scale. The third major assumption is that complete alignment is assumed for MSSM-M and MSSM-DM. This causes the neutrinos to be massless at tree-level, while acquiring masses at the loop level. Thus, in this analysis, explicit neutrino masses do only appear in MSSM-D.

The analysis of Chapter 4 shows that MSSM-D easily fulfils the current experimental upper limits on the lepton flavour violating decays, $l \to l'\gamma$. But even more importantly, this model can not be ruled out even if the upper limits where to be improved by a factor 1000. Such an improvement may be achieved in the near future [24, 25].

The analysis of MSSM-M has been focused on a study of the R-parity violating couplings. These parameters greatly enhance the decay rates. It is also interesting to note that the existence of the trilinear couplings λ'_{ijk} makes it possible for quarks (and squarks) to enter these lepton flavour violating decay rates. Upper limits on the R-parity violating couplings have been obtained from different textures on λ_{ijk} and λ'_{ijk}. It has been shown that the uniform textures leads to the most stringent bounds for these couplings.

For MSSM-DM the analysis has been focused on the couplings between the right-

handed gauge singlets and the other fields, i.e., on the couplings labelled by $\lambda'''_{\alpha i}$. It has been shown that the neutrino masses give equal tight upper bounds as the decay rates.

For all three models the supergravity inspired scenario have been used. But smaller violations of this scenario have also been studied. This analysis shows that the experimental limits could easily be violated if these supergravity inspired boundary conditions are violated.

Future theoretical studies of MSSM-D, MSSM-M and MSSM-DM should include the loop induced neutrino masses and loop corrections to the neutral scalar potential and the neutral scalar masses. Other processes, like the $g - 2$ experiment and other lepton number violating processes are also important to include in a future phenomenological analysis of these three models. New experiments involving the decay rates studied in this thesis have been approved [24], and may lower the upper bounds for $\mu \to e\gamma$ by a factor 1000. Or this experiment could show that this decay channel is small, buy still open. Due to their strong experimental limits and their sensitivity to new physics, these decay channel will be very interesting to study in the future.

Appendix A

Notation and supersymmetry

In this section the notation will be presented along with some general results regarding supersymmetry. This appendix does not aim to be a general introduction neither to the field of supersymmetry, nor to the literature dealing with this theory. The sole purpose of this appendix is to collect some of the most important relations and results for easy reference.

There exist many well written books and articles on the theory and phenomenology of supersymmetry, both at the introductory and at the expert level. Some of the references, which has been very useful in this work, are Refs. [28, 29, 32, 47, 35].

A.1 Notation

The metric is chosen as,

$$g_{\mu\nu} = \text{diag}(1, -1, -1, -1), \tag{A.1}$$

and the speed of light, c, and the reduced Planck constant, $\hbar$, are both set equal to 1, i.e.,

$$\hbar = c = 1, \tag{A.2}$$

and the charge of the electron is $-e$. The Feynman-notation for 4-vectors is used, e.g.,

$$\not{p} = \gamma_\mu p^\mu = \gamma^\mu p_\mu. \tag{A.3}$$

The γ-matrices fulfil the Clifford-algebra

$$\{\gamma^\mu, \gamma^\nu\} = \gamma^\mu\gamma^\nu + \gamma^\nu\gamma^\mu = 2g^{\mu\nu}, \tag{A.4}$$

and the γ^5-matrix is defined by

$$\gamma^5 = i\gamma^0\gamma^1\gamma^2\gamma^3. \tag{A.5}$$

A Grassmann variable, θ, is an anti-commuting variable, i.e.,

$$\{\theta, \theta\} = 0, \quad \text{or} \quad \theta^2 = 0. \tag{A.6}$$

Due to this property any function of Grassmann variables can be expressed as

$$f(\theta) = a + b\theta. \tag{A.7}$$

Integration over Grassmann variables are also made possible by the definitions,

$$\int d\theta = 0 \quad \text{and} \quad \int d\theta\, \theta = 1. \tag{A.8}$$

For a function $f(\theta) = a + b\theta$ these definitions lead to the remarkable result that integration and derivation of $f(\theta)$ are equal operations, i.e.,

$$\frac{\partial f(\theta)}{\partial \theta} = \int d\theta\, f(\theta) = b. \tag{A.9}$$

The Pauli matrices are defined [62] as

$$\sigma^1 = \begin{pmatrix} 0 & 1 \\ 1 & 0 \end{pmatrix}, \; \sigma^2 = \begin{pmatrix} 0 & -i \\ i & 0 \end{pmatrix}, \; \sigma^3 = \begin{pmatrix} 1 & 0 \\ 0 & -1 \end{pmatrix}. \tag{A.10}$$

Also the 4-vector version of the Pauli matrices is defined as

$$\sigma^\mu = (1, \boldsymbol{\sigma}), \quad \hat{\sigma}^\mu = (1, -\boldsymbol{\sigma}), \tag{A.11}$$

where

$$\boldsymbol{\sigma} = (\sigma^1, \sigma^2, \sigma^3). \tag{A.12}$$

The two-component Weyl spinors are the fundamental building elements of any quantum field theory. Also General Relativity may be described in terms of Weyl spinors [63]. The Weyl spinor, ψ_A, $A = 1, 2$, is a two-component Grassmann variable. It is defined to transform under a matrix $M \in \mathrm{SL}(2, C)$, as

$$\psi'_A = M_A^B\, \psi_B, \quad A, B = 1, 2. \tag{A.13}$$

Spinors transforming according to (A.13) are called left-handed Weyl spinors. Right-handed Weyl spinors are defined as two-component Weyl spinors transforming according to

$$\overline{\psi}'_{\dot{A}} = (M^*)_{\dot{A}}^{\dot{B}}\, \psi_B, \quad \dot{A}, \dot{B} = 1, 2, \tag{A.14}$$

and $*$ means complex conjugation.

The indices of these Weyl spinors can be raised and lowered by use of the metric ε_{AB}, i.e.,

$$\varepsilon_{AB} = \begin{pmatrix} 0 & -1 \\ 1 & 0 \end{pmatrix}, \; \varepsilon^{AB} = \varepsilon^T_{AB} = \begin{pmatrix} 0 & 1 \\ -1 & 0 \end{pmatrix}, \tag{A.15}$$

$$\bar{\varepsilon}_{\dot{A}\dot{B}} = \begin{pmatrix} 0 & -1 \\ 1 & 0 \end{pmatrix}, \; \bar{\varepsilon}^{\dot{A}\dot{B}} = \bar{\varepsilon}^T_{\dot{A}\dot{B}} = \begin{pmatrix} 0 & 1 \\ -1 & 0 \end{pmatrix}. \tag{A.16}$$

That is,

$$\psi^A = \varepsilon^{AB}\,\psi_B, \tag{A.17}$$

$$\overline{\psi}'^{\dot{A}} = \varepsilon^{\dot{A}\dot{B}}\,\overline{\psi}'_{\dot{B}}. \tag{A.18}$$

These two last spinors transform according to $M^{-1\,T}$ and $M^{*-1\,T}$, respectively.

Note that for Weyl spinors the following summation convention is used

$$\psi\xi \equiv \psi^A\,\xi_A, \tag{A.19}$$

$$\bar{\psi}\bar{\xi} \equiv \bar{\psi}_{\dot{A}}\,\bar{\xi}^{\dot{A}}. \tag{A.20}$$

Assume that the following Weyl spinors exist,

$$\eta_A,\; \bar{\eta}_{\dot{A}},\; \bar{\xi}_{\dot{A}},\; \xi_A.$$

Then the following 4-component spinors can be defined,

$$\Psi = \begin{pmatrix} \xi_A \\ \eta^{\dot{A}} \end{pmatrix}, \qquad \bar{\Psi} = \left(\eta^A \;\; \bar{\xi}_{\dot{A}}\right), \tag{A.21}$$

$$\Psi^{\mathrm{C}} = \begin{pmatrix} \eta_A \\ \bar{\xi}^{\dot{A}} \end{pmatrix}, \quad \bar{\Psi}^C = \left(\xi^A \;\; \bar{\eta}_{\dot{A}}\right), \tag{A.22}$$

where C means charge conjugation and T is transposition.

A 4-component Majorana spinor is defined by

$$(\Psi_M)^C = \Psi_M \qquad \text{or} \qquad \Psi_M = \begin{pmatrix} \xi_A \\ \bar{\xi}^{\dot{A}} \end{pmatrix}. \tag{A.23}$$

The left- and right-handed projection operators are defined as

$$P_{L,R} = \frac{1}{2}\,(1 \mp \gamma_5). \tag{A.24}$$

Assume that the two 4 component spinors exists,

$$\Psi_1 = \begin{pmatrix} (\xi_1)_A \\ (\bar{\eta}_1)^{\dot{A}} \end{pmatrix}, \quad \Psi_2 = \begin{pmatrix} (\xi_2)_A \\ (\bar{\eta}_2)^{\dot{A}} \end{pmatrix}. \tag{A.25}$$

By using the projection operators from Eq. (A.24) one finds the following very useful relations,

$$\bar{\Psi}_1 P_L \Psi_2 = \eta_1 \xi_2, \qquad \bar{\Psi}_1 P_R \Psi_2 = \bar{\eta}_2 \bar{\xi}_1, \tag{A.26}$$

$$\bar{\Psi}_1 \gamma^\mu P_L \Psi_2 = \bar{\xi}_1 \bar{\sigma}^\mu \xi_2, \quad \bar{\Psi}_1 \gamma^\mu P_R \Psi_2 = -\bar{\eta}_2 \bar{\sigma}^\mu \eta_1. \tag{A.27}$$

Other useful identities, and details regarding calculations involving two- and four-spinors, can be found in Refs. [28, 29].

A.2 A short introduction to supersymmetry

Motivation for supersymmetry

Supersymmetry is a symmetry that generalises the space-time symmetries defined by the Poincarè group. The most important feature of supersymmetry is that it transforms fermions into bosons and visa versa. In elementary particle physics this symmetry has not been observed in any experiment or observation. Though a version of supersymmetry adopted for studies of the nucleus has been observed [64]. Still, supersymmetry is well motivated from both theoretical and phenomenological considerations.

The hierarchy and naturalness problems are important phenomenological motivations for supersymmetry. The hierarchy problem means that the mass of the Standard Model Higgs particle receives large quantum corrections from all particles which couple to it. It is therefore difficult to understand why this mass should be of the same order as the electroweak scale. One possible solution to this problem is to fine tune the couplings to one part in 10^{28}. This fine tuning is referred to as the naturalness problem. Even if such a fine tuning is possible a more fundamental mechanism is search for.

Supersymmetry avoids both of these problems since the symmetry between fermions and bosons leads to cancellations among the dangerous terms. This cancellation works even for broken supersymmetry, as long as the soft-breaking parameters are involved. At this point it should be mentioned that an alternative, the so-called "little-Higgs"-models [65] has recently been proposed as an alternative to supersymmetry, with respect to the hierarchy problem. This model has created a lot of activity, but we will not make any further comments or analysis of this model in this thesis.

A theoretical motivation for supersymmetry is stated in the "no-go" theorem of Coleman and Mandula [66]. This theorem says that supersymmetry is the only symmetry which connects the internal symmetries with the necessary symmetries of the S-matrix (see also Ref. [29]).

An even deeper theoretical motivation for supersymmetry is the observation that local supersymmetry includes gravity. Thus supersymmetry may be an important ingredient to unify quantum field theory and gravity. Supersymmetry is also important for string theories, e.g., to define the fermionic degrees of freedom.

Finally, it should be mentioned that supersymmetry is not only used in the study of quantum field theories, but is also an important tool in quantum mechanics [67].

These arguments does not means that supersymmetry has to exists, but they give a rationale for studying supersymmetric models.

Superfields and Lagrangian

Superspace is an extension of the Minkowski space, and a point in superspace is defined in terms of super-coordinates. That is, a point is defined in terms of the usual four Minkowski space-time coordinates, x^μ, and four additional anti-commuting numbers. These Grassmann numbers are the four Weyl spinors defined in Eqs. (A.13) and (A.14).

A superfield $\Phi(x, \theta, \bar{\theta})$ is defined [29] as an operator valued function on superspace. It is to be expanded as a power series in θ^A and $\bar{\theta}_{\dot{A}}$, i.e.,

$$\begin{aligned}\Phi(x,\theta,\bar{\theta}) = {} & f(x) + \theta^A\,\phi_A(x) + \bar{\theta}_{\dot{A}}\,\bar{\chi}^{\dot{A}}(x) \\ & + (\theta\theta)\,m(x) + (\theta\theta)\,n(x) + (\theta\sigma^\mu\theta)\,V_\mu(x) \\ & + (\theta\theta)\bar{\theta}_{\dot{A}}\,\bar{\lambda}^{\dot{A}}(x) + (\bar{\theta}\bar{\theta})\theta^A\,\psi_A(x) + (\theta\theta)(\bar{\theta}\bar{\theta})\,d(x). \end{aligned} \tag{A.28}$$

The following convention has been used for products of spinors,

$$(\theta\theta) = \theta^A\theta_A, \qquad (\bar{\theta}\bar{\theta}) = \bar{\theta}_{\dot{A}}\bar{\theta}^{\dot{A}}. \tag{A.29}$$

The component fields have the following properties:

$f(x)$, $m(x)$, $n(x)$ and $d(x)$	are scalar or pseudo-scalar fields,
$\psi(x)$ and $\phi(x)$	are left-handed Weyl spinor fields,
$\chi(x)$ and $\bar{\lambda}$	are right-handed Weyl spinor fields,
$V_\mu(x)$	is a Lorentz 4-vector field.

From the general expression of a superfield, three important superfields are defined.

These are the left- and right-handed chiral superfields, i.e.,

$$\Phi(y,\theta) = A(y) + \sqrt{2}\theta\psi(y) + (\theta\theta)F(y), \tag{A.30}$$

$$\Phi^{+}(z,\bar{\theta}) = A^{*}(z) + \sqrt{2}\bar{\theta}\bar{\psi}(y) + (\bar{\theta}\bar{\theta})F^{*}(y), \tag{A.31}$$

where

$$y^{\mu} = x^{\mu} + i\theta\sigma^{\mu}\bar{\theta}, \tag{A.32}$$

$$z^{\mu} = x^{\mu} - i\theta\sigma^{\mu}\bar{\theta}. \tag{A.33}$$

It is important to observe that a product of left-(right-) handed chiral superfields will also be a left-(right-) handed chiral superfield. That is, by using Eq. (A.30) one finds,

$$\begin{aligned}\Phi_i\Phi_j = {} & A_i(y)A_k(y) + \sqrt{(}2)\theta\left[A_i(y)\psi_j(y) + \psi_i(y)A_j(y)\right] \\ & + (\theta\theta)[A_i(y)F_k(y) + F_i(y)A_k(y) - \psi_i(y)\psi_j(y)],\end{aligned} \tag{A.34}$$

$$\begin{aligned}\Phi_i\Phi_j\Phi_k = {} & A_i(y)A_j(y)A_k(y) + \sqrt{(}2)\theta\left[A_i(y)A_j(y)\psi_k(y)\right. \\ & + A_i(y)\psi_j(y)A_k(y) + \psi_i(y)A_j(y)A_k(y)] \\ & + (\theta\theta)[A_i(y)A_j(y)F_k(y) + A_i(y)F_j(y)A_k(y) + F_i(y)A_j(y)A_k(y) \\ & - \psi_i(y)\psi_j(y)A_k(y) - \psi_i(y)A_j(y)\psi_k(y) - A_i(y)\psi_j(y)\psi_k(y)].\end{aligned} \tag{A.35}$$

A vector superfield is defined from the general superfield of Eq. (A.28), i.e.,

$$\begin{aligned}V(x,\theta,\bar{\theta}) = {} & V^{+}(x,\theta,\bar{\theta}) \\ = {} & C(x) + \theta\phi(x) + \bar{\theta}\bar{\phi}(x) \\ & + (\theta\theta)M(x) + (\bar{\theta}\bar{\theta})M^{*}(x) + \theta\sigma^{\mu}\bar{\theta}V_{\mu}(x) \\ & + (\theta\theta)\bar{\theta}\left(\bar{\lambda}(x) - \frac{i}{2}\bar{\sigma}^{\mu}\partial_{\mu}\phi(x)\right) + (\bar{\theta}\bar{\theta})\theta\left(\lambda(x) - \frac{i}{2}\sigma^{\mu}\partial_{\mu}\bar{\phi}(x)\right) \\ & + (\theta\theta)(\theta\theta)\left(D(x) - \frac{1}{4}\,\Box\, C(x)\right),\end{aligned} \tag{A.36}$$

and $\Box = \partial^{\mu}\partial_{\mu}$.

By using the two chiral superfields along with the vector superfield, i.e., Eqs. (A.30), (A.31) and (A.36), the supersymmetric version of an Abelian gauge transformation can be defined,

$$\begin{aligned}V(x,\theta,\bar{\theta}) \rightarrow {} & V'(x,\theta,\bar{\theta}) \\ = {} & V(x,\theta,\bar{\theta}) + i\left(\Lambda(x,\theta,\bar{\theta}) - \Lambda^{+}(x,\theta,\bar{\theta})\right),\end{aligned} \tag{A.37}$$

where $\Phi(x,\theta,\bar{\theta}) = i\Lambda(x,\theta,\bar{\theta})$ is an arbitrary chiral superfield.

The non-Abelian gauge transformation of the chiral- and vector-superfields along with the field strength, Λ, extends this definition, i.e.,

$$\Phi \to \Phi' = e^{-g\Lambda}\Phi, \tag{A.38}$$

$$e^{gV} =\to e^{gV'} = e^{-g\Lambda^*} e^{gV} e^{g\Lambda}. \tag{A.39}$$

From the vector superfield one can define the supersymmetric field strengths, which are invariant under Abelian and non-Abelian gauge transformations, respectively,

$$W'_A = -\frac{1}{4}(\bar{D}\bar{D})\, D_A\, V', \tag{A.40}$$

$$W_A = -\frac{1}{8g}(\bar{D}\bar{D}) e^{-2gV}\, D_A\, e^{2gV}. \tag{A.41}$$

The covariant derivative in use has been defined as,

$$D_A = \partial_A + 2i\sigma^\mu\bar{\theta}\partial_\mu. \tag{A.42}$$

One also need the superpotential $W(\Phi)$. This is a function of the left-handed chiral fields alone. By demanding renormalizability [29] one finds that the most general form of the superpotential is,

$$W = A\Phi + B\Phi^2 + C\Phi^3. \tag{A.43}$$

The supersymmetric Lagrangian is defined in terms of a supersymmetric action integral over superspace, i.e.,

$$S = \int d^4x \int d^4\theta\, \mathcal{L} = \int d^4x \int d^2\theta\, d^2\bar{\theta}\, \mathcal{L}. \tag{A.44}$$

The supersymmetric Lagrangian can now be formulated in terms of the chiral superfields, the supersymmetric field strength and the superpotential, that is, in terms of,

$$\Phi^+ e^{2gV+g'V'}\Phi, \quad \frac{1}{4k}Tr(W^a W_a) \quad \text{and} \quad W(\Phi). \tag{A.45}$$

Supersymmetry must be broken, and all possible soft breaking terms must be included. These terms were found in Ref. [37].

As for the Standard Model, one must also fix a gauge e.g., the Feynman gauge, and also include ghost terms. For details on this topic see Ref. [47].

This outlines the principles on how the supersymmetric Lagrangian is constructed. Further details on the construction of a supersymmetric version of Quantum Flavour Dynamic (QFD), can be found in Ref. [68].

Superfields	Boson fields	Fermionic partners
B_μ	$\tilde{B}_\mu$	λ_B
Λ^i_μ	$\tilde{\Lambda}^i_\mu$	λ^i_Λ
G^a_μ	$\tilde{G}^a_\mu$	λ^a_G
$\hat{H}_u$	$(H^1_u, H^2_u) = (H^+_u, H^0_u)$	$\psi_{H_u} = \left(\psi_{H^1_u}, \psi_{H^2_u}\right) = \left(\psi_{H^+_u}, \psi_{H^0_u}\right)$
$\hat{H}_d$	$(H^1_d, H^2_d) = (H^0_d, H^-_d)$	$\psi_{H_d} = \left(\psi_{H^1_d}, \psi_{H^2_d}\right) = \left(\psi_{H^0_d}, \psi_{H^-_d}\right)$
L_I	$(\tilde{L}^1_I, \tilde{L}^2_I) = (\tilde{L}^0_I, \tilde{L}^-_I)$	$\psi_{L_I} = \left(\psi_{L^1_I}, \psi_{L^2_I}\right) = \left(\psi_{L^0_I}, \psi_{L^-_I}\right)$
Q_I	$(\tilde{Q}^1_I, \tilde{Q}^2_I)$	$\psi_{Q_I} = \left(\psi_{Q^1_I}, \psi_{Q^2_I}\right)$
e_I	$\tilde{e}_I$	ψ_{e_I}
n_I	$\tilde{n}_I$	ψ_{n_I}
u_I	$\tilde{u}_I$	ψ_{u_I}
d_I	$\tilde{d}_I$	ψ_{d_I}.

Table A.1: The table shows the field content of the models studied in this thesis. The labels are such that μ is the space-time index from special relativity, and $i = 1, 2, 3$ labels the $SU(2)$ triplet of gauge bosons and $a = 1, 2, \ldots, 8$ labels $SU(3)$ gauge bosons. Finally, the index $I = 1, 2, 3$ labels the 3 flavours of (s)leptons and (s)quarks.

A.2.1 Field content

The gauge group from the Standard Model is used for all models, i.e., $SU(3) \times SU(2) \times U(1)$, with gauge coupling constants g_3, g_2 and g_1, respectively.

The field content consists of the gauge group multiplets and the matter multiplets, see Table A.1. All three models, studied in this thesis, contains these fields, except for MSSM-M which does not contain the three right-handed gauge singlets n_I.

Note that the superfield e is a left-handed chiral superfield. Thus a term like

$$(Y_e)_{ij}\, L_i \hat{H}_d c_j, \quad i, j = 1, 2, 3, \tag{A.46}$$

is a product between three left-handed chiral superfields, and can therefore be expanded by use of Eq. (A.35). The right-handed component of the electron is therefore contained in the right-handed superfield e^+_I. This also means that the electric charge for each L_I is negative, while each e_I has positive electric charge.

A.3 R-parity

R-parity is a discrete multiplicative quantum number, defined [35] by

$$P_R = (-1)^{3(B-L)+2s}, \tag{A.47}$$

for each particle of the model.

This quantum number is important since particles within the same supermultiplet have different R-parity. All particles of the Standard Model, and the Higgs bosons, have R-parity equal to $+1$. While their supersymmetric partners have R-parity equal to -1. R-parity can therefore be used to distinguish between particles and sparticles, that is, particles are defined as the states with $P_R = +1$, and sparticles are the states with $P_R = -1$.

If R-parity is conserved, as in MSSM and MSSM-D, there can be no mixing between particles and sparticles. Furthermore, the interaction vertices of these models must involve an even number of sparticles. This has some interesting phenomenological consequences:

- The lightest sparticle is stable. This particle is referred to as the lightest supersymmetric particle or LSP.
- All particles, other than the LSP, must decay into this stable particle.

R-parity is closely related to matter parity, which is defined [35], as

$$P_M = (-1)^{3(B-L)}, \tag{A.48}$$

for each particle of the theory. Matter parity can be conserved even if lepton number and baryon number is violated. Such violations will occur due to non-perturbative electroweak effects [35]. Such effects will not be studied in this thesis. The definitions (A.47) and (A.48) shows that matter parity and R-parity conservation are equivalent, since the product of $(-1)^{2s}$ is equal to $+1$ for the particles involved in any interaction vertex in a theory that conserves angular momentum [35].

It is important to emphasise that the conservation of lepton number and baryon number in the Standard Model is not imposed on the model, but is a consequence of including all renormalizable and gauge invariant interaction. This is often referred to as an accidental symmetry [16]. On the other hand R-parity must be introduced on the model by hand in order to avoid certain renormalizable and gauge invariant interactions. That is, MSSM is defined to conserve R-parity. The models discussed in this thesis are defined in terms of their conservation of lepton numbers. Conservation or violation of R-parity is therefore a consequence of conservation of lepton and baryon number.

URN:NBN:no-7281

Appendix B

Form factors and amplitudes

B.1 Form factors and matrix elements

A general expression for the amplitudes contributing to the decay rates $l \to l'\gamma$ can be obtained by Lorentz decomposing the amplitude as follows [30],

$$\begin{aligned}\mathcal{M} &= \varepsilon^{\lambda} < l'|J^{\rm em}_{\lambda}|l > \\ &= \overline{u}_{l'}\left(p_2\right)\left[iq^{\nu}\sigma_{\lambda\nu}\left(A + B\gamma_5\right) + \gamma_{\lambda}\left(C + D\gamma_5\right) + q_{\lambda}\left(E + F\gamma_5\right)\right]u_l\left(p_1\right), \end{aligned} \tag{B.1}$$

where $J^{\rm em}_{\lambda}$ is the electromagnetic current, $\varepsilon^{\lambda}(q)$ is photon polarisation, and A, B, C, D, E and F are Lorentz-invariant amplitudes. Electromagnetic gauge invariance

$$\partial^{\lambda} J^{\rm em}_{\lambda} - 0, \qquad \text{or} \qquad q^{\lambda} J^{\rm em}_{\lambda} - 0, \tag{B.2}$$

means that

$$-m_l(C + D\gamma_5) + m_{l'}(C - D\gamma_5) + q^2(E + F\gamma_5) = 0, \tag{B.3}$$

or

$$C = D = 0, \tag{B.4}$$

for an on-shell photon, i.e., for $q^2 = 0$. Due to the relation $\varepsilon^{\lambda} q_{\lambda} = 0$, the on-shell amplitude is a magnetic transition [30], i.e.,

$$\mathcal{M} = \varepsilon^{\lambda}\overline{u}_{l'}\left(p_2\right)\left[iq^{\nu}\sigma_{\lambda\nu}\left(A + B\gamma_5\right)\right]u_l\left(p_1\right). \tag{B.5}$$

This is a non-renormalizable dimension 5 term, known as a Pauli-term, and must be represented by a set of loop-diagrams. These diagrams results in a finite amplitude, since there can be no counterterms associated with non-renormalizable terms. This is also the reason why the $(g-2)$ anomalous magnetic moment of the electron must be finite in QED.

This simplifies the calculations considerably, since all terms which can not be reduced to the magnetic term of Eq. (B.5) are simply ignored. By using a Gordon decomposition, the amplitude $\mathcal{M}$ of Eq. (B.5) may be rewritten [30] as,

$$\mathcal{M} = \overline{u}_{l'}(p_2)(A + B\gamma_5)(2(p_1\varepsilon) - m_\mu \not{\varepsilon})\, u_l(p_1)\,. \tag{B.6}$$

The terms proportional to γ^μ are cancelled by terms of similar form from diagrams where the photon is attached to the external fermions, see e.g. Ref. [30]. Thus the relevant contribution to the amplitudes under study comes from the terms which are proportional to $(p_1\varepsilon)$.

It is useful to rewrite this part of the amplitude into the following form,

$$\mathcal{M} = (p\varepsilon)\left\{F_L\mathcal{M}_L + F_R\mathcal{M}_R\right\}, \tag{B.7}$$

where $\mathcal{M}_L$ and $\mathcal{M}_R$ are defined by

$$\mathcal{M}_L = \overline{u}_e(p_2)\, P_L u_\mu(p_1)\,, \tag{B.8}$$
$$\mathcal{M}_R = \overline{u}_e(p_2)\, P_R u_\mu(p_1)\,. \tag{B.9}$$

The projection operators $P_{R,L} = 1/2(1 \pm \gamma_5)$ have been used.

B.2 The decay rate

By including the kinematic terms and integrating over the phase space the following expression for the decay rate is obtained, i.e.,

$$\Gamma(l \to l'\gamma) = \frac{\alpha^3}{8\pi^2} m_l^3 \left(1 + y^2\right)\left\{\left(1 + y^2\right)\left(|F_R|^2 + |F_L|^2\right) + 4y\,\mathrm{Re}\left(F_R^* F_L\right)\right\}, \tag{B.10}$$

where the mass relation y have been defined as,

$$y = \frac{m_{l'}}{m_l}. \tag{B.11}$$

Note that if the mass of the outgoing fermion is neglected, i.e., $m_{l'} = 0$ or equivalently $y = 0$, the decay rate takes the simpler form,

$$\Gamma(l \to l'\gamma) = \frac{\alpha^3}{8\pi^2} m_l^3 \left(|F_R|^2 + |F_L|^2\right). \tag{B.12}$$

From Appendices B.4 and G.1 one finds that F_L and F_R have mass dimension m^{-1}, and the decay rates are therefore measured in m. These decay rates will be compared with the observed upper limits presented in Eqs. (2.4) - (2.6).

B.3 A toy model

In this section the expression for the branching ratio of $\mu \to e\gamma$, that was found in Ref. [30], i.e., Eq. 2.21, will be discussed by use of a simple toy model. The model is defined in a two flavour model by use of a 2×2 mass matrix. A simple series expansion is found by expanding the decay rate in terms of the off-diagonal elements of this mass matrix. This simple model still captures some of the most important characteristics of the more complicated models analysed in the main part of this thesis.

The starting point is the following factor from Eq. 2.21,

$$\Delta m^2 = |m_i^2 U_{\mu i} U_{ei}|^2, \quad i = 1, .., n, \tag{B.13}$$

where the summation is over the number of families, i.e., $n = 2$. This factor is to be interpreted as a sum over squared mass differences. Thus, the decay rates $l \to l'\gamma$, will increase for increasing values of this mass differences. It also shows that if the masses are completely degenerate then there are no contributions to the decay rates.

For simplicity the following mass matrix is assumed

$$M = \begin{pmatrix} a & x \\ x & b \end{pmatrix}. \tag{B.14}$$

Its eigenvalues and eigenvectors are found as

$$m_{\binom{1}{2}} = \frac{1}{2}\left(a + b \pm \sqrt{(a-b)^2 + 4x^2}\right), \tag{B.15}$$

$$U = \begin{pmatrix} \cos\theta & \sin\theta \\ -\sin\theta & \cos\theta \end{pmatrix}, \quad \tan 2\theta = \frac{2x}{a-b}. \tag{B.16}$$

By using these expressions a series expansion for Δm^2 in terms of x, can easily be obtained,

$$\Delta m^2 = \frac{a^4 + b^4}{(a-b)^2} x^2 - \frac{4ab(a^2+b^2)}{(a-b)^4} x^4 + \mathcal{O}(x^6). \tag{B.17}$$

This expression shows that for small values of x, and for large values of $a - b$, the decay rate for $l \to l'\gamma$ will follow a power law in its dependency on the off-diagonal element x from the mass matrix, i.e.,

$$\Gamma(l \to l'\gamma) \sim x^2. \tag{B.18}$$

Note that if a and b are nearly equal this series expansion is not valid. In this case one can assume that

$$b = a(1 - \varepsilon), \tag{B.19}$$

were ε is a small dimensionless parameter. The following series expansion is now obtained,

$$\Delta m^2 = \frac{x^4}{2} + 3a^2(1 - \varepsilon)x^2 + a^4\left(\frac{1}{2} - \varepsilon\right) + \mathcal{O}(\varepsilon^2). \tag{B.20}$$

From Eqs. (B.17) and (B.20) one sees that the decay rate for $\mu \to e\gamma$ follows a simple power law in its dependency on x. One also sees that the decay rate does not depend upon the sign of x. This is also confirmed by inspection of the general expression for Δm^2.

One should also remember that the eigenvalues, m_i of a $n \times n$-matrix M will obey a simple sum rule,

$$\sum_{i=1}^{n} m_i = \mathrm{Tr}\, M. \tag{B.21}$$

This means that the off-diagonal elements of the mass matrices presented in Chapters 4 - 6 will not alter the sum of the mass eigenstates. On the other hand, the off-diagonal elements do alter the mass differences and the mixing matrices. This will cause a non-vanishing contribution to the decay rates under study. Its actual size will depend on the details of the model.

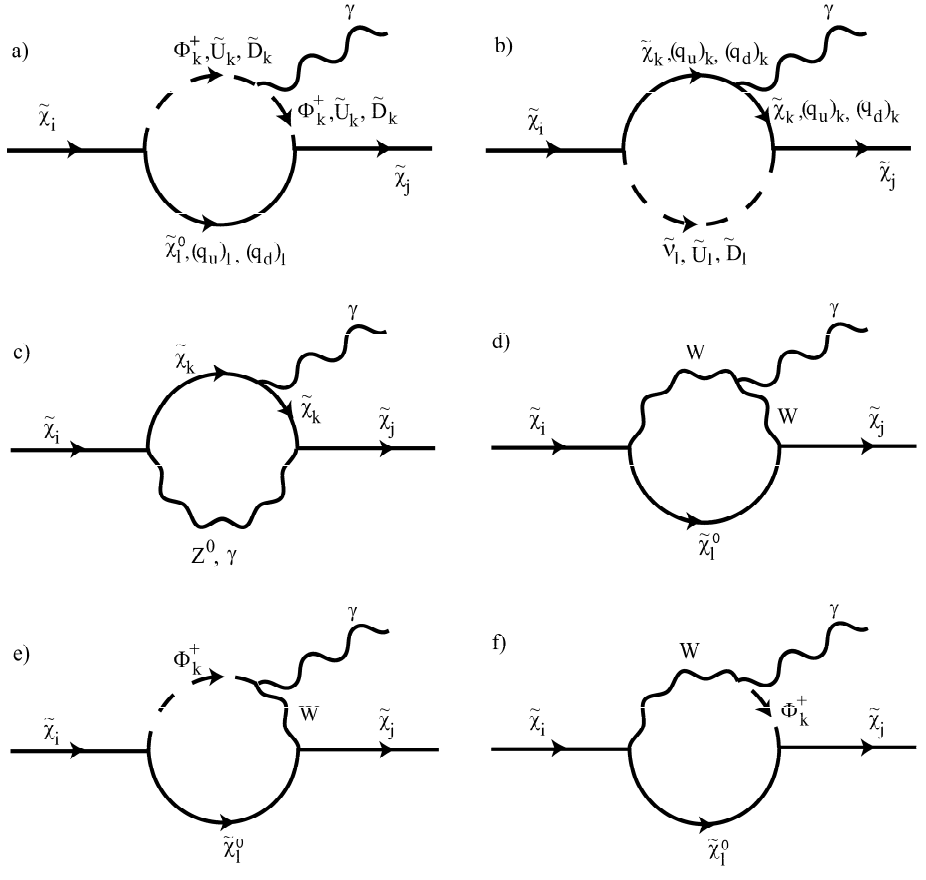

Figure B.1: The figure shows the amplitudes which may contribute to the decay rates $l \to l'\gamma$ in MSSM-DM.

B.4 Amplitudes in MSSM-DM

The amplitudes, which may contribute to the decay rates under study, are shown in Fig. B.1. Note that the amplitudes of Figs. B.1 a) and b) show that quarks and squarks also will contribute. This is a consequence of the R-parity violating coupling λ'_{ijk}, which exists in MSSM-M and MSSM-DM.

The relevant Feynman rules are presented in Appendices E.1 and E.3. The vertex factors A, B and F are all defined in these appendices, i.e., in Appendices E.1 and E.3. The Veltman-Passarino integrals, i.e., the integrals labelled as C_0, C_{11}, C_{12}, C_{21}, C_{22} and C_{23} are all defined, and solutions are presented in Appendix G.1. The direct calculations of these amplitudes shows that they lead to a finite result, in accordance with the general discussion of Appendix B.1.

Diagram a)

The diagram shown in Fig. B.1 a) consists of intermediate charged scalars and neutral fermions, or intermediate quarks and squarks. By picking out only those terms which are proportional to p^μ one obtains the following general expression for this amplitude,

$$\begin{aligned} ie\varepsilon_\mu \left(\Gamma_b^\mu\right)_{ijkl} = (p\varepsilon)\, \frac{iq^3}{8\pi^2} u\left(p'\right) \Big\{ \big[& m_i B_{ikl} B^*_{jkl} \left(C_{11} + C_{12} - C_{21} - C_{23}\right) \\ & - m_j A_{ikl} A^*_{jkl} \left(C_{12} - C_{23}\right) + m_k A_{ikl} B^*_{jkl} \left(C_0 - C_{11}\right) \big] P_L \\ & + \big[m_i A_{ikl} A^*_{jkl} \left(C_{11} + C_{12} - C_{21} - C_{23}\right) \\ & - m_j B_{ikl} B^*_{jkl} \left(C_{12} - C_{23}\right) + m_k B_{ikl} A^*_{jkl} \left(C_0 - C_{11}\right) \big] P_R \Big\} u\left(p\right), \end{aligned} \tag{B.22}$$

where q is the electric charge of the positron, and the external fermions are labelled by $i, j = 1, 2, \ldots, 5$. The intermediate particles are labelled by $k = 1, 2, \ldots, 8$ and $l - 1, 2, \ldots, 10$ for intermediate charged scalars and neutral fermions, and $k - 1, 2, 3$ and $l = 1, 2, \ldots, 6$ for intermediate quarks and squarks.

Diagram b)

The diagram shown in Fig. B.1 b) consists of intermediate charged fermions and neutral scalars, or intermediate quarks and squarks. By picking out only those terms which are proportional to p^μ one obtains the following general expression for this amplitude,

$$\begin{aligned} ie\varepsilon_\mu \left(\Gamma_a^\mu\right)_{ijkl} = (p\varepsilon)\, \frac{iq^3}{8\pi^2} u\left(p'\right) \Big\{ \big[& m_i \left(C_{11} + C_{12} + C_{21} + C_{23}\right) B_{ikl} B^*_{jkl} \\ & - m_j \left(C_{12} + C_{23}\right) A_{ikl} A^*_{jkl} + m_k C_{11} A_{ikl} B^*_{jkl} \big] P_L \\ & + \big[m_i \left(C_{11} + C_{12} + C_{21} + C_{23}\right) A_{ikl} A^*_{jkl} \\ & - m_j \left(C_{12} + C_{23}\right) B_{ikl} B^*_{jkl} + m_k C_{11} B_{ikl} A^*_{jkl} \big] P_R \Big\} u\left(p\right), \end{aligned} \tag{B.23}$$

where q is the electric charge of the positron, and the external fermions are labelled by $i, j = 1, 2, \ldots, 5$. The intermediate particles are labelled by $k = 1, 2, \ldots, 5$ and $l = 1, 2, \ldots, 16$ for intermediate charged fermions and neutral scalars, and $k = 1, 2, 3$ and $l = 1, 2, \ldots, 6$ for intermediate quarks and squarks.

Diagram c)

The diagram shown in Fig. B.1 c) consists of intermediate charged fermions and neutral gauge bosons. There are no contribution involving an intermediate photon

since such a contribution only contributes to the renormalization of the electric charge, i.e., it is not proportional to p^μ. By picking out only those terms proportional to p^μ one obtains the following general expression for this amplitude,

$$\begin{aligned} ie\varepsilon_\mu \left(\Gamma_d^\mu\right)_{ijk} = -2\left(p\varepsilon\right)\frac{ie^2q}{8\pi^2}u\left(p'\right)\Big\{\Big[&2m_k B_{ik}B_{jk}^*\left(C_0 - C_{11}\right) \\ &+ m_i A_{ik}B_{jk}^*\left(C_0 + 2C_{11} + C_{21} + C_{22} + C_{23}\right) \\ &+ m_j B_{ik}A_{jk}^*\left(C_0 + C_{11} - C_{12} - C_{23}\right)P_L \\ &+ \Big[2m_k A_{ik}A_{jk}^*\left(C_0 - C_{11}\right) \\ &+ m_i B_{ik}A_{jk}^*\left(C_0 + 2C_{11} + C_{21} + C_{22} + C_{23}\right) \\ &+ m_j A_{ik}B_{jk}^*\left(C_0 + C_{11} - C_{12} - C_{23}\right)\Big]P_R\Big\}u\left(p\right), \end{aligned} \tag{B.24}$$

where q is the electric charge of the positron, and the external fermions are labelled by $i, j = 1, 2, \ldots, 5$. The intermediate charged fermions are labelled by $k = 1, 2, \ldots, 5$.

Diagram d)

The diagram shown in Fig. B.1 d) consists of intermediate charged gauge bosons and neutral fermions. By picking out only those terms which are proportional to p^μ one obtains the following general expression for this amplitude,

$$\begin{aligned} ie\varepsilon_\mu \left(\Gamma_c^\mu\right)_{ijk} = -\left(p\varepsilon\right)\frac{ie^3}{8\pi^2}u\left(p'\right)\Big\{\Big[&m_k\left(8C_0 + 5C_{11}\right)A_{ik}A_{jk}^* \\ &- m_i B_{ik}A_{jk}^*\left(4C_{11} + 3C_{12} + 2C_{21} + 2C_{23}\right) \\ &+ m_j A_{ik}B_{jk}^*\left(3C_{12} - C_{11} + 2C_{23}\right)\Big]P_L \\ &+ \Big[m_k\left(8C_0 + 5C_{11}\right)B_{ik}B_{jk}^* \\ &- m_i A_{ik}B_{jk}^*\left(4C_{11} + 3C_{12} + 2C_{21} + 2C_{23}\right) \\ &+ m_j B_{ik}A_{jk}^*\left(3C_{12} - C_{11} + 2C_{23}\right)P_R\Big\}u\left(p\right), \end{aligned} \tag{B.25}$$

where q is the electric charge of the positron, and the external fermions are labelled by $i, j = 1, 2, \ldots, 5$. The intermediate neutral fermions are labelled by $k = 1, 2, \ldots, 10$.

Diagrams e) and f)

The diagrams shown in Fig. B.1 e) and f) consists of intermediate charged fermions, charged scalars and neutral fermions. They appear explicitly in the Feynman-gauge

used throughout the calculations. In the unitary gauge these Feynman diagrams vanish, and their effect is included in the propagators for the gauge bosons. By picking out only those terms proportional to p^μ one obtains the following general expression for this amplitude,

$$ie\varepsilon_\mu \left(\Gamma_e^\mu\right)_{ijlk} = (p\varepsilon)\frac{ie^2q}{8\pi^2}F_l\left(C_{11}+C_{12}\right)u\left(p'\right)\left(A_{ik}C_{jlk}P_R + B_{ik}D_{jlk}P_L\right)u\left(p\right), \quad \text{(B.26)}$$

$$ie\varepsilon_\mu \left(\Gamma_f^\mu\right)_{ijlk} = -(p\varepsilon)\frac{ie^2q}{8\pi^2}F_lC_{12}u\left(p'\right)\left(A_{ik}^*C_{jlk}^*P_L + B_{ik}^*D_{jlk}^*P_R\right)u\left(p\right), \quad \text{(B.27)}$$

where q is the electric charge of the positron, and the external fermions are labelled by $i,j=1,2,\ldots,5$. The intermediate charged scalars are labelled by $k=1,2,\ldots,6$, and intermediate neutral fermions are labelled by $k=1,2,\ldots,10$.

B.5 Amplitudes in MSSM-M

The amplitudes, which contribute in MSSM-M, are almost equal to the ones contributing in MSSM-DM. The difference is that in MSSM-M there are no right-handed gauge singlet fields. This affects the general expressions of Eqs. (B.22) - (B.27) in two ways. First, the Feynman rules are changed according to the discussion in Appendix E.2. Secondly, the indices labelling the intermediate particles have to be modified a bit. That is, there are only 7 neutral fermions and 10 neutral scalars in MSSM-M. On the other hand, the charged fermions and charged scalars are not affected by whether the right-handed singlets exist or not.

B.6 Amplitudes in MSSM-D

The 8 kind of diagrams, which may contribute to the decay rates $l \to l'\gamma$, are shown in Fig. 4.8 on page 41.

The amplitudes, represented by these diagrams, can be obtained from the general expressions of Eqs. (B.22) - (B.27), with two modifications. First, the Feynman rules of MSSM-D must be used to define the vertex factors. These rules are presented in Appendix E.1. Second, the indices of Eqs. (B.22) - (B.27) must be modified in accordance with the particle content of MSSM-D. Also, note that since lepton number is conserved in MSSM-D, there are no R-parity violating couplings, and consequently no (s)quark-contribution. By the same reason the superfields H_d and L_i do not mix together.

Appendix C

Scalarpotentials

In this appendix the scalar potential of MSSM-DM will be presented. The neutral part of this scalar potential, the neutral scalar potential, will also be presented. Also, details regarding the tadpole method will be discussed. This method is used to solve the minimisation conditions for MSSM-D.

The scalar potential of MSSM-DM is huge and complicated due to the existence of both right-handed gauge singlets and R-parity violating couplings. In preceding appendices it has been shown that also (s)quarks will contribute. This scalar potential is important in order to find the squared mass matrices for both neutral and charged scalars.

C.1 Tree-level scalar potential

In this appendix the tree-level scalar potential for the model MSSM-DM will be shown. Since the models MSSM-D and MSSM-M can both be obtained from MSSM-DM, the scalar potential presented in this section is therefore valid for all three models.

The superpotential and soft-breaking terms are respectively,

$$\begin{aligned} W_{\rm DM} &= Y_u Q H_u u + \frac{1}{2}\lambda_{\alpha\beta k} L_\alpha L_\beta e_k + \lambda'_{\alpha jk} L_\alpha Q_j d_k + \mu_\alpha L_\alpha H_u \\ &+ \frac{1}{2}\lambda''_{ijk} u_i d_j d_k + \lambda'''_{\alpha j} L_\alpha H_u n_j \\ &+ \frac{1}{6} A_{ijk} n_i n_j n_k + \frac{1}{2} B_{ij} n_i n_j + C_i n_i, \end{aligned} \tag{C.1}$$

and

$$\begin{aligned} -\mathcal{L}_{\rm soft} &= M_Q^2 \tilde{Q}^\dagger \tilde{Q} + M_{H_u}^2 H_u^\dagger H_u + \left(M_L^2\right)_{\alpha\beta} \tilde{L}_\alpha^\dagger \tilde{L}_\beta \\ &+ M_u^2 \tilde{u}\tilde{u}^* + M_d^2 \tilde{d}\tilde{d}^* + M_e^2 \tilde{e}\tilde{e}^* + M_\nu^2 \tilde{n}\tilde{n}^* \\ &+ \Bigg[b_\alpha \tilde{L}_\alpha H_u + a_u \tilde{Q} H_u \tilde{u} + \frac{1}{2}\lambda^{\rm s}_{\alpha\beta k} \tilde{L}_\alpha \tilde{L}_\beta \tilde{e}_k + \lambda'^{\rm s}_{\alpha jk} \tilde{L}_\alpha \tilde{Q}_j \tilde{d}_k \\ &+ \frac{1}{2}\lambda''^{\rm s}_{ijk} \tilde{u}_i \tilde{d}_j \tilde{d}_k + \lambda'''^{\rm s}_{\alpha j} \tilde{L}_\alpha H_u \tilde{n}_j \\ &+ \frac{1}{6} A^{\rm s}_{ijk} \tilde{n}_i \tilde{n}_j \tilde{n}_k + \frac{1}{2} B^{\rm s}_{ij} \tilde{n}_i \tilde{n}_j \\ &+ \frac{1}{2}\left(M_1 \tilde{B}\tilde{B} + M_2 \tilde{W}^a \tilde{W}^a + M_3 \tilde{g}\tilde{g}\right) + \text{h.c.} \Bigg]. \end{aligned} \tag{C.2}$$

The tree-level scalar potential becomes [28]

$$V_{\rm scalar} = V_F + V_D + V_{\rm soft}, \tag{C.3}$$

where the soft part is given by

$$V_{\rm soft} = -\mathcal{L}. \tag{C.4}$$

The F-term is obtained from

$$V_F = \sum_\phi \left| \frac{dW_{\rm DM}}{d\phi} \right|^2, \tag{C.5}$$

where ϕ is the scalar part of all chiral fields. This gives

$$
\begin{aligned}
V_F = {} & (Y_u)_{ij}\,(Y_u^*)_{ik}\,|H_u|^2\,\tilde{u}_j\tilde{u}_k^* + \lambda'_{\alpha jk}\lambda'^*_{\beta jl}\tilde{L}^i_\alpha\tilde{L}^{i*}_\beta\tilde{d}_k\tilde{d}_l^* \\
& - \Big[(Y_u)_{ij}\,\lambda'^*_{\alpha il}H_u^i\tilde{L}^{i*}_\alpha\tilde{u}_j\tilde{u}_l^* + \text{h.c.}\Big] \\
& + \lambda_{\alpha\beta k}\lambda^*_{\alpha\rho l}\tilde{L}^i_\beta\tilde{L}^{i*}_\rho\tilde{e}_k\tilde{e}_l^* + \lambda'_{\alpha jk}\lambda'^*_{\alpha lm}\tilde{Q}^i_j\tilde{Q}^{i*}_l\tilde{d}_k\tilde{d}_m^* \\
& + |\mu_\alpha|^2\,|H_u|^2 + \lambda'''_{\alpha j}\lambda'''^*_{\alpha k}\,|H_u|^2\,\tilde{n}_j\tilde{n}_k^* \\
& + \Big[\mu_\alpha\lambda^*_{\alpha\beta k}H_u^i\tilde{L}^{i*}_\beta\tilde{e}_k^* + \mu_\alpha\lambda'^*_{\alpha jk}H_u^i\tilde{Q}^{i*}_j\tilde{d}_k^* + \mu_\alpha\lambda'''^*_{\alpha j}\,|H_u|^2\,\tilde{n}_j \\
& + \lambda_{\alpha\beta k}\lambda'^*_{\alpha jl}\tilde{L}^i_\beta\tilde{Q}^{i*}_j\tilde{e}_k\tilde{d}_l^* + \lambda_{\alpha\beta k}\lambda'''^*_{\alpha j}\tilde{L}^i_\beta H^{i*}_u\tilde{e}_k\tilde{n}_j^* \\
& + \lambda'_{\alpha jk}\lambda'''^*_{\alpha l}\tilde{Q}^i_j H^{i*}_u\tilde{d}_k\tilde{n}_l^* + \text{h.c.}\Big] \\
& + (Y_u)_{ij}\,(Y_u^*)_{mn}\,\tilde{Q}^i_i\tilde{Q}^{i*}_m\tilde{u}_j\tilde{u}_n^* + \mu_\alpha\mu^*_\beta\tilde{L}^i_\alpha\tilde{L}^{i*}_\beta + \lambda'''_{\alpha j}\lambda'''^*_{\beta k}\tilde{L}^i_\alpha\tilde{L}^{i*}_\beta\tilde{n}_j\tilde{n}_k^* \\
& + \Big[\mu_\alpha\,(Y_u^*)_{ij}\,\tilde{L}^i_\alpha\tilde{Q}^{i*}_i\tilde{u}_j^* + \mu_\alpha\lambda'''^*_{\beta j}\tilde{L}^i_\alpha\tilde{L}^{i*}_\beta\tilde{n}_j^* \\
& + (Y_u)_{ij}\,\lambda'''^*_{\alpha k}\tilde{Q}^i_i\tilde{L}^{i*}_\alpha\tilde{u}_j\tilde{n}_k + \text{h.c.}\Big] \\
& + (Y_u)_{il}\,(Y_u^*)_{jl}\,\tilde{Q}^i_i H^j_u\left(\tilde{Q}^{i*}_j H^{j*}_u - \tilde{Q}^{j*}_j H^{i*}_u\right) \\
& + \frac{1}{4}\lambda''_{ljk}\lambda''^*_{lmn}\tilde{d}_j\tilde{d}_k\tilde{d}^*_m\tilde{d}^*_n + \left[\frac{1}{2}\,(Y_u)_{il}\,\lambda''^*_{ljk}\tilde{Q}^i_i H^j_u\tilde{d}^*_j\tilde{d}^*_k\varepsilon_{ij} + \text{h.c.}\right] \\
& + \lambda'_{\alpha jl}\lambda'^*_{\beta kl}\tilde{L}^i_\alpha\tilde{Q}^j_j\left(\tilde{L}^{i*}_\beta\tilde{Q}^{j*}_k - \tilde{L}^{j*}_\beta\tilde{Q}^{i*}_k\right) \\
& + \lambda''_{ijl}\lambda''^*_{mnl}\tilde{u}_i\tilde{u}^*_m\tilde{d}_j\tilde{d}^*_n + \left[\lambda'_{\alpha jl}\lambda''^*_{ikl}\tilde{L}^i_\alpha\tilde{Q}^j_j\tilde{u}^*_i\tilde{d}^*_k\varepsilon_{ij} + \text{h.c.}\right] \\
& + \frac{1}{2}\lambda_{\alpha\beta l}\lambda^*_{\rho\sigma l}\tilde{L}^i_\alpha\tilde{L}^j_\beta\tilde{L}^{i*}_\rho\tilde{L}^{j*}_\sigma \\
& + \lambda'''_{\alpha l}\lambda'''^*_{\beta l}\tilde{L}^i_\alpha H^j_u\left(\tilde{L}^{i*}_\beta H^{j*}_u - \tilde{L}^{j*}_\beta H^{i*}_u\right) + \frac{1}{4}A_{ijl}A^*_{pql}\tilde{n}_i\tilde{n}_j\tilde{n}^*_p\tilde{n}^*_q \\
& + B_{il}B_{jl}\tilde{n}_i\tilde{n}_j^* + |C_l|^2 \\
& + \left[\frac{1}{2}\lambda'''_{\alpha l}A^*_{ijl}\tilde{L}^i_\alpha H^j_u\tilde{n}^*_i\tilde{n}^*_j\varepsilon_{ij} + \lambda'''_{\alpha l}B^*_{il}\tilde{L}^i_\alpha H^j_u\tilde{n}^*_i\varepsilon_{ij} + \lambda'''_{\alpha l}C^*_l L^i_\alpha H^j_u\varepsilon_{ij}\right. \\
& \left. + \frac{1}{2}A_{ijl}B^*_{kl}\tilde{n}_i\tilde{n}_j\tilde{n}^*_k + \frac{1}{2}A_{ijl}C^*_l\tilde{n}_i\tilde{n}_j + B_{il}C^*_l\tilde{n}_i + \text{h.c.}\right]. \qquad \text{(C.6)}
\end{aligned}
$$

Here ε_{ij} is the antisymmetric tensor used to sum over $SU(2)$ indices. It is defined by $\varepsilon_{12} = 1$.

The D-term is obtained from

$$V_D = \frac{1}{2}\left[D^a D^a + (D')^2\right], \qquad \text{(C.7)}$$

which gives

$$
\begin{aligned}
V_D = \frac{1}{8}g^2 \Bigg\{ & \left(\left|H_u\right|^2 - \left|\tilde{L}_\alpha\right|^2 - \left|\tilde{Q}_m\right|^2 \right)^2 \\
& - 2\sum_{\alpha\neq\beta} \left|\tilde{L}^i_\alpha \tilde{L}^i_\beta\right|^2 - 2\sum_{m\neq n} \tilde{Q}^i_m \tilde{Q}^i_n \\
& + 4\left|H^{*i}_u \tilde{L}^i_\alpha\right|^2 + 4\left|H^{i*}_u \tilde{Q}^i_m\right|^2 + 4\left|\tilde{L}^i_\alpha \tilde{Q}^i_m\right|^2 \Bigg\} \\
& + \frac{1}{8}g'^2 \Bigg[\left|H_u\right|^2 - \left|\tilde{L}_\alpha\right|^2 + 2\left|\tilde{e}_m\right|^2 + \frac{1}{3}\left|\tilde{Q}_m\right|^2 \\
& - \frac{4}{3}\left|\tilde{u}_m\right|^2 + \frac{2}{3}\left|\tilde{d}_m\right|^2 \Bigg]^2 .
\end{aligned}
\tag{C.8}
$$

Note that since the neutrino superfields are gauge singlets and they consequently do not show up in the D-term.

C.1.1 Neutral scalar potential

The neutral part of this scalar potential becomes

$$
\begin{aligned}
V = & \left(M^2_{H_u} + \left|\mu_\alpha\right|^2\right)\left|H_u\right|^2 + \left(\left(M^2_L\right)_{\alpha\beta} + \mu_\alpha \mu^*_\beta\right)\tilde{L}^i_\alpha \tilde{L}^{i*}_\beta \\
& + \left(\varepsilon_{ij} b_\alpha \tilde{L}^i_\alpha H^j_u + \text{h.c.}\right) + \frac{1}{8}\left(g^2 + g'^2\right)\left(\left|H_u\right|^2 - \left|\tilde{L}_\alpha\right|^2\right)^2 \\
& + \frac{1}{2}g'^2\left|H^{i*}_u L^i_\alpha\right|^2 + \frac{1}{2}g'^2 \sum_{\alpha\neq\beta}\left|\tilde{L}^{i*}_\alpha \tilde{L}^i_\beta\right|^2 + \lambda'''_{\alpha j}\lambda'''^*_{\alpha k}\left|H_u\right|^2 \tilde{n}_j \tilde{n}^*_k \\
& + \left(M^2_\nu\right)_{ij}\tilde{n}_i \tilde{n}^*_j + \Bigg(\frac{1}{2}B^s_{ij}\tilde{n}_i\tilde{n}_j + \varepsilon_{ij}\lambda'''^s_{\alpha j}\tilde{L}^i_\alpha H^j_u \tilde{n}_j \\
& + \frac{1}{6}A^s_{ijk}\tilde{n}_i\tilde{n}_j\tilde{n}_k + \mu_\alpha \lambda'''^*_{\alpha j}\left|H_u\right|^2 \tilde{n}_j + \mu_\alpha \lambda'''^*_{\beta j}\tilde{L}^i_\alpha \tilde{L}^{i*}_\beta \tilde{n}^*_j + \text{h.c.}\Bigg) \\
& + \lambda'''_{\alpha j}\lambda'''^*_{\beta k}\tilde{L}^i_\alpha \tilde{L}^{i*}_\beta \tilde{n}_j \tilde{n}^*_k + \frac{1}{2}\lambda_{\alpha\beta l}\lambda^*_{\rho\sigma l}\tilde{L}^i_\alpha \tilde{L}^j_\beta \tilde{L}^{i*}_\rho \tilde{L}^{j*}_\sigma \\
& + \lambda'''_{\alpha l}\lambda'''^*_{\beta l}\tilde{L}^i_\alpha H^j_u\left(\tilde{L}^{i*}_\beta H^{j*}_u - \tilde{L}^{j*}_\beta H^{i*}_u\right) + \frac{1}{4}A^*_{pql}A_{ijl}\tilde{n}_i\tilde{n}_j\tilde{n}^*_p\tilde{n}^*_q \\
& + B_{il}B_{jl}\tilde{n}_i\tilde{n}^*_j + \left|C_l\right|^2 \\
& + \Bigg[\frac{1}{2}\lambda'''^*_{\alpha l}A^*_{ijl}\tilde{L}^i_\alpha H^j_u \tilde{n}^*_i \tilde{n}^*_j \varepsilon_{ij} + \lambda'''_{\alpha l}B^*_{il}\tilde{L}^i_\alpha H^j_u \tilde{n}^*_i \varepsilon_{ij} + \lambda'''_{\alpha l}C^*_l L^i_\alpha H^j_u \varepsilon_{ij} \\
& + \frac{1}{2}A_{ijl}\bar{B}^\dagger_{kl}\bar{n}_i\bar{n}_j\bar{n}^\dagger_k + \frac{1}{2}A_{ijl}\bar{C}^\dagger_l \bar{n}_i\bar{n}_j + \bar{B}_{il}\bar{C}^\dagger_l \bar{n}_i + \text{h.c.}\Bigg] .
\end{aligned}
\tag{C.9}
$$

Note that by assuming that the right-handed gauge singlet fields vanish the neutral

scalar potential simplifies considerably, i.e.,

$$V = \left(M_{H_u}^2 + |\mu_\alpha|^2\right)|H_u|^2 + \left(\left(M_L^2\right)_{\alpha\beta} + \mu_\alpha\mu_\beta^*\right)\tilde{L}_\alpha^i\tilde{L}_\beta^i + \left(-\varepsilon_{ij}b_\alpha\tilde{L}_\alpha^i H_u^j + \text{h.c.}\right) + \frac{1}{8}\left(g^2+g'^2\right)\left(|H_u|^2 - \left|\tilde{L}_\alpha\right|^2\right)^2 + \frac{1}{2}g^2\left|H_u^{i*}L_\alpha^j\varepsilon_{ij}\right|^2. \tag{C.10}$$

Here ε_{ij} is the antisymmetric tensor used to sum over $SU(2)$ indices. It is defined by $\varepsilon_{12} = 1$.

This is the neutral part of the scalar potential for the model MSSM-M, which is studied in Sec. 5.4.

C.2 The tadpole method

In this appendix the one-loop contributions to the scalar Higgs-potential in MSSM is found by use of the tadpole method [38]. In Ref. [38] the contributions to the minimisation conditions for the scalar potential was found under the assumption of flavour conservation. In this appendix flavour changing for the fermions and sfermions are taken into account along with the contributions from the right-handed sneutrinos. Also some minor errors in Ref. [38] are corrected.

C.2.1 The tree-level scalar potential

For MSSM-D the superpotential is given by

$$W = Y_u Q\hat{H}_u U - Y_d Q\hat{H}_d D - Y_e L\hat{H}_d R + Y_\nu L\hat{H}_u n + \mu\hat{H}_u\hat{H}_d, \tag{C.11}$$

where both $SU(2)$ and $SU(3)$ indices are suppressed. The Higgs fields are given by

$$H_u = \begin{pmatrix} H_u^+ \\ H_u^0 \end{pmatrix} \equiv \begin{pmatrix} H_u^+ \\ \frac{1}{\sqrt{2}}\left(\psi_u + v_u + i\phi_u\right) \end{pmatrix}, \tag{C.12}$$

$$H_d = \begin{pmatrix} H_d^0 \\ H_d^- \end{pmatrix} \equiv \begin{pmatrix} \frac{1}{\sqrt{2}}\left(\psi_d + v_d + i\phi_d\right) \\ H_d^- \end{pmatrix}. \tag{C.13}$$

The sign convention in Eq. (C.11) is the same as in Ref. [35], which gives positive Yukawa-couplings for the Standard Model fermions. The Yukawa-couplings Y_ν will be neglected due their smallness for the rest of the calculation. That is, the scalarpotential, Eq. (C.11) becomes equal to the one from MSSM.

The scalar potential is found from

$$V_{\text{scalar}} = V_F + V_D + V_{\text{soft}}, \tag{C.14}$$

where the scalar potential is given in Eq. (3.3), i.e.,

$$\begin{aligned} V_{\text{soft}} = {} & M_{\tilde{Q}}^2 \tilde{Q}^\dagger \tilde{Q} + M_{\tilde{L}}^2 \tilde{L}^\dagger \tilde{L} + M_{H_u}^2 H_u^\dagger H_u + M_{H_d}^2 H_d^\dagger H_d \\ & + M_{\tilde{u}}^2 \tilde{u}\tilde{u}^* + M_{\tilde{d}}^2 \tilde{d}\tilde{d}^* + M_{\tilde{e}}^2 \tilde{e}\tilde{e}^* + M_{\tilde{\nu}}^2 \tilde{n}\tilde{n}^* \\ & + \Big[a_u \tilde{Q} H_u \tilde{u} + a_d \tilde{Q} H_d \tilde{d} + a_e \tilde{L} H_d \tilde{e} + a_\nu \tilde{L} H_u \tilde{n} + b H_u H_d \\ & + \frac{1}{2} M_1 \tilde{B}^0 \tilde{B}^0 + \frac{1}{2} M_2 \tilde{W}^a \tilde{W}^a + \frac{1}{2} M_3 \tilde{G}^a \tilde{G}^a + \text{h.c.} \Big], \end{aligned} \tag{C.15}$$

and

$$V_D = \frac{1}{2} \left[D^a D^a + (D')^2 \right]. \tag{C.16}$$

And finally the contribution from the superpotential,

$$V_F = \sum_\phi \left| \frac{dW}{d\phi} \right|^2, \tag{C.17}$$

These equations gives the following neutral part of the scalar potential,

$$\begin{aligned} V_0 = {} & \left(m_{H_u}^2 + \mu^2 \right) |H_u|^2 + \left(m_{H_d}^2 + \mu^2 \right) |H_d|^2 + b \left(H_u H_d + h.c. \right) + Y_\nu L H_u n \\ & + \frac{1}{8} \left(g^2 + g'^2 \right) \left[|H_u|^2 - |H_d|^2 \right]^2 + \frac{1}{2} g^2 |H_u H_d|^2. \end{aligned} \tag{C.18}$$

C.2.2 Tree-level tadpoles

By substituting Eqs. (C.12) and (C.13) into the scalar potential (C.14) we can identify

$$V_{\text{tadpole}} = t_u \psi_u + t_d \psi_d,$$

where t_u and t_d are the tree-level tadpoles, i.e.,

$$\begin{aligned} t_u &= \left(m_{H_u}^2 + \mu^2 \right) v_u + b v_u - \frac{1}{8} \left(g^2 + g'^2 \right) v_u \left(v_d^2 - v_u^2 \right), \\ t_d &= \left(m_{H_d}^2 + \mu^2 \right) v_d + b v_d + \frac{1}{8} \left(g^2 + g'^2 \right) v_d \left(v_d^2 - v_u^2 \right). \end{aligned}$$

The minimum of the Higgs potential is determined by,

$$\frac{\partial V_0}{\partial \psi_i} = \frac{\partial V_{\text{tadpole}}}{\partial \psi_i} = 0. \tag{C.19}$$

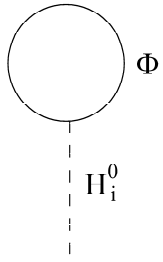

Figure C.1: The figure shows the one-loop tadpole with the two neutral Higgs scalars, H and h, along with all other possible fields, Φ.

Therefore the tadpoles t_u and t_d must vanish at the minimum. By performing a rotation of the tadpoles we find

$$\begin{pmatrix} T_u \\ T_d \end{pmatrix} = \begin{pmatrix} \cos\beta & -\sin\beta \\ \sin\beta & \cos\beta \end{pmatrix} \begin{pmatrix} t_u \\ t_d \end{pmatrix},$$

we find

$$T_u = v\left[\frac{1}{2}\left(m_{H_u}^2 + m_{H_d}^2 + 2\mu^2\right)\sin 2\beta + b\right], \tag{C.20}$$

$$T_d = v\left[\left(m_{H_d}^2 + \mu^2\right)\cos^2\beta - \left(m_{H_u}^2 + \mu^2\right)\sin^2\beta + \frac{1}{2}M_Z^2\cos 2\beta\right]. \tag{C.21}$$

Setting $T_u = 0$ and dividing by v gives the familiar tree-level condition, i.e.,

$$-b = \frac{1}{2}\left(m_{H_u}^2 + m_{H_d}^2 + 2\mu^2\right)\sin 2\beta. \tag{C.22}$$

Also by setting $T_d = 0$ and dividing by $v\cos 2\beta$ gives the other tree-level condition, i.e,

$$\frac{1}{2}M_Z^2 = \frac{m_{H_d}^2 - m_{H_u}^2\tan^2\beta}{\tan^2\beta - 1} - \mu^2. \tag{C.23}$$

C.2.3 The one-loop tadpoles

In this section the contribution from the one-loop tadpoles will be calculated. The physical Higgs bosons H and h are obtained from the neutral fields H_u^0 and H_d^0 by,

$$\begin{pmatrix} h \\ H \end{pmatrix} = \begin{pmatrix} \cos\alpha & -\sin\alpha \\ \sin\alpha & \cos\alpha \end{pmatrix} \begin{pmatrix} H_u^0 \\ H_d^0 \end{pmatrix}. \tag{C.24}$$

Here α is defined [47] by

$$\tan 2\alpha = \tan 2\beta \frac{2b + M_Z^2 \sin 2\beta}{2b - M_Z^2 \sin 2\beta}. \tag{C.25}$$

These one-loop diagrams are shown in Fig. (C.1). The field Φ is a shorthand notation for all fields which couples to the Higgs fields. The tadpole contributions are regularized by the $\overline{\text{DM}}$ method.

It is useful to define the linear combinations J and $J_\perp$,

$$\begin{pmatrix} J \\ J_\perp \end{pmatrix} = \begin{pmatrix} \cos(\alpha+\beta) & -\sin(\alpha+\beta) \\ \sin(\alpha+\beta) & \cos(\alpha+\beta) \end{pmatrix} \begin{pmatrix} H \\ h \end{pmatrix}.$$

or

$$\begin{pmatrix} H \\ h \end{pmatrix} = \begin{pmatrix} \cos(\alpha+\beta) & \sin(\alpha+\beta) \\ -\sin(\alpha+\beta) & \cos(\alpha+\beta) \end{pmatrix} \begin{pmatrix} J \\ J_\perp \end{pmatrix}. \tag{C.26}$$

The relevant interaction term is

$$\mathcal{L}_{\text{int}} = g_H H \phi_i^* \phi_j + g_h h \phi_i^* \phi_j,$$

where ϕ_i is an arbitrary field. By using Eq. (C.26) we find

$$\begin{aligned} \mathcal{L}_{\text{int}} &= (g_H \cos(\alpha+\beta) - g_h \sin(\alpha+\beta)) J \phi_i^* \phi_j \\ &\quad + (g_H \sin(\alpha+\beta) + g_h \cos(\alpha+\beta)) J_\perp \phi_i^* \phi_j \\ &\equiv V(J\phi_i^*\phi_j) J \phi_i^* \phi_j + V(J_\perp \phi_i^* \phi_j) J_\perp \phi_i^* \phi_j. \end{aligned} \tag{C.27}$$

We will also need the definitions

$$Z_R = \begin{pmatrix} -\sin\alpha & \cos\alpha \\ \cos\alpha & \sin\alpha \end{pmatrix},$$

and

$$B_R^i = v_d Z_R^{1i} - v_u Z_R^{2i},$$

that is,

$$\begin{aligned} B_R^1 &= v_d Z_R^{11} - v_u Z_R^{21} = -v \sin(\alpha+\beta), \\ B_R^2 &= v_d Z_R^{12} - v_u Z_R^{22} = v \cos(\alpha+\beta). \end{aligned}$$

By rotating to J and $J_\perp$ we find

$$\begin{aligned}
V\left(JU_iU_i\right) &= -ig\frac{2}{3}\frac{M_Z\sin^2\theta_W}{\cos\theta_W}\left[1+\frac{3-8\sin^2\theta_W}{4\sin^2\theta_W}\left(Z_U^{Ii}\right)^2\right] \\
&\quad + i\left(Y_u^I\right)^2 v\sin^2\beta\left(\left(Z_U^{Ii}\right)^2+\left(Z_U^{(I+3)i}\right)^2\right) \\
&\quad - i\sqrt{2}\sin\beta a_u^{IJ}Z_U^{Ii}Z_U^{(J+3)i}+i\sqrt{2}\cos\beta\mu Y_u^I Z_U^{Ii}Z_U^{(I+3)i}, \qquad \text{(C.28)} \\
V\left(J_\perp U_iU_i\right) &= -i\left(Y_u^I\right)^2 v\sin\beta\cos\beta\left(\left(Z_U^{Ii}\right)^2+\left(Z_U^{(I+3)i}\right)^2\right) \\
&\quad + i\sqrt{2}\cos\beta a_u^{IJ}Z_U^{Ii}Z_U^{(J+3)i}+i\sqrt{2}\sin\beta\mu Y_u^I Z_U^{Ii}Z_U^{(I+3)i}, \qquad \text{(C.29)}
\end{aligned}$$

$$\begin{aligned}
V\left(JD_iD_i\right) &= ig\frac{1}{3}\frac{M_Z\sin^2\theta_W}{\cos\theta_W}\left[1+\frac{3-4\sin^2\theta_W}{4\sin^2\theta_W}\left(Z_D^{Ii}\right)^2\right] \\
&\quad - i\left(Y_d^I\right)^2 v\cos^2\beta\left(\left(Z_D^{Ii}\right)^2+\left(Z_D^{(I+3)i}\right)^2\right) \\
&\quad - i\sqrt{2}\cos\beta a_d^{IJ}Z_D^{Ii}Z_D^{(J+3)i}-i\sqrt{2}\sin\beta\mu Y_d^I Z_D^{Ii}Z_D^{(I+3)i}, \qquad \text{(C.30)} \\
V\left(J_\perp D_iD_i\right) &= -i\left(Y_d^I\right)^2 v\sin\beta\cos\beta\left(\left(Z_D^{Ii}\right)^2+\left(Z_D^{(I+3)i}\right)^2\right) \\
&\quad - i\sqrt{2}\sin\beta a_d^{IJ}Z_D^{Ii}Z_D^{(J+3)i}+i\sqrt{2}\cos\beta\mu Y_d^I Z_D^{Ii}Z_D^{(I+3)i}, \qquad \text{(C.31)}
\end{aligned}$$

$$\begin{aligned}
V\left(JL_iL_i\right) &= ig\frac{M_Z\sin^2\theta_W}{\cos\theta_W}\left[1+\frac{1-4\sin^2\theta_W}{2\sin^2\theta_W}\left(Z_L^{Ii}\right)^2\right] \\
&\quad - i\left(Y_e^I\right)^2 v\cos^2\beta\left(\left(Z_L^{Ii}\right)^2+\left(Z_L^{(I+3)i}\right)^2\right) \\
&\quad - i\sqrt{2}\cos\beta a_e^{IJ}Z_L^{Ii}Z_L^{(J+3)i}-i\sqrt{2}\sin\beta\mu Y_e^I Z_L^{Ii}Z_L^{(I+3)i}, \qquad \text{(C.32)} \\
V\left(J_\perp L_iL_i\right) &= -i\left(Y_e^I\right)^2 v\sin\beta\cos\beta\left(\left(Z_L^{Ii}\right)^2+\left(Z_L^{(I+3)i}\right)^2\right) \\
&\quad - i\sqrt{2}\sin\beta a_e^{IJ}Z_L^{Ii}Z_L^{(J+3)i}+i\sqrt{2}\cos\beta\mu Y_e^I Z_L^{Ii}Z_L^{(I+3)i}. \qquad \text{(C.33)}
\end{aligned}$$

The quark (squark) and lepton (slepton) contribution

$$\begin{aligned}
\Delta T_1^{(q)} = & \frac{3g}{8\pi^2 M_W}\left\{\left(m_u^I\right)^4\left(\ln\frac{\left(m_u^I\right)^2}{Q^2}-1\right)-\left(m_d^I\right)^4\left(\ln\frac{\left(m_d^I\right)^2}{Q^2}-1\right)\right\} \\
& +\frac{3}{16\pi^2}\left\{m_{U_i}^2\left(\ln\frac{m_{U_i}^2}{Q^2}-1\right)\left[-\left(Y_u^I\right)^2 v\sin^2\beta\left(\left(Z_U^{Ii}\right)^2+\left(Z_U^{(I+3)i}\right)^2\right)\right.\right. \\
& +\sqrt{2}\sin\beta a_u^{IJ} Z_U^{Ii} Z_U^{(J+3)i}-\sqrt{2}\mu\cos\beta Y_u^I Z_U^{Ii} Z_U^{(I+3)i} \\
& \left.+\frac{2gM_Z\sin^2\theta_W}{3\cos\theta_W}\left(1+\frac{3-8\sin^2\theta_W}{4\sin^2\theta_W}\left(Z_U^{Ii}\right)^2\right)\right] \\
& +m_{D_i}^2\left(\ln\frac{m_{D_i}^2}{Q^2}-1\right)\left[\left(Y_d^I\right)^2 v\cos^2\beta\left(\left(Z_D^{Ii}\right)^2+\left(Z_D^{(I+3)i}\right)^2\right)\right. \\
& +\sqrt{2}\cos\beta a_d^{IJ} Z_D^{Ii} Z_D^{(J+3)i}+\sqrt{2}\mu\sin\beta Y_d^I Z_D^{Ii} Z_D^{(I+3)i} \\
& \left.\left.-\frac{gM_Z\sin^2\theta_W}{3\cos\theta_W}\left(1+\frac{3-4\sin^2\theta_W}{2\sin^2\theta_W}\left(Z_D^{Ii}\right)^2\right)\right]\right\},
\end{aligned} \tag{C.34}$$

$$\begin{aligned}
\Delta T_2^{(q)} = & -\frac{3g}{8\pi^2 M_W}\left\{\left(m_u^I\right)^4\left(\ln\frac{\left(m_u^I\right)^2}{Q^2}-1\right)\cot\beta+\left(m_d^I\right)^4\left(\ln\frac{\left(m_d^I\right)^2}{Q^2}-1\right)\tan\beta\right\} \\
& +\frac{3}{16\pi^2}\left\{m_{U_i}^2\left(\ln\frac{m_{U_i}^2}{Q^2}-1\right)\left[\left(Y_u^I\right)^2 v\sin\beta\cos\beta\left(\left(Z_U^{Ii}\right)^2+\left(Z_U^{(I+3)i}\right)^2\right)\right.\right. \\
& \left.-\sqrt{2}\cos\beta a_u^{IJ} Z_U^{Ii} Z_U^{(J+3)i}-\sqrt{2}\sin\beta\mu Y_u^I Z_U^{Ii} Z_U^{(I+3)i}\right] \\
& +m_{D_i}^2\left(\ln\frac{m_{D_i}^2}{Q^2}-1\right)\left[\left(Y_d^I\right)^2 v\sin\beta\cos\beta\left(\left(Z_D^{Ii}\right)^2+\left(Z_D^{(I+3)i}\right)^2\right)\right. \\
& \left.\left.+\sqrt{2}\sin\beta a_d^{IJ} Z_D^{Ii} Z_D^{(J+3)i}-\sqrt{2}\mu\cos\beta Y_d^I Z_D^{Ii} Z_D^{(I+3)i}\right]\right\},
\end{aligned} \tag{C.35}$$

$$\begin{aligned}
\Delta T_1^{(l)} = & -\frac{1}{4\pi^2 v}\left(m_e^I\right)^4\left(\ln\frac{\left(m_e^I\right)^2}{Q^2}-1\right) \\
& +\frac{1}{16\pi^2}\left\{m_{L_i}^2\left(\ln\frac{m_{L_i}^2}{Q^2}-1\right)\left[\left(Y_c^I\right)^2 v\cos^2\beta\left(\left(Z_L^{Ii}\right)^2+\left(Z_L^{(I+3)i}\right)^2\right)\right. \\
& +\sqrt{2}\cos\beta a_e^{IJ} Z_L^{Ii} Z_L^{(J+3)i}+\sqrt{2}\mu\sin\beta Y_e^I Z_L^{Ii} Z_L^{(I+3)i} \\
& \left.-\frac{gM_Z\sin^2\theta_W}{\cos\theta_W}\left(1+\frac{1-4\sin^2\theta_W}{2\sin^2\theta_W}\left(Z_L^{Ii}\right)^2\right)\right] \\
& \left.+\frac{M_Z^2 m_{\tilde{\nu}}^2}{v}\left(\ln\frac{m_{\tilde{\nu}}^2}{Q^2}-1\right)\right\},
\end{aligned} \tag{C.36}$$

$$\Delta T_2^{(l)} = -\frac{1}{4\pi^2 v}\left(m_e^I\right)^4\left(\ln\frac{\left(m_e^I\right)^2}{Q^2}-1\right)\tan\beta$$
$$+\frac{1}{16\pi^2}\left\{m_{L_i}^2\left(\ln\frac{m_{L_i}^2}{Q^2}-1\right)\left[\left(Y_e^I\right)^2 v\cos\beta\sin\beta\left(\left(Z_L^{Ii}\right)^2+\left(Z_L^{(I+3)i}\right)^2\right)\right.\right.$$
$$\left.\left.+\sqrt{2}\sin\beta a_e^{IJ}Z_L^{Ii}Z_L^{(J+3)i}-\sqrt{2}\mu\cos\beta Y_e^I Z_L^{Ii}Z_L^{(I+3)i}\right]\right\}. \quad \text{(C.37)}$$

Note that the extra factor of 4 associated with the fermions is because a Dirac fermion has 4 degrees of freedom. The factor of -1 is due to normal ordering for the fermions. Also note that a Majorana fermion only has 2 degrees of freedom.

The neutralino mass matrix is given by

$$M_N = \begin{pmatrix} M_1 & 0 & -M_Z\cos\beta\sin\theta_W & M_Z\sin\beta\sin\theta_W \\ 0 & M_2 & M_Z\cos\beta\cos\theta_W & M_Z\sin\beta\cos\theta_W \\ M_{\bar{Z}}\cos\beta\sin\theta_W & M_{\bar{Z}}\cos\beta\cos\theta_W & 0 & \mu \\ M_Z\sin\beta\sin\theta_W & M_Z\sin\beta\cos\theta_W & -\mu & 0 \end{pmatrix}.$$

This matrix is diagonalised by the unitary matrix Z_N, i.e.,

$$M_{\text{diag}} = Z_N^T M_N Z.$$

From Ref. [47] (note the corrected expression in the errata) we find the following couplings after a rotation to J and $J_\perp$,

$$V\left(J\tilde{\chi}_i^0\tilde{\chi}_i^0\right) = ig\left(Z_N^{1i}\tan\theta_W - Z_N^{2i}\right)\left[Z_N^{3i}\cos\beta + Z_N^{4i}\sin\beta\right],$$
$$V\left(J_\perp\tilde{\chi}_i^0\tilde{\chi}_i^0\right) = ig\left(Z_N^{1i}\tan\theta_W - Z_N^{2i}\right)\left[Z_N^{3i}\sin\beta - Z_N^{4i}\cos\beta\right].$$

This gives the following contribution to the minimisation conditions,

$$\Delta T_1^{(\chi^0)} = -\frac{g}{8\pi^2}\sum_{i=1}^{4} M_{\chi_i^0}^3\left(Q'_{ii}\cos\beta + S'_{ii}\sin\beta\right)\left(\ln\frac{M_{\chi_i^0}^2}{Q^2}-1\right), \quad \text{(C.38)}$$

$$\Delta T_2^{(\chi^0)} = -\frac{g}{8\pi^2}\sum_{i=1}^{4} M_{\chi_i^0}^3\left(Q'_{ii}\sin\beta - S'_{ii}\cos\beta\right)\left(\ln\frac{M_{\chi_i^0}^2}{Q^2}-1\right), \quad \text{(C.39)}$$

where

$$Q'_{ii} = \varepsilon_i\left[Z_N^{3i}\left(Z_N^{2i} - Z_N^{1i}\tan\theta_W\right)\right], \quad \text{(C.40)}$$
$$S'_{ii} = \varepsilon_i\left[Z_N^{4i}\left(Z_N^{2i} - Z_N^{1i}\tan\theta_W\right)\right]. \quad \text{(C.41)}$$

Here ε_i is the sign of the ith eigenvalue of the neutralino mass matrix.

Note that the neutralinos are Majorana fermions, that is, they only have two degrees of freedom.

The chargino mass matrix is given by

$$M_C = \begin{pmatrix} M_2 & \sqrt{2}M_W \sin\beta \\ \sqrt{2}M_W \cos\beta & \mu \end{pmatrix}.$$

This mass matrix is not diagonal and must be diagonalised by two matrices Z_+ and Z_-, i.e.,

$$M_{\text{diag}} = (Z_-)^T M_C Z_+.$$

From Ref. [47] we find the following couplings after a rotation to J and $J_\perp$,

$$V\left(J\tilde{\chi}_i\tilde{\chi}_i\right) = -\frac{ig}{\sqrt{2}}\left[Z_{2i}^- Z_{1i}^+ \cos\beta - Z_{1i}^- Z_{2i}^+ \sin\beta\right],$$
$$V\left(J_\perp\tilde{\chi}_i\tilde{\chi}_i\right) = -\frac{ig}{\sqrt{2}}\left[Z_{2i}^- Z_{1i}^+ \sin\beta + Z_{1i}^- Z_{2i}^+ \cos\beta\right].$$

This gives the following contributions to the minimisation conditions,

$$\Delta T_1^{(\tilde{\chi})} = -\frac{g}{4\pi^2}\sum_{i=1}^{2} M_{\tilde{\chi}_i}^3 \left[Q_{ii}\cos\beta - S_{ii}\sin\beta\right]\left(\ln\frac{M_{\tilde{\chi}_i}^2}{Q^2} - 1\right), \tag{C.42}$$

$$\Delta T_2^{(\tilde{\chi})} = -\frac{g}{4\pi^2}\sum_{i=1}^{2} M_{\tilde{\chi}_i}^3 \left[Q_{ii}\sin\beta + S_{ii}\cos\beta\right]\left(\ln\frac{M_{\tilde{\chi}_i}^2}{Q^2} - 1\right), \tag{C.43}$$

where

$$Q_{ii} = \frac{1}{\sqrt{2}} Z_{2i}^- Z_{1i}^+, \tag{C.44}$$

$$S_{ii} = \frac{1}{\sqrt{2}} Z_{1i}^- Z_{2i}^+. \tag{C.45}$$

The gauge boson contribution is found from Ref. [47], after a rotation to J and $J_\perp$,

$$V\left(JWW\right) = igM_W g^{\mu\nu}\cos\left(2\beta\right),$$
$$V\left(J_\perp WW\right) = igM_W g^{\mu\nu}\sin\left(2\beta\right),$$
$$V\left(JZZ\right) = \frac{igM_Z}{\cos\theta_W} g^{\mu\nu}\cos\left(2\beta\right),$$
$$V\left(J_\perp ZZ\right) = \frac{igM_Z}{\cos\theta_W} g^{\mu\nu}\sin\left(2\beta\right),$$

which gives the following contributions to the minimisation conditions,

$$\begin{aligned}\Delta T_1^{(GB)} &= \frac{3gM_W^3}{16\pi^2}\cos(2\beta)\left(\ln\frac{M_W^2}{Q^2}-1\right)\\ &\quad+\frac{3gM_Z^3}{32\pi^2\cos\theta_W}\cos(2\beta)\left(\ln\frac{M_Z^2}{Q^2}-1\right),\end{aligned}\tag{C.46}$$

$$\begin{aligned}\Delta T_2^{(GB)} &= \frac{3gM_W^3}{16\pi^2}\sin(2\beta)\left(\ln\frac{M_W^2}{Q^2}-1\right)\\ &\quad+\frac{3gM_Z^3}{32\pi^2\cos\theta_W}\sin(2\beta)\left(\ln\frac{M_Z^2}{Q^2}-1\right).\end{aligned}\tag{C.47}$$

The factor of 3 is because the gauge bosons have 3 degrees of freedom after the electroweak symmetry breaking.

The Higgs bosons give the following contribution to the minimisation condition,

$$\begin{aligned}\Delta T_1^{(H)} &= \frac{gM_{H^\pm}^2}{32\pi^2}\left(2M_W-\frac{M_Z}{\cos\theta_W}\right)\cos 2\beta\left(\ln\frac{M_{H^\pm}^2}{Q^2}-1\right)\\ &\quad+\frac{gM_ZM_h^2}{64\pi^2\cos\theta_W}(-2\cos 2\alpha+\cos 2\beta)\left(\ln\frac{M_h^2}{Q^2}-1\right)\\ &\quad+\frac{gM_ZM_H^2}{64\pi^2\cos\theta_W}(2\cos 2\alpha+\cos 2\beta)\left(\ln\frac{M_H^2}{Q^2}-1\right)\\ &\quad-\frac{gM_ZM_A^2}{64\pi^2\cos\theta_W}\cos 2\beta\left(\ln\frac{M_A^2}{Q^2}-1\right),\end{aligned}\tag{C.48}$$

$$\begin{aligned}\Delta T_2^{(H)} &= \frac{gM_WM_{H^\pm}^2}{16\pi^2}\sin 2\beta\left(\ln\frac{M_{H^\pm}^2}{Q^2}-1\right)\\ &\quad+\frac{gM_ZM_h^2}{64\pi^2\cos\theta_W}(\sin 2\alpha+\sin 2\beta)\left(\ln\frac{M_h^2}{Q^2}-1\right)\\ &\quad+\frac{gM_ZM_H^2}{64\pi^2\cos\theta_W}(-\sin 2\alpha+\sin 2\beta)\left(\ln\frac{M_H^2}{Q^2}-1\right).\end{aligned}\tag{C.49}$$

In the Landau gauge the Goldstone bosons are absorbed by the gauge bosons, and do contribute to the minimisation condition only through the gauge bosons.

URN:NBN:no-7281

Appendix D

Mass- and mixing-matrices

D.1 Field content of MSSM-D

In this appendix the field content of MSSM-D will be reviewed, and the mass matrices, relevant for the calculations, will be presented.

The difference between MSSM and MSSM-D is that MSSM-D also contain three right-handed gauge singlet chiral superfields, n_I. The superpotential and soft-breaking parameters of MSSM-D are shown in Eqs. (3.2) and (3.3). The relevant doublets are

$$\hat{H}_u = \begin{pmatrix} \hat{H}_u^1 \\ \hat{H}_u^2 \end{pmatrix}, \quad \hat{H}_d = \begin{pmatrix} \hat{H}_d^1 \\ \hat{H}_d^2 \end{pmatrix}, \quad \text{and} \quad L_I = \begin{pmatrix} L_I^1 \\ L_I^2 \end{pmatrix}, \tag{D.1}$$

where $I = 1, 2, 3$. The right-handed part of the electron and neutrinos are contained in the supermultiplets e_I and n_I. Note that these fields are left-handed, such that a term like $(Y_\nu)_{IJ}\, L_I\, \hat{H}_u\, n_J$ can be expanded by use of Eq. (A.35).

D.2 Mass matrices and mixing in MSSM-D

The neutrinos of MSSM-D are Dirac fermions, and their masses are determined from the electroweak symmetry breaking, and one Yukawa matrix, Y_ν. Except for the neutrino masses and the extension of the squared sneutrino mass matrix, all mass matrices of MSSM-D and MSSM are equal. However, for completeness and easy referencing the mass matrices for the charginos and neutralinos, and also the squared mass matrix for the selectrons, will be presented.

Sneutrinos

In the basis $\Phi_{\tilde{\nu}}^T = (\tilde{L}_1^1, \tilde{L}_2^1, \tilde{L}_3^1, \tilde{n}_1, \tilde{n}_2, \tilde{n}_3)$, the 6×6 sneutrino mass matrix becomes,

$$M_{\tilde{\nu}}^2 = \begin{pmatrix} M_L^2 + M_\nu^2 + \frac{1}{2} M_Z^2 \cos 2\beta & v\,(a_\nu \sin\beta - \mu Y_\nu \cos\beta) \\ v\left(a_\nu^\dagger \sin\beta - \mu^* Y_\nu^\dagger \cos\beta\right) & M_n^2 + M_\nu^2 \end{pmatrix}. \tag{D.2}$$

This symmetric matrix is diagonalized by one unitary matrix, i.e.,

$$Z_{\tilde{\nu}}^\dagger M_{\tilde{\nu}}^2 Z_{\tilde{\nu}} = \mathrm{diag}(m_{\tilde{\nu}_1}^2, m_{\tilde{\nu}_2}^2, m_{\tilde{\nu}_3}^2, m_{\tilde{\nu}_4}^2, m_{\tilde{\nu}_5}^2, m_{\tilde{\nu}_6}^2). \tag{D.3}$$

By using the mixing matrix matrix $Z_{\tilde{\nu}}$ the 6 mass eigenstates, $\tilde{\nu}_i$, can be expressed in terms of the 3 gauge eigenstates, L_I^1 and n_I, i.e.,

$$L_I^1 = Z_{\tilde{\nu}}^{Ij}\, \tilde{\nu}_j, \quad n_I = Z_{\tilde{\nu}}^{(I+3)j*}\, \tilde{\nu}_j, \quad I = 1,2,3, \quad j = 1,2,\ldots,6. \tag{D.4}$$

Selectrons

In the basis $\Phi_{\tilde{L}}^T = (\tilde{L}_1^2, \tilde{L}_2^2, \tilde{L}_3^2, \tilde{e}_1, \tilde{e}_2, \tilde{e}_3)$, The 6×6 selectron mass matrix is

$$M_{\tilde{l}}^2 = \begin{pmatrix} M_L^2 + M_l^2 + \Delta_L & v\,(a_e \cos\beta - \mu Y_e \sin\beta) \\ v\left(a_e^\dagger \cos\beta - \mu^* Y_e^\dagger \sin\beta\right) & M_e^2 + M_l^2 + \Delta_e \end{pmatrix}, \tag{D.5}$$

where

$$\Delta_L = M_Z^2 \left(\frac{1}{2} + \sin^2\theta_W\right) \cos(2\beta), \tag{D.6}$$

$$\Delta_e = M_Z^2 \sin^2\theta_W \cos(2\beta). \tag{D.7}$$

This matrix is diagonalized by one unitary matrix, i.e.,

$$Z_L^\dagger M_{\tilde{l}}^2 Z_L = \mathrm{diag}(M_{\tilde{L}_1}^2, M_{\tilde{L}_2}^2, M_{\tilde{L}_3}^2, M_{\tilde{L}_4}^2, M_{\tilde{L}_5}^2, M_{\tilde{L}_6}^2). \tag{D.8}$$

By using the mixing matrix Z_L the 6 mass eigenstates, L_i^+, and the gauge eigenstates, L_I^2 and e_I, i.e.,

$$L_I^2 = Z_L^{Ij*}\, L_i^-, \quad e_I = Z_L^{(I+3)j}\, L_j^+, \quad I = 1,2,3, \quad j = 1,2,\ldots,6. \tag{D.9}$$

Charginos

In the gauge-eigenstate basis $(\psi^\pm)^T = \left(\tilde{W}^+, \psi_{H_u^1}, \tilde{W}^-, \psi_{H_d^2}\right)$, the chargino mass matrix is

$$M_{\tilde{\chi}} = \begin{pmatrix} 0 & X^T \\ X & 0 \end{pmatrix}, \tag{D.10}$$

where

$$X = \begin{pmatrix} M_2 & \sqrt{2}\, M_W \sin\beta \\ \sqrt{2}\, M_W \cos\beta & \mu \end{pmatrix}. \tag{D.11}$$

This mass matrix may be diagonalized by using two 2×2 unitary matrices, i.e.,

$$\left(Z^-\right)^T X Z^+ = \mathrm{diag}(m_{\tilde{\chi}_1}, m_{\tilde{\chi}_2}). \tag{D.12}$$

Analytically, the mass eigenstates and the corresponding mixing matrices become [28],

$$\begin{aligned} m^2_{\tilde{\chi}^+} = \frac{1}{2}\Big\{ & M_2^2 + \mu^2 + 2M_W^2 \\ & \pm[(M_2^2 - \mu^2)^2 + 4M_W^2(M_2^2 + \mu^2 + 2M_2\,\mu \sin 2\beta)]^{1/2}\Big\} \end{aligned} \tag{D.13}$$

$$Z^- = O_-, \qquad Z^+ = \begin{cases} O_+ & \text{if } \det X \geq 0, \\ \sigma_3 O_+ & \text{if } \det X < 0, \end{cases} \tag{D.14}$$

where the Pauli matrix σ_3 have been inserted and the matrices $O_\pm$ have been defined as

$$O_\pm = \begin{pmatrix} \cos\phi_\pm & \sin\phi_\pm \\ -\sin\phi_\pm & \cos\phi_\pm \end{pmatrix}. \tag{D.15}$$

The mixing angles are determined by the relations

$$\tan 2\phi_- = 2\sqrt{2}\, \frac{M_W(\mu\cos\theta_W + M_2 \sin\theta_W)}{M_2^2 - \mu^2 + 2M_W^2 \cos 2\theta_W}, \tag{D.16}$$

$$\tan 2\phi_- = 2\sqrt{2}\, \frac{M_W(\mu\sin\theta_W + M_2 \cos\theta_W)}{M_2^2 - \mu^2 - 2M_W^2 \cos 2\theta_W}. \tag{D.17}$$

By using the mixing matrices $Z^\pm$, the mass eigenstates and gauge eigenstates are related as follows,

$$\psi_{H_u^1} = Z^+_{2i}\chi_i^+, \quad \psi_{H_d^2} = Z^-_{2i}\chi_i^-, \tag{D.18}$$

$$W^\pm = iZ_1^\pm \chi_i^\pm, \quad \tilde{\chi}_i = \begin{pmatrix} \chi_i^+ \\ \bar{\chi}_i^- \end{pmatrix}, \quad i = 1, 2. \tag{D.19}$$

Neutralinos

In the gauge eigenbasis $\psi_0^T = \left(\tilde{B}, \tilde{W}^0, \psi_{H_d^1}, \psi_{H_u^2}\right)$ the neutralino mass matrix is

$$M_N = \begin{pmatrix} M_1 & 0 & -M_Z \cos\beta \sin\theta_W & M_Z \sin\beta \sin\theta_W \\ 0 & M_2 & M_Z \cos\beta \cos\theta_W & -M_Z \sin\beta \cos\theta_W \\ -M_Z \cos\beta \sin\theta_W & M_Z \cos\beta \cos\theta_W & 0 & -\mu \\ M_Z \sin\beta \sin\theta_W & -M_Z \sin\beta \cos\theta_W & -\mu & 0 \end{pmatrix}. \tag{D.20}$$

This mass matrix is diagonalized by the unitary matrix Z_N, i.e.,

$$Z_N^\dagger \, M_N \, Z_N = \mathrm{diag}(m_{\tilde{\chi}_1^0}, m_{\tilde{\chi}_1^0}, m_{\tilde{\chi}_1^0}, m_{\tilde{\chi}_1^0}). \tag{D.21}$$

By using this mixing matrix the mass eigenstates and gauge eigenstates are related as follows,

$$\tilde{B} = i Z_N^{1i} \chi_i^0, \qquad \tilde{W}^0 = i Z_N^{2i} \chi_i^0, \tag{D.22}$$

$$\psi_{H_d^0} = Z_N^{3i} \chi_i^0, \qquad \psi_{H_u^0} = Z_N^{4i} \chi_i^0, \tag{D.23}$$

$$\tilde{\chi}_i^0 = \begin{pmatrix} \chi_i^0 \\ \bar{\chi}_i^0 \end{pmatrix}, \qquad i = 1, 2, 3, 4. \tag{D.24}$$

Though analytic expressions can be found for the eigenvalues and the mixing matrix, numerical methods, provided by the NAG-library[55], have been used throughout this work.

D.3 Field content of MSSM-DM

The field content is equal in MSSM-DM and MSSM-D, that is, all fields of MSSM are present, in addition to the right-handed gauge singlets n_I, $I = 1, 2, 3$. However, due to the existence of a $U(4)$ symmetry the superfields $\hat{H}_d$ and L_I will mix together. This makes it convenient to define the $U(4)$-vector

$$L_\alpha = (\hat{H}_d, L_I), \quad I = 1, 2, 3, \tag{D.25}$$

where the doublets $\hat{H}_d$ and L_I was defined in Eq. (D.1). Equations (A.34) and (A.35) have been used extensively in order to find the mass matrices.

D.4 Mass-matrices in MSSM-DM

In this section the mass-matrices for MSSM-DM are presented. The particle spectrum of this model consists of 10 neutral Majorana fermions, 5 charged Dirac fermions, 8 charged scalars, 16 neutral scalars, and also a quark sector almost identical to the one in MSSM.

D.4.1 Neutral fermions in MSSM-DM

In the gauge-basis $\Phi_N^T = \left(\tilde{B}, \tilde{W}^3, \psi_{H_u^2}, \psi_{L_\alpha^1}, \psi_{n_i}\right)$, the masses for the neutral fermions are determined from the following 10×10 symmetric matrix, i.e.,

$$M_N = \begin{pmatrix} M_1 & 0 & M_Z s_\theta s_\beta & -M_Z s_\theta v_\alpha/v & 0 \\ 0 & M_2 & -M_Z c_\theta s_\beta & M_Z c_\theta v_\beta/v & 0 \\ M_Z s_\theta s_\beta & -M_Z c_\theta s_\beta & 0 & \hat{\mu}_\alpha & \frac{1}{\sqrt{2}}\lambda'''_{\alpha j} v_\alpha \\ -M_Z s_\theta v_\alpha/v & M_Z c_\theta v_\beta/v & \hat{\mu}_\alpha & 0 & \frac{1}{\sqrt{2}}\lambda'''_{\alpha j} v_u \\ 0 & 0 & \frac{1}{\sqrt{2}}\lambda'''_{\alpha j} v_\alpha & \frac{1}{\sqrt{2}}\lambda'''_{\alpha j} v_u & \frac{1}{2}\left(\frac{1}{\sqrt{2}} A_{ijk} w_k + B_{ij}\right) \end{pmatrix}, \tag{D.26}$$

where $s_\theta = \sin\theta_W$, $c_\theta = \cos\theta_W$, $s_\beta = \sin\beta$, and $\hat{\mu}_\alpha$ as defined by Eq. (6.22) has been used. This symmetric matrix is diagonalized by one matrix, Z_N, i.e.,

$$Z_N^T M_N Z_N = \mathrm{diag}\,(m_{\tilde{\chi}_i}), \quad i = 1, \ldots, 10. \tag{D.27}$$

D.4.2 Charged Dirac fermions

In the gauge-basis

$$\Psi^{-T} = \left(\tilde{W}^-, \psi_{L_\alpha^2}\right) \text{ and } \Psi^{+T} = \left(\tilde{W}^+, \psi_{H_u^+}, \psi_{e_i}\right), \tag{D.28}$$

the 5×5 mass-matrix for the charged fermions become [49],

$$M_C = \begin{pmatrix} M_2 & \sqrt{2} M_W \sin\beta & 0_{1\times 3} \\ \sqrt{2} M_W \cos\beta\, \hat{e}_\alpha & -\hat{\mu}_\alpha & -\frac{1}{\sqrt{2}}\lambda_{\alpha\beta k} v_\beta \end{pmatrix}. \tag{D.29}$$

Here the unit vector $\hat{e}_\alpha$ is defined, i.e., $\hat{e}_\alpha = (1, 0, 0, 0)$.

D.4.3 Charged scalars

By using the field definitions from Eqs. (6.12) - (6.14), the following gauge basis is defined, $\Phi_{\mathrm{cs}}^T = \left(H_u^\downarrow, \tilde{L}_\beta^{2*}, \tilde{e}_k\right)$, the 8×8 squared mass-matrix for the charged scalars become [49],

$$M_{\mathrm{cs}}^2 = \begin{pmatrix} (M_{\mathrm{cs}}^2)_u & (M_{\mathrm{cs}}^2)_{u\beta} & (M_{\mathrm{cs}}^2)_{uj} \\ (M_{\mathrm{cs}}^2)_{\alpha u} & (M_{\mathrm{cs}}^2)_{\alpha\beta} & (M_{\mathrm{cs}}^2)_{\alpha j} \\ (M_{\mathrm{cs}}^2)_{iu} & (M_{\mathrm{cs}}^2)_{i\beta} & (M_{\mathrm{cs}}^2)_{ij} \end{pmatrix}, \tag{D.30}$$

where

$$\left(M^2_{\rm cs}\right)_{\hat{u}} = M^2_{H_{\hat{u}}} + |\hat{\mu}_\alpha|^2 + \frac{1}{8}\left(g^2 - g'^2\right)\left(|v_u|^2 - |v_d|^2\right), \tag{D.31}$$

$$\left(M^2_{\rm cs}\right)_{u\beta} = \hat{b}_\beta + \frac{1}{4}g^2 v_\beta v_u + \frac{1}{2}v_u v_\rho \lambda'''_{\beta l}\lambda'''^*_{\rho l}, \tag{D.32}$$

$$\left(M^2_{\rm cs}\right)_{uj} = \frac{1}{\sqrt{2}}v_\beta \hat{\mu}_\alpha \lambda_{\alpha\beta j}, \tag{D.33}$$

$$\left(M^2_{\rm cs}\right)_{\alpha\beta} = \left(M^2_L\right)_{\alpha\beta} + \hat{\mu}_\alpha\hat{\mu}_\beta + \frac{1}{8}\left(g^2 - g'^2\right)\left(|v_u|^2 - |v_d|^2\right)\delta_{\alpha\beta} + \frac{1}{4}g^2 v_\alpha v_\beta + \frac{1}{2}v_\rho v_\sigma \lambda_{\alpha\beta l}\lambda_{\rho\sigma l}, \tag{D.34}$$

$$\left(M^2_{\rm cs}\right)_{\alpha j} = \frac{1}{\sqrt{2}}\left(v_\rho \lambda^{\rm s}_{\rho\alpha j} - v_u \hat{\mu}_\rho \lambda_{\rho\alpha j}\right), \tag{D.35}$$

$$\left(M^2_{\rm cs}\right)_{ij} = \left(M^2_e\right)_{ij} + \frac{1}{2}v_\alpha v_\beta \lambda_{\rho\alpha i}\lambda_{\rho\beta j} + \frac{1}{4}g'^2\left(|v_u|^2 - |v_d|^2\right)\delta_{KM}. \tag{D.36}$$

Charged mass matrix ν_i-basis

The v_i-basis is defined by

$$v_i = 0 \text{ and } \hat{\mu}_i = 0.$$

In the ν_i-basis the squared mass matrix takes the simpler form

$$\begin{aligned}
\left(M^2_{\rm cs}\right)_u &= M^2_{H_u} + |\hat{\mu}|^2 - \frac{M^2_Z}{2}\cos 2\theta \cos 2\beta,\\
\left(M^2_{\rm cs}\right)_{u\beta} &= \hat{b}_\beta + \frac{M^2_W}{2}\sin 2\beta\,\delta_{\beta 0},\\
\left(M^2_{\rm cs}\right)_{uj} &= 0,\\
\left(M^2_{\rm cs}\right)_{\alpha\beta} &= \left(M^2_L\right)_{\alpha\beta} + \hat{\mu}^2\,\delta_{\alpha 0}\,\delta_{\beta 0} - \frac{M^2_Z}{2}\cos 2\theta\cos 2\beta\,\delta_{\alpha\beta} - \frac{M^2_W}{2}\sin 2\beta\,\delta_{\alpha 0}\,\delta_{\beta 0},\\
\left(M^2_{\rm cs}\right)_{\alpha j} &= \frac{1}{\sqrt{2}}\left(v_d \lambda^{\rm s}_{0\alpha j} - v_u \hat{\mu}\lambda_{0\alpha j}\right),\\
\left(M^2_{\rm cs}\right)_{ij} &= \left(M^2_e\right)_{ij} + M^2_l\,\delta_{ij} - M^2_W\tan^2\theta\cos 2\beta\,\delta_{KM}.
\end{aligned}$$

Here we have defined

$$\hat{b}_\beta = b_\beta + \frac{1}{\sqrt{2}}\lambda'''^{\rm s}_{\beta j}w_j + \lambda'''_{\beta l}\left[\frac{1}{8}w_i w_j \Lambda_{ijl} + \frac{1}{\sqrt{2}}w_i B_{il} + C_l\right], \tag{D.37}$$

and also the diagonal matrix M_l, whose diagonal elements are the three charged leptons of the Standard Model, i.e.,

$$M_l = \mathrm{diag}\left(m_e, m_\mu, m_\tau\right). \tag{D.38}$$

Note that this matrix is symmetric. It can therefore be diagonalized by using only one unitary matrix, i.e.,

$$Z_{\rm cs} M^2_{\rm cs} Z^T_{\rm cs} = \text{diag}\left(m_1^2, m_2^2, \ldots, m_8^2\right).$$

D.4.4 Neutral scalars

CP-even neutral scalars By using the field definitions from Eqs. (6.12) - (6.14), the following gauge basis can be defined $\Phi^T_{\rm even} = (\chi_u, \chi_\alpha, \xi_i)$ as basis for the CP-even neutral scalar particles, the squared mass-matrix becomes [49],

$$M^2_{\rm even} = \begin{pmatrix} (M^2_{\rm even})_u & (M^2_{\rm even})_{u\alpha} & (M^2_{\rm even})_{uj} \\ (M^2_{\rm even})_{\alpha u} & (M^2_{\rm even})_{\alpha\beta} & (M^2_{\rm even})_{\alpha j} \\ (M^2_{\rm even})_{iu} & (M^2_{\rm even})_{i\beta} & (M^2_{\rm even})_{ij} \end{pmatrix}, \tag{D.39}$$

where

$$\left(M^2_{\rm even}\right)_u = \frac{M_Z^2}{2}\frac{3v_u^2 - v_d^2}{v^2} + |\hat{\mu}_\alpha|^2 + M^2_{H_u} + \frac{1}{4}\lambda'''_{\alpha j}\lambda'''_{\beta j} v_\alpha v_\beta, \tag{D.40}$$

$$\left(M^2_{\rm even}\right)_{u\alpha} = -M_Z^2\frac{v_u v_\alpha}{v^2} + \hat{b}_\alpha + v_u v_\beta \lambda'''_{\alpha l}\lambda'''_{\beta l}, \tag{D.41}$$

$$\left(M^2_{\rm even}\right)_{ui} = \frac{v_\alpha}{\sqrt{2}}\left(\lambda'''^{\rm s}_{\alpha i} + \lambda'''_{\alpha l}\left(B_{il} + \frac{1}{\sqrt{2}} w_j A_{ijl}\right)\right) + \sqrt{2} v_u \hat{\mu}_\alpha \lambda'''_{\alpha i}, \tag{D.42}$$

$$\left(M^2_{\rm even}\right)_{\alpha\beta} = \begin{cases} \frac{M_Z^2}{2}\frac{3v_p^2 - v_u^2}{v^2}\delta_{\alpha\beta} + (M_L^2)_{\alpha\beta} + \hat{\mu}_\alpha\hat{\mu}_\beta + \frac{1}{2}v_u^2\lambda'''_{\alpha l}\lambda'''_{\beta l}, & \text{for } \alpha = \beta, \\ M_Z^2\frac{v_\alpha v_\beta}{v^2} + (M_L^2)_{\alpha\beta} + \hat{\mu}_\alpha\hat{\mu}_\beta + \frac{1}{2}v_u^2\lambda'''_{\alpha l}\lambda'''_{\beta l}, & \text{for } \alpha \neq \beta, \end{cases} \tag{D.43}$$

$$\left(M^2_{\rm even}\right)_{\alpha i} = \frac{v_u}{\sqrt{2}}\left(\lambda'''^{\rm s}_{\alpha i} + \lambda'''_{\alpha l}\left(B_{il} + \frac{1}{\sqrt{2}} w_j A_{ijl}\right)\right) + \frac{1}{\sqrt{2}} v_\beta\left(\hat{\mu}_\alpha \lambda'''_{\beta i} + \hat{\mu}_\beta \lambda'''_{\alpha i}\right), \tag{D.44}$$

$$\begin{aligned}\left(M^2_{\rm even}\right)_{ij} &= \left(M^2_\nu\right)_{ij} + B^{\rm s}_{ij} + \frac{1}{\sqrt{2}} w_k A^{\rm s}_{ijk} + \frac{1}{2}v_u^2\lambda'''_{\alpha i}\lambda'''_{\alpha j} + \frac{1}{2}v_\alpha v_\beta \lambda'''_{\alpha i}\lambda'''_{\beta j} \\ &\quad + \frac{1}{4} w_m w_n \left(A_{ijl}A_{mnl} + 2A_{iml}A_{jnl}\right) + A_{il}A_{jl} + \frac{1}{2}v_\alpha v_u \lambda'''_{\alpha l} A_{ijl} \qquad \text{(D.45)} \\ &\quad + \frac{1}{2\sqrt{2}} w_k \left[A_{ijl}B_{kl} + A_{ikl}B_{jl} + A_{jkl}B_{il}\right] + C_l A_{ijl}. \qquad \text{(D.46)}\end{aligned}$$

CP-odd neutral scalars By using the field definitions from Eqs. (6.12) - (6.14), the following gauge basis can be defined $\Phi^T_{\text{even}} = (\phi_u, \phi_\alpha, \zeta_i)$ as basis for the CP-even neutral scalar particles, the squared mass-matrix becomes [49],

$$M^2_{\text{odd}} = \begin{pmatrix} (M^2_{\text{odd}})_u & (M^2_{\text{odd}})_{u\alpha} & (M^2_{\text{odd}})_{ui} \\ (M^2_{\text{odd}})_{\alpha u} & (M^2_{\text{odd}})_{\alpha\beta} & (M^2_{\text{odd}})_{\alpha i} \\ (M^2_{\text{odd}})_{iu} & (M^2_{\text{odd}})_{i\alpha} & (M^2_{\text{odd}})_{ij} \end{pmatrix}, \tag{D.47}$$

where

$$\left(M^2_{\text{odd}}\right)_u = \frac{M_Z^2}{2}\frac{v_u^2 - v_d^2}{v^2} + |\hat{\mu}_\alpha|^2 + M^2_{H_u} + \frac{1}{2}v_\alpha v_\beta \lambda'''_{\alpha l}\lambda'''_{\beta l}, \tag{D.48}$$

$$\left(M^2_{\text{odd}}\right)_{u\hat{\alpha}} = \hat{b}_\alpha, \tag{D.49}$$

$$\left(M^2_{\text{odd}}\right)_{ui} = \frac{1}{\sqrt{2}}v_\alpha\left(-\lambda'''^{\text{s}}_{\alpha i} + \frac{1}{\sqrt{2}}\lambda'''_{\alpha l}\left(B_{il} + w_j A_{ijl}\right)\right),$$

$$\left(M^2_{\text{odd}}\right)_{\alpha\beta} = \frac{M_Z^2}{2}\frac{v_\alpha^2 - v_u^2}{v^2} + \left(M^2_L\right)_{\alpha\beta} + \hat{\mu}_\alpha\hat{\mu}_{\hat{\beta}} + \frac{1}{2}v_u^2\lambda'''_{\alpha l}\lambda'''_{\beta l}, \tag{D.50}$$

$$\left(M^2_{\text{odd}}\right)_{\alpha i} = \frac{1}{\sqrt{2}}v_u\left(-\lambda'''^{\text{s}}_{\alpha i} + B_{il}\lambda'''_{\alpha l}\right) + \frac{1}{\sqrt{2}}v_\rho\left(\hat{\mu}_\alpha\lambda'''_{\rho i} + \hat{\mu}_\rho\lambda'''_{\alpha i}\right), \tag{D.51}$$

$$\begin{aligned}\left(M^2_{\text{odd}}\right)_{ij} = {} & \left(M^2_\nu\right)_{ij} - B^{\text{s}}_{ij} - \sqrt{2}w_k A^{\text{s}}_{ijk} + \frac{1}{2}v_u^2\lambda'''_{\alpha i}\lambda'''_{\alpha j} + \frac{1}{2}v_\alpha v_\beta\lambda'''_{\alpha i}\lambda'''_{\beta j} \\ & + \frac{1}{4}w_p w_q\left(2A_{ipl}A_{jql} - A_{ijl}A_{pql}\right) + B_{il}B_{jl} + \frac{1}{2}v_\alpha v_u\lambda'''_{\alpha l}A_{ijl} \\ & + \sqrt{2}w_k\left(B_{kl}A_{ijl} + B_{il}A_{jkl} + B_{jl}A_{ikl}\right) - C_l A_{ijl}.\end{aligned} \tag{D.52}$$

Neutral scalar mass matrices in ν_i-basis

In the ν_i-basis these squared mass-matrices for the neutral scalars becomes

$$M^2_{\text{even}} = \begin{pmatrix} M_Z^2\cos^2\beta + b_0\cot\beta & -M_Z^2\cos\beta\sin\beta - b_0 & \hat{b}_j & (M^2_{\text{even}})_{1,5+j} \\ -M_Z^2\cos\beta\sin\beta - b_0 & M_Z^2\cos^2\beta + b_0\tan\beta & \hat{b}_j\tan\beta & (M^2_{\text{even}})_{2,5+j} \\ \hat{b}_i & \hat{b}_i\tan\beta & (M^2_{\text{even}})_{2+i,2+j} & (M^2_{\text{even}})_{2+i,5+j} \\ (M^2_{\text{even}})_{5+j,1} & (M^2_{\text{even}})_{2,5+j} & (M^2_{\text{even}})_{5+i,2+j} & (M^2_{\text{even}})_{5+i,5+j} \end{pmatrix}, \tag{D.53}$$

$$\begin{aligned}
\left(M^2_{\text{even}}\right)_{1,5+i} &= \left(M^2_{\text{even}}\right)_{5+i,1} \\
&= \frac{1}{\sqrt{2}} v \cos\beta \left(\lambda'''^{\text{s}}_{0i} + \lambda'''_{0l}\hat{B}_{il}\right) + \sqrt{2} v \sin\beta \hat{\mu}_0 \lambda'''_{0i}, && \text{(D.54)} \\
\left(M^2_{\text{even}}\right)_{2,5+i} &= \left(M^2_{\text{even}}\right)_{5+i,2} \\
&= \frac{1}{\sqrt{2}} v \sin\beta \left(\lambda'''^{\text{s}}_{0i} + \lambda'''_{0l}\hat{B}_{il}\right) + \sqrt{2} v \cos\beta \hat{\mu}_0 \lambda'''_{0i}, && \text{(D.55)} \\
\left(M^2_{\text{even}}\right)_{2+i,2+j} &= \left(M^2_L\right)_{ij} + \frac{M_Z^2}{2}\cos 2\beta\, \delta_{ij} + \frac{1}{2} v_u^2 \lambda'''_{il}\lambda'''_{jl}, && \text{(D.56)} \\
\left(M^2_{\text{even}}\right)_{2+i,5+j} &= \frac{v_u}{\sqrt{2}}\left[\lambda'''^{\text{s}}_{ij} + \lambda'''_{il}\left(B_{jl} + \frac{1}{\sqrt{2}} w_k A_{jkl}\right)\right], && \text{(D.57)} \\
\left(M^2_{\text{even}}\right)_{5+i,5+j} &= \left(M^2_\nu\right)_{ij} + B^{\text{s}}_{ij} + \frac{1}{\sqrt{2}} w_k \Lambda^{\text{s}}_{ijk} + \frac{1}{2} v_u^2 \lambda'''_{li}\lambda'''_{lj} \\
&\quad + \frac{1}{4} w_p w_q \left(2 A_{ipl} A_{jql} + A_{ijl} A_{pql}\right) + B_{il} B_{jl} \\
&\quad + \frac{1}{2\sqrt{2}} w_k \left(B_{kl}\Lambda_{ijl} + B_{il}\Lambda_{jkl} + B_{jl}\Lambda_{ikl}\right) + C_l \Lambda_{ijl}. && \text{(D.58)}
\end{aligned}$$

$$M^2_{\text{odd}} = \begin{pmatrix}
b_0 \cot\beta & b_0 & \hat{b}_j & \left(M^2_{\text{odd}}\right)_{1,5+j} \\
b_0 & b_0 \tan\beta & \hat{b}_j \tan\beta & \left(M^2_{\text{odd}}\right)_{2,5+j} \\
\hat{b}_i & \hat{b}_i \tan\beta & \left(M^2_{\text{odd}}\right)_{2+i,2+j} & \left(M^2_{\text{odd}}\right)_{2+i,5+j} \\
\left(M^2_{\text{odd}}\right)_{5+j,1} & \left(M^2_{\text{odd}}\right)_{5+j,2} & \left(M^2_{\text{odd}}\right)_{5+i,2+j} & \left(M^2_{\text{odd}}\right)_{5+i,5+j}
\end{pmatrix}, \qquad \text{(D.59)}$$

$$\begin{aligned}
\left(M^2_{\text{odd}}\right)_{1,5+i} &= \left(M^2_{\text{odd}}\right)_{5+i,1} = \frac{1}{\sqrt{2}} v \cos\beta \left(-\lambda'''^{\text{s}}_{0i} + \lambda'''_{0l}\hat{B}_{il}\right), && \text{(D.60)} \\
\left(M^2_{\text{odd}}\right)_{2,5+i} &= \left(M^2_{\text{odd}}\right)_{5+i,2} = \frac{1}{\sqrt{2}} v \sin\beta \left(-\lambda'''^{\text{s}}_{0i} + \lambda'''_{0l}\hat{B}_{il}\right), && \text{(D.61)} \\
\left(M^2_{\text{odd}}\right)_{2+i,2+j} &= \left(M^2_L\right)_{ij} + \frac{M_Z^2}{2}\cos 2\beta\, \delta_{ij} + \frac{1}{2} v_u^2 \lambda'''_{il}\lambda'''_{jl}, && \text{(D.62)} \\
\left(M^2_{\text{odd}}\right)_{2+i,5+j} &= \frac{v_u}{\sqrt{2}}\left(-\lambda'''^{\text{s}}_{ij} + \lambda'''_{il} B_{jl} + \frac{1}{\sqrt{2}} v_d \lambda'''_{ji}\right), && \text{(D.63)} \\
\left(M^2_{\text{odd}}\right)_{5+i,5+j} &= \left(M^2_\nu\right)_{ij} - B^{\text{s}}_{ij} - \sqrt{2} w_k A^{\text{s}}_{ijk} + \frac{1}{2} v_u^2 \lambda'''_{li}\lambda'''_{lj} \\
&\quad + \frac{1}{4} w_p w_q \left(2\Lambda_{ipl}\Lambda_{jql} - \Lambda_{ijl}\Lambda_{pql}\right) + B_{il} B_{jl} \\
&\quad + \frac{1}{2\sqrt{2}} w_k \left(B_{kl} A_{ijl} + B_{il} A_{jkl} + B_{jl} A_{ikl}\right) - C_l A_{ijl}. && \text{(D.64)}
\end{aligned}$$

The elements $(M^2_{\rm even})_{5+i,5+j}$ and $(M^2_{\rm odd})_{5+i,5+j}$ are assumed to be very heavy, as discussed in Sec. 6.3. It is also argued, in Sec. 6.5, that all elements of A_{ijk} and $A^{\rm s}_{ijk}$ can be assumed to vanish. This further simplifies the mass matrices $M^2_{\rm even}$ and $M^2_{\rm odd}$.

D.5 Mass-matrices in MSSM-M

The mass-matrices for MSSM-M can be found from the general expressions shown in the last section. The important difference between MSSM-DM and MSSM-M is that in MSSM-M there are no right-handed neutrino fields. Thus all the couplings $\lambda'''_{\alpha i}$, $\lambda'''_{\alpha i}$ vanish along with the terms A_{ijk}, B_{ij}, C_i, $A^{\rm s}$ and $B^{\rm s}$. Also there are only 7 neutral fermions and 10 neutral scalars in MSSM-M. The other mass matrices are not altered by these changes.

Appendix E

Feynman-rules

This appendix shows the Feynman-rules relevant for the calculations made in this thesis. Reference [47] shows the complete set of Feynman-rules for MSSM. This appendix generalises these Feynman-rules to MSSM-M and MSSM-D. The notation of Ref. [47] will be followed as close as possible.

E.1 Feynman-rules in MSSM-D

The relevant Feynman-rules for MSSM-D are almost identical to the corresponding ones for MSSM [47]. The difference is that for MSSM-D the neutrinos have mass-terms, and that the squared mass matrix for the sneutrinos is a 6×6 symmetric matrix. This alters the mixing matrices a bit compared to MSSM. For easy reference all relevant Feynman rules relevant for this thesis are now presented.

The mixing matrices appearing in these Feynman rules, i.e., Z_N, Z_L, Z_ν, Z^+, Z^-, Z_{II} and Z_R, are all defined in Appendix D.2. Following Ref. [47] the Yukawa matrix Y_e is assumed diagonal with diagonal elements l^i. The eigenvalues of the neutrino Yukawa-matrix, Y_ν, is denoted by n^i, and the neutrino mixing matrix (the MNS matrix) is denoted by C. This matrix is in analogy to the CKM-matrix in the quark sector.

Lepton - slepton - neutralino
This case is equal to the corresponding interaction in MSSM [47], i.e.,

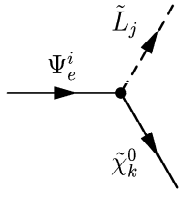

$ie(A_{ijk}\,P_L + B_{ijk}\,P_R)$,

$$A_{ijk} = \frac{1}{\sqrt{2}\,\sin\theta\,\cos\theta} Z_L^{ij}(Z_N^{1j}\sin\theta + Z_N^{2j}\cos\theta) + \frac{l^i}{c} Z_L^{(i+3)j} Z_N^{3j}, \tag{E.1}$$

$$B_{ijk} = -\frac{\sqrt{2}}{\cos\theta} Z_L^{(i+3)j} Z_N^{1j\star} + \frac{l^i}{e} Z_L^{ij} Z_N^{3j\star}, \tag{E.2}$$

$$i = 1,2,3;\ j = 1,2,\ldots,6;\ k = 1,2,\ldots,4 \tag{E.3}$$

Lepton - sneutrino - chargino

This case is analogous to the quark-squark-chargino case in MSSM [47], i.e.,

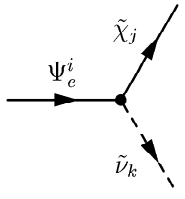

$$ie(A_{ijk}\,P_L + B_{ijk}\,P_R),$$

$$A_{ijk} = -\frac{1}{\sin\theta} Z_\nu^{pi\star}(Z_{1j}^{+} + \frac{n^p}{c} Z_\nu^{(p+3)i\star} Z_{2j}^{+}) C^{ip}, \tag{E.4}$$

$$B_{ijk} = -\frac{l^i}{e} Z_\nu^{pi\star} Z_{2j}^{-\star} C^{ip}, \qquad i = 1,2,3;\ j = 1,2;\ k = 1,2,\ldots,6 \tag{E.5}$$

Lepton - neutrino - charged gauge boson

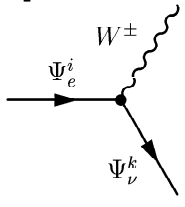

$$-\frac{ie}{\sqrt{2}\,\sin\theta} C^{ik}\gamma^\mu P_L. \qquad i,k = 1,2,3. \tag{E.6}$$

Lepton - lepton - neutral gauge boson

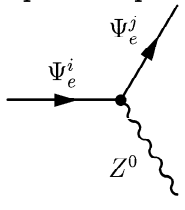

$$ie(A_{ij}\,P_L + B_{ij}\,P_R),$$

$$A_{ij} = \frac{1}{\sin\theta\,\cos\theta}\left(\frac{1}{2} - \sin^2\theta\right)\delta_{ij}, \tag{E.7}$$

$$B_{ij} = -\tan\theta\,\delta_{ij}, \qquad i,j = 1,2,3. \tag{E.8}$$

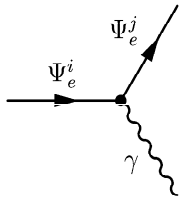

$$ie\gamma^\mu\,\delta_{ij} \qquad i,j=1,2,3. \tag{E.9}$$

Lepton - neutrino - charged Higgs

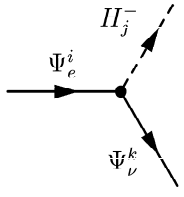

$ie(A_{ij}\,P_L + B_{ij}\,P_R),$

$$A_{ijk} = \frac{m_k}{M_W}\frac{1}{\sqrt{2}\,\sin\beta\,\sin\theta}Z_H^{2j}C^{ik}, \tag{E.10}$$

$$B_{ijk} - \frac{m_\nu^k}{M_W}\frac{1}{\sqrt{2}\,\cos\beta\,\sin\theta}Z_H^{1j}C^{ik} \qquad i,k-1,2,3;\ j-1,2. \tag{E.11}$$

Lepton - lepton - neutral Higgs

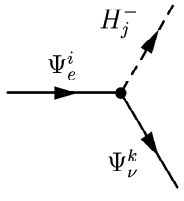

$$ie\frac{m^i}{M_W}\frac{1}{2\cos\beta\,\sin\theta}Z_R^{1k}\delta_{ij}, \tag{E.12}$$

$$ie\frac{m^i}{M_W}\frac{1}{2\cos\beta\,\sin\theta}Z_H^{1k}\gamma_5\delta_{ij} \qquad i,j=1,2,3;\ k=1,2. \tag{E.13}$$

Chargino - chargino - neutral gauge boson

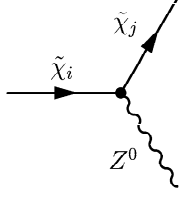

$$-ie\gamma^\mu\,\delta_{ij} \qquad i,j=1,2. \tag{E.14}$$

Slepton - slepton - neutral gauge boson

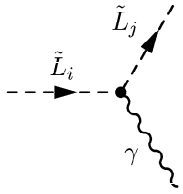

$$ie\delta^{ij}(p+k)^{\mu} \qquad i,j=1,2,\ldots,6. \tag{E.15}$$

Charged gauge boson - charged gauge boson - neutral gauge boson

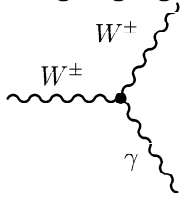

$$ie\left[g^{\nu\lambda}(k_1-k_2)^{\mu}+g^{\lambda\mu}(k_2-k_3)^{\nu}+g^{\mu\nu}(k_3-k_1)^{\lambda}\right]. \tag{E.16}$$

Charged Higgs - charged Higgs - photon

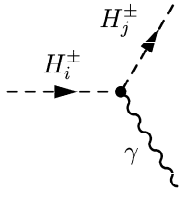

$$ie\delta^{ij}(p+k)^{\mu} \qquad i,j=1,2. \tag{E.17}$$

Charged Higgs - charged Higgs - photon

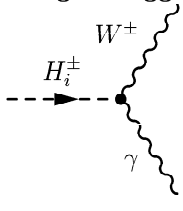

$$ieM_W g^{\mu\nu}. \tag{E.18}$$

E.2 Feynman rules for MSSM-M and MSSM-DM

In this appendix the Feynman rules for MSSM-M and MSSM-DM will be presented. These Feynman rules differs from the ones presented in Ref. [17] in two ways. First, there are R-parity violating couplings explicitly appearing in these Feynman rules. Second, the $U(4)$-symmetry described in Sec. 5.3 makes the superfields H_d and L_i to mix. The Feynman rules are therefore written in the $U(4)$ manifest notation presented in Sec. 5.3. The Feynman rules are first presented for MSSM-DM, and then the Feynman rules of MSSM-M are obtained as a subset.

E.2.1 Weyl-spinors and mass-eigenstates

In order to formulate the Feynman rules properly the gauge-bases, which are used, will be reviewed.

Neutral fermions
In MSSM-DM there are 10 neutral Majorana fermions. The following gauge-basis is used,

$$\left(\psi_i^0\right)^T = \left(\lambda_B, \lambda_A^3, \psi_{H_u}^2, \psi_{L_\alpha}^1, \psi_{\nu_j}\right). \tag{E.19}$$

These bases extend the gauge bases used in MSSM. The major difference is the inclusion of right-handed neutrino fields, ψ_{ν_j}, and the use of the $U(4)$-spinor $\psi_{L_\alpha}^1$.

The corresponding mass matrix is shown in Eq. (6.29). It is a 10×10 symmetric matrix and is therefore diagonalised by only one matrix, i.e.,

$$Z_N^T\, M_N\, Z_N = \mathrm{diag}\left(m_{\tilde{\chi}_i^0}\right), \qquad i = 1, 2, \ldots, 10. \tag{E.20}$$

In terms of the mixing matrix Z_N the gauge-eigenstates and mass-eigenstates are related as follows,

$$\lambda_B = iZ_N^{1i}\psi_i^0, \qquad \lambda_A^3 = iZ_N^{2i}\psi_i^0, \tag{E.21}$$

$$\psi_{H_u}^2 = Z_N^{3i}\psi_i^0, \qquad \psi_{L_\alpha}^1 = Z_N^{(4+\alpha)i}\psi_i^0, \tag{E.22}$$

$$\psi_{\nu_j} = Z_N^{(7+j)i}\psi_i^0. \tag{E.23}$$

These Weyl spinors makes up 10 Majorana spinors, that is, the 10 neutral fermions of MSSM-DM,

$$\tilde{\chi}_i^0 = \begin{pmatrix} \psi_i^0 \\ \bar{\psi}_i^0 \end{pmatrix}, \qquad i = 1, 2, \ldots, 10. \tag{E.24}$$

Charged fermions
Also the charged fermions associated with the superfields $\hat{H}_d$ and L_α mix together.

Thus in MSSM-DM (and MSSM-M) there are 5 charged Dirac spinors. The following gauge-basis will be used, i.e.,

$$\psi_i = \left(\lambda_A^1, \lambda_A^2, \psi_{H_u}^1, \psi_{L_\alpha}^{2\dagger}, \psi_{R,i}\right). \tag{E.25}$$

The charged fermions of MSSM-DM are thus made up of the charginos and charged leptons of MSSM. As for the charginos in MSSM the charged fermions of MSSM-DM will have positive electric charge. The mass matrix of the charged fermions is a generalisation of the chargino mass matrix of MSSM, i.e.,

$$M_C = \begin{pmatrix} 0 & X^T \\ X & 0 \end{pmatrix}, \tag{E.26}$$

where X is shown in Eq. (6.38). This mass matrix is not diagonal and has to be diagonalised by use of two unitary matrices, i.e.,

$$\left(Z^-\right)^T X Z^+ = \text{diag}\left(\tilde{\chi}_i^+\right), \qquad i = 1, 2, \ldots, 5. \tag{E.27}$$

These Weyl-spinors make up the following 5 charged Dirac fermions,

$$\tilde{\chi}_i = \begin{pmatrix} \tilde{\chi}_i^+ \\ \bar{\tilde{\chi}}_i^- \end{pmatrix}, \quad i = 1, 2, \ldots, 5. \tag{E.28}$$

By using the mixing matrices Z^- and Z^+ the gauge-eigenstates and the mass-eigenstates are related as follows,

$$i\lambda_A^\pm = i\frac{\lambda_A^1 \mp i\lambda_A^2}{\sqrt{2}} = -Z_{1i}^\pm \tilde{\chi}_i^\pm \tag{E.29}$$

$$\psi_{H_u}^1 = Z_{2i}^+ \tilde{\chi}_i^+, \tag{E.30}$$

$$\psi_{L_\alpha}^2 = Z_{2+\alpha,i}^- \tilde{\chi}_i^-, \tag{E.31}$$

$$\psi_{R,j} = Z_{2+j,i}^+ \tilde{\chi}_i^+. \tag{E.32}$$

Charged scalars

The charged scalars of the superfields $\hat{H}_d$ and L_α will mix and define 8 charged scalars. The following gauge-basis will be used,

$$\Phi_{\text{CS}} = \left(H_u^1, L_\alpha^2, c_{Ri}\right). \tag{E.33}$$

The squared mass matrix, shown in Eq. (6.44), is diagonal and is therefore diagonalised by only one matrix, i.e.,

$$Z_L^\dagger M_{\text{CS}} Z_L = \text{diag}\left(\tilde{L}_i\right), i = 1, 2, \ldots, 8. \tag{E.34}$$

By using this mixing matrix the gauge-eigenstates and the mass eigenstates are related as follows,

$$H_u^{1} = Z_L^{1\prime} L_i^{+}, \tag{E.35}$$
$$L_\alpha^{2} = Z_L^{(2+\alpha)i*} L_i^{-}, \tag{E.36}$$
$$e_{Rj} = Z_L^{5+j,i} L_i^{+}. \tag{E.37}$$

Neutral scalars

In MSSM the neutral Higgs scalars are divided into two groups according their CP eigenvalues. On the other hand, the sneutrinos are complex neutral scalars with no defined CP eigenvalue. In MSSM-DM all these neutral scalars mix together. By using the CP eigenvalues there are now two groups of neutral scalars, with the following gauge-basis.

$$\phi_{\text{even}} = (\chi_u, \chi_\alpha, \eta_i)\,, \tag{E.38}$$
$$\phi_{\text{odd}} = (\phi_u, \phi_\alpha, \rho_i)\,. \tag{E.39}$$

Their squared mass matrices are shown in Eqs. (D.39) and (D.47), respectively.

These squared mass matrices are each diagonalised by one matrix, i.e.,

$$Z_R^T\, M_E^2\, Z_R = \text{diag}\,(\Phi_i)\,, \tag{E.40}$$
$$Z_H^T\, M_O^2\, Z_H = \text{diag}\,(\Phi_i)\,, i = 1, 2, \ldots, 8. \tag{E.41}$$

The gauge eigenstates can now be written in terms of the mass eigenstates. However, the general formulas for the amplitudes, developed in Appendix B.4, used Feynman rules on a form not taking the CP eigenvalues into account. Therefore, in order to easily be able to use these formulas a new scalar field is defined, i.e.,

$$\Phi_{NS} = \begin{pmatrix} \phi_{\text{even}} \\ \phi_{\text{odd}} \end{pmatrix}.$$

The squared mass matrix for these eigenstates are therefore given by the 16×16-dimensional matrix,

$$M_{\text{NS}}^2 = \begin{pmatrix} M_E^2 & 0 \\ 0 & M_O^2 \end{pmatrix}. \tag{E.42}$$

This matrix is symmetric and is therefore diagonalised by the use of only one matrix Z_{NS},

$$Z_{NS} = \begin{pmatrix} Z_R & 0 \\ 0 & Z_H \end{pmatrix} \tag{E.43}$$

By using this mixing matrix the gauge eigenstates and the 16 neutral mass eigenstates with well defined CP eigenvalues are related by,

$$\chi_u = Z_{NS}^{1i}\Phi_{NS}^i, \tag{E.44}$$
$$\phi_u = Z_{NS}^{9i}\Phi_{NS}^i, \tag{E.45}$$
$$\chi_\alpha = Z_{NS}^{2+\alpha,i}\Phi_{NS}^i, \tag{E.46}$$
$$\phi_\alpha = Z_{NS}^{10+\alpha,i}\Phi_{NS}^i, \tag{E.47}$$
$$\eta_j = Z_{NS}^{5+j,i}\Phi_{NS}^i, \tag{E.48}$$
$$\rho_j = Z_{NS}^{13+j,i}\Phi_{NS}^i, \tag{E.49}$$

where $i = 1, 2, \ldots, 16$.

Of course one can also relate the gauge eigenstates with no well defined CP eigenvalues to the neutral scalars,

$$H_u^2 = \frac{1}{\sqrt{2}}\left(\chi_u + i\phi_u\right) = \frac{1}{\sqrt{2}}\left(Z_{NS}^{1i} + iZ_{NS}^{9i}\right)\Phi_{NS,i}, \tag{E.50}$$
$$\tilde{L}_\alpha^1 = \frac{1}{\sqrt{2}}\left(\chi_\alpha + i\phi_\alpha\right) = \frac{1}{\sqrt{2}}\left(Z_{NS}^{2+\alpha,i} + iZ_{NS}^{10+\alpha,i}\right)\Phi_{NS,i}, \tag{E.51}$$
$$\tilde{n}_j^* = \frac{1}{\sqrt{2}}\left(\eta_j + i\rho_j\right) = \frac{1}{\sqrt{2}}\left(Z_{NS}^{5+j,i} + iZ_{NS}^{13+j,i}\right)\Phi_{NS,i}^*, \tag{E.52}$$

where $i = 1, 2, \ldots, 16$.

Quarks and squarks

The quark and squarks do enter the Feynman rules due to the trilinear R-parity violating coupling λ'_{ijk}. Their mass matrices and consequently mixing matrices are not altered in MSSM-DM compared to their appearance in MSSM. We still shows these mixing matrices for easy referencing and completeness.

The quark masses are obtained from the superpotential, i.e.,

$$Y_u Q_i H_u u_j + \lambda'_{\alpha jk} L_\alpha Q_j d_k + \text{h.c.}$$

This term of the superpotential shows that the masses for the up-quarks are not affected by the R-parity violating terms, as long as λ''_{ijk} is assumed to vanish. The masses for the down-quarks will, however, depend on the trilinear coupling λ'_{ijk}. However, in the v_i-basis the down-quark mass matrix does only depend on $\lambda_{0ij} = Y_d$, analogous to the charged fermions, see Eq. (6.38).

The mixing among the up- and down-quarks is determined by the CKM-matrix [23],

$$C_{\text{CKM}} = \begin{pmatrix} c_{12}c_{13} & s_{12}c_{13} & s_{13} \\ -s_{12}c_{23} - c_{12}s_{23}s_{13}e^{i\delta_{13}} & c_{12}c_{23} - s_{12}s_{23}s_{13}e^{i\delta_{13}} & s_{23}c_{13} \\ s_{12}s_{23} - c_{12}c_{23}s_{13}e^{i\delta_{13}} & -c_{12}s_{23} - s_{12}c_{23}s_{13}e^{i\delta_{13}} & c_{23}c_{13} \end{pmatrix}. \tag{E.53}$$

The corresponding Dirac spinors q_u and q_d then become,

$$q_{u,i} = \begin{pmatrix} \psi^1_{Q_i} \\ \psi_{u,i} \end{pmatrix}, \tag{E.54}$$

$$q_{d,i} = \begin{pmatrix} \psi^2_{Q_i} \\ \psi_{d,i} \end{pmatrix}. \tag{E.55}$$

The 6 up-squarks, $\tilde{U}_i$, and down-squarks, $\tilde{D}_i$, are defined [47] as follows,

$$\tilde{Q}^1_j = Z_U^{ji} U_i^+, \qquad \tilde{u}_j = Z_U^{3+j,i} U_i^-, \tag{E.56}$$

$$\tilde{Q}^2_j = Z_D^{ji} D_i^-, \qquad \tilde{d}_j = Z_D^{3+j,i} D_i^+. \tag{E.57}$$

The mass eigenstates and mixing matrices in this section were obtained for MSSM-DM. However, the difference to MSSM-M is that in MSSM-M there are no right-handed singlet superfield n_i. This means that all results from this section are also valid for MSSM-M only with minor corrections.

First, the neutral fermion mass matrix is a 7×7 symmetric matrix. That is, the index of Eq. (E.20) only runs to 7, and only equations Eqs. (E.21) and (E.22) are used.

Also the neutral scalars in MSSM-M will not depend on the scalar fields η_i and ρ_i, see Eq. (E.38) and (E.39). This means that the neutral scalars ϕ_{even} and ϕ_{odd} each consist of 5 elements. Consequently, the neutral scalar field which is to be used, i.e., Φ_{NS} will be a 10-dimensional vector. This gives

$$\chi_u = Z_{NS}^{1i} \Phi^i_{NS}, \tag{E.58}$$

$$\phi_u = Z_{NS}^{6i} \Phi^i_{NS}, \tag{E.59}$$

$$\chi_\alpha = Z_{NS}^{2+\alpha,i} \Phi^i_{NS}, \tag{E.60}$$

$$\phi_\alpha = Z_{NS}^{7+\alpha,i} \Phi^i_{NS}. \tag{E.61}$$

and

$$H_u^2 = \frac{1}{\sqrt{2}} (\chi_u + i\phi_u) = \frac{1}{\sqrt{2}} \left(Z_{NS}^{1i} + i Z_{NS}^{6i} \right) \Phi_{NS,i}, \tag{E.62}$$

$$L_\alpha^1 = \frac{1}{\sqrt{2}} (\chi_\alpha + i\phi_\alpha) = \frac{1}{\sqrt{2}} \left(Z_{NS}^{2+\alpha,i} + i Z_{NS}^{7+\alpha,i} \right) \Phi_{NS,i}, \tag{E.63}$$

where $i = 1, 2, \ldots, 10$.

E.3 Feynman rules

By using the mass eigenstates of the last section it is now straight forward to generalise the Feynman rules of Ref. [47].

Also note that

$$\frac{1}{e} = \frac{v}{2M_W \sin\theta_W}. \tag{E.64}$$

Charged fermion - charged fermion - neutral scalar

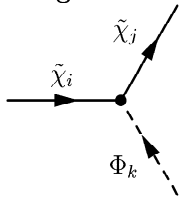

$ie(A_{ijk}\,P_L + B_{ijk}\,P_R)$, $i,j = 1,2,\ldots,5$, $k = 1,2,\ldots,16$,

$$\begin{aligned} A_{ijk} = &-\frac{1}{\sqrt{2}\sin\theta} Z^{-*}_{2+\alpha,i} Z^{+*}_{1j} \left(Z^{2+\alpha,k}_{NS} + i Z^{10+\alpha,k}_{NS} \right) \\ &+ \frac{1}{2\sqrt{2}} \frac{\lambda_{\alpha\beta l}}{e} Z^{+}_{2+l,i} \Big[Z^{-}_{2+\alpha,j} \left(Z^{2+\beta,k}_{NS} + i Z^{10+\beta,k}_{NS} \right) \\ &\qquad - Z^{-}_{2+\beta,j} \left(Z^{2+\alpha,k}_{NS} + i Z^{10+\alpha,k}_{NS} \right) \Big], \end{aligned} \tag{E.65}$$

$$\begin{aligned} B_{ijk} = &-\frac{1}{\sqrt{2}\sin\theta} Z^{-*}_{1i} Z^{+*}_{2j} \left(Z^{1k}_{NS} - i Z^{9k}_{NS} \right) \\ &+ \frac{1}{\sqrt{2}} \frac{\lambda'''_{\alpha p}}{e} Z^{-*}_{2+\alpha,i} Z^{+}_{2j} \left(Z^{5+p,k}_{NS} - i Z^{13+p,k}_{NS} \right). \end{aligned} \tag{E.66}$$

Charged fermion - charged fermion - charged scalar

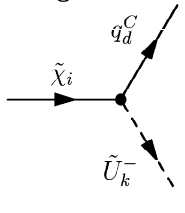

$ie(A_{ijk}\,P_L + B_{ijk}\,P_R)$, $i = 1,2,\ldots,5$, $j,k = 1,2,3$,

$$A_{ijk} = -\frac{1}{\sin\theta} Z^{Ik}_{U} Z^{+*}_{1i} C^{Ij} + \frac{1}{e} \left(Y_u\right)_{jl} Z^{+}_{2i} Z^{3+l,k}_{U}, \tag{E.67}$$

$$B_{ijk} = \frac{1}{e} \lambda'_{\alpha lj} Z^{-*}_{2+\alpha,i} Z^{lk}_{U}. \tag{E.68}$$

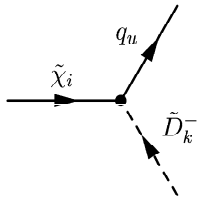

$$ie(A_{ijk}\,P_L + B_{ijk}\,P_R),\ i = 1,2,\ldots,5,\ j,k = 1,2,3,$$

$$A_{ijk} = \frac{1}{e}\,(Y_u)_{lj}\,Z_{2i}^{+}Z_D^{lk}P_L - \frac{1}{\sin\theta}Z_D^{lk}Z_{1i}^{-*}C^{lj}, \tag{E.69}$$

$$B_{ijk} = \frac{1}{e}\lambda'_{\alpha jl}Z_{2+\alpha,i}^{-}Z_D^{3+l,k} \tag{E.70}$$

Charged fermion - neutral fermion - charged scalar

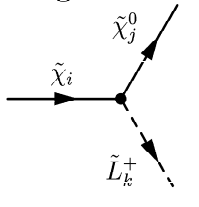

$$ie(A_{ijk}\,P_L + B_{ijk}\,P_R),\ i = 1,2,\ldots,5,\ j = 1,2\ldots,10,\ k = 1,2,\ldots,8,$$

$$\begin{aligned}
A_{ijk} = &-\frac{1}{\sqrt{2}\sin\theta\cos\theta}Z_{2i}^{+}Z_L^{1k*}\left(Z_N^{1j}\sin\theta + Z_N^{2j}\cos\theta\right)\\
&+\frac{1}{\sin\theta}Z_{1i}^{+}Z_N^{3j}Z_L^{1k*} - \frac{1}{\sqrt{2}\cos\theta}Z_N^{1j}Z_{2+l,i}^{+}Z_L^{5+l,k*}\\
&+\frac{1}{2}\frac{\lambda_{\alpha\beta l}}{e}\Big[Z_{2+l,i}^{+}\left(Z_L^{2+\alpha,k*}Z_N^{4+\beta,j} - Z_L^{2+\beta,k*}Z_N^{4+\alpha,j}\right)\\
&\qquad + Z_L^{5+l,k*}\left(Z_{2+\alpha,i}^{-*}Z_N^{4+\beta,j*} - Z_{2+\beta,i}^{-*}Z_N^{4+\alpha,j*}\right)\Big]\\
&+\frac{\lambda'''_{\alpha l}}{e}\left(Z_L^{2+\alpha,k*}Z_{2i}^{+}Z_N^{7+l,j} + Z_{2+\alpha,i}^{-*}Z_L^{1k*}Z_N^{7+l,j*}\right),
\end{aligned} \tag{E.71}$$

$$\begin{aligned}
B_{ijk} = &\frac{1}{\sqrt{2}\sin\theta\cos\theta}Z_{2+\alpha,i}^{-*}Z_L^{2+\alpha,k}\left(Z_N^{1j}\sin\theta - Z_N^{2j}\cos\theta\right)\\
&-\frac{1}{\sin\theta}Z_{1i}^{-*}Z_N^{4+\alpha,j*}Z_L^{2+\alpha,k}.
\end{aligned} \tag{E.72}$$

Charged fermion - charged fermion - neutral gauge boson

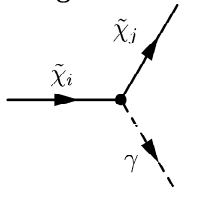

$$-ie\gamma^{\mu}\delta_{ij}, \quad i,j = 1,2,\ldots,5. \tag{E.73}$$

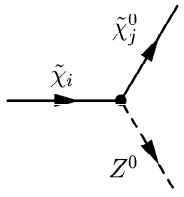

$$ie(A_{ijk}\,P_L + B_{ijk}\,P_R),\ i = 1,2,\ldots,5,\ j = 1,2,\ldots,10,$$

$$A_{ijk} = -\frac{1}{2\sin\theta\cos\theta}\gamma^\mu\left(Z_{2j}^{+*}Z_{2i}^{+} + \delta_{ij}\cos 2\theta\right), \tag{E.74}$$

$$B_{ijk} = -\frac{1}{2\sin\theta\cos\theta}\gamma^\mu\left(Z_{2+\alpha,j}^{-}Z_{2+\alpha,i}^{-*} + \delta_{ij}\cos 2\theta\right). \tag{E.75}$$

Charged fermion - neutral fermion - charged gauge boson

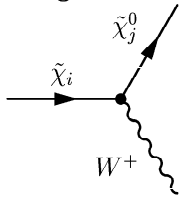

$$ie(A_{ijk}\,P_L + B_{ijk}\,P_R),\ i = 1,2,\ldots,5,\ j = 1,2,\ldots,10,$$

$$A_{ijk} = Z_N^{1j}Z_{1,i}^{-*} + \frac{1}{\sqrt{2}}Z_N^{4+\alpha,j}Z_{2+\alpha,i}^{-*},$$

$$B_{ijk} = \frac{1}{\sin\theta}\gamma^\mu\left(Z_N^{1j*}Z_{1,i}^{+} - \frac{1}{\sqrt{2}}Z_N^{3j*}Z_{2i}^{+}\right). \tag{E.76}$$

Neutral gauge boson - charged gauge boson - charged gauge boson

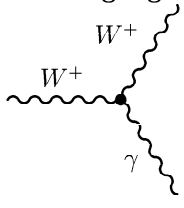

$$ie\left[g^{\nu\lambda}(k_1-k_2)^\mu + g^{\lambda\mu}(k_2-k_3)^\nu + g^{\mu\nu}(k_3-k_1)^\lambda\right]. \tag{E.77}$$

Neutral gauge boson - charged gauge boson - charged scalar

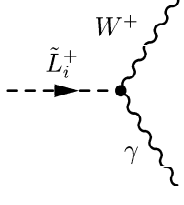

$$ie\left(\sin\beta Z_L^{1i} - \frac{v_\alpha}{v}Z_L^{2+\alpha,i}\right)M_W, \qquad i = 1,2,\ldots,8. \tag{E.78}$$

E.4 Feynman rules for MSSM-M

The Feynman rules for MSSM-M are obtained as a subset of the Feynman rules of MSSM-DM. To see this first one put $\lambda''_{\alpha j}$ to zero. Next, use the transformations of the neutral fermions and neutral scalars as explained at the end of Appendix E.2.1. This reduces the number of neutral fermions from 10 to 7, and the neutral scalars from 16 to 10.

URN:NBN:no-7281

Appendix F

Renormalisation group equations

F.1 MSSM-D

The two-loop renormalization group equations (RGE's) for a general MSSM like model were presented in Ref. [34]. Also the one-loop RGE's for the lepton sector involving right-handed neutrino superfields were presented in Ref. [69]. For completeness the two-loop RGE's for the gauge couplings and gaugino masses are presented, along with the one-loop RGE's for the superpotential parameters and soft-breaking terms. The notation from Ref. [34] is used throughout.

Gauge couplings and gaugino masses
The two-loop RGE's for the gauge-couplings and for the gaugino masses are as in MSSM, see Ref. [34].

$$\frac{d}{dt}g_a = \frac{g_a^3}{16\pi^2}\,B_a^{(1)} + \frac{g_a^3}{(16\pi^2)^2}\left[\sum_{b=1}^{3} B_{ab}^{(2)} g_b^2 - \sum_{x=u,d,e} C_a^x \mathrm{Tr}(Y_x^\dagger Y_x)\right], \tag{F.1}$$

$$\frac{d}{dt}M_a - \frac{2g_a^2}{16\pi^2}\,B_a^{(1)} M_a + \frac{2g_a^2}{(16\pi^2)^2}\left[\sum_{b=1}^{3} B_{ab}^{(2)} g_b^2 (M_a + M_b)\right.$$

$$\left. + \sum_{x=u,d,e} C_a^x \left(\mathrm{Tr}[Y_x^\dagger h_x] - M_a \mathrm{Tr}[Y_x^\dagger Y_x]\right)\right]. \tag{F.2}$$

Where $B_a^{(1)} = (33/5, 1, -3)$ for $U(1)_Y$ (in a GUT normalisation, see e.g., Ref. [53]), $SU(2)$ and $SU(3)$ respectively, and

$$B_{ab}^{(2)} = \begin{pmatrix} 199/25 & 27/5 & 88/5 \\ 9/5 & 25 & 24 \\ 11/5 & 9 & 14 \end{pmatrix} \quad \text{and} \quad C_a^{u,d,e} = \begin{pmatrix} 26/5 & 14/5 & 18/5 \\ 6 & 6 & 2 \\ 4 & 4 & 0 \end{pmatrix}. \tag{F.3}$$

Superpotential parameters
The one-loop RGE's for the superpotential parameters can be written as

$$\frac{d}{dt}\mu = \frac{1}{16\pi^2}\beta_\mu, \tag{F.4}$$

$$\frac{d}{dt}\boldsymbol{Y}_{u,d,c,n} = \frac{1}{16\pi^2}\beta_{\boldsymbol{Y}_{u,d,e,n}}, \tag{F.5}$$

where

$$\beta_\mu = \mu\left\{\mathrm{Tr}(3\boldsymbol{Y}_u\boldsymbol{Y}_u^\dagger + 3\boldsymbol{Y}_d\boldsymbol{Y}_d^\dagger + \boldsymbol{Y}_e\boldsymbol{Y}_e^\dagger)\right\}, \tag{F.6}$$

$$\beta_{\boldsymbol{Y}_u} = \boldsymbol{Y}_u\left\{\mathrm{Tr}[3\boldsymbol{Y}_u\boldsymbol{Y}_u^\dagger + \boldsymbol{Y}_\nu\boldsymbol{Y}_\nu^\dagger] + 3\boldsymbol{Y}_u^\dagger\boldsymbol{Y}_u + \boldsymbol{Y}_d^\dagger\boldsymbol{Y}_d - \frac{13}{15}g_1^2 - 3g_2^2 - \frac{16}{3}g_3^2\right\}, \tag{F.7}$$

$$\beta_{\boldsymbol{Y}_d} = \boldsymbol{Y}_d\left\{\mathrm{Tr}[3\boldsymbol{Y}_d\boldsymbol{Y}_d^\dagger + \boldsymbol{Y}_e\boldsymbol{Y}_c^\dagger] + 3\boldsymbol{Y}_d^\dagger\boldsymbol{Y}_d + \boldsymbol{Y}_u^\dagger\boldsymbol{Y}_u - \frac{7}{15}g_1^2 - 3g_2^2 - \frac{16}{3}g_3^2\right\}, \tag{F.8}$$

$$\beta_{\boldsymbol{Y}_e} = \boldsymbol{Y}_e\left\{\mathrm{Tr}[3\boldsymbol{Y}_d\boldsymbol{Y}_d^\dagger + \boldsymbol{Y}_e\boldsymbol{Y}_e^\dagger] + 3\boldsymbol{Y}_e^\dagger\boldsymbol{Y}_e + \boldsymbol{Y}_\nu^\dagger\boldsymbol{Y}_\nu - \frac{9}{5}g_1^2 - 3g_2^2\right\}, \tag{F.9}$$

$$\beta_{\boldsymbol{Y}_\nu} = \boldsymbol{Y}_\nu\left\{\mathrm{Tr}[3\boldsymbol{Y}_u\boldsymbol{Y}_u^\dagger + \boldsymbol{Y}_\nu\boldsymbol{Y}_\nu^\dagger] + 3\boldsymbol{Y}_\nu^\dagger\boldsymbol{Y}_\nu + \boldsymbol{Y}_e^\dagger\boldsymbol{Y}_e - \frac{3}{5}g_1^2 - 3g_2^2\right\}. \tag{F.10}$$

These expressions shows that the β-function for a superpotential coupling is proportional to this coupling. This is a consequence of the non-renormalization theorem of supersymmetry [34].

Soft breaking terms
The one-loop RGE's for the soft breaking terms can all be written as

$$\frac{d}{dl}\boldsymbol{a}_{u,d,e,n} = \frac{1}{16\pi^2}\beta_{\boldsymbol{a}_{u,d,e,n}}, \tag{F.11}$$

$$\frac{d}{dt}B = \frac{1}{16\pi^2}\beta_B, \tag{F.12}$$

$$\frac{d}{dt}M^2_{H_u,H_d,Q,L,u,d,e,n} = \frac{1}{16\pi^2}\beta_{M^2_{H_u,H_d,Q,L,u,d,e,n}}. \tag{F.13}$$

$$\beta_{\boldsymbol{a}_u} = \boldsymbol{a}_u \left\{ \mathrm{Tr}[3\boldsymbol{Y}_u\boldsymbol{Y}_u^\dagger + \boldsymbol{Y}_\nu\boldsymbol{Y}_\nu^\dagger] + 5\boldsymbol{Y}_u^\dagger\boldsymbol{Y}_u + \boldsymbol{Y}_d^\dagger\boldsymbol{Y}_d - \frac{13}{15}g_1^2 - 3g_2^2 - \frac{16}{3}g_3^2 \right\}$$
$$+ \boldsymbol{Y}_u \left\{ \mathrm{Tr}[6\boldsymbol{a}_u\boldsymbol{Y}_u^\dagger + 2\boldsymbol{a}_\nu\boldsymbol{Y}_\nu^\dagger] + 4\boldsymbol{Y}_u^\dagger\boldsymbol{a}_u + 2\boldsymbol{Y}_d^\dagger\boldsymbol{a}_d \right.$$
$$\left. + \frac{26}{15}g_1^2 M_1 + 6g_2^2 M_2 + \frac{32}{3}g_3^2 M_3 \right\}, \tag{F.14}$$

$$\beta_{\boldsymbol{a}_d} = \boldsymbol{a}_e \left\{ \mathrm{Tr}[3\boldsymbol{Y}_d\boldsymbol{Y}_d^\dagger + \boldsymbol{Y}_e\boldsymbol{Y}_e^\dagger] + 5\boldsymbol{Y}_d^\dagger\boldsymbol{Y}_d + \boldsymbol{Y}_u^\dagger\boldsymbol{Y}_u - \frac{7}{15}g_1^2 - 3g_2^2 - \frac{16}{3}g_3^2 \right\}$$
$$+ \boldsymbol{Y}_d \left\{ \mathrm{Tr}[6\boldsymbol{a}_d\boldsymbol{Y}_d^\dagger + 2\boldsymbol{a}_e\boldsymbol{Y}_e^\dagger] + 4\boldsymbol{Y}_d^\dagger\boldsymbol{a}_d + 2\boldsymbol{Y}_u^\dagger\boldsymbol{a}_u \right.$$
$$\left. + \frac{14}{15}g_1^2 + 6g_2^2 M_2 + \frac{32}{3}g_3^2 M_3 \right\}, \tag{F.15}$$

$$\beta_{\boldsymbol{a}_e} = \boldsymbol{a}_e \left\{ \mathrm{Tr}[3\boldsymbol{Y}_d\boldsymbol{Y}_d^\dagger + \boldsymbol{Y}_e\boldsymbol{Y}_e^\dagger] + 5\boldsymbol{Y}_e^\dagger\boldsymbol{Y}_e + \boldsymbol{Y}_\nu^\dagger\boldsymbol{Y}_\nu - 3g_2^2 - \frac{9}{5}g_1^2 \right\}$$
$$+ \boldsymbol{Y}_e \left\{ \mathrm{Tr}[6\boldsymbol{a}_d\boldsymbol{Y}_d^\dagger + 2\boldsymbol{a}_e\boldsymbol{Y}_e^\dagger] + 4\boldsymbol{Y}_e^\dagger\boldsymbol{a}_e + 2\boldsymbol{Y}_\nu^\dagger\boldsymbol{a}_\nu \right.$$
$$\left. - 6g_2^2 M_2 - \frac{18}{5}g_1^2 M_1 \right\}, \tag{F.16}$$

$$\beta_{\boldsymbol{a}_\nu} = \boldsymbol{a}_\nu \left\{ \mathrm{Tr}[3\boldsymbol{Y}_u\boldsymbol{Y}_u^\dagger + \boldsymbol{Y}_\nu\boldsymbol{Y}_\nu^\dagger] + 5\boldsymbol{Y}_\nu^\dagger\boldsymbol{Y}_\nu + \boldsymbol{Y}_e^\dagger\boldsymbol{Y}_e - 3g_2^2 - \frac{3}{5}g_1^2 \right\}$$
$$+ \boldsymbol{Y}_\nu \left\{ \mathrm{Tr}[6\boldsymbol{a}_u\boldsymbol{Y}_u^\dagger + 2\boldsymbol{a}_\nu\boldsymbol{Y}_\nu^\dagger] + 4\boldsymbol{Y}_\nu^\dagger\boldsymbol{a}_\nu + 2\boldsymbol{Y}_e^\dagger\boldsymbol{a}_e \right.$$
$$\left. - \frac{6}{5}g_1^2 M_1 - 6g_2^2 M_2 \right\}, \tag{F.17}$$

$$\beta_B = B \left\{ \mathrm{Tr}(3\boldsymbol{Y}_u\boldsymbol{Y}_u^\dagger + 3\boldsymbol{Y}_d\boldsymbol{Y}_d^\dagger + \boldsymbol{Y}_e\boldsymbol{Y}_e^\dagger + \boldsymbol{Y}_\nu\boldsymbol{Y}_\nu^\dagger) - \frac{3}{5}g_1^2 - 3g_2^2 \right\}$$
$$+ \mu \left\{ \mathrm{Tr}(6\boldsymbol{a}_u\boldsymbol{Y}_u^\dagger + 6\boldsymbol{a}_d\boldsymbol{Y}_d^\dagger + 2\boldsymbol{a}_e\boldsymbol{Y}_e^\dagger + \boldsymbol{a}_\nu\boldsymbol{Y}_\nu^\dagger) + \frac{6}{5}g_1^2 M_1 + 3g_2^2 M_2 \right\}. \tag{F.18}$$

$$\beta_{M_{H_u}^2} = 6\mathrm{Tr}[(M_{H_u}^2 + M_Q^2)\boldsymbol{Y}_u^\dagger \boldsymbol{Y}_u + \boldsymbol{Y}_u^\dagger M_u^2 \boldsymbol{Y}_u + \boldsymbol{a}_u^\dagger \boldsymbol{a}_u] - 6g_2^2|M_2|^2 - \frac{6}{5}g_1^2|M_1|^2 + \frac{3}{5}S, \tag{F.19}$$

$$\beta_{M_{H_d}^2} = \mathrm{Tr}[6(M_{H_d}^2 + M_Q^2)\boldsymbol{Y}_d^\dagger \boldsymbol{Y}_d + 6\boldsymbol{Y}_d^\dagger M_d^2 \boldsymbol{Y}_d + 2(M_{H_d}^2 + M_L^2)\boldsymbol{Y}_e^\dagger \boldsymbol{Y}_e + 2\boldsymbol{Y}_e^\dagger M_e^2 \boldsymbol{Y}_e + 6\boldsymbol{a}_d^\dagger \boldsymbol{a}_d + 2\boldsymbol{a}_e^\dagger \boldsymbol{a}_e] - \frac{6}{5}g_1^2|M_1|^2 - 6g_2^2|M_2|^2 - \frac{3}{5}S, \tag{F.20}$$

$$\beta_{\boldsymbol{M}_Q^2} = \left(\boldsymbol{M}_Q^2 + 2M_{H_u}^2\right)\boldsymbol{Y}_u^\dagger \boldsymbol{Y}_u + \left(\boldsymbol{M}_Q^2 + 2M_{H_d}^2\right)\boldsymbol{Y}_d^\dagger \boldsymbol{Y}_d + [\boldsymbol{Y}_u^\dagger \boldsymbol{Y}_u + \boldsymbol{Y}_d^\dagger \boldsymbol{Y}_d]M_Q^2 + 2\boldsymbol{Y}_u^\dagger \boldsymbol{M}_u^2 \boldsymbol{Y}_u + 2\boldsymbol{Y}_d^\dagger \boldsymbol{M}_d^2 \boldsymbol{Y}_d + 2\boldsymbol{a}_u^\dagger \boldsymbol{a}_u + 2\boldsymbol{a}_d^\dagger \boldsymbol{a}_d - \frac{2}{15}g_1^2|M_1|^2 - 6g_2^2|M_2|^2 - \frac{32}{3}g_3^2|M_3|^2 + \frac{1}{5}g_1^2 S, \tag{F.21}$$

$$\beta_{\boldsymbol{M}_L^2} = \left(\boldsymbol{M}_L^2 + 2M_{H_d}^2\right)\boldsymbol{Y}_e^\dagger \boldsymbol{Y}_e + 2\boldsymbol{Y}_e^\dagger \boldsymbol{M}_e^2 \boldsymbol{Y}_e + \boldsymbol{Y}_e^\dagger \boldsymbol{Y}_e \boldsymbol{M}_L^2 + 2\boldsymbol{a}_e^\dagger \boldsymbol{a}_e + \left(\boldsymbol{M}_L^2 + 2M_{H_u}^2\right)\boldsymbol{Y}_\nu^\dagger \boldsymbol{Y}_\nu + 2\boldsymbol{Y}_\nu^\dagger \boldsymbol{M}_\nu^2 \boldsymbol{Y}_\nu + \boldsymbol{Y}_\nu^\dagger \boldsymbol{Y}_\nu \boldsymbol{M}_L^2 + 2\boldsymbol{a}_\nu^\dagger \boldsymbol{a}_\nu - \frac{6}{5}g_1^2|M_1|^2 - 6g_2^2|M_2|^2 - \frac{3}{5}g_1^2 S, \tag{F.22}$$

$$\beta_{\boldsymbol{M}_u^2} = \left(2\boldsymbol{M}_u^2 + 4M_{H_u}^2\right)\boldsymbol{Y}_u \boldsymbol{Y}_u^\dagger + 4\boldsymbol{Y}_u \boldsymbol{M}_Q^2 \boldsymbol{Y}_u^\dagger + 2\boldsymbol{Y}_u \boldsymbol{Y}_u^\dagger \boldsymbol{M}_u^2 + 4\boldsymbol{a}_u \boldsymbol{a}_u^\dagger - \frac{32}{15}g_1^2|M_1|^2 - \frac{32}{3}g_3^2|M_3|^2 - \frac{6}{5}g_1^2 S, \tag{F.23}$$

$$\beta_{\boldsymbol{M}_d^2} = \left(2\boldsymbol{M}_d^2 + 4M_{H_d}^2\right)\boldsymbol{Y}_d \boldsymbol{Y}_d^\dagger + 4\boldsymbol{Y}_d \boldsymbol{M}_Q^2 \boldsymbol{Y}_d^\dagger + 2\boldsymbol{Y}_d \boldsymbol{Y}_d^\dagger \boldsymbol{M}_d^2 + 4\boldsymbol{a}_d \boldsymbol{a}_d^\dagger - \frac{8}{15}g_1^2|M_1|^2 - \frac{32}{3}g_3^2|M_3|^2 + \frac{2}{5}g_1^2 S, \tag{F.24}$$

$$\beta_{\boldsymbol{M}_e^2} = \left(2\boldsymbol{M}_e^2 + 4M_{H_d}^2\right)\boldsymbol{Y}_e \boldsymbol{Y}_e^\dagger + 4\boldsymbol{Y}_e \boldsymbol{M}_L^2 \boldsymbol{Y}_e^\dagger + 2\boldsymbol{Y}_e \boldsymbol{Y}_e^\dagger \boldsymbol{M}_e^2 + 4\boldsymbol{a}_e \boldsymbol{a}_e^\dagger - \frac{24}{5}g_1^2|M_1|^2 + \frac{6}{5}g_1^2 S, \tag{F.25}$$

$$\beta_{\boldsymbol{M}_\nu^2} = \left(2\boldsymbol{M}_\nu^2 + 4M_{H_u}^2\right)\boldsymbol{Y}_\nu \boldsymbol{Y}_\nu^\dagger + 4\boldsymbol{Y}_\nu \boldsymbol{M}_L^2 \boldsymbol{Y}_\nu^\dagger + 2\boldsymbol{Y}_\nu \boldsymbol{Y}_\nu^\dagger \boldsymbol{M}_\nu^2 + 4\boldsymbol{a}_\nu \boldsymbol{a}_\nu^\dagger, \tag{F.26}$$

where

$$S = M_{H_u}^2 - M_{H_d}^2 + \mathrm{Tr}\left[\boldsymbol{M}_Q^2 - \boldsymbol{M}_L^2 - 2\boldsymbol{M}_u^2 + \boldsymbol{M}_d^2 + \boldsymbol{M}_e^2\right]. \tag{F.27}$$

F.2 MSSM-DM

The superpotential of MSSM-DM is given by

$$\begin{aligned} W_{\rm DM} = & Y_u Q H_u u + \frac{1}{2}\lambda_{\alpha\beta k} L_\alpha L_\beta e_k + \lambda'_{\alpha jk} L_\alpha Q_j d_k + \mu_\alpha L_\alpha H_u \\ & + \frac{1}{2}\lambda''_{ijk} u_i d_j d_k + \lambda'''_{\alpha j} L_\alpha H_u n_j \\ & + \frac{1}{6} A_{ijk} n_i n_j n_k + \frac{1}{2} B_{ij} n_i n_j + C_i n_i . \end{aligned} \tag{F.28}$$

And the soft-breaking terms are given by

$$\begin{aligned} \mathcal{L}_{\rm soft} = & M_Q^2 \tilde{Q}^\dagger \tilde{Q} + M_{H_u}^2 H_u^\dagger H_u + \left(M_L^2\right)_{\alpha\beta} \tilde{L}_\alpha^\dagger \tilde{L}_\beta + M_u^2 \tilde{u}\tilde{u}^* \\ & + M_d^2 \tilde{d}\tilde{d}^* + M_e^2 \tilde{e}\tilde{e}^* + M_n^2 \tilde{n}^* \tilde{n} \\ & + \Bigg[b_\alpha L_\alpha H_u + a_u \tilde{Q} H_u \tilde{u} + \frac{1}{2}\lambda^{\rm s}_{\alpha\beta k} \tilde{L}_\alpha \tilde{L}_\beta \tilde{e}_k \\ & + \lambda'^{\rm s}_{\alpha jk} \tilde{L}_\alpha \tilde{Q}_j \tilde{d}_k + \frac{1}{2}\lambda''^{\rm s}_{ijk} \tilde{u}_i \tilde{d}_j \tilde{d}_k + \lambda'''^{\rm s}_{\alpha j} \tilde{L}_\alpha H_u \tilde{n}_j \\ & + \frac{1}{6} A^{\rm s}_{ijk} \tilde{n}_i \tilde{n}_j \tilde{n}_k + \frac{1}{2} B^{\rm s}_{ij} \tilde{n}_i \tilde{n}_j \\ & + \frac{1}{2}\left(M_1 \tilde{B}\tilde{B} + M_2 \tilde{W}^a \tilde{W}^a + M_3 \tilde{g}\tilde{g} \right) + \text{h.c.} \Bigg] . \end{aligned} \tag{F.29}$$

Note that a linear supersymmetry breaking term is not allowed [37].

F.2.1 Quantum numbers and group properties

The $SU(3)_C \times SU(2)_L \times U(1)_Y$ quantum numbers for the chiral fields are

$$\begin{aligned} & Q : \left(3, 2, \frac{1}{6}\right), \quad L : \left(1, 2, -\frac{1}{2}\right), \quad H_u : \left(1, 2, \frac{1}{2}\right), \\ & u : \left(3, 1, \frac{2}{3}\right), \quad d : \left(3, 1, -\frac{1}{3}\right), \quad e : (1, 1, 1), \\ & n : (0, 0, 0) . \end{aligned}$$

These quantum numbers are related to the electric charge, q, by,

$$q = I_{3W} - Y_W . \tag{F.30}$$

Note that since the right-handed sneutrino fields have no gauge quantum numbers they can not interact with the gauge bosons; they are so-called sterile neutrinos.

If one considers a group G with representation matrices $t^A \equiv \left(t^A\right)_i^j$. Then the quadratic Casimir, $C(R)$, of a representation R is defined by

$$\left(t^A t^A\right)_i^j = C(R)\,\delta_i^j. \tag{F.31}$$

For the gauge group of the Standard Model $SU(3)$ triplets q and for $SU(2)$ doublets L we have

$$C_{SU(3)}(q) = \frac{4}{3},\; C_{SU(2)}(L) = \frac{3}{4},\; C_{U(1)}(f) = \frac{3}{5}Y^2(f), \tag{F.32}$$

where $Y(f)$ is the hypercharge of the chiral field f. The factor $3/5$ is a grand unified normalisation, see e.g., Ref. [53].

For the adjoint representation of a group, G, of dimension $d(G)$, one has

$$C(G)\,\delta^{AB} = f^{ACD} f^{BCD}, \tag{F.33}$$

where f^{ABC} are the structure constants. For the Standard Model gauge group one finds

$$C\left(SU(3)_C\right) = 3,\; C\left(SU(2)_L\right) = 2,\; C\left(U(1)_Y\right) = 0. \tag{F.34}$$

The Dynkin index, $S(R)$, is defined by

$$Tr_R\left[t^A t^B\right] = S(R)\,\delta^{AB}. \tag{F.35}$$

For the fundamental representations we find

$$SU(3)_C,\, SU(2)_L:\; S(f) = \frac{1}{2}, \tag{F.36}$$

$$U(1):\; S(f) = \frac{3}{2}Y^2(f), \tag{F.37}$$

where again the GUT normalisation has been used.

Using these relations, and the general expressions from Ref. [34], all RGE's for MSSM-DM are obtained.

F.2.2 Gauge-couplings and gaugino-masses

The two-loop RGE's for the gauge couplings was obtained in Ref. [53],

$$\frac{d}{dt}g_1 = \frac{g_1^3}{16\pi^2}B_1^{(1)} + \frac{g_1^3}{(16\pi^2)^2}\left[\sum_{b=1}^{3} B_{1b}^{(2)} g_b^2 \right.$$
$$- g_1^2\left(\frac{26}{5}\left(Y_u\right)_{ik}\left(Y_u^*\right)_{ik} + \frac{18}{10}\lambda_{\alpha\beta k}\lambda^*_{\alpha\beta k} + \frac{14}{5}\lambda'_{\alpha jk}\lambda'^*_{\alpha jk}\right.$$
$$\left.\left. + \frac{12}{5}\lambda''_{ijk}\lambda''^*_{ijk} + \frac{6}{5}\lambda'''_{\alpha j}\lambda'''^*_{\alpha j}\right)\right], \tag{F.38}$$
$$\frac{d}{dt}g_2 = \frac{g_2^3}{16\pi^2}B_2^{(1)} + \frac{g_2^3}{(16\pi^2)^2}\left[\sum_{b-1}^{3} B_{2b}^{(2)} g_b^2 \right.$$
$$- g_2^2\left(6\left(Y_u\right)_{ik}\left(Y_u^*\right)_{ik} + \lambda_{\alpha\beta k}\lambda^*_{\alpha\beta k} + 6\lambda'_{\alpha jk}\lambda'^*_{\alpha jk}\right.$$
$$\left.\left. + 2\lambda'''_{\alpha j}\lambda'''^*_{\alpha j}\right)\right], \tag{F.39}$$
$$\frac{d}{dt}g_3 = \frac{g_3^3}{16\pi^2}B_3^{(1)} + \frac{g_3^3}{(16\pi^2)^2}\left[\sum_{b-1}^{3} B_{3b}^{(2)} g_b^2 \right.$$
$$\left. - 4g_3^2\left(\left(Y_u\right)_{ik}\left(Y_u^*\right)_{ik} + \lambda'_{\alpha jk}\lambda'^*_{\alpha jk} + \lambda''_{ijk}\lambda''^*_{ijk}\right)\right]. \tag{F.40}$$

Here the following matrices have been defined

$$B_a^{(1)} = \left(33/5, 1, -3\right), \tag{F.41}$$
$$B_{ab}^{(2)} = \begin{pmatrix} 199/25 & 27/5 & 88/5 \\ 9/5 & 25 & 24 \\ 11/5 & 9 & 14 \end{pmatrix}, \tag{F.42}$$

The RGE's for the gaugino-masses are

$$\frac{d}{dt}M_1 = \frac{2g_1^2}{16\pi^2}B_1^{(1)}M_1 + \frac{2g_1^2}{(16\pi^2)^2}\left[\sum_{b=1}^{3} B_{1b}^{(2)} g_b^2\left(M_1 + M_b\right)\right.$$
$$+ \frac{26}{5}\left(\left(Y_u^*\right)_{ik}\left(a_u\right)_{ik} - M_1\left(Y_u\right)_{ik}\left(Y_u^*\right)_{ik}\right)$$
$$+ \frac{18}{10}\left(\lambda^{s}_{\alpha\beta k}\lambda^*_{\alpha\beta k} - M_1\lambda_{\alpha\beta k}\lambda^*_{\alpha\beta k}\right)$$
$$+ \frac{14}{5}\left(\lambda'^{s}_{\alpha jk}\lambda'^*_{\alpha jk} - M_1\lambda'_{\alpha jk}\lambda'^*_{\alpha jk}\right)$$
$$+ \frac{12}{5}\left(\lambda''^{s}_{ijk}\lambda''^*_{ijk} - M_1\lambda''_{ijk}\lambda''^*_{ijk}\right)$$
$$\left. + \frac{6}{5}\left(\lambda'''^{s}_{\alpha j}\lambda'''^*_{\alpha j} - M_1\lambda'''_{\alpha j}\lambda'''^*_{\alpha j}\right)\right], \tag{F.43}$$

$$\begin{aligned}\frac{d}{dt}M_2 = \frac{2g_2^2}{16\pi^2}B_2^{(1)}M_2 + \frac{2g_2^2}{(16\pi^2)^2}\Bigg[&\sum_{b=1}^{3}B_{2b}^{(2)}g_b^2\left(M_2+M_b\right)\\ &+6\left(\left(Y_u^*\right)_{ik}\left(a_u\right)_{ik}-M_2\left(Y_u\right)_{ik}\left(Y_u^*\right)_{ik}\right)\\ &+\left(\lambda^{\mathrm{s}}_{\alpha\beta k}\lambda^*_{\alpha\beta k}-M_2\lambda_{\alpha\beta k}\lambda^*_{\alpha\beta k}\right)\\ &+6\left(\lambda'^{\mathrm{s}}_{\alpha jk}\lambda'^*_{\alpha jk}-M_2\lambda'_{\alpha jk}\lambda'^*_{\alpha jk}\right)\\ &+2\left(\lambda'''^{\mathrm{s}}_{\alpha j}\lambda'''^*_{\alpha j}-M_2\lambda'''_{\alpha j}\lambda'''^*_{\alpha j}\right)\Bigg],\end{aligned} \tag{F.44}$$

$$\begin{aligned}\frac{d}{dt}M_3 = \frac{2g_3^2}{16\pi^2}B_3^{(1)}M_3 + \frac{2g_3^2}{(16\pi^2)^2}\Bigg[&\sum_{b=1}^{3}B_{3b}^{(2)}g_b^2\left(M_3+M_b\right)\\ &+4\left[\left(Y_u^*\right)_{ik}\left(a_u\right)_{ik}-M_3\left(Y_u\right)_{ik}\left(Y_u^*\right)_{ik}\right.\\ &+\left(\lambda'^{\mathrm{s}}_{\alpha jk}\lambda'^*_{\alpha jk}-M_3\lambda'_{\alpha jk}\lambda'^*_{\alpha jk}\right)\\ &\left.+\left(\lambda''^{\mathrm{s}}_{ijk}\lambda''^*_{ijk}-M_3\lambda''_{ijk}\lambda''^*_{ijk}\right)\right].\end{aligned} \tag{F.45}$$

F.2.3 Superpotential parameters

The RGE's for the superpotential parameters are most easily expressed in terms of the anomalous dimensions,

$$\gamma^{1j}_{1i} = \left(Y_u^*\right)_{pi}\left(Y_u\right)_{pj} + \lambda'^*_{\alpha ik}\lambda'_{\alpha jk} - \left(\frac{1}{30}g_1^2+\frac{3}{2}g_2^2+\frac{8}{3}g_3^2\right)\delta_i^j, \tag{F.46}$$

$$\gamma^{2\beta}_{2\alpha} = \lambda^*_{\alpha\rho q}\lambda_{\beta\rho q} + 3\lambda'^*_{\alpha pq}\lambda'_{\beta pq} + \lambda'''^*_{\alpha p}\lambda'''_{\beta p} - \left(\frac{3}{10}g_1^2 + \frac{3}{2}g_2^2\right)\delta_\alpha^\beta, \tag{F.47}$$

$$\gamma^3_3 = 3\left(Y_u^*\right)_{pq}\left(Y_u\right)_{pq} + \lambda'''^*_{\alpha p}\lambda'''_{\alpha p} - \left(\frac{3}{10}g_1^2+\frac{3}{2}g_2^2\right), \tag{F.48}$$

$$\gamma^{4j}_{4i} = 2\left(Y_u^*\right)_{pi}\left(Y_u\right)_{pj} + \lambda''^*_{ipq}\lambda''_{jpq} - \left(\frac{8}{15}g_1^2+\frac{8}{3}g_3^2\right)\delta_i^j, \tag{F.49}$$

$$\gamma^{5j}_{5i} = 2\lambda'^*_{\alpha qi}\lambda'_{\alpha qj} + 2\lambda''^*_{ipq}\lambda''_{jpq} - \left(\frac{2}{15}g_1^2+\frac{8}{3}g_3^2\right)\delta_i^j, \tag{F.50}$$

$$\gamma^{6j}_{6i} = \lambda^*_{\rho\sigma i}\lambda_{\rho\sigma j} - \frac{6}{5}g_1^2\,\delta_i^j, \tag{F.51}$$

$$\gamma^{7j}_{7i} = \lambda'''^*_{\alpha i}\lambda'''_{\alpha j} + A^*_{ipq}A_{jpq}. \tag{F.52}$$

Using these expressions the RGE's for the superpotential parameters becomes

$$16\pi^2 \frac{d}{dt}(Y_u)_{ij} = (Y_u)_{ip}\gamma^{4_j}_{4_p} + (Y_u)_{pj}\gamma^{1_i}_{1_p} + (Y_u)_{ij}\gamma^3_3, \tag{F.53}$$

$$16\pi^2 \frac{d}{dt}\lambda_{\alpha\beta k} = \lambda_{\alpha\beta p}\gamma^{6_k}_{6_p} + \lambda_{\rho\beta k}\gamma^{2_\alpha}_{2_\rho} + \lambda_{\alpha\rho k}\gamma^{2_\beta}_{2_\rho}, \tag{F.54}$$

$$16\pi^2 \frac{d}{dt}\lambda'_{\alpha jk} = \lambda'_{\alpha jp}\gamma^{5_k}_{5_p} + \lambda'_{\rho jk}\gamma^{2_\alpha}_{2_\rho} + \lambda'_{\alpha pk}\gamma^{1_j}_{1_p}, \tag{F.55}$$

$$16\pi^2 \frac{d}{dt}\lambda''_{ijk} = \lambda''_{ijp}\gamma^{5_k}_{5_p} + \lambda''_{pjk}\gamma^{4_i}_{4_p} + \lambda''_{ipk}\gamma^{5_j}_{5_p}, \tag{F.56}$$

$$16\pi^2 \frac{d}{dt}\lambda'''_{\alpha j} = \lambda'''_{\alpha p}\gamma^{7_j}_{7_p} + \lambda'''_{\rho j}\gamma^{2_\alpha}_{2_\rho} + \lambda'''_{\alpha j}\gamma^3_3, \tag{F.57}$$

$$16\pi^2 \frac{d}{dt}A_{ijk} = A_{ijp}\gamma^{7_k}_{7_p} + A_{kjp}\gamma^{7_i}_{7_p} + A_{ipk}\gamma^{7_j}_{7_p}, \tag{F.58}$$

$$16\pi^2 \frac{d}{dt}\mu_\alpha = \mu_\alpha\gamma^3_3 + \mu_\rho\gamma^{2_\alpha}_{2_\rho}, \tag{F.59}$$

$$16\pi^2 \frac{d}{dt}B_{ij} = B_{ip}\gamma^{7_j}_{7_p} + B_{jp}\gamma^{7_i}_{7_p}, \tag{F.60}$$

$$16\pi^2 \frac{d}{dt}C_i = C_p\gamma^{7_i}_{7_p}. \tag{F.61}$$

F.2.4 Soft-breaking terms

Trilinear terms

$$\begin{aligned}
\beta_{(a_u)_{ij}} = {} & 2\,(a_u)_{il}\left[(Y_u^*)_{ml}\,(Y_u)_{mj} + \lambda''^*_{lmn}\lambda''_{jmn}\right] \\
& + (a_u)_{lj}\left[(Y_u^*)_{lm}\,(Y_u)_{im} + \lambda'^*_{\rho lm}\lambda'_{\rho im}\right] \\
& + (a_u)_{ij}\left[3\,(Y_u^*)_{mn}\,(Y_u)_{mn} + \lambda'''^*_{\rho m}\lambda'''_{\rho m}\right] \\
& + 4\,(Y_u)_{il}\left[(Y_u^*)_{ml}\,(a_u)_{mj} + \lambda''^*_{lmn}\lambda''^{\rm s}_{jmn}\right] \\
& + 2\,(Y_u)_{lj}\left[(Y_u^*)_{lm}\,(a_u)_{im} + \lambda'^*_{\rho lm}\lambda'^{\rm s}_{\rho im}\right] \\
& + 2\,(Y_u)_{ij}\left[3\,(Y_u^*)_{mn}\,(a_u)_{mn} + \lambda'''^*_{\rho m}\lambda'''^{\rm s}_{\rho m}\right] \\
& - (a_u)_{ij}\left(\frac{13}{15}g_1^2 + 3g_2^2 + \frac{16}{3}g_3^2\right) \\
& + (Y_u)_{ij}\left(\frac{26}{15}g_1^2M_1 + 6g_2^2M_2 + \frac{32}{3}g_3^2M_3\right),
\end{aligned} \tag{F.62}$$

$$\begin{aligned}\beta_{\lambda^{s}_{\alpha\beta k}} = {} & \lambda^{s}_{\alpha\beta l}\lambda_{\rho\sigma l}\lambda_{\rho\sigma k} + 3\lambda^{s}_{\rho\beta k}\lambda'_{\rho pq}\lambda'_{\alpha pq} \\ & + \lambda^{s}_{\rho\beta k}\left[\lambda_{\rho\sigma q}\lambda_{\alpha\sigma q} + \lambda'''_{\rho q}\lambda'''_{\alpha q}\right] + \lambda^{s}_{\alpha\rho k}\lambda_{\sigma\rho l}\lambda_{\sigma\beta l} \\ & + 2\lambda_{\alpha\beta l}\lambda_{\rho\sigma l}\lambda^{s}_{\rho\sigma k} + 6\lambda_{\rho\beta k}\lambda'_{\rho pq}\lambda'^{s}_{\alpha pq} \\ & + 2\lambda_{\rho\beta k}\left[\lambda_{\rho\sigma q}\lambda^{s}_{\alpha\sigma q} + \lambda'''_{\rho q}\lambda'''^{s}_{\alpha q}\right] + 2\lambda_{\alpha\rho k}\lambda_{\sigma\rho l}\lambda^{s}_{\sigma\beta l} \\ & - \lambda^{s}_{\alpha\beta k}\left(\frac{9}{5}g_1^2 + 3g_2^2\right) + \lambda_{\alpha\beta k}\left(\frac{18}{5}g_1^2 M_1 + 6g_2^2 M_2\right), \end{aligned} \tag{F.63}$$

$$\begin{aligned}\beta_{\lambda'^{s}_{\alpha jk}} = {} & 2\lambda'^{s}_{\alpha jl}\left[\lambda'^{*}_{\rho pl}\lambda'_{\rho pk} + \lambda''^{*}_{plq}\lambda''_{pqk}\right] \\ & + \lambda'^{s}_{\rho jk}\left[3\lambda'^{*}_{\rho pq}\lambda'_{\alpha pq} + \lambda'''^{*}_{\rho q}\lambda'''_{\alpha q}\right] + \frac{1}{2}\lambda'^{s}_{\alpha jk}\lambda^{*}_{\rho\sigma q}\lambda_{\rho\sigma q} \\ & + \lambda'^{s}_{\alpha lk}\left[\left(Y_u^{*}\right)_{lq}\left(Y_u\right)_{jq} + \lambda'^{*}_{\rho lq}\lambda'_{\rho jq}\right] \\ & + 2\lambda'_{\alpha jl}\left[\lambda'^{*}_{\rho pl}\lambda'^{s}_{\rho pk} + \lambda''^{*}_{plq}\lambda''^{s}_{pqk}\right] \\ & + 2\lambda'_{\rho jk}\left[3\lambda'^{*}_{\rho pq}\lambda'^{s}_{\alpha pk} + \lambda'''^{*}_{\rho q}\lambda'''^{s}_{\alpha q}\right] + \lambda'_{\alpha jk}\lambda^{*}_{\rho\sigma q}\lambda^{s}_{\rho\sigma q} \\ & + 4\lambda'_{\alpha lk}\left[\left(Y_u^{*}\right)_{lq}\left(a_u\right)_{jq} + \lambda'^{*}_{\rho lq}\lambda'^{s}_{\rho jq}\right] \\ & - \lambda'^{s}_{\alpha jk}\left(\frac{7}{15}g_1^2 + 3g_2^2 + \frac{16}{3}g_3^2\right) \\ & + \lambda'_{\alpha jk}\left(\frac{14}{15}g_1^2 M_1 + 6g_2^2 M_2 + \frac{32}{3}g_3^2 M_3\right), \end{aligned} \tag{F.64}$$

$$\begin{aligned}\beta_{\lambda''^{s}_{ijk}} = {} & 2\lambda''^{s}_{ijl}\left[\lambda'^{*}_{\rho ql}\lambda'_{\rho qk} + \lambda''^{*}_{plq}\lambda''_{pqk}\right] \\ & + \lambda''^{s}_{lkj}\left[\left(Y_u^{*}\right)_{pl}\left(Y_u\right)_{pi} + \lambda''^{*}_{lpq}\lambda''_{ipq}\right] \\ & + 2\lambda''^{s}_{iki}\left[\lambda'^{*}_{\rho qi}\lambda'_{\rho qj} + \lambda''^{*}_{piq}\lambda''_{pqj}\right] \\ & + 4\lambda''_{ijl}\left[\lambda'^{*}_{\rho ql}\lambda'^{s}_{\rho qk} + \lambda''^{*}_{plq}\lambda''^{s}_{pqk}\right] \\ & + 2\lambda''_{lkj}\left[\left(Y_u^{*}\right)_{pl}\left(a_u\right)_{pi} + \lambda''^{*}_{lpq}\lambda''^{s}_{ipq}\right] \\ & + 4\lambda''_{ikl}\left[\lambda'^{*}_{\rho ql}\lambda'^{s}_{\rho qj} + \lambda''^{*}_{plq}\lambda''^{s}_{pqj}\right] \\ & - \lambda''^{s}_{ijk}\left(\frac{3}{5}g_1^2 + \frac{8}{3}g_3^2\right) + \lambda''_{ijk}\left(\frac{6}{5}g_1^2 M_1 + \frac{16}{3}g_3^2 M_3\right), \end{aligned} \tag{F.65}$$

$$\begin{aligned}\beta_{\lambda'''^{s}_{\alpha j}} = & \lambda'''^{s}_{\alpha l}\lambda'''^{*}_{\rho l}\lambda'''_{\rho j} + 3\lambda'''^{s}_{\rho j}\lambda'^{*}_{\rho pq}\lambda'_{\alpha pq} + \lambda'''^{s}_{\alpha l}A^{*}_{lmn}A_{mnj} \\ & + \lambda'''^{s}_{\rho j}\lambda^{*}_{\rho\sigma q}\lambda_{\alpha\sigma q} + \lambda'''^{s}_{\rho j}\lambda'''^{*}_{\rho q}\lambda'''_{\alpha q} \\ & + \lambda'''^{s}_{\alpha j}\left[3\left(Y^{*}_{u}\right)_{pq}\left(Y_{u}\right)_{pq} + \lambda'''^{*}_{\rho q}\lambda'''_{\rho q}\right] \\ & + 2\lambda'''_{\alpha l}\lambda'''^{*}_{\rho l}\lambda'''^{s}_{\rho j} + 6\lambda'''_{\rho j}\lambda'^{*}_{\rho pq}\lambda'^{s}_{\alpha pq} + \lambda'''_{\alpha l}A^{*}_{lmn}A^{s}_{mnj} \\ & + 2\lambda'''_{\rho j}\lambda^{*}_{\rho\sigma q}\lambda^{s}_{\alpha\sigma q} + 2\lambda'''_{\rho j}\lambda'''^{*}_{\rho q}\lambda'''^{s}_{\alpha q} \\ & + 2\lambda'''_{\alpha j}\left[3\left(Y^{*}_{u}\right)_{\bar{p}\bar{q}}\left(a_{u}\right)_{\bar{p}\bar{q}} + \lambda'''^{*}_{\bar{\rho}\bar{q}}\lambda'''^{s}_{\bar{\rho}\bar{q}}\right] \\ & - \lambda'''^{s}_{\alpha j}\left(\frac{3}{5}g_1^2 + \frac{3}{2}g_2^2\right) + \lambda'''_{\alpha j}\left(\frac{6}{5}g_1^2 + 3g_2^2\right), \end{aligned} \tag{F.66}$$

$$\begin{aligned}\beta_{A^{s}_{ijk}} = & A^{s}_{ijl}\left(A_{lmn}A_{mnk} + \lambda'''^{*}_{\rho l}\lambda'''_{\rho k}\right) \\ & + A^{s}_{kjl}\left(A_{lmn}A_{mni} + \lambda'''^{*}_{\rho l}\lambda'''_{\rho n}\right) \\ & + A^{s}_{ikl}\left(A_{lmn}A_{mnj} + \lambda'''^{*}_{\rho l}\lambda'''_{\rho j}\right) \\ & + 2\left[A_{ijl}\left(A_{lmn}A^{s}_{mnk} + \lambda'''^{*}_{\rho l}\lambda'''^{s}_{\rho k}\right)\right. \\ & + A_{kjl}\left(A_{lmn}A^{s}_{mni} + \lambda'''^{*}_{\rho l}\lambda'''^{s}_{\rho i}\right) \\ & \left. + A_{ikl}\left(A_{lmn}A^{s}_{mnj} + \lambda'''^{*}_{\rho l}\lambda'''^{s}_{\rho j}\right)\right]. \end{aligned} \tag{F.67}$$

Scalar masses

It is convenient to define

$$S = M_{H_u}^2 - Tr\left[M_L^2\right] - Tr\left[M_Q^2 - 2M_u^2 + M_d^2 + M_e^2\right]. \tag{F.68}$$

$$\begin{aligned}\beta_{b_\alpha} = & b_\alpha\left(3\left(Y_u^{*}\right)_{mn}\left(Y_u\right)_{mn} + \lambda'''^{*}_{\rho q}\lambda'''_{\rho q} - \frac{3}{5}g_1^2 - 3g_2^2\right) \\ & + b_\rho\left(\lambda'''^{*}_{\rho l}\lambda'''_{\alpha l} + 3\lambda'^{*}_{\rho pq}\lambda'_{\alpha pq} + \lambda^{*}_{\rho\sigma q}\lambda_{\sigma\alpha q} + 2\lambda'''^{*}_{\rho q}\lambda'''_{\alpha q}\right) \\ & + \mu_\alpha\left(3\left(Y_u^{*}\right)_{mn}\left(a_u\right)_{mn} + \lambda'''^{*}_{\rho q}\lambda'''^{s}_{\rho q} + \frac{6}{5}g_1^2M_1 + 6g_2^2M_2\right) \\ & + \mu_\rho\left(\lambda'''^{*}_{\rho l}\lambda'''^{s}_{\alpha l} + \lambda'^{*}_{\rho pq}\lambda'^{s}_{\alpha pq} + \lambda^{*}_{\rho\sigma q}\lambda^{s}_{\sigma\alpha q} + 2\lambda'''^{*}_{\alpha l}\lambda'''^{s}_{\rho l}\right), \end{aligned} \tag{F.69}$$

$$\begin{aligned}\beta_{B^{\rm s}_{ij}} = & B^{\rm s}_{il}\left(\frac{1}{2}A^*_{lmn}A_{mnj}+\lambda'''^*_{\rho l}\lambda'''_{\rho j}\right)\\ & +2A_{ijl}\left(\frac{1}{2}A_{lmn}B^{\rm s}_{mn}+\lambda'''^*_{\rho l}b_\rho\right)\\ & +B_{il}\left(A^*_{lmn}A^{\rm s}_{mnj}+2\lambda'''^*_{\rho l}\lambda'''^{\rm s}_{\rho j}\right)\\ & +B^{\rm s}_{jl}\left(\frac{1}{2}A^*_{lmn}A_{mni}+\lambda'''^*_{\rho l}\lambda'''_{\rho i}\right)\\ & +B_{jl}\left(A^*_{lmn}A^{\rm s}_{mni}+2\lambda'''^*_{\rho l}\lambda'''^{\rm s}_{\rho i}\right).\end{aligned} \tag{F.70}$$

$$\begin{aligned}\beta_{H_u} = & \left(6\left(Y^*_u\right)_{pq}\left(Y_u\right)_{pq}+2\lambda'''^*_{\rho q}\lambda'''_{\rho q}\right)M^2_{H_u}\\ & +6\left(Y^*_u\right)_{pq}\left(Y_u\right)_{pr}\left(M^2_u\right)_{qr}+6\left(Y^*_u\right)_{qp}\left(Y_u\right)_{rp}\left(M^2_Q\right)_{qr}\\ & +2\lambda'''^*_{\rho q}\lambda'''_{\alpha r}\left(M^2_n\right)_{qr}+2\lambda'''^*_{\rho p}\lambda'''_{\sigma p}\left(M^2_L\right)_{\rho\sigma}\\ & +6\left(a^*_u\right)_{pq}\left(a_u\right)_{pq}+2\lambda'''^{\rm s}_{\rho q}\lambda'''^{\rm s}_{\rho q}\\ & -\left(\frac{6}{5}g'^2_1M'^2_1+6g'^2_2M'^2_2-\frac{3}{5}g'^2_1S\right),\end{aligned} \tag{F.71}$$

$$\begin{aligned}\beta_{\left(M^2_Q\right)_{ij}} = & \left(Y^*_u\right)_{iq}\left(Y_u\right)_{uq}\left(M^2_Q\right)_{nj}+\lambda'^*_{\rho iq}\lambda'_{\rho nq}\left(M^2_Q\right)_{nj}\\ & +\left(Y^*_u\right)_{jq}\left(Y_u\right)_{nq}\left(M^2_Q\right)_{ni}+\lambda'^*_{\rho jq}\lambda'_{\rho nq}\left(M^2_Q\right)_{ni}\\ & +2\left(Y^*_u\right)_{iq}\left(Y_u\right)_{jr}\left(M^2_u\right)_{rq}+2\lambda'^*_{\rho iq}\lambda'_{\rho jr}\left(M^2_Q\right)_{rq}\\ & +2\left(Y^*_u\right)_{iq}\left(Y_u\right)_{jq}M^2_{H_u}+2\lambda'^*_{\rho iq}\lambda'_{\sigma jq}\left(M^2_L\right)_{\rho\sigma}\\ & +2\left(a^*_u\right)_{iq}\left(a_u\right)_{jq}+2\lambda'^{*{\rm s}}_{\rho iq}\lambda'^{\rm s}_{\rho jq}\\ & -\left(\frac{2}{15}g'^2_1\left|M_1\right|^2+6g'^2_2\left|M_2\right|^2+\frac{32}{3}g'^2_3\left|M_3\right|^2+\frac{3}{5}g'^2_1S\right)\delta_{ij},\end{aligned} \tag{F.72}$$

$$\begin{aligned}\beta_{\left(M^2_L\right)_{\alpha\beta}} = & \left(M^2_L\right)_{\rho\beta}\left(\lambda^*_{\alpha\sigma q}\lambda_{\sigma\rho q}+3\lambda'^*_{\alpha pq}\lambda'_{\rho pq}+\lambda'''^*_{\alpha q}\lambda'''_{\rho q}\right)\\ & +\left(M^2_L\right)_{\rho\alpha}\left(\lambda^*_{\beta\sigma q}\lambda_{\sigma\rho q}+3\lambda'^*_{\beta pq}\lambda'_{\rho pq}+\lambda'''^*_{\beta q}\lambda'''_{\rho q}\right)\\ & +6\left(M^2_d\right)_{rq}\lambda'^*_{\alpha pr}\lambda'_{\beta pq}+2\left(M^2_e\right)_{rq}\lambda^*_{\alpha\rho r}\lambda_{\beta\rho q}\\ & +6\left(M^2_Q\right)_{rq}\lambda'^*_{\alpha rp}\lambda'_{\beta qp}+2\left(M^2_L\right)_{\rho\sigma}\lambda^*_{\alpha\sigma p}\lambda_{\beta\rho p}\\ & +2\left(M^2_n\right)_{rq}\lambda'''^*_{\alpha q}\lambda'''_{\beta r}+2M^2_{H_u}\lambda'''^*_{\alpha p}\lambda'''_{\beta p}\\ & +2\lambda^{*{\rm s}}_{\alpha\rho q}\lambda^{\rm s}_{\beta\rho q}+6\lambda'^{*{\rm s}}_{\alpha pq}\lambda'^{\rm s}_{\beta pq}+2\lambda'''^{*{\rm s}}_{\alpha q}\lambda'''^{\rm s}_{\beta q}\\ & -\left(\frac{6}{5}g^2_1\left|M_1\right|^2+6g^2_2\left|M_2\right|^2+\frac{3}{5}g^2_1S\right)\delta_{\alpha\beta},\end{aligned} \tag{F.73}$$

$$\begin{aligned}\beta_{(M_u^2)_{ij}} = & 2\left(Y_u^*\right)_{pi}\left(Y_u\right)_{pn}\left(M_u\right)_{nj} + 2\left(Y_u^*\right)_{pj}\left(Y_u\right)_{pn}\left(M_u\right)_{ni} \\ & + \left(Y_u^*\right)_{pi}\left(Y_u\right)_{pn}\left(M_Q^2\right)_{nj} + \lambda''^*_{ipq}\lambda''_{npq}\left(M_u^2\right)_{nj} \\ & + \left(Y_u^*\right)_{pj}\left(Y_u\right)_{pn}\left(M_Q^2\right)_{ni} + \lambda''^*_{jpq}\lambda''_{npq}\left(M_u^2\right)_{ni} \\ & + 4\left(Y_u^*\right)_{pi}\left(Y_u\right)_{pj}M_{H_u}^2 + 2\left(Y_u^*\right)_{qi}\left(Y_u\right)_{rj}\left(M_Q^2\right)_{rq} \\ & + 4\lambda''^*_{ipq}\lambda''_{jpq}\left(M_u^2\right)_{rq} + 4\left(a_u^*\right)_{pi}\left(a_u\right)_{pj} + 2\lambda''^{\mathrm{s}*}_{ipq}\lambda''^{\mathrm{s}}_{jpr} \\ & - \left(\frac{32}{5}g_1^2\left|M_1\right|^2 + \frac{32}{3}g_3^2\left|M_3\right|^2 - \frac{3}{5}g_1^2 S\right)\delta_{ij}, \end{aligned} \tag{F.74}$$

$$\begin{aligned}\beta_{\left(M_d^2\right)_{ij}} = & \left(M_d^2\right)_{nj}\left(\lambda'^*_{\rho iq}\lambda'_{\rho qn} + \lambda''^*_{qip}\lambda''_{qpn}\right) \\ & + \left(M_d^2\right)_{ni}\left(\lambda'^*_{\rho jq}\lambda'_{\rho qn} + \lambda''^*_{qjp}\lambda''_{qpn}\right) \\ & + 2\lambda'^*_{\rho iq}\lambda'_{\rho jr}\left(M_Q^2\right)_{rq} + 2\lambda'^*_{\rho pi}\lambda'_{\sigma pj}\left(M_L^2\right)_{\rho\sigma} \\ & + 2\lambda''^*_{qip}\lambda''_{rjp}\left(M_u^2\right)_{rq} + 2\lambda''^*_{piq}\lambda''_{pjr}\left(M_u^2\right)_{rq} \\ & + 2\lambda'^{\mathrm{s}*}_{\rho qi}\lambda'^{\mathrm{s}}_{\rho qj} + 2\lambda''^{\mathrm{s}*}_{qip}\lambda''^{\mathrm{s}}_{qjp} \\ & - \left(\frac{8}{15}g_1^2\left|M_1\right|^2 + \frac{32}{3}g_3^2\left|M_3\right|^2 - \frac{2}{5}g_1^2 S\right)\delta_{ij}, \end{aligned} \tag{F.75}$$

$$\begin{aligned}\beta_{(M_e^2)_{ij}} = & \left(M_e^2\right)_{nj}\lambda^*_{\rho\sigma i}\lambda_{\rho\sigma n} + \left(M_e^2\right)_{ni}\lambda^*_{\rho\sigma j}\lambda_{\rho\sigma n} \\ & + 2\left(M_L^2\right)_{\delta\sigma}\lambda^*_{\rho\sigma i}\lambda_{\rho\delta j} + \lambda'^{\mathrm{s}*}_{\rho\sigma i}\lambda'^{\mathrm{s}}_{\rho\sigma j} \\ & - \left(\frac{24}{5}g_1^2\left|M_1\right|^2 - \frac{6}{5}g_1^2 S\right)\delta_{ij}, \end{aligned} \tag{F.76}$$

$$\begin{aligned}\beta_{(M_n^2)_{ij}} = & \left(M_n^2\right)_{nj}\left(\lambda'''^*_{\rho i}\lambda'''_{\rho n} + A^*_{ipq}A_{pqn}\right) \\ & + \left(M_n^2\right)_{ni}\left(\lambda'''^*_{\rho j}\lambda'''_{\rho n} + A^*_{jpq}A_{pqn}\right) \\ & + 2\lambda'''^*_{\rho i}\lambda'''_{\rho j}M_{H_u}^2 + 2\lambda'''^*_{\rho i}\lambda'''_{\sigma j}\left(M_L^2\right)_{\rho\sigma} \\ & + 2A^*_{ipq}A_{jpr}\left(M_n^2\right)_{rq} + 2\lambda'''^{\mathrm{s}*}_{\rho i}\lambda'''^{\mathrm{s}}_{\rho j} + A^{\mathrm{s}*}_{ipq}A^{\mathrm{s}}_{jpq}. \end{aligned} \tag{F.77}$$

URN:NBN:no-7281

Appendix G

Veltman-Passarino integrals

G.1 Veltman-Passarino integrals

In this appendix the one-loop integrals, used for the calculations, will be presented. These integrals will be solved by use of a series expansion. For a general treatment of these so-called Veltman-Passarino integrals see e.g. Refs. [70, 71].

The integrals needed are the so-called C-integrals, defined as

$$C_{\{0,\mu,\mu\nu\}} = \frac{1}{i\pi^2}\int d^n q \frac{q_{\{0,\mu,\mu\nu\}}}{\left[(p+q)^2 - m_1^2\right]\left[(p'+q)^2 - m_1^2\right]\left[q^2 - m_2^2\right]}, \tag{G.1}$$

where $q_{\mu\nu} = q_\mu q_\nu$, and $n \to 4$.

These integrals can be expanded in terms of the external momenta (see e.g., Refs. [70, 71, 72]), i.e.,

$$C_\mu = p_\mu C_{11} + p'_\mu C_{12}, \tag{G.2}$$

$$C_{\mu\nu} = p_\mu p_\nu C_{21} + p'_\mu p'_\nu C_{22} + \left(p_\mu p'_\nu + p_\nu p'_\mu\right) C_{23} + + g_{\mu\nu} C_{24}. \tag{G.3}$$

This expansion clearly shows the Lorentz structure of the C-integrals.

In order to solve these integrals the following two relations are used

$$\frac{1}{abc} = \int_0^1 \int_0^1 \frac{2x}{\left((a-b)\,xy + (b-c)\,x + c\right)^3}\, dx\, dy, \tag{G.4}$$

$$\frac{1}{2A} = \frac{1}{i\pi^2}\int d^4 q \frac{1}{\left[q^2 + A\right]^3}. \tag{G.5}$$

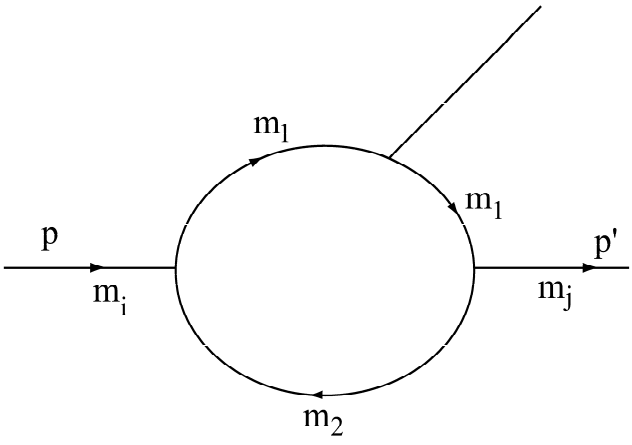

Figure G.1: The figure shows the convention used for the momenta and masses in the C-integrals.

By using Eq. (G.4) the denominator of Eq. (G.1) can be rewritten, i.e.,

$$\begin{aligned}
a-b &= \left((p+q)^2 - m_1^2\right) - \left((p'+q)^2 - m_1^2\right) \\
&= p^2 + q^2 + 2pq - m_1^2 - p'^2 - q^2 - 2p'q + m_1^2 \\
&= p^2 - p'^2 + 2q(p-p'), \\
b-c &= \left((p'+q)^2 - m_1^2\right) - \left(q^2 - m_2^2\right) \\
&= p'^2 + q^2 + 2p'q - m_1^2 - q^2 + m_2^2 \\
&= p'^2 + 2p'q + m_2^2 - m_1^2 \\
(a-b)\,xy + (b-c)\,x + c & \\
&= (q + p_y x)^2 - \left[(m_i^2 - (m_i^2 - m_j^2)(1-y))x^2\right. \\
&\quad \left. + \left(m_j^2 - m_i^2\right)xy + \left(m_1^2 - m_2^2 - m_j^2\right)x + m_2^2\right].
\end{aligned}$$

Here the following definition is used

$$p_y = (p - p')y + p', \tag{G.6}$$

which gives

$$p_y^2 = m_i^2 - (m_i^2 - m_j^2)(1-y). \tag{G.7}$$

One should also remember that the photon is on-shell, i.e., $k^2 = 0$.

Using these relations the integral of Eq. (G.1) can be rewritten as,

$$C_{\{0,\mu,\mu\nu\}} = \frac{1}{i\pi^2}\int_0^1\int_0^1\int d^n q\, dx\, dy \frac{2x\, q_{\{0,\mu,\mu\nu\}}}{\left[(q+p_y x)^2 + A\right]^3}, \tag{G.8}$$

where

$$A = -\left[\left(m_i^2 - \left(m_i^2 - m_j^2\right)(1-y)\right)x^2 + \left(m_j^2 - m_i^2\right)xy + \left(m_1^2 - m_2^2 - m_j^2\right)x + m_2^2\right]. \tag{G.9}$$

Now the integrals defined by Eqs. (G.2) and (G.3) can be found. The first of these integrals, the C_0 integral, becomes,

$$\begin{aligned} C_0 &= \frac{1}{i\pi^2}\int_0^1\int_0^1\int d^4q\,dx\,dy \frac{2x}{\left[(q+p_yx)^2 + A\right]^3} \\ &= \int_0^1\int_0^1 dx\,dy\,\frac{x}{A} \\ &= \frac{1}{m_i^2 - m_j^2}\int_0^1 \frac{dx}{1-x}\ln\frac{m_i^2x^2 + (m_1^2 - m_2^2 - m_i^2)x + m_2^2}{m_j^2x^2 + (m_1^2 - m_2^2 - m_j^2)x + m_2^2}. \end{aligned} \tag{G.10}$$

The integral C_μ is now rewritten in terms of the external momenta, i.e.,

$$\begin{aligned} C_\mu &= p_\mu C_{11} + p'_\mu C_{12} \\ &= \frac{1}{i\pi^2}\int_0^1\int_0^1\int d^4q\,dx\,dy\,\frac{2x\,q_\mu}{\left[(q+p_yx)^2 + A\right]^3} \\ &= \frac{1}{i\pi^2}\int_0^1\int_0^1\int d^4q'\,dx\,dy\,\frac{2x\,(q' - p_yx)_\mu}{[q'^2 + A]^3} \\ &= -\frac{1}{i\pi^2}\int_0^1\int_0^1\int d^4q'\,dx\,dy\,\frac{2x^2\,(p\,y + p'(1-y))_\mu}{[q'^2 + A]^3} \\ &= -\int_0^1\int_0^1 dx\,dy\,\frac{p_\mu\,x^2y + p'_\mu x^2(1-y)}{A}. \end{aligned} \tag{G.11}$$

The integrals C_{11} and C_{12}, defined from C_μ, therefore becomes,

$$C_{11} = -\int_0^1\int_0^1 dx\,dy\,\frac{x^2\,y}{A}, \tag{G.12}$$

$$C_{12} = \int_0^1\int_0^1 dx\,dy\,\frac{x^2\,(1-y)}{A}, \tag{G.13}$$

with A given by Eq. (G.9).

The integral $C_{\mu\nu}$ is also rewritten in terms of the external momenta, i.e.,

$$\begin{aligned}
C_{\mu\nu} &= p_\mu p_\nu C_{21} + p'_\mu p'_\nu C_{22} + \left(p_\mu p'_\nu + p_\nu p'_\mu\right) C_{23} + g_{\mu\nu} C_{24} \\
&= \frac{1}{i\pi^2} \int_0^1 \int_0^1 \int d^n q dx dy \frac{2x\, q_\mu q_\nu}{\left[(q + p_y x)^2 + A\right]^3} \\
&= \frac{1}{i\pi^2} \int_0^1 \int_0^1 \int d^n q' dx dy \frac{2x\, (q' - p_y x)_\mu (q' - p_y x)_\nu}{\left[q'^2 + A\right]^3} \\
&= \frac{1}{i\pi^2} \int_0^1 \int_0^1 \int d^n q' dx dy \frac{2x\, \left(q'_\mu - x\left(p_\mu + p'_\mu (1-y)\right)\right)\left(q'_\nu - x\left(p_\nu + p'_\nu (1-y)\right)\right)}{\left[(q + p_y x)^2 + A\right]^3} \\
&= \frac{1}{i\pi^2} \int_0^1 \int_0^1 \int d^n q' dx dy \frac{2x^3 \left(p_\mu p_\nu + p'_\mu p'_\nu (1-y)^2 + \left(p_\mu p'_\nu + p_\nu p'_\mu\right)(1-y)\right) + 2x q'_\mu q'_\nu}{\left[q'^2 + A\right]^3}.
\end{aligned} \tag{G.14}$$

The integral C_{24} is logarithmically divergent, but this particular integral will not contribute to the decay rates under study, see comments in Appendix B.1. The other three integrals are now found as

$$C_{21} = \int_0^1 \int_0^1 dx\, dy\, \frac{x^3}{A}, \tag{G.15}$$

$$C_{23} = \int_0^1 \int_0^1 dx\, dy\, \frac{x^3\, (1-y)}{A}, \tag{G.16}$$

$$C_{22} = \int_0^1 \int_0^1 dx\, dy\, \frac{x^3\, (1-y)^2}{A} \tag{G.17}$$

with A given by Eq. (G.9).

The y-integration is easily performed, since the denominator, i.e., A from Eq. (G.9), is linear in y. This integration gives,

$$C_0 = \frac{1}{m_i^2 - m_j^2} \int_0^1 dx\, I_0(x), \tag{G.18}$$

$$C_{11} = -\frac{1}{m_i^2 - m_j^2} \int_0^1 dx\, x I_1(x), \tag{G.19}$$

$$C_{12} = \frac{1}{m_i^2 - m_j^2} \int_0^1 dx\, x(I_0(x) - I_1(x)), \tag{G.20}$$

$$C_{21} = \frac{1}{m_i^2 - m_j^2} \int_0^1 dx\, x^2 I_0(x), \tag{G.21}$$

$$C_{22} = \frac{1}{m_i^2 - m_j^2} \int_0^1 dx\, x^2 (I_0(x) - 2I_1(x) + I_2(x)), \tag{G.22}$$

$$C_{23} = \frac{1}{m_i^2 - m_j^2} \int_0^1 dx\, x^2 (I_0(x) - I_1(x)), \tag{G.23}$$

where the $I_n(x)$-functions are defined as follows

$$I_0(x) = \frac{1}{1-x} \ln \frac{m_i^2 x^2 + (m_1^2 - m_2^2 - m_i^2)x + m_2^2}{m_j^2 x^2 + (m_1^2 - m_2^2 - m_j^2)x + m_2^2}, \tag{G.24}$$

$$I_1(x) = \frac{1}{1-x} \left[1 + \frac{m_j^2 x^2 + (m_1^2 - m_2^2 - m_j^2)x + m_2^2}{(m_i^2 - m_j^2)x(1-x)} \right.$$
$$\left. \times \ln \frac{m_i^2 x^2 + (m_1^2 - m_2^2 - m_i^2)x + m_2^2}{m_j^2 x^2 + (m_1^2 - m_2^2 - m_j^2)x + m_2^2} \right] \tag{G.25}$$

$$I_2(x) = \frac{1}{1-x} \left[\frac{1}{2} + \frac{m_j^2 x^2 + (m_1^2 - m_2^2 - m_j^2)x + m_2^2}{(m_i^2 - m_j^2)x(1-x)} \right.$$
$$\left. + \left(\frac{m_j^2 x^2 + (m_1^2 - m_2^2 - m_j^2)x + m_2^2}{(m_i^2 - m_j^2)x(1-x)} \right)^2 \ln \frac{m_i^2 x^2 + (m_1^2 - m_2^2 - m_i^2)x + m_2^2}{m_j^2 x^2 + (m_1^2 - m_2^2 - m_j^2)x + m_2^2} \right]. \tag{G.26}$$

All of the functions Eqs. (G.24) - (G.26) are finite for $x \to 1$.

The integrals, Eqs. (G.18) - (G.23), can all be solved by analytic methods, see e.g. Ref. [71]. However, it is more convenient to perform the calculations by use of numerical methods. The Fortran libraries FF and Looptools [72] are often used to this task. Unfortunately, these libraries do not seem to give numerical stable results for the case with one intermediate mass very large compared to the other masses. Such integrals appear in the analysis of MSSM-D and MSSM-DM. In MSSM-D the neutrino masses are small, but non-vanishing, and in MSSM-DM the right-handed neutral particles are assumed to take very large values. Therefore, to obtain stable results a series expansion of the integrals, Eqs. (G.18) - (G.22), has been used. This series expansion is presented in next section.

G.2 Solution by series expansion

The necessity of calculating the integrals of Eqs. (G.18) - (G.22), with great precision is clearly seen in MSSM-DM. In this model light left-handed components mix with much heavier right-handed components. Thus to obtain the necessary accuracy and stability in the numerical calculations of the Veltman-Passarino integrals, a series expansion have been used.

Unfortunately, such a series expansion can not be obtained by a straightforward expansion of the C-integrals, i.e., of the integrals in Eqs. (G.18) -(G.22). The reason is that an expansion in terms of a light neutral mass, m_2, or in terms of $1/m_1$, both lead to logarithmic divergences.

The proper way to handle these integrals is to use another expansion parameter. Following Ref. [73] the logarithm, which appear in all C-integrals, is rewritten, i.e.,

$$\ln \frac{m_i^2 x^2 + (m_1^2 - m_2^2 - m_i^2)x + m_2^2}{m_j^2 x^2 + (m_1^2 - m_2^2 - m_j^2)x + m_2^2} = \ln \frac{1-\varepsilon}{1-\eta}, \tag{G.27}$$

where

$$\varepsilon = \left(\frac{m_i}{m_1}\right)^2 \frac{x(1-x)}{x + m(1-x)}, \tag{G.28}$$

$$\eta = \left(\frac{m_j}{m_1}\right)^2 \frac{x(1-x)}{x + m(1-x)}, \tag{G.29}$$

$$m = \left(\frac{m_2}{m_1}\right)^2. \tag{G.30}$$

By expanding this logarithm in terms of ε and η the proper series expansion of the logarithm is now obtained, i.e.,

$$\ln \frac{1-\varepsilon}{1-\eta} = -\sum_{n=1}^{\infty} \frac{m_i^{2n} - m_j^{2n}}{m_1^{2n}} \frac{1}{n} \frac{x^n (1-x)^n}{(x + m(1-x))^n}. \tag{G.31}$$

In order to proceed it is useful to define the following family of integrals,

$$J_{p,q,r}(m) = \int_0^1 dx \, \frac{x^p \, (1-x)^q}{(x + m(1-x))^r}, \qquad p, q \geq 0, \; r \leq 0, \tag{G.32}$$

where the definition of m from Eq. (G.30) has been used.

This integral can be solved by a rather straightforward method. First, note that if $r = 0$ or $m = 1$, then the integrals can be solved in terms of the so-called Beta-function [74], i.e.,

$$\begin{aligned} J_{p,q,r}(m) &= \int_0^1 dx \, x^p \, (1-x)^q \\ &= B(1+p, 1+q), \text{ for } r = 0 \text{ or } m = 1, \end{aligned} \tag{G.33}$$

$$B(p,q) = \int_0^1 dx x^{p-1} (1-x)^{q-1} = \frac{\Gamma(p)\,\Gamma(q)}{\Gamma(p+q)}. \tag{G.34}$$

This formula is not well suited for numerical calculations. The reason is that p, q and r are integers, while m is a continuous positive parameter. Therefore, in order to increase the stability a series expansion around $m = 1$ of $J_{p,q,r}(m)$ in terms of m have been used, i.e.,

$$J_{p,q,r}(m) = \sum_{n=0}^{\infty} \binom{n+r-1}{n} (1-m)^n B(1+p, 1+n+q). \tag{G.35}$$

Also, the case where $m = 0$ and $r > 0$ is easily solved, i.e.,

$$\begin{aligned} J_{p,q,r}(m) &= \int_0^1 dx\, x^{p-r}\,(1-x)^q \\ &= B(1+p-r, 1+q),\ p-r \geq 0. \end{aligned} \tag{G.36}$$

At this point it is useful to introduce the following family of integrals [71],

$$\begin{aligned} f_n(a,b) &= \int_0^1 dx\, \frac{ax^n}{ax+b}, \qquad a > 0 \\ &= \left(-\frac{b}{a}\right)^n \ln\frac{a+b}{b} + \sum_{i=0}^{n-1} \frac{1}{n-i}\left(-\frac{b}{a}\right)^i. \end{aligned} \tag{G.37}$$

By using these integrals the solution for $r = 1$ is obtained, i.e.,

$$\begin{aligned} J_{p,q,1}(m) &= \int_0^1 dx\, \frac{x^p\,(1-x)^q}{x+m(1-x)} \\ &= \sum_{i=0}^{q} \binom{q}{i} (-1)^i \int_0^1 dx\, \frac{x^{p+i}}{(1-m)x+m} \\ &= \frac{1}{1-m} \sum_{i=0}^{q} \binom{q}{i} (-1)^i\, f_{p+i}(1-m, m). \end{aligned} \tag{G.38}$$

To obtain the solution for the general case, that is, for $r > 0$ and $m \neq 0$ or 1, the following change of variables is made,

$$u = (1-m)x + m. \tag{G.39}$$

Also the family of functions $g_a(m)$ is defined, i.e.,

$$g_a(m) = \int_m^1 dx\, x^a = \begin{cases} (1 - m^{1+a})/(1+a) & \text{for } a \neq -1, \\ -\ln(m) & \text{for } a = -1. \end{cases} \tag{G.40}$$

The general integral with $r > 1$ now becomes

$$\begin{aligned} J_{p,q,r}(m) &= \int_0^1 dx \, \frac{x^p \, (1-x)^q}{((1-m)x+m)^r} \\ &= \sum_{i=0}^{q} \binom{q}{i} (-1)^i \int_0^1 dx \, \frac{x^{p+i}}{((1-m)x+m)^r} \\ &= \sum_{i=0}^{q} \binom{q}{i} \frac{(-1)^i}{(1-m)^{1+p+i}} \int_m^1 du \frac{(u-m)^{p+i}}{u^r} \\ &= \sum_{i=0}^{q} \binom{q}{i} \frac{(-1)^i}{(1-m)^{1+p+i}} \sum_{j=0}^{p+i} \binom{p+i}{j} (-m)^{p+i-j} \, g_{j-r}(m). \end{aligned} \tag{G.41}$$

Thus the family of integrals, represented by $J_{p,q,r}(m)$, are now completely solved by Eqs. (G.33), (G.36) and (G.41), for all parameters of interest.

By using $J_{p,q,r}(m)$ it is now possible to obtain the series expansion of the following integrals,

$$\int_0^1 dx x^k I_0(x) = -\sum_{n-1}^{\infty} \frac{\sigma^n - \tau^n}{n} J_{n+k,n-1,n}(m), \tag{G.42}$$

$$\begin{aligned} \int_0^1 dx x^k I_1(x) = \tau J_{1+k,0,1}(m) - \frac{1}{\sigma-\tau} \sum_{n=2}^{\infty} \frac{\sigma^n - \tau^n}{n} \left[\tau J_{n+k+1,n-2,n}(m) \right. \\ \left. +(1-m-\tau) J_{n+k,n-2,n}(m) + m J_{n+k-1,n-2,n}(m) \right], \end{aligned} \tag{G.43}$$

$$\begin{aligned} \int_0^1 dx x^k I_2(x) = R_k(m) - \frac{1}{(\sigma-\tau)^2} \sum_{n=3}^{\infty} \frac{\sigma^n - \tau^n}{n} \left[\tau^2 \, J_{n+k+2,n-3,n}(m) \right. \\ + 2\tau(1-m-\tau) \, J_{n+k+1,n-3,n}(m) \\ + (1+m^2+\tau^2-2m(1-2\tau)-2\tau) \, J_{n+k,n-3,n}(m) \\ \left. +2m(1-m-\tau) \, J_{n+k-1,n-3,n}(m) + m^2 \, J_{n+k-2,n-3,n}(m) \right], \end{aligned} \tag{G.44}$$

where

$$\begin{aligned} R_k(m) = \frac{\tau}{\sigma-\tau} \left[\frac{\tau(\sigma+\tau)}{2} \, J_{k+3,0,2}(m) \right. \\ + \left(\sigma(1-m-\tau) + \frac{\tau(\sigma-\tau)}{2} \right) J_{k+2,0,2}(m) \\ \left. +m\sigma \, J_{k+1,0,2}(m) \right]. \end{aligned} \tag{G.45}$$

Here the following mass ratios have been used

$$\sigma = \left(\frac{m_i}{m_1}\right)^2 \quad \text{and} \quad \tau = \left(\frac{m_j}{m_1}\right)^2, \tag{G.46}$$

along with the parameter m defined by Eq. (G.30).

These series expansions, along with the definition of $J_{p,q,r}(m)$, Eq. (G.32), clearly shows that all of these integrals are well behaved for $x = 1$.

This completes the series expansion of the integrals shown in Eqs. (G.18) - (G.22).

The series expansion for the C-integrals converges very fast and only a few terms are needed to obtain the integrals to the necessary accuracy. Also, by combining the solutions of Eqs. (G.42) - (G.44) with the multiple precision library FM [59, 60] the C-integrals can be solved to any accuracy.

URN:NBN:no-7281

Appendix H

Numerical methods

This appendix gives additional details regarding the numerical methods used in this thesis.

For each of the models MSSM-D, MSSM-M and MSSM-DM a computer program has been written. These programs have as their input the free parameters of each model, and as output the decay rates under study. The computer code has been written in Fortran and compiled on a Digital compiler by use of the software package Compaq Visual Fortran[1]. The compiled program has been executed on various computers, such as a 1.7 GHz Pentium M. Even though the code extends over many lines the programs are fast and return an answer in less than a second, and roughly 10 seconds if multiple precision is used in the calculation of the Veltman-Passarino integrals. Various numerical routines have been used to test for speed and stability. Most of the numerical routines have been provided by NAG [55], but also the library IMSL [75] and the multiple precision library FM [59, 60] have been used.

The numerical routines are all build in the same manner, and follow the same work-flow in the numerical calculations, i.e.,

1. Define the parameters of the model.
2. Solve the renormalization group equations, and minimisation conditions.
3. Determine mass eigenstates and mixing matrices.
4. Determine the proper Feynman rules.
5. Solve the Veltman-Passarino integrals.
6. Calculate each contributing amplitude.
7. Calculate the decay rate and present the result.

[1]Earlier releases of this software package are traded under the names Microsoft Powerstation and Digital Visual Fortran.

Each of the items above has been solved in terms of several subroutines, e.g., one subroutine for each mass matrix. This modulation of the computer code has made it easier to check the code, and also to extend the calculations.

The above items will now be discussed in greater detail.

Define the parameters of the model. The collection of all parameters for each model have been referred to as the parameter space. To find constraints on the parameter space from the lepton flavour violating decay rates has been one of the main objectives in this thesis. Several assumptions and textures have been analysed, and results are presented in the main part of this thesis.

One expects the decay rates to be continuous functions of the free parameters. This continuity serves as a consistency check on the stability of the computer code. The final versions of each computer code all give continuous results for continuous input parameters.

Solve the renormalization group equations. The input parameters are defined at the electroweak and at the GUT scale. And the renormalization group equations connect these two scales. The renormalization group equations have been obtained from Ref. [34], and written in the analytic software package Maple [61]. First, several special cases have been tested by use of analytical and numerical methods in Maple. Next, the Fortran generator of Maple has been used to convert the renormalization group equations into Fortran-77. This workflow has made it easier to check this large set of differential equations.

To numerically solve the renormalization group equations several routines, all provided by NAG have been used. This system of equations does not show any form of stiffness, and a Runge-Kutta method (D02BAF and D02BDF), has been used.

At the electroweak scale, the minimisation conditions have been solved. This set of equations can be iterated between the electroweak and the GUT scale, in order to match the boundary conditions at each scale. The results of this procedure have been presented in Secs. 4.4, 5.7 and 6.5.

Determine mass eigenstates and mixing angles. A subroutine has been written for each mass matrix. The eigenvalues and mixing matrices are easily found from these mass matrices. Numerically, this has been achieved by use of numerical routines from NAG, i.e., by F02ABF.

These routines have been checked, both analytically and numerically, by use of Maple, for some special cases.

Determine the proper Feynman rules. After the mass eigenstates and mixing matrices are found the Feynman rules, as presented in Appendix E, have been obtained.

Solve the Veltman-Passarino integrals. The solution of the Veltman-Passarino integrals turned out to be more challenging than first expected. The numerical library FF [72] was first used, but it did not give stable results in all cases. In the

final version of each program the series expansion presented in Appendix G.1 was chosen. This procedure did give stable results, as can be shown in e.g., Fig. 5.10.

The last two items on the list are now easily calculated.

The Fortran codes and the Maple code can be obtained by request from the author, i.e.,

Terje R. Meisler
Gunnerus gate 1, 7004 Trondheim

terje.meisler@iaf.hist.no

URN:NBN:no-7281

Bibliography

[1] J. J. Thompson, Philosophical Magzine **44**, 293 (1897).

[2] L. M. Brown, A. Pais, and S. B. Pippard, *Twentieth Century Physics* (AIP Press, New York, 1995), chap. Elementary particle physics in the second half of the twentieth century, Fitch, Val L. and Rosner, Jonathan L.

[3] M. L. Perl *et al.*, Phys. Rev. Lett. **35**, 1489 (1975).

[4] http://www.ethbib.ethz.ch/exhibit/pauli/.

[5] DONUT, K. Kodama *et al.*, Phys. Lett. **B504**, 218 (2001), hep-ex/0012035.

[6] K. Hagiwara *et al.*, Phys. Rev. D **66**, 010001+ (2002).

[7] J. Davis, Raymond, D. S. Harmer, and K. C. Hoffman, Phys. Rev. Lett. **20**, 1205 (1968).

[8] Super-Kamiokande, Y. Fukuda *et al.*, Phys. Rev. Lett. **81**, 1562 (1998), hep-ex/9807003.

[9] SNO, Q. R. Ahmad *et al.*, Phys. Rev. Lett. **87**, 071301 (2001), nucl-ex/0106015.

[10] SNO, Q. R. Ahmad *et al.*, Phys. Rev. Lett. **89**, 011301 (2002), nucl-ex/0204008.

[11] SAGE, V. N. Gavrin, Nucl. Phys. Proc. Suppl. **91**, 36 (2001).

[12] MACRO, M. Spurio, (2000), hep-ex/0101019.

[13] K2K, S. H. Ahn *et al.*, Phys. Lett. **B511**, 178 (2001), hep-ex/0103001.

[14] KamLAND, K. Eguchi *et al.*, Phys. Rev. Lett. **90**, 021802 (2003), hep-ex/0212021.

[15] M. Apollonio *et al.*, Eur. Phys. J. **C27**, 331 (2003), hep-ex/0301017.

[16] S. Weinberg, *The Quantum Theory of Fields* (Cambridge University Press, Cambridge, 1995).

[17] T. P. Cheng and L.-F. Li, Phys. Rev. Lett. **45**, 1908 (1980).

[18] S. L. Glashow, J. Iliopoulos, and L. Maiani, Phys. Rev. **D2**, 1285 (1970).

[19] Z. Maki, M. Nakagawa, and S. Sakata, Prog. Theor. Phys. **28**, 870 (1962).

[20] H. V. Klapdor-Kleingrothaus, (2002), hep-ph/0211037.

[21] S. M. Bilenkii, C. Giunti, and W. Grimus, (1998), hep-ph/9812360.

[22] http://neutrinooscillation.org.

[23] D. E. Groom *et al.*, Eur. Phys. J. **C15**, 1 (2000).

[24] T. Mori, Nucl. Phys. Proc. Suppl. **111**, 194 (2002).

[25] D. F. Carvalho, J. R. Ellis, M. E. Gomez, S. Lola, and J. C. Romao, (2002), hep-ph/0206148.

[26] H. Fusaoka and Y. Koide, Phys. Rev. **D57**, 3986 (1998), hep-ph/9712201.

[27] B. Pontecorvo, Sov. Phys. JETP **26**, 984 (1968).

[28] H. E. Haber and G. L. Kane, Phys. Rep. **117**, 75 (1985).

[29] H. J. W. Müller-Kirsten and A. Wiedeman, *Supersymmetry - An Introduction with Conceptual and Calculational Details* (World Scientific, 1987).

[30] T.-P. Cheng and L.-F. Li, *Gauge theory of elementary particle physics* (Oxford University Press, New York, 1984).

[31] H. E. Haber, (1997), hep-ph/9709450.

[32] D. Bailin and A. Love, *Supersymmetric Gauge Field Theory and String Theory* (IOP Publishing, 1994).

[33] J. Wess and J. Bagger, *Supersymmetry and Supergravity*, second ed. (Princeton University Press, 1992).

[34] S. P. Martin and M. T. Vaughn, Phys. Rev. **D50**, 2282 (1994), hep-ph/9311340.

[35] S. P. Martin, (1997), hep-ph/9709356.

[36] S. Dimopoulos and D. Sutter, Nucl. Phys. **B452**, 496 (1995), hep-ph/9504415.

[37] L. Girardello and M. T. Grisaru, Nucl. Phys. **B194**, 65 (1982).

[38] V. Barger, M. S. Berger, and P. Ohmann, Phys. Rev. **D49**, 4908 (1994), hep-ph/9311269.

[39] M. C. Gonzalez-Garcia and Y. Nir, (2002), hep-ph/0202058.

[40] http://www-spires.slac.stanford.edu/spires/hep/.

[41] B. C. Allanach, A. Dedes, and H. K. Dreiner, Phys. Rev. **D60**, 075014 (1999), hep-ph/9906209.

[42] B. Pendleton and G. G. Ross, Phys. Lett. **B98**, 291 (1981).

[43] C. T. Hill, Phys. Rev. **D24**, 691 (1981).

[44] M. B. Einhorn and D. R. T. Jones, Nucl. Phys. **B196**, 475 (1982).

[45] L. E. Ibanez and C. Lopez, Nucl. Phys. **B233**, 511 (1984).

[46] G. Kane, C. Kolda, L. Roszkowski, and J. D. Wells, Phys. Rev. **D49**, 6173 (1994).

[47] J. Rosiek, Phys. Rev. **D41**, 3464 (1990), Erratum hep-ph/9511250.

[48] G. Jungman, K. Kamionkowski, and K. Griest, Phys. Rep. **267**, 195 (1996).

[49] C. hsi Chang and T. fu Feng, (1999), hep-ph/9908295.

[50] Y. Grossman and H. E. Haber, (1999), hep-ph/9906310.

[51] C. Caso *et al.*, Eur. Phys. J. **C3**, 1 (1998).

[52] J. R. Ellis, Nucl. Phys. Proc. Suppl. **91**, 503 (2000), hep-ph/0008334.

[53] B. C. Allanach, A. Dedes, and H. K. Dreiner, Phys. Rev. **D60**, 056002 (1999), hep-ph/9902251.

[54] M. T. Grisaru, W. Siegel, and M. Rocek, Nucl. Phys. **B159**, 429 (1979).

[55] http://www.nag.com.

[56] W. H. Press, *Numerical Recipes in Fortran* (Cambridge University Press, 1986).

[57] J. R. Espinosa and R.-J. Zhang, Nucl. Phys. **B586**, 3 (2000), hep-ph/0003246.

[58] M. S. Berger, Phys. Rev. **D41**, 225 (1990).

[59] D. M. Smith, ACM Trans. Math. Softw. **17**, 273 (1991), http://www.lmu.edu/acad/personal/faculty/dmsmith2/FMLIB.html.

[60] D. M. Smith, ACM Trans. Math. Softw. **24**, 359 (1998), http://www.lmu.edu/acad/personal/faculty/dmsmith2/FMLIB.html.

[61] http://www.maplesoft.com.

[62] C. Itzykson and J.-B. Zuber, *Quantum Field Theory* (McGraw-Hill, 1980).

[63] C. W. Misner, K. S. Thorne, and J. A. Wheeler, *Gravitation* (Freeman, San Francisco, 1973).

[64] A. Metz *et al.*, Phys. Rev. Lett. **83**, 1542 (1999).

[65] N. Arkani-Hamed, A. G. Cohen, and H. Georgi, Phys. Lett. **B513**, 232 (2001), hep-ph/0105239.

[66] S. R. Coleman and J. Mandula, Phys. Rev. **159**, 1251 (1967).

[67] F. Cooper, A. Khare, and U. Sukhatme, Phys. Rept. **251**, 267 (1995), hep-th/9405029.

[68] I. Simonsen, (1995), hep-ph/9506369.

[69] J. Hisano, T. Moroi, K. Tobe, and M. Yamaguchi, Phys. Rev. **D53**, 2442 (1996), hep-ph/9510309.

[70] G. Passarino and M. Veltman, Nucl. Phys. **B160**, 151 (1979).

[71] J. Fujimoto, M. Igarashi, N. Nakazawa, Y. Shimizu, and K. Tobimatsu, Prog. Theor. Phys. Suppl. **100**, 1 (1990).

[72] T. Hahn and M. Perez-Victoria, Comp. Phys. Comm. **118**, 153 (1999), hep-ph/9807565.

[73] K.-i. Aoki, Z. Hioki, R. Kawaba, M. Konuma, and T. Muta, Suppl. Prog. Th. Phys. **73**, 1 (1982).

[74] M. Abramowitz and I. A. Stegun, *Handbook of Mathematical Functions* (Dover Publications, New York, 1972).

[75] http://www.vni.com.